ILMATIETEEN LAITOS
METEOROLOGISKA INSTITUTET
FINNISH METEOROLOGICAL INSTITUTE

163
CONTRIBUTIONS

AIR QUALITY TRENDS IN FINLAND, 1994-2018

PIA ANTTILA

FINNISH METEOROLOGICAL INSTITUTE
CONTRIBUTIONS
No. 163

Air Quality Trends in Finland, 1994–2018

Pia Anttila

Institute of Atmospheric and Earth System Research/Physics
Faculty of Science
University of Helsinki
Helsinki, Finland

ACADEMIC DISSERTATION in physics

To be presented, with the permission of the Faculty of Science of the University of Helsinki, for public examination in lecture room D101, Physicum, Gustaf Hällströmin katu 2, on the 27th of October, 2020 at 12 o'clock.

Finnish Meteorological Institute
Helsinki, 2020

Author: Pia Anttila
Finnish Meteorological Institute
P.O. Box 503, FI-00101 Helsinki, Finland
pia.anttila@fmi.fi

Supervisor: Research Professor Hannele Hakola
Finnish Meteorological Institute
Atmospheric Composition Research
Helsinki, Finland

Reviewers: Professor Heikki Junninen
University of Tartu, Institute of Physics
Laboratory of Environmental Physics
Tartu, Estonia

Associate Professor Topi Rönkkö
Tampere University, Physics unit
Aerosol Physics Laboratory
Tampere, Finland

Opponent: Professor Øystein Hov
The Norwegian Meteorological Institute
Oslo, Norway

Custos: Academician, Academy Professor Markku Kulmala
University of Helsinki, Faculty of Science
Institute for Atmospheric and Earth System Research
(INAR) / Physics

ISBN 978-952-336-101-0 (paperback)
ISBN 978-952-336-102-7 (pdf)
ISSN 0782-6117
https://doi.org/10.35614/isbn.9789523361027

Edita Prima Oy
Helsinki, 2020

To my grandchildren

Eko, Kimo and Kaïa

“Air quality is the composition of the air

in terms of how much pollution it contains.”

Collins English Dictionary

ILMATIETEEN LAITOS
METEOROLOGISKA INSTITUTET
FINNISH METEOROLOGICAL INSTITUTE

Published by	Finnish Meteorological Institute	Series title, number, and report code
	(Erik Palménin aukio 1), P.O. Box 503	FMI Contributions, 163, FMI-CONT-163
	FIN-00101 Helsinki, Finland	Date October 2020

Author
Pia Anttila

Title
Air quality trends in Finland, 1994–2018

Abstract

In this thesis, long-term, multicomponent, high-resolution (time and accuracy) air quality monitoring data from about 400 sites across Finland since 1994 are integrated into a single unified and compact view to demonstrate past air quality development and to assess the reasons behind the development at the national level.

This thesis demonstrates that internationally launched and nationally implemented regulatory controls have had an important role in improving air quality in Finland. The pollutants subject to long-term ambitious international abatement strategies (like SO_2 and persistent organic pollutants) have decreased the most. Also, NO_x emission control has been successful, but urban roadside NO_2 concentrations have not decreased as expected. The increase in diesel cars (and their potentially high primary NO_2 emissions) may have been one factor in slowing down the decline of concentrations. However, the development of emission reduction technologies together with the improved type approval test procedures have resulted in a reduction in the significance of primary NO_2 emissions in Europe. In Finland, our relatively old car fleet and the increased import of old diesel cars cause uncertainty for future development.

Due to the use of studded tyres and manifested as elevated concentrations of PM_{10}, springtime street dust is a local air pollution problem. This thesis suggests that local abatement measures (e.g., reducing traffic, changes in the car fleet, road maintenance activities) have been moving in the right direction, and the springtime street dust levels have been reduced. Although air quality standards are not exceeded today, street dust remains a persistent flaw in our otherwise good air quality.

In Finland, the ozone peak levels have been declining since 2006. Similar development has been detected in Europe and North America, and it is related to decreasing anthropogenic precursor emissions of NO_x and VOCs. For Finland, high background concentrations are more problematic, and reducing them would require international and even hemispheric cooperation.

The available long-term background data of PAH concentrations suggest that no widespread decrease in concentrations has occurred. This is not necessarily surprising as the major global sources are small-scale solid fuel combustion and wildfires. Efforts to reduce these emissions have been relatively limited or non-existent so far.

Publishing unit
Atmospheric Composition Research/Air Quality

Classification (UDC)	Keywords	
502.3:613.15 (air quality)	pollution, monitoring, data-analysis,	
303.446.3 (time series study)	time development, abatement	
ISSN and series title	ISBN	
0782-6117	978-952-336-101-0 (paperback)	
Finnish Meteorological Institute Contributions	978-952-336-102-7 (pdf)	
DOI	Language	Pages
10.35614/isbn.9789523361027	English	54

ILMATIETEEN LAITOS
METEOROLOGISKA INSTITUTET
FINNISH METEOROLOGICAL INSTITUTE

Julkaisija	Ilmatieteen laitos (Erik Palménin aukio 1) PL 503, 00101 Helsinki	Julkaisun sarja, numero ja raporttikoodi Contributions, 163, FMI-CONT-163 Päiväys Lokakuu 2020

Tekijä

Pia Anttila

Nimeke

Ilmanlaatutrendit Suomessa 1994–2018

Tiivistelmä

Tässä väitöskirjassa on koottu yhteen Suomen ilmanlaadun mittaustiedot yli parinkymmenen vuoden ajalta ja noin 400 mittausasemalta. Aineistosta arvioidaan ilmanlaadun kehitystä ja syitä havaittuun kehitykseen kansallisella tasolla.

Tämä opinnäyte osoittaa, että kansainvälisesti käynnistetyillä ja kansallisesti toteutetuilla päästöjen rajoittamistoimilla on ollut tärkeä rooli ilmanlaadun parantamisessa Suomessa. Epäpuhtaudet, joihin on kohdistunut pitkäaikaisia kunnianhimoisia kansainvälisiä päästöstrategioita (kuten SO_2 ja pysyvät orgaaniset ympäristömyrkyt), ovat vähentyneet eniten. Myös NO_x-päästöjen vähentäminen on onnistunut, mutta kaupungeissa NO_2-pitoisuudet eivät ole vähentyneet odotetusti. Dieselautojen lisääntynyt määrä (ja niiden mahdollisesti korkeat suorat NO_2-päästöt) on saattanut olla yksi tekijä, joka on hidastanut NO_2-pitoisuuksien laskua. Päästöjen vähentämistekniikoiden ja tyyppihyväksyntämenettelyjen kehittyminen on kuitenkin vähentänyt suorien NO_2-päästöjen merkitystä Euroopan tasolla. Suomessa suhteellisen vanha autokanta ja vanhojen dieselautojen lisääntynyt tuonti aiheuttavat epävarmuutta tulevaisuuden kehitykselle.

Kevään katupöly, joka johtuu nastarenkaiden käytöstä ja joka ilmenee korkeina PM_{10}-pitoisuuksina, on paikallinen ilmanlaatuongelma. Tämä opinnäyte viittaa siihen, että paikalliset vähennystoimenpiteet (esim. liikennemäärien vähentäminen, muutokset autokannassa, tienhoitotoimet) ovat olleet oikeansuuntaisia ja kevään katupölytasot ovat vähentyneet. Vaikka ilmanlaatunormeja ei tällä hetkellä ylitetä, katupöly on edelleen sitkeä ilmanlaatuhaitta muuten hyvässä ilmanlaadussamme.

Suomessa otsonin huipputasot ovat laskeneet vuodesta 2006. Vastaavaa kehitystä on havaittu Euroopassa ja Pohjois-Amerikassa, ja se on liitetty typen oksidien (NO_x) ja haihtuvien orgaanisten yhdisteiden (VOC) päästöjen vähentämiseen. Suomessa kuitenkin korkeat taustapitoisuudet ovat ongelmallisempia, ja niiden alentaminen edellyttää laajaa kansainvälistä yhteistyötä.

PAH-pitoisuuksissa ei ole tapahtunut laaja-alaista laskua. Tämä ei ole välttämättä yllättävää, koska suurimpia lähteitä maailmanlaajuisesti ovat pienpoltto ja metsä- ja maastopalot. Pyrkimykset näiden päästöjen vähentämiseksi ovat toistaiseksi olleet suhteellisen vähäisiä tai olemattomia.

Julkaisijayksikkö

Ilmakehän koostumuksen tutkimus/Ilmanlaatu

Luokitus (UDK) 502.3:613.15 303.446.3	Asiasanat ilmansaasteet, seuranta, aikakehitys, torjunta, lähteet
ISSN ja avainnimeke 0782-6117 Contributions	ISBN 978-952-336-101-0 (paperback) 978-952-336-102-7 (pdf)
DOI 10.35614/isbn.9789523361027	Kieli englanti Sivumäärä 54

Preface

Seriously, this thesis has been underway for almost ten years. Its slow progress is not only because of my personal deficiencies as a researcher but also because of other tasks that have more strongly drawn my interest. Of those, I want to mention my participation in modernising the national air quality information system and its integration with other FMI ITC systems, the expert tasks in air quality capacity building projects in Balkan and Central Asia, and my long-lasting interest in communicating information about ambient air quality. To me, these years have been both interesting and meaningful, and I greatly appreciate the efforts, support and help I have received from my colleagues during various projects. These activities have also shaped my perception of the air quality in general and have strongly influenced how this thesis finally came to be.

I've been very fortunate to have spent most of my professional life at the Finnish Meteorological Institute, where I have had the opportunity to create such a varied career among different aspects of air quality, and for this, I express my gratitude.

I thank Academician, Academy Professor Markku Kulmala for believing that my (fragmented) research on air quality could finally make a coherent story worthy of becoming a doctoral dissertation. Of course, it helped that I have had the privilege to co-write my articles with brilliant researchers, for which I am truly grateful. I thank my pre-examiners, Professor Heikki Junninen and Associate Professor Topi Rönkkö for their supportive, sound advice. And warm thanks to my supervisor, Research Professor Hannele Hakola, who has been encouraging me towards this dissertation during these years.

And finally, special thanks are due to the Finnish air quality community, the hundreds of air quality data producers in municipalities, industries and institutions, colleagues in the reference laboratory of air quality, and the data flow and repository managers at FMI. Without your input, this work would not have been possible.

In Helsinki, Ilmala, 20 February 2020

Pia Anttila

Abbreviations

ACF	Autocorrelation function
AICC	Bias-corrected Akaike information criterion
AirBase	European air quality database maintained by the EEA
AMAP	Arctic Monitoring and Assessment Programme under the Arctic Council
Ant	Anthracene
AQM	Air quality monitoring
ARMA	Autoregressive moving-average
BaA	Benz(a)anthracene
BaP	Benzo(a)pyrene
BbF	Benzo(b)fluoranthene
BkF	Benzo(k)fluoranthene
BP	Benzo(ghi)perylene
BAPMoN	WMO Background Air Pollution Monitoring Network
CDPF	Catalytic diesel particulate filters
CEN	European Committee for Standardization
Chr	Chrysene
CLRTAP	Convention on Long-range Transboundary Air Pollution
CO	Carbon monoxide
DDD	Dichlorodiphenyldichloroethane
DDE	Dichlorodiphenyldichloroethylene
DDT	Dichlorodiphenyltrichloroethane
DhA	Dibenz(a,h)anthracene
EEA	European Environment Agency
EGAP	Group of experts on airborne pollution of the Baltic Sea area under HELCOM
EMEP	UNECE European Monitoring and Evaluation Programme
EU	European Union
FAQDMS	Finnish air quality data management system
Fl	Fluoranthene
FMI	Finnish Meteorological Institute
GAW	WMO Global Atmosphere Watch
GDP	Gross Domestic Product
GLS	Generalised least square
HCH	Hexachlorocyclohexane
HELCOM	Baltic Marine Environment Protection Commission – Helsinki Commission
HSY	Helsinki Region Environmental Services Authority (Helsingin seudun ympäristöpalvelut –kuntayhtymä)
IcP	Indeno(1,2,3-cd)pyrene
iid	independent and identically distributed
IM	UNECE Integrated Monitoring Network
INSPIRE	Directive of the Infrastructure for Spatial Information in the European Community
IPR	Directive of the reciprocal exchange of information and reporting on ambient air quality
ISO	International Organization for Standardization
IVL	Swedish Environmental Research Institute
LRT	Long-range transport

MLE	Maximum likelihood estimation
NEDC	New European Driving Cycle
NO	Nitrogen monoxide
NO_2	Nitrogen dioxide
NO_x	$NO+NO_2$
O_3	Ozone
OCP	Organochlorine pesticide
OLS	Ordinary least square
PAH	Polycyclic aromatic hydrocarbon
ppbv	parts per billion by volume
PCB	Polychlorinated biphenyl
PEMS	Portable emission measurement system
Phe	Phenanthrene
PM	Particulate matter
PM_{10}	Particles less than 10 µm in aerodynamic diameter
$PM_{2.5}$	Particles less than 2.5 µm in aerodynamic diameter
PMF	Positive matrix factorization
POP	Persistent organic pollutant
Pyr	Pyrene
RDE	Real Driving Emissions
SECA	Sulphur Emission Control Area
SIA	Secondary inorganic aerosols
SO_2	Sulphur dioxide
STD	Standard deviation
TM	Trace metals
TSP	Total suspended particles
TWC	Three-way catalytic converters
UNECE	United Nations Economic Commission for Europe
WMO	World Meteorological Organisation
WN	White noise
VOC	Volatile organic compound
WLTP	Worldwide harmonised light vehicle test procedure
WSI	Water soluble ions

gas	conversion between µg/m^3 and ppbv (293 K, 101.3 kPa)
SO_2	1 µg/m^3 = 0.376 ppb
NO_2	1 µg/m^3 = 0.523 ppb
NO	1 µg/m^3 = 0.802 ppb
O_3	1 µg/m^3 = 0.500 ppb
CO	1 µg/m^3 = 0.86 ppb

Contents

Publications of the thesis

This thesis consists of five original articles and a synthesis where these articles are reviewed in the framework of the research field in focus. The articles with their original abstracts are listed below. All measurements were either performed by the co-authors or validated data were retrieved from open-data archives. The AQM data for **Papers I** and **IV** originate from the Finnish air quality monitoring networks and were downloaded from the FMI AQ database. Data for **Paper II** were provided by the co-author at HSY. The long-term persistent organic pollutants' (POPs) data in **Paper III** were provided by the co-authors from the IVL chemical laboratory. The data for **Paper V** were received directly from the co-authors at FMI. I am responsible for the overall planning of the papers, data analysis and calculations, except in **Paper V** Lic.Sc. Sirkka Leppänen conducted the PMF calculations. Interpretation of the results was made together with the co-authors, and the co-authors also contributed to the writing of the papers.

I Anttila, P., Tuovinen, J.-P., 2010. Trends of primary and secondary pollutant concentrations in Finland in 1994–2007. Atmos. Environ., 44, 38–49.

The trends in the atmospheric concentrations of the main gaseous and particulate pollutants in urban, industrial and rural environments across Finland were estimated for the period of 1994–2007. The statistical analysis was based on generalized least-squares regression with classical decomposition and autoregressive moving-average (ARMA) errors, which were applied to monthly-averaged data. In addition, three alternative methods were tested. Altogether, 102 pollutant time series from 42 sites were analysed. During the study period, the concentrations of SO_2, CO and NO_x declined considerably and widely across Finland. The SO_2 concentrations at urban and industrial sites were approaching background levels. The reductions in NO_x and CO concentrations were comparable to those in national road traffic emissions. A downward trend was detected in half of the NO_2 time series studied, but the reductions were not as large as would be expected on the basis of emission trends, or from NO_x concentrations. For O_3, neither the mean nor the peak values showed large changes in background areas, but they were increasing in the urban data. For PM_{10}, 5 of the 12 urban time series showed decreasing mean levels. However, the highest concentrations, typically attributable to the problematic springtime street dust, did not decrease as widely. The reduction of the long-range transported major ions, mainly driven by the large-scale reduction in sulphur emissions, possibly plays a significant part in the decreases in the mean PM_{10} concentrations. It was shown that the handling of the serially correlated data with the ARMA processes improved the analysis of monthly values. The use of monthly rather than annually-averaged data helped to identify the weakest trends.

II Anttila, P., Tuovinen, J.-P., Niemi, J.V., 2011. Primary NO_2 emissions and their role in the development of NO_2 concentrations in a traffic environment. Atmos. Environ., 45, 986–992.

An assessment of the formation of NO_2 concentrations in heavily traffic-influenced environments in Helsinki, Finland was carried out. The proportion of primary NO_2 emissions from road traffic was estimated using a statistical model for the relationship between the mixing ratios of nitrogen oxides ($NO + NO_2$) and total oxidant ($O_3 + NO_2$) measured in 1994–2009. Based on this analysis, a quantitative estimate was derived for the relative importance of the primary NO_2 emissions, ambient $NO–NO_2–O_3$ equilibrium and background concentrations in the observed NO_2 concentrations. The proportion of primary NO_2 in the vehicular NO_x

emissions increased from below 10% in the 1990s to about 20% in 2009, with a more distinctive increase during the most recent years. This development was related to the changes in the proportion of diesel-powered passenger cars in Finland. Between 1994 and 2004, the photochemical NO-to-NO_2 conversion comprised on average 51% of the mean NO_2 concentration, while the primary NO_2 emissions contributed 31%. The role of the primary NO_2 emissions was limited by the steeply-decreasing total NO_x emissions. More recent data (2005–2009) yielded higher primary NO_2 emission fractions (15–21%), with a clearly increasing trend. As a result, the contribution of chemical conversion steadily decreased from 54% in 2005 to 43% in 2009, while that of the primary NO_2 emissions increased from 32 to 44%. In order not to exceed in future the annual limit of NO_2 concentration, set by the European Union, in the busiest street canyons in downtown Helsinki, the primary NO_2 emissions need to be addressed alongside the total NO_x emissions.

III Anttila, P., Brorström-Lundén, E., Hansson, K., Hakola, H., Vestenius, M., 2016. Assessment of the spatial and temporal distribution of persistent organic pollutants (POPs) in the Nordic atmosphere. Atmos. Environ., 140, 22–33.

Long-term atmospheric monitoring data (1994–2011) of persistent organic pollutants (POPs) were assembled from a rural site in southern Sweden, Råö, and a remote, sub-Arctic site in Finland, Pallas. The concentration levels, congener profiles, seasonal and temporal trends, and projections were evaluated in order to assess the status of POPs in the Scandinavian atmosphere. Our data include atmospheric concentrations of polycyclic aromatic hydrocarbons (PAHs), polychlorinated biphenyls (PCBs) and organochlorine pesticides (OCPs), altogether comprising a selection of 27 different compounds.

The atmospheric POP levels were generally higher in the south, closer to the sources (primary emissions) of the pollutants. The levels of low-chlorinated PCBs and chlordanes were equal at the two sites, and one of the studied POPs, α-HCH, showed higher levels in the north than in the south.

Declining temporal trends in the atmospheric concentrations for the legacy POPs — PCBs (2–4% per year), HCHs (6–7% per year), chlordanes (3–4% per year) and DTTs (2–5% per year) — were identified both along Sweden's west coast and in the sub-Arctic area of northern Finland. Most of PAHs did not show any significant long-term trends.

The future projections for POP concentrations suggest that in Scandinavia, low-chlorinated PCBs and p,p′-DDE will remain in the atmospheric compartment the longest (beyond 2030). HCH's and PCB180 will be depleted from the Nordic atmosphere first, before 2020, whereas chlordanes and rest of the PCBs will be depleted between the years 2020 and 2025. PCBs tend to deplete sooner and chlordanes later from the sub-Arctic compared to the south of Sweden.

This study demonstrates that the international bans on legacy POPs have successfully reduced the concentrations of these substances in the Nordic atmosphere. However, the most long-lived compounds may continue in the atmospheric cycle for another couple of decades.

IV Anttila, P., Salmi, T., 2006. Characterizing temporal and spatial patterns of urban PM_{10} using six years of Finnish monitoring data. Boreal Env. Res., 11, 463–479.

Data from the Finnish Meteorological Institute's Air Quality Monitoring Data Management System (ILSE) for 1998–2003 were used to examine the temporal and spatial patterns of urban PM_{10} in Finland. Long term means of PM_{10} at 24 Finnish urban stations vary between 11 and 24 $\mu g/m^3$. The seasonal variation of PM_{10} at all stations was dominated by the spring maximum. A strong influence of traffic on the urban PM_{10} concentrations is shown. However, the highly synchronized day-to-day variation at a variety of sites across the country highlights the role of

large-scale weather patterns also in the formation of spring episodes. Every year, most often in August, September and October, there were also 1–5 irregular regional PM_{10} episodes, lasting from one day to six days and most likely caused by long-range transported particles. During these regional events, the PM_{10} concentrations may well reach the typical spring peak concentration levels.

V Anttila, P., Makkonen, U., Hellén, H., Pyy, K., Leppänen, S., Saari, H., Hakola, H., 2008. Impact of the open biomass fires in spring and summer of 2006 on the chemical composition of background air in south-eastern Finland, Atmos. Environ., 42, 6472–6486.

In the spring and summer of 2006, the air quality in southern Finland was affected by two major biomass fire smoke episodes. At the Virolahti background station, closest to the eastern fire areas, the episodes lasted altogether several weeks. The high point in spring was 25 April and in summer 13 August. In spring the aerosol detected at Virolahti originated at distances of even hundreds of kilometres to the south and south-east, and consequently was a mixture of material from biomass burning and from other sources (both LRT and local), all of which contributed to the detected elevation of PM_{10} concentrations. The elevated concentrations of trace elements (Cd, Pb, Zn) during the most intense biomass fire episode were associated with other anthropogenic emissions.

In contrast, during August 2006, the PM_{10} at Virolahti was quite exclusively impacted by close (ca. 50–100 km) biomass fire sources. The presumably organic component comprised, at its highest, as much as 90% of the total PM_{10}. In addition to record high PM_{10} and $PM_{2.5}$ concentrations, the concentrations of polycyclic aromatic hydrocarbons were considerably elevated, even reaching values more typical of wintertime urban environments. During the peaks of the episodes in August, the total gaseous mercury concentration in the air was more than double its background value. In general, the trace elements did not exceed their background values.

The publications are referred to in the text by their Roman numerals. The publications are reproduced with the permission of the journals concerned.

New but comparable material has also been downloaded from the FMI AQ database and is presented in this thesis.

1 Introduction

Measurements and research of outdoor, ground-level ambient air quality have been made routinely in Finland for many decades. The number of sites and pollutants measured started to expand substantially in the early 1990s following the implementation of the European Union (EU) legislation. The first major instrument was the Air Quality Framework Directive 96/62/EC and its three daughter directives. The directives established standards for pollutants, including sulphur dioxide (SO_2), nitrogen dioxide (NO_2), particulate matter (PM_{10}) and lead (Pb) in 1999; benzene (C_6H_6) and carbon monoxide (CO) in 2000; and ozone (O_3) in 2001. These were later consolidated into the Ambient Air Quality Directive 2008/50/EC (EU, 2008), which set objectives for fine particulate matter ($PM_{2.5}$). Together with Directive 2004/107/EC (EU, 2004, relating arsenic (As), cadmium (Cd), mercury (Hg), and nickel (Ni) and polycyclic aromatic hydrocarbons (PAHs)), the Ambient Air Quality Directive provides the current framework for the control of ambient concentrations of air pollution in the European Union (EU).

In addition to setting the air quality standards, the directives determined the required quantity and quality of mandatory monitoring in relation to the prevailing pollution situation and potentially exposed population as well as details of the required reporting and dissemination of information. The implementation of EU legislation in Finland strongly involved municipalities and industry in air quality monitoring in their own territories, but they also opened it up to nationwide co-operation. Nowadays, municipalities and local industry often perform the necessary monitoring tasks in economic and/or technical co-operation. The Finnish Meteorological Institute is responsible for background air quality monitoring as well as collecting, reporting, assessing and disseminating AQ information at the national level.

The objectives of air quality monitoring (AQM) are typically to establish the levels of exposure (human and/or ecosystem), to ensure compliance with legislation and to demonstrate the effectiveness of control measures. For these purposes, data are summarised as various annual statistics in accordance with the rules of the mandate in question. Such statistics serve to check compliance, but one aspect – long term trends – is not fully covered in this regulatory context.

Understanding the status and developments of air quality is crucial to supporting national air quality management and the implementation of control measures. In this work, long-term, multicomponent, high-resolution (time and accuracy) AQM data available from about 400 Finnish sites since 1994 are utilised to demonstrate past air quality development at the national level.

The focus is on Finland and Finnish monitoring results, but due to the transboundary nature of air pollution, research on a European or even a hemispheric scale is needed.

The objectives of this thesis are

- to aggregate the available long-term AQM data and process them into unified and compact information
- to answer how the air quality in Finland has developed
- to explain which factors are behind the observed air quality development.

2 Material

In Finland, systematic air quality monitoring can be said to have started in the early 1970s with the SO_2, sulphate and TSP measurements at a couple of background sites operated by FMI. In the same decade, first urban networks were also initiated in Helsinki and Oulu. The Air Protection Act of 1982 (67/1982) proclaimed that the municipalities shall see to the necessary air quality monitoring within their territories according to local conditions. The law also included a provision for the establishment of an "Air protection data register" (Ilmansuojelun tietorekisteri) to provide data for the necessary planning, control and research of air protection.

FMI continues to be responsible for the background air quality monitoring (see, e.g. Joffre et al., 1990; Ruoho-Airola, 2004; Makkonen, 2014). From the 1970s to the early 1990s, background monitoring was mainly driven by international research programmes (CLRTAP, EMEP, BAPMoN, EGAP, IM, AMAP, GAW), but from the 1990s onwards, the EU has also become an important actor in background monitoring by setting new components to be monitored and new measurement techniques to be used. In the mid-2000s, monitoring of trace elements, PAHs and Hg was started at three background sites as provided by Directive 2004/107/EC.

Since 2000, the national reference laboratory operated by FMI has been an important quality assurance resource to improve the reliability and comparability of the automatic analysers used in compliance monitoring (Waldén, 2009; Waldén et al., 2004; 2008; 2010; 2015; Walden and Vestenius 2018). In FMI's background network, methods based on the sampling and chemical analyses are widely used. From the beginning, chemical analyses used in the various international programmes were intercompared annually and sampling equipment a couple years later (see, e.g. Karlsson et al., 2007). Sampling and analysis methods of EU compliance monitoring are defined in the directives and are based on CEN or ISO standards. In 1997, the first accreditation of FMI's atmospheric chemistry laboratory was approved.

The air quality data register initiated in 1982 has evolved into the Finnish Air Quality Data Management System (FAQDMS) operated by FMI. This system, among other things, collects the validated air quality monitoring data (and metadata) of the FMI network and urban/industrial monitoring networks since 1973 and 1985, respectively. FMI's AQ archive aggregates Finnish data originating from long-term international research programmes, data that aim to check the compliance with air quality standards, and long-term monitoring data obliged by environmental permits.

Validated data are updated annually and processed and reported to the EU Commission, the EEA (IPR compatible) and other international organisations (e.g. EMEP). The system also processes the (near) real-time data received hourly from the stations and transfers the information to the website (https://en.ilmatieteenlaitos.fi/air-quality) and FMI's INSPIRE-compatible open data service interface (https://en.ilmatieteenlaitos.fi/open-data).

At present, around 30 independent operators (most of them municipalities) perform the compliance AQM in Finland. The biggest of these, FMI and HSY, both have a dozen fixed monitoring sites with comprehensive measurement programmes (ilmatieteenlaitos.fi/seurantamittaukset; hsy.fi/fi/asukkaalle/ilmanlaatu/). These data are also

widely used as supplementary or principal material in scientific works, while the rest of the monitoring data are not as widely exploited for scientific purposes.

The expansion in air quality monitoring is illustrated in Figure 1, which shows the steep increase in the number of continuous hourly measurements starting in the mid-1980s. The figure also reflects changes in the priorities of air quality monitoring during these decades. In 1993, sulphur dioxide levels were monitored at almost one hundred measuring stations, and since then, that number has been cut in half. Meanwhile, the number of size-selective PM mass measurements (PM_{10} or $PM_{2.5}$) has increased from fewer than 30 to over 100.

Over the years, in some cities/communities, AQM has discontinued, owing to the decline of the local smokestack (basic manufacturing/energy production) industries (e.g. Inkoo, Kaskinen, Koverhar, Valkeakoski). The focus has shifted more and more to the monitoring of pollutants generated (directly or indirectly) from vehicular emissions and other small-scale combustion, i.e. NO_x and particles. Such developments have also been enhanced by the increasing focus on the health impacts of air pollution and the role of pollutants in climate change.

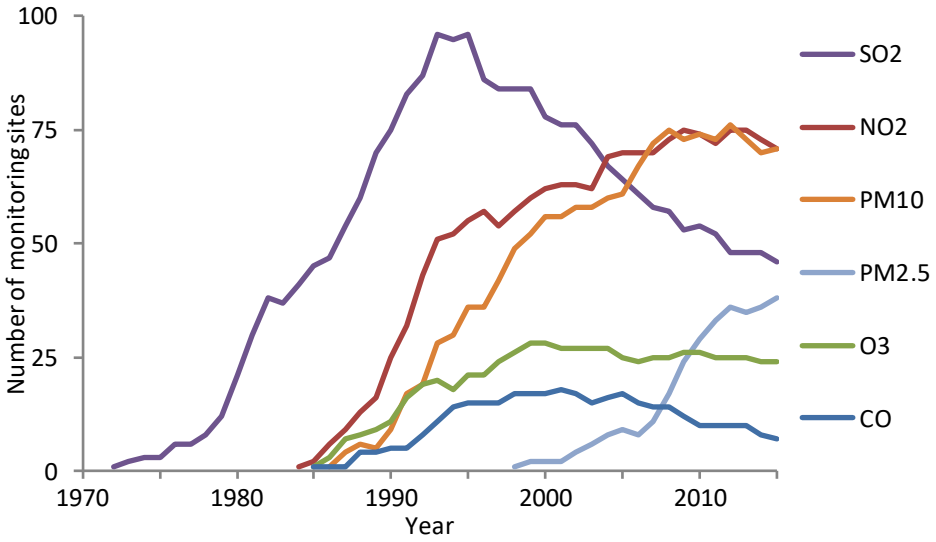

Figure 1. Number of operative air quality monitoring sites per year and per component in Finland.

Kukkonen et al. (1999) published the first review of urban air quality based on the Finnish AQM data from 1990–1993. This work focused on the comparison of concentrations to the national air quality guideline values issued in 1996. Anttila et al. (2003) compiled a summary of the AQM data from 1985–2000. By that time, it had become meaningful to make statistical analyses of air quality trends as well as comparisons to other European cities.

The data in this thesis are measured with European reference methods (or the equivalent) or with the methods determined in the international research programme in question. The set of pollutants is determined by the availability of long-term time series and is restricted to the ones studied in **Papers I**–**V**. Trends of atmospheric heavy metals at a subarctic (Pallas) site during 1996–2018 were presented in a recent paper by Kyllönen et al. (2020).

A summary of the monitoring data included in the original papers of this thesis is shown in Table 1 and the site map in Figure 2.

Table 1. List of the monitoring sites, the chemical species and PM mass size fractions included from each site in **Papers I–V**

Network/ City	Municipality/ Site	NO_2/ NO_x	O_3	SO_2	CO	SIA[1]	WSI[2]	TM[3]	PAH[4]	POP[5]	$PM_{2.5}$	PM_{10}
FMI	Ilomantsi		**I**									
	Raja-Jooseppi		**I**	**I**								
	Utö	**I**	**I**	**I**		**I**						
	Lammi Evo		**I**									
	Pallas		**I**	**I**					**III**	**III**		
	Oulanka		**I**	**I**		**I**						
	Virolahti	**I,V**	**I,V**	**I,V**		**I,V**	**V**	**V**	**V**		**V**	
	Ähtäri	**I**	**I**	**I**								
Harjavalta	Kaleva			**I**								
	Pirkkala			**I**								
	Torttila			**I**								
HSY	Espoo Leppävaara2	**IV**										**IV**
	Espoo Luukki	**I,II**	**I,II**	**I**								**IV**
	Helsinki Kallio1	**IV**										**IV**
	Helsinki Mannerheimint	**II**	**II**									
	Helsinki Töölö	**I,II**	**I,II**		**I**							**I,IV**
	Helsinki Vallila	**I**		**I**	**I**							**I,IV**
	Vantaa Tikkurila2		**I**									
	Vantaa Tikkurila3	**I**			**I**							**I,IV**
Hämeenlinna	Raatihuoneenkatu	**IV**										**IV**
Imatra	Imatra Rautionkylä[6]	**I,IV**		**I**								**I,IV**
	Imatra Teppanala											**I**
	Imatra Mansikkala	**IV**		**I**								**IV**
	Lappeenranta Keskusta	**IV**										**IV**
	Lappeenranta Lauritsala	**I**										
	Lappeenranta Tirilä			**I**								
IVL	Råö (Sweden)								**III**	**III**		
Jyväskylä	Lyseo	**I**		**I**								**I,IV**
Kajaani	Keskusta	**I**										**IV**
Kokkola	Keskusta	**IV**										**IV**
Kotka	Kirjastotalo	**I,IV**										**IV**
Kouvola	Keskusta	**I**										**I,IV**
	Valkeala Lappakoski			**I**								
Kuopio	Kasarmipuisto				**I**							
	Keskusta	**IV**										**IV**
Lahti	Kisapuisto	**I**										
	Vesku	**I**			**I**							
Lohja	Nahkurintori	**IV**										**IV**
Oulu	Keskusta	**I**			**I**							**I,IV**
	Pyyköjärvi	**I**										**I,IV**
	Nokela			**I**								
Pietarsaari	Bottenviksvägen			**I**								**IV**
Pori	Itätulli	**IV**										**IV**
	Lampaluoto			**I**								
Neste	Porvoo Mustijoki	**I**		**I**								
Rauma	Sinisaari			**I**								
Seinäjoki	Vapaudentie	**I**										

Network/ City	Municipality/ Site	NO_2/ NO_x	O_3	SO_2	CO	SIA[1]	WSI[2]	TM[3]	PAH[4]	POP[5]	$PM_{2.5}$	PM_{10}
Tampere	Lielahti[6]	**I**										
Turku	Naantali Keskusta	**IV**										**IV**
	Raisio Keskusta	**I**										**I,IV**
	Raisio Kaanaa			**I**								
	Turku Kauppatori	**I**										**I,IV**
Varkaus	Pääterveysasema	**IV**										**I,IV**

[1] Secondary inorganic aerosols: SO_4^{2-} (p), NO_3^- (g+p), $NH4^+$ (g+p)
[2] Water-Soluble Inorganic Ions: Na^+, K^+, Mg^{2+}, Ca^{2+}, Cl^-
[3] Trace Metals: Hg (g), Al, As, Cd, Co, Cr, Cu, Fe, Mn, Ni, Pb, V, Zn
[4] Polycyclic aromatic hydrocarbons (g+p): Phe, Ant, Fl, Pyr, BaA, Chr, BbF, BkF, BaP, DhA, BP, IcP
[5] Persistent organic pollutants (g+p): polychlorinated biphenyls (seven PCB congeners), organochlorine pesticides (α- and γ-HCH, chlordanes, DDT, DDE, DDD)
[6] no NO_x

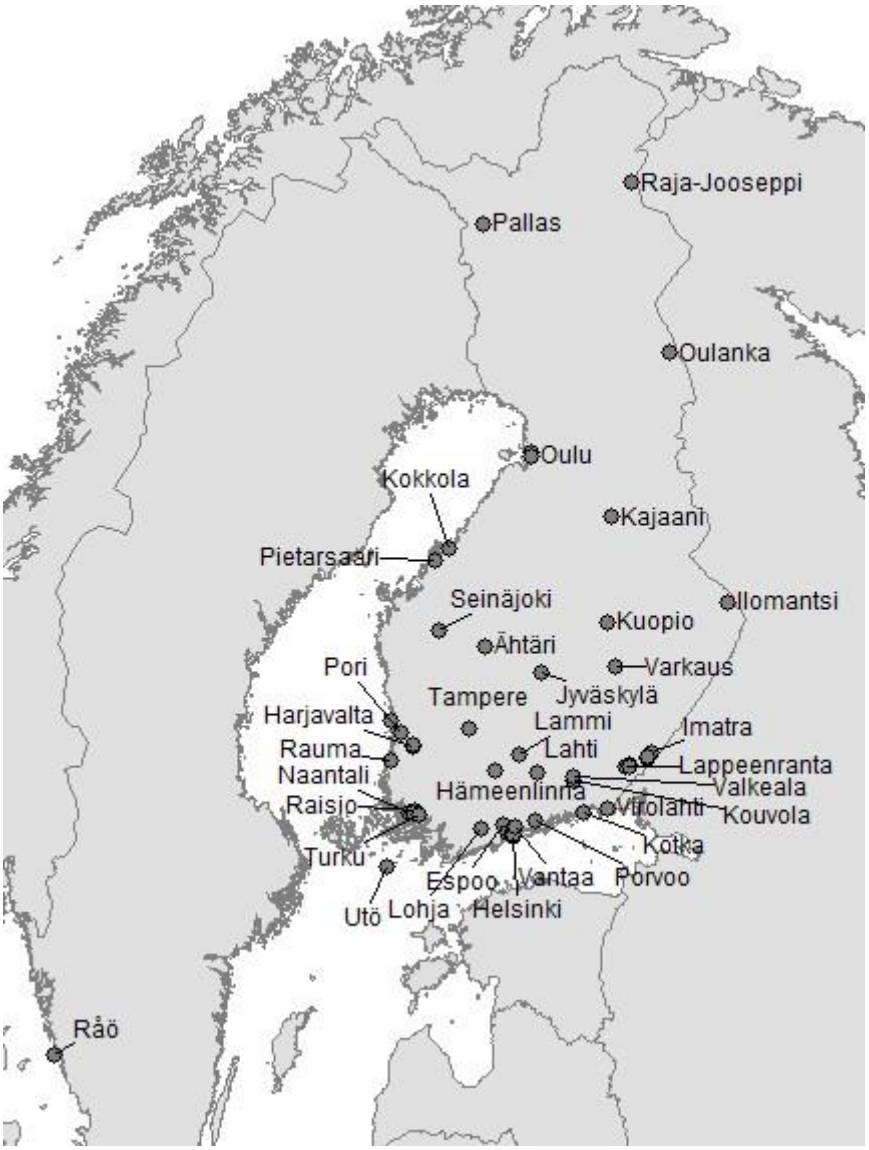

Figure 2. Locations of the air quality monitoring sites in **Papers I**–**V**.

3 Data analysis method

3.1 Generalised least squares (GLS) regression with ARMA errors

The generalised least squares regression with ARMA errors (GLS-ARMA) method is essential time series analysis method in **Papers I** and **III**.. A light methodological background and practical implementation of the method is presented here. Chapters 3.1.1 and 3.1.2 are based on the general time series analysis framework presented, e.g. by Hamilton (1994) and Brockwell and Davies (2002). The application of the method is demonstrated in chapter 3.1.3.

3.1.1 Generalisation of ordinary least squares regression

In standard linear regression, the errors (or residuals of the fit) are assumed to be independent and identically distributed (iid) (Hamilton, 1994). In an air quality time series, this assumption is typically violated due to cyclic dependencies (e.g. diurnal, seasonal) in the observed data. Generalised least squares (GLS) regression with ARMA errors extends the ordinary least squares (OLS) estimation of the linear model by providing for possible correlations between different residuals and for possibly unequal residual variances (Brockwell and Davis, 2002; Hamilton, 1994).

Let us first consider the ordinary least squares (OLS) regression model in matrix form,

$$y = X\beta + \varepsilon \quad , \qquad \text{(Eq. 1)}$$

where y is the vector of n observations of some random variable Y at times $t = 1,\ldots, n$, (y is a nx1 matrix). X is the design matrix of the explanatory variables (non-stochastic); its columns can be, e.g. any function of time t. β is the vector of regression coefficients and ε is the vector of random errors (nx1). The goal is to obtain the OLS estimators $\hat{\beta}_{\mathrm{OLS}}$ of vector β, so that

$$y = X\hat{\beta}_{\mathrm{OLS}} + e \ , \qquad \text{(Eq. 2)}$$

where e is the residual vector (nx1) of the OLS fit.

The OLS estimator $\hat{\beta}_{\mathrm{OLS}}$ minimises the sum of squared residuals (prime denotes the transpose)

$$\sum e_t^2 = e'e = (y - X\hat{\beta}_{\mathrm{OLS}})'(y - X\hat{\beta}_{\mathrm{OLS}}) \ . \qquad \text{(Eq. 3)}$$

Expanding this out, differentiating with respect to $\hat{\beta}_{\mathrm{OLS}}$ and setting to zero, we find that

$$\hat{\beta}_{\mathrm{OLS}} = (X'X)^{-1}X'y, \qquad \text{(Eq. 4)}$$

i.e. the OLS coefficients can be calculated as a function of data matrix X and observation vector y.

To find the "significance" of the trend, we need to determine the standard error (SE) of the slope coefficient, i.e. one of the terms of the OLS estimator $\hat{\beta}_{\mathrm{OLS}}$. For this, we need to make use of the iid assumptions of the residuals of this OLS fit; $e_t \sim \mathrm{N}(0, \sigma^2 I)$, where σ^2 is the true error variance and I is the identity matrix.

The variance of any random variable is the expectation of the squared deviation of its expected value. For the random vector $\hat{\beta}_{\mathrm{OLS}}$,

$$\mathrm{Var}\,\hat{\beta}_{\mathrm{OLS}} = \mathrm{E}\left[\left(\hat{\beta}_{\mathrm{OLS}} - \mathrm{E}(\hat{\beta}_{\mathrm{OLS}})\right)\left(\hat{\beta}_{\mathrm{OLS}} - \mathrm{E}(\hat{\beta}_{\mathrm{OLS}})\right)'\right] \quad , \qquad \text{(Eq. 5)}$$

where E stands for the expected value.

After some matrix calculus (not shown), we get

$$\mathrm{Var}\,\hat{\beta}_{\mathrm{OLS}} = (X'X)^{-1}X'\mathrm{E}(ee')X(X'X)^{-1} \quad . \qquad \text{(Eq. 6)}$$

The term $\mathrm{E}(ee')$ is the covariance matrix of e which, under OLS assumptions ($e_t \sim \mathrm{N}(0, \sigma^2 I)$ is $\mathrm{E}(ee')=\sigma^2 I$ and (Eq. 6) reduces to

$$\mathrm{Var}\,\hat{\beta}_{\mathrm{OLS}} = \sigma^2(X'X)^{-1} \text{ and SE } \hat{\beta}_{\mathrm{OLS}} = \sigma\sqrt{(X'X)^{-1}} \quad . \qquad \text{(Eq. 7)}$$

The true error variance σ^2 is unknown, but it is estimated based on the regression residuals (mean squared error)

$$\hat{\sigma}^2 \sim \frac{1}{n-2}\sum_{t=1}^{n} e_t^2 \quad . \qquad \text{(Eq. 8)}$$

This is where the OLS method goes: statistical packages give the regression parameters from (Eq. 4) and estimates of the standard errors from (Eq. 7) and (Eq. 8).

If residual errors are not independent and identically distributed (iid), we need a specification of how the dependence varies with time. This dependence can be parameterised in the variance–covariance matrix and can be fitted by generalised least squares (GLS). In this case, the residual covariance matrix term in (Eq. 6) is $\mathrm{E}(ee') = \mathrm{Cov}(e) = \Gamma$, where Γ is any matrix so that $e_t \sim \mathrm{N}(0, \Gamma)$. Different diagonal entries in Γ correspond to non-constant error variances, while nonzero off-diagonal entries correspond to correlated errors.

The GLS solution lies in transforming the original linear regression model to $y^* = X^*\beta + e^*$ so that we can then estimate the $\hat{\beta}$ matrix by OLS on the transformed variables, i.e.

$$\mathrm{Cov}(e^*) = \mathrm{E}(e^* e^{*\prime}) = \sigma^2 I \quad . \qquad \text{(Eq. 9)}$$

For this, we define matrix T so that

$$T'T = \sigma^2 \Gamma^{-1} \text{ and hence (not shown) } T\Gamma T' = \sigma^2 I \; . \qquad \text{(Eq. 10)}$$

If we now multiply (Eq. 2) by matrix T, we get

$$Ty = TX\beta + Te \quad , \qquad \text{(Eq. 11)}$$

a regression equation with coefficient vector β, data vector Ty, design matrix TX, and error vector Te. The covariance matrix of the transformed error term will be

$$\begin{aligned} \text{Cov}\,(Te) &= \text{E}(Te(Te)') \\ &= T\text{E}(ee')T' \\ &= T\Gamma T' = \sigma^2 I\,, \end{aligned} \qquad \text{(Eq. 12)}$$

so the transformed model (Eq. 11) has uncorrelated, zero mean errors, each with variance σ^2. The estimator of β in terms of Ty can be obtained by applying an OLS estimation to the transformed regression equation (Eq. 11). This gives the generalised least squares (GLS) estimator $\hat{\beta}_{\text{GLS}}$

$$\hat{\beta}_{\text{GLS}} = \left(X'\Gamma^{-1}X\right)^{-1}X'\Gamma^{-1}y \qquad \text{(Eq. 13)}$$

with the covariance matrix

$$\text{Cov}\,\hat{\beta}_{\text{GLS}} = \left(X'\Gamma^{-1}X\right)^{-1} \quad . \qquad \text{(Eq. 14)}$$

The error covariance matrix Γ is not known, and it must be estimated from the data along the regression coefficients, e.g. by the maximum likelihood method; for this, further restrictions are needed due to too many elements in Γ ($n(n+1)/2$).

In our case (and more generally, in time series data), after transformations, the error e_t terms are already stationary. But they are serially correlated, and the covariance of two errors depends only upon their separation in time: voilà, this is exactly what ARMA processes can provide.

3.1.2 Autoregressive moving-average (ARMA) models

Autoregressive moving-average (ARMA) models (e.g. Hamilton, 1994; Brockwell and Davies, 2002) provide a commonly used description of a stationary time series e_t in terms of two polynomials: one describes the value of the time series as a function of its lagged values (this is the so-called autoregressive (AR) part), and the second describes the effect of lagged random terms (the moving average (MA) part).

The ARMA(p,q) process is defined as

$$e_t = \phi_1 e_{t-1} + \ldots + \phi_p e_{t-p} + Z_t + \theta_1 Z_{t-1} + \ldots + \theta_q Z_{t-q} \quad , \qquad \text{(Eq. 15)}$$

where ϕ_i, i=1,…, p and θ_j, j=1,..., q are constants and $Z_t \sim \text{WN}(0, \sigma^2)$; p is the number of autoregressive parameters, and q is the number of moving-average parameters (Brockwell and Davis, 2002).

The next step is to find the most satisfactory ARMA(p, q) model to represent the residual series e_t in order to eliminate the remaining dependencies and finally get the white noise error terms. The parameters ϕ_i, i=1,…, p and θ_j j=1,..., q are estimated with the maximum likelihood method. The selection of the parameters p, q is based on the bias-corrected Akaike information criterion (AICC) (Akaike, 1973; Hurvich and Tsai, 1989). All combinations of p and q (within the pre-set ranges) are walked through, and the combination of p and q values that returns the maximum likelihood model with the smallest AICC value is chosen.

So, we build the error covariance matrix with the ARMA processes and estimate the unknown parameters ($\hat{\phi}_i$, $\hat{\theta}_j$, $\hat{\beta}_{\mathrm{GLS}}$) using the maximum likelihood method.

3.1.3 Application of GLS-ARMA in AQ trend analysis

The purpose of trend testing is to determine whether the values of a random variable generally increase (or decrease) over some period in statistical terms. The concentrations of airborne pollutants are our random variables C_t, and the observed concentrations c_t are the realisation of these variables. The time resolution of our original data (**Papers I** and **III**) varied from one hour to one week, but all data have been averaged to monthly means, resulting in a time series with consecutive measurements taken at equally spaced time intervals; the independent variable, time t, gets the values from 1 to n. The Windows-based computer package ITSM2000 (B and D Enterprises, Inc. 7.3 (Professional) Oct 1, 2005) was used in the computations.

The application of the method is demonstrated with the help of diagnostic plots from an example: the monthly time series of NO_2 concentrations at Oulu Keskusta station in 1994–2007 (**Paper I**) with the extension of new data up to the end of 2015 (n = 168 + 96 monthly values) (Figure 3).

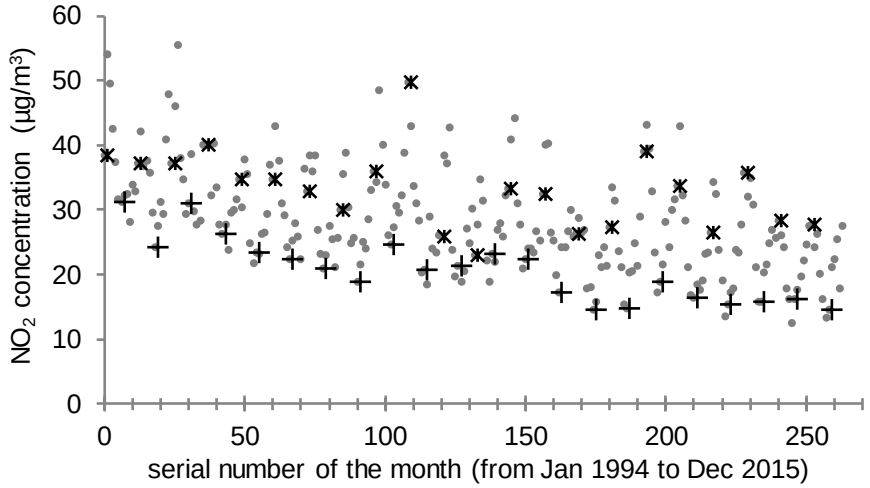

Figure 3. Scatterplot of the monthly mean concentrations of NO_2 at Oulu Keskusta station in 1994–2015. January and July values are denoted with stars and crosses, respectively.

The trend analysis begins with the examination of the detected time series (c_t) plot. The plot (Figure 3) reveals that there are no obvious exponential changes or heteroscedasticity (strongly increasing or decreasing variance), which suggests that a linear model could be appropriate. We

also see seasonal variation (concentrations are systematically higher in winter months) and trend (decreasing mean) patterns (Figure 3).

Before introducing the GLS-ARMA, we do a preliminary transformation of the observed time series c_t; seasonal adjustment is needed as most of the ambient air pollutants have a strong seasonal variation. This is done here by applying a moving average filter to c_t, calculating the monthly indices and subtracting them from the original time series c_t (see details in **Paper I**).

Now, the deseasonalised time series c_t^{ds} becomes our dependent variable, and we fit an OLS line, $c_t^{\mathrm{ds}} = \hat{\beta}_1 + \hat{\beta}_2 t + e_t$, where $\hat{\beta}_1$ and $\hat{\beta}_2$ are the regression parameters and e_t are the residuals of this fit to this remaining time series (Figure 4a). Now, we have the OLS approximation of the regression parameters (Eq. 4) and their standard errors (in parentheses) (Eq. 7 and (Eq. 8),

$$\hat{\beta}_1 = 34.88(0.5164) \text{ and } \hat{\beta}_2 = \text{-}0.05175(0.003378) \quad . \qquad \text{(Eq. 16)}$$

It is time to study the residuals e_t of this fit. In a valid regression model, the residuals need to be independent and identically distributed (iid), i.e. normally distributed with a zero mean and constant variance and not serially autocorrelated. So, the residuals must be investigated for the normality, homoscedasticity and autocorrelation to ensure the appropriateness of our linear regression model. This can be done using descriptive plots and formal statistical tests.

Figure 4b suggests that residuals e_t now have ~zero mean and constant variance; both Breusch–Pagan and White tests suggest homoscedasticity with *p*-values 0.084 and 0.225, respectively. Figure 4c shows that residuals are moderately close to normal distribution; the Kolmogorov–Smirnov test does not reject normal distribution, while the Jarque–Bera and Shapiro–Wilk tests reject normality assumption. We conclude that the deviation from normality is so small that we continue with the selected model.

However, the sample autocorrelation function in Figure 4d displays high autocorrelations of the residuals e_t up to a lag of five months. Hence, our residual sequence e_t is not (yet) iid, and we must introduce additional terms – ARMA processes – into our model to account for the autocorrelation.

We can then use the ARMA processes to model the remaining dependences (autocorrelation) of the residuals and finally use them (ARMA processes) in conjunction with the trend to re-estimate the parameters (and standard errors) of the original model.

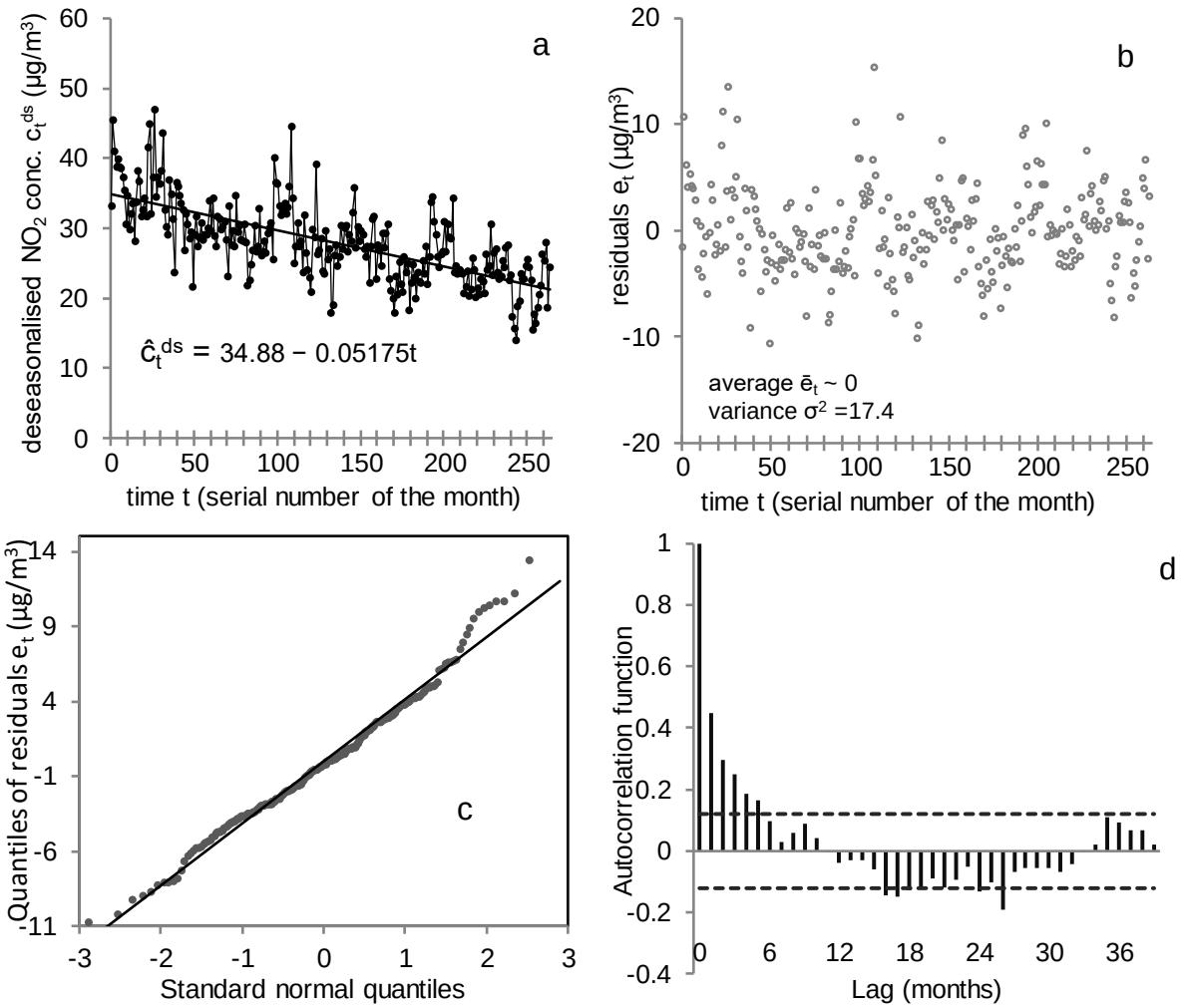

Figure 4. (a) seasonally adjusted c_t^{ds} together with the fitted OLS line $\hat{c}_t^{\text{ds}}$, (b) residual e_t time series, (c) a quantile-quantile plot of a the residuals e_t versus the standard normal quantiles with an OLS line as a reference, and (d) the autocorrelation plot of the residuals e_t (the horizontal lines are the 95% confidence level bounds).

Next, we fit the maximum likelihood ARMA(p, q) values for all p and q (in a specified range) and select from these the model with the smallest AICC value. In ITSM software, the maximum likelihood estimation of the ARMA(p, q) model is based on the innovation algorithm (see Brockwell and Davies, 2002).

In our example, the minimum AICC model for the OLS regression residuals e_t turns out to be an ARMA(1,1) model with $\hat{\phi}_1 = 0.7331$, $\hat{\theta}_1 = -0.3747$. Thus, our new model for c_t^{ds} is

$$\begin{aligned} c_t^{\text{ds}} &= 34.88(0.5164) - 0.05175(0.003378)t \\ &+ 0.7331(0.09079)e_{t-1} + Z_t - 0.3747(0.1279)Z_{t-1} \end{aligned}, \qquad \text{(Eq. 17)}$$

where $Z_t \sim \text{WN}(0, 13.564996)$.

Next, both the ARMA parameters ($\hat{\phi}$ and $\hat{\theta}$) and the regression coefficients ($\hat{\beta}$) are reestimated with the maximum likelihood estimation. MLE is repeated until all parameters are

stabilised. After several iterations, we arrive at the final model with the following maximum likelihood estimators (the standard errors in parentheses):

$$c_t^{ds} = 34.92(1.044) - 0.05177(0.006803)t + 0.7332(0.09076)e_{t-1} + Z_t - 0.3748(0.1279)Z_{t-1} \quad \text{(Eq. 18)}$$

and $Z_t \sim \text{WN}(0, 13.5648)$.

The residuals of this GLS-ARMA model are (Brockwell and Davis, 2002)

$$\hat{e}_t^{\text{GLS-ARMA}} = (e_t - \hat{e}_t)/\sqrt{r_{t-1}} \ , \quad \text{(Eq. 19)}$$

where $\hat{e}_t$ is a one-step predictor of e_t, $r_{t-1} = \text{E}(e_t - \hat{e}_t)^2/\sigma^2$ and σ^2 is the white noise variance of the fitted model.

The next step is to check the model for goodness of fit. The statistical confidence intervals for the zero autocorrelation (null hypothesis) are estimated as follows: For iid noise ~N(0, σ^2), the sample autocorrelations are approximately iid N(0,1/*n*) for large *n* (see, e.g. Brockwell and Davis, 2002). Hence, approximately 95% of the autocorrelations should fall between the bounds $\pm 1.96/\sqrt{n} = \pm 0.12$ (since 1.96 is the 0.975 quantile of the standard normal distribution, and *n* is 264).

While the OLS residuals e_t failed to meet the iid assumptions (due to autocorrelation; see Figure 4d), the ACF of the GLS-ARMA residuals $\hat{e}_t^{\text{GLS-ARMA}}$ shows that all but one of the 40 sample autocorrelations calculated fall between the 95% bounds, and there is no cause to reject the fitted model based on the autocorrelations (see Figure 5). (Other tests of randomness were comparable to previously presented OLS residual tests.)

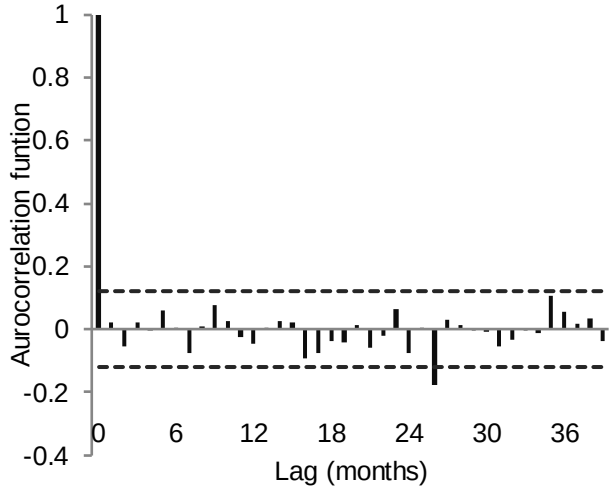

Figure 5. ACF plot of the residuals $\hat{e}_t^{\text{GLS-ARMA}}$. The horizontal lines are the 95% confidence level bounds.

Next, we decide whether there is a statistically significant trend. The null hypothesis H0 (no trend, i.e. slope is zero) is tested against the alternative hypothesis H1 where there is a trend (slope $\neq 0$).

Estimated 95% confidence bounds for the slope using this GLS-ARMA estimate are slope ± 1.96 x standard error = −0.0518 ± 1.96 x 0.0068 = (−0.0651, −0.0384). Zero does not belong to this interval, and we reject the null hypothesis and conclude that there is a significant decreasing trend in our time series at a 95% confidence level.

The final trend equation, with standard errors, is

$$\hat{c}_t^{\mathrm{ds}} = ((34.9 \pm 1.0) - 0.0518 \pm 0.0068)t \quad . \qquad \text{(Eq. 20)}$$

If we had settled for the OLS (Eq. 16) instead of GLS in this example, the standard error estimates of the slope and intercept would have been about half of the resulting GLS estimates (Eq. 20). So, ignoring the autocorrelation of the residuals would have led to an underestimation of the standard errors – and an overestimation of the significance. But on the other hand, both methods would have suggested a decreasing trend even at a 99.9% confidence level.

In **Paper I**, the slopes and significance of the trends calculated with the GLS-ARMA method were compared with three other trend analysis methods, i.e. deseasonalised monthly OLS regression, annual OLS regression and annual non-parametric Sen's slope and the Mann-Kendall significance test (Salmi et al., 2002).

4 Results

In **Paper I**, the atmospheric concentration time series of the main inorganic gases, secondary inorganic ions and PM_{10} mass from 42 Finnish rural, urban or industrial AQM sites (Table 1) between 1994 and 2007 were analysed with GLS-ARMA for potential trends. Analogously, in **Paper III**, the long-term temporal trends of 27 persistent organic pollutant species from 1996 to 2011 from two Scandinavian rural background sites (Råö and Pallas) were investigated (Table 1). **Paper II** accompanies **Paper I** by focusing on the urban NO_x anomaly in more detail. **Papers IV** and **V** are case studies that provide supportive material for the AQ trend analysis.

4.1 Sulphur dioxide (SO_2) and sulphate (SO_4^{2-}) trends

In Europe, the abatement of long-range transboundary air pollution started under the United Nations Economic Commission for Europe (UNECE) in 1979 with the signature of the Convention on Long-range Transboundary Air Pollution (CLRTAP) by 32 governments and the European Community. The first sulphur protocol under the CLRTAP was adopted in 1985 (UNECE, 1985). The acidification of ecosystems was the main driving force for SO_2 emission abatement in Europe in the 1980s (see, e.g. Kauppi et al., 1990). The timing and implementation of emission reductions varied between countries, but the major reduction measures generally included the shift to cleaner, low-sulphur fuels, the adoption of flue gas desulphurisation and advances in technologies and industrial processes (Crippa et al., 2016; Vestreng et al., 2007). Rafaj et al. (2014) emphasise the role of reduced energy intensity (energy/GDP) in SO_2 emission reduction. In Finland, SO_2 emission reduction was enhanced by a comprehensive legislative package approved by the government in 1987, which limited the maximum allowed sulphur content of light and diesel oil and coal as well as SO_2 emissions in heavy oil and coal-fuelled power plants, the pulp industry, sulphuric acid plants and oil refineries (e.g. Huutoniemi et al., 2006).

As a result, in Finland as in the whole of Europe, SO_2 emissions have been declining for over 40 years now (Vestreng et al., 2007; Crippa et al., 2016; EEA, 2018). These reductions of SO_2 emissions were reflected in the decreasing ambient SO_2 (-3% to -8%/yr) concentrations at 15 sites during the study period, 1994–2007 (**Paper I**). Comparable downward trends have been reported in both urban and rural environments in Europe (Jones and Harrison, 2011; Henschel et al., 2013; Guerreiro et al., 2014; Crippa et al., 2016; Tørseth et al., 2012; Colette et al., 2016) and in Finland (Ruoho-Airola et al., 2015; Riuttanen et al., 2013; Nieminen et al., 2014). Aas et al. (2019) report that an average reduction in SO_2 concentrations was -5.03%/yr (STD=2.04; *n*=20) in European background areas between 1980 and 1990 and -7.56%/yr (1.81; 43) and -4.23%/yr (3.17; 51) in 1990−2000 and 2000−2010, respectively.

Figure 6 summarises all the Finnish SO_2 monitoring data available at the FAQDMS since 1987. After removing years with data captures below 70%, the data set contained 1406 individual annual values from 201 separate sites. Caution is required when averaging data from a monitoring network containing multiple time series of variable durations. Movement, opening and closing of monitoring sites may introduce biases into the average trend. However, an aggregate view of the overall changes in concentrations offers an interesting perspective.

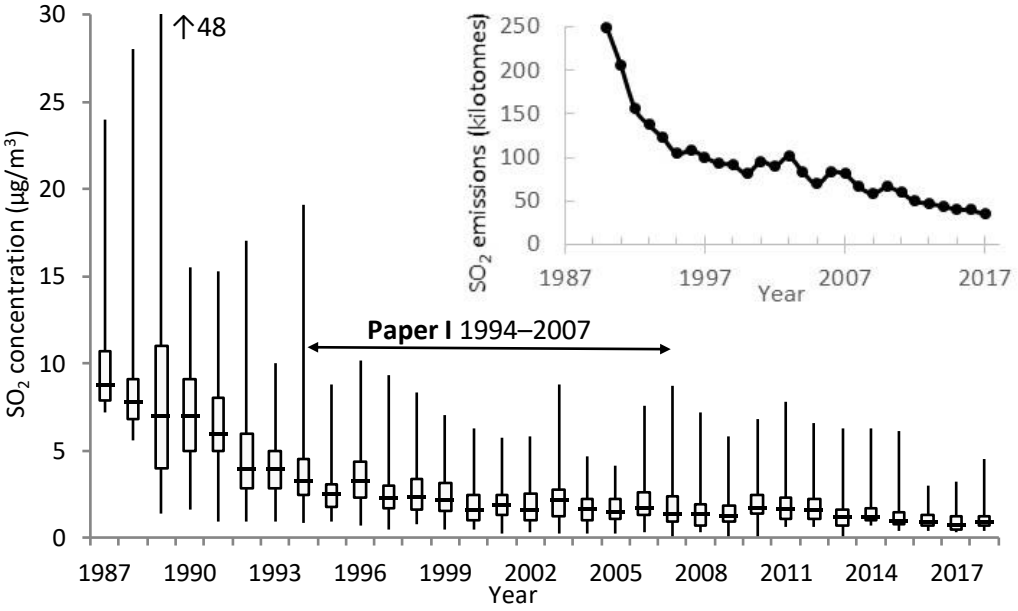

Figure 6. Distribution of annual mean concentrations of SO_2 measured at the Finnish monitoring sites in 1987−2018. At least a 70% annual data capture was required for each site and year. For each year, the lowest, highest and median values together with the 25th and 75th percentile values (box) are shown. The number of sites included varies from 6 in 1987 to 76 in 1993, and after that, there is a gradual decrease to 36 sites in 2018. A total of 1406 annual values were included. The subplot shows the development of the annual SO_2 emissions in Finland (SYKE, 2019a).

Figure 6 demonstrates the steepest decline in SO_2 concentrations in the late 1980s and early 1990s and a moderate decrease in 1994–2007 (**Paper I**). Overall, SO_2 concentration levels are lower now than 10 years ago, but the decline has not been as straightforward as anticipated in **Paper I**. The high end of the SO_2 concentration distribution nowadays (2016–2018) is occupied by industrial monitoring sites in Harjavalta, Imatra, Kokkola, Lappeenranta, Porvoo and Raahe. The annual means of SO_2 have varied (2016–2018) between 2–5 µg/m^3, and hourly values have occasionally reached maximums of 1000 µg/m^3. European air quality standards are not exceeded anywhere.

In Finnish background areas, the SO_2 concentration level is around 0.5–1 µg/m^3. Nowadays (2016–2018) in Finnish background areas, the lowest SO_2 concentrations (hourly, daily, annual) are observed at Utö, and the highest are in northernmost Lapland (Raja-Jooseppi and Kevo) under the influence of the ongoing and still partly obscure emissions in the Kola Peninsula (e.g. Prank et al., 2010). On the other hand, the worst SO_2 episode of the last decade in Lapland was due to the volcanic plume coming from the Icelandic Holuhraun fissure eruption in September 2014 (Ialongo et al., 2015). The highest SO_2 hourly values were 188 µg/m^3, 172 µg/m^3 and 88 µg/m^3 at Pallas/Sammaltunturi, Oulanka and Raja-Jooseppi, respectively.

As of 1 January, 2015, the stricter Sulphur Emission Control Area (SECA) regulations (IMO, 2008; EU, 2016) came into force in the North Sea and the Baltic Sea, reducing the maximum sulphur content allowed in marine fuels from 1.0% to 0.1%. By means of three chemical transport models, Karl et al. (2019) estimated that in Finnish southern coastal areas in the pre-SECA conditions (2012), the contribution of ship emissions to the SO_2 concentrations was around 0.2–0.5 µg/m^3. Indeed, at Utö, the difference between the observed daily SO_2 means in the pre-SECA period, 2012–2014 (0.72 ±0.70 µg/m^3), and the post-SECA period, 2015–2017

(0.4 ±0.4 µg/m^3), was -0.3 µg/m^3 ($p<0.0001$). A similar stepwise reduction is also clearly visible in the SO_4^{2-} concentrations (Figure 7).

In the atmosphere, gaseous SO_2 becomes oxidised to form particulate sulphate (SO_4^{2-}). Figure 7 assembles the monthly time series of SO_4^{2-} concentrations at FMI's three monitoring stations between 1994 and 2018. At the beginning of 2007, the change of the main ions' sampling method was introduced (Ruoho-Airola et al., 2015), so the demonstrative OLS lines are drawn in two parts (Figure 7). The decrease in concentrations has also continued after 2006, the end of the study period in **Paper I**.

For SO_4^{2-}, Aas et al. (2019) gave a European average trend of -2.67%/yr (2.03; 36) for the 2000–2015 period, which is in line with the Finnish observations (-2% to -3%/yr in 1994–2006) reported in **Paper I**.

Since the late 1970s, the European-wide co-operation to tackle acid rain and its impacts on ecosystems has been followed by a number of policies (both under the EU and the UN) that either directly or indirectly act to reduce SO_2 emissions. Through these actions, SO_2 emissions, acid rain and ecosystem impacts have decreased (see, e.g. Grennfelt et al., 2019). Simultaneously, marked sulphur-related air quality improvements have been achieved, and the protection of human health from air pollution has substantially benefitted.

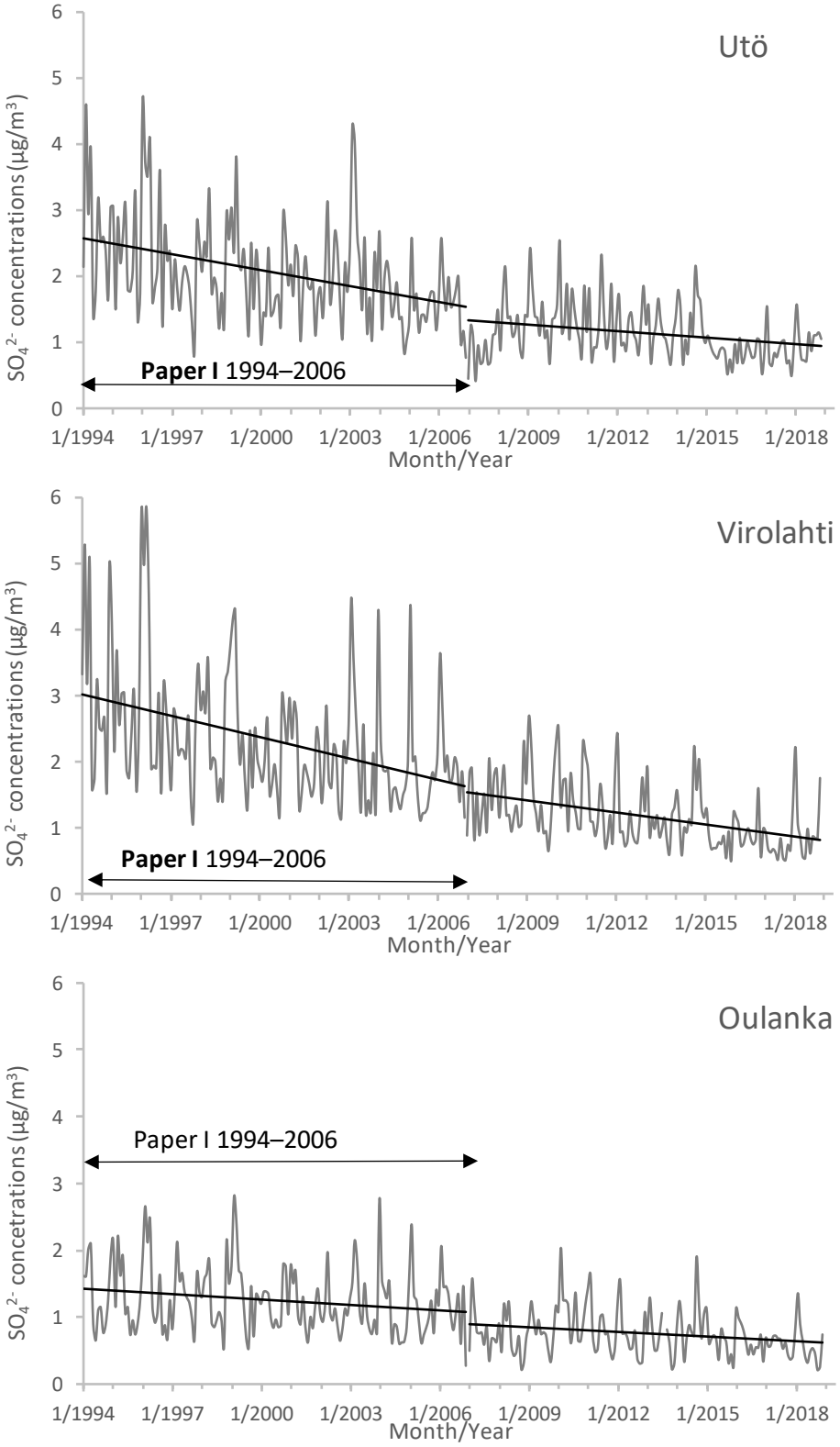

Figure 7. Monthly time series of SO_4^{2-} concentrations at Utö, Virolahti and Oulanka in 1994–2018. OLS lines are drawn for visualisation.

4.2 Nitrogen oxides (NO_x) trends

As in the case of SO_2, the control of NO_x ($NO+NO_2$) emissions was agreed under the UNECE in 1988 (UNECE, 1988); only stabilisation was mandated. In Europe, a major step

forward in limiting road transport emissions was the introduction of the first of the so-called Euro emission standards, Euro 1, in 1992. In practice, then, a three-way catalytic converter (TWC) became mandatory in all new petrol vehicles. TWCs reduce the emission of the three primary pollutants NO_x, CO and VOCs. The introduction of TWCs to petrol cars has reduced these emissions significantly in Finland (Table 2) and in Europe (Guerreiro et al., 2014; EEA, 2018).

Table 2. Annual anthropogenic emissions of NO_x, CO and VOC in Finland in 1994 and 2017 (SYKE, 2019b).

	Finnish anthropogenic emissions (1000 tonnes)				Reduction	
	1994		2017		%	
	total	traffic	total	traffic	total	traffic
NO_x	293	179	130	58	56	68
CO	700	490	379	141	46	71
VOC	208	101	89	15	57	85

In **Paper I,** the concentration time series of NO_2 and NO_x from 22 and 20 monitoring sites during 1994–2007 (Table 1) were studied. Half of the NO_2 time series displayed a statistically significant decreasing trend, while as much as 70% of the studied NO_x time series were decreasing. The typical annual reductions were 1–2% and 3–5% for NO_2 and NO_x, respectively, typically occuring in traffic-influenced environments. During the same period, the national total NO_x emissions and road traffic emissions were reduced by 2% and 5%, respectively, so the decrease in NO_x concentrations was generally consistent with the national NO_x emission data (**Paper I**).

Figure 8 summarises the Finnish NO_2 and NO monitoring results up to 2018. Visually, the downward trends of NO_2 have continued throughout the 1994–2018 period. Statistically, the trends were decreasing (OLS, *t*-test, $p<0.001$) for all percentiles except the time series consisting of the highest annual means. Also, the post-2007 trends were decreasing ($p<0.05$) apart from the minimum time series. Analogously, NO concentrations (Figure 8) decreased throughout the whole period ($p<0.01$ for all studied percentiles), while the post-2007 trends were decreasing but were not statistically significant ($p>0.05$).

The air quality directive (EU, 2008) sets two limit values for NO_2 for the protection of human health: the NO_2 hourly mean value may not exceed 200 µg/m^3 more than 18 times in a year, and the NO_2 annual mean value may not exceed 40 µg/m^3; both are to be met from 2010 onwards. In Finland, the hourly limit value of NO_2 is not critical, but the annual limit value was exceeded beyond 2010 in the busiest street canyons in Helsinki. Since 2016, the annual limit value of NO_2 has not been exceeded at any monitoring station.

During 1994–2017, Finnish total and traffic NO_x emissions decreased by 56% and 68%, respectively (Table 2). At the same time, NO concentrations decreased by 80% (calculated from the medium values in Figure 8) and NO_2 concentrations by 50%. In the past twenty years or so, the NO_2 concentrations have been decreasing, albeit slower than NO_x emissions and NO concentrations, and nowadays, the air quality standards for the protection of human health are not exceeded (since 2016).

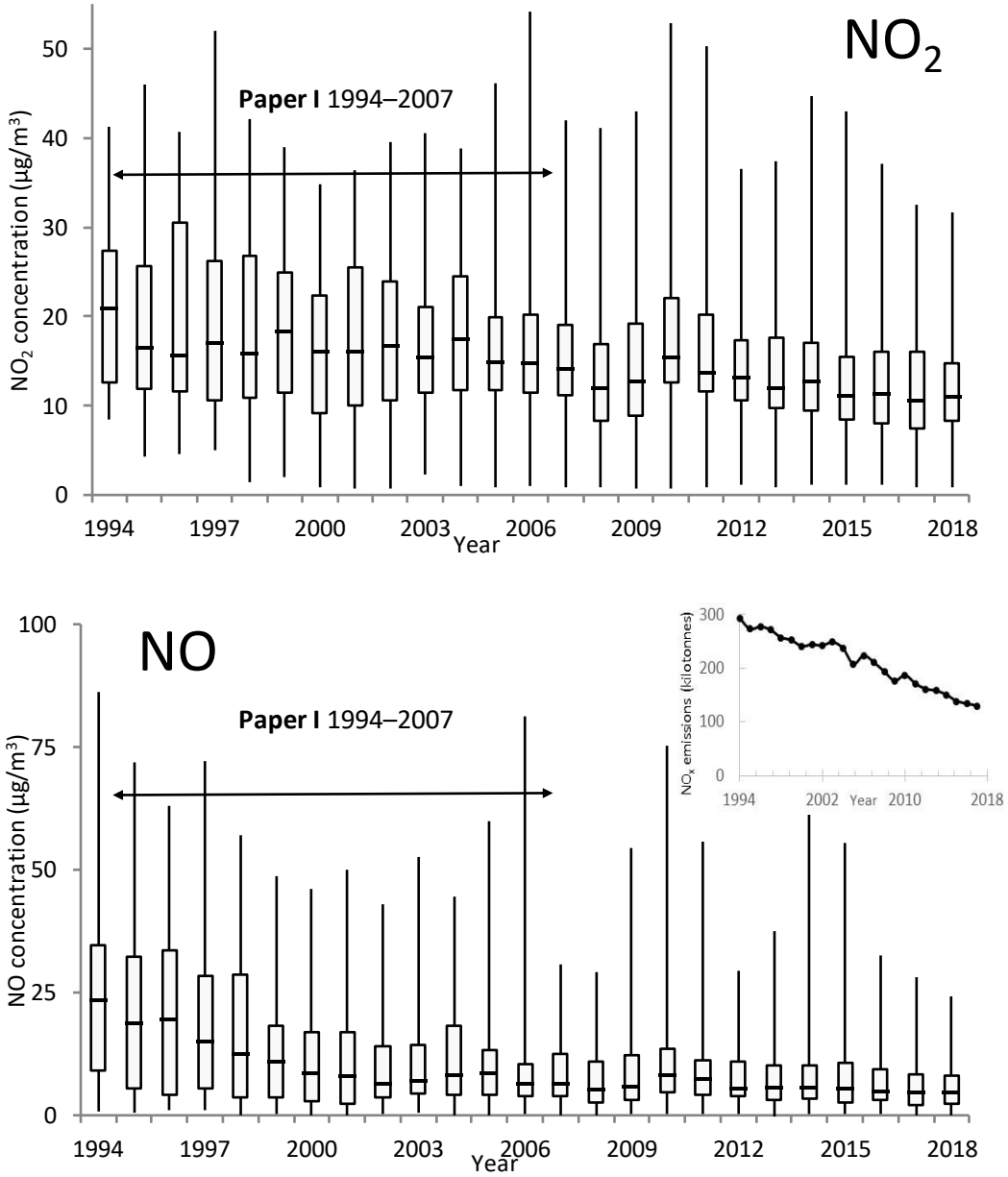

Figure 8. Distribution of annual mean concentrations of NO_2 and NO (lower) measured at the Finnish monitoring sites in 1994−2018. At least a 75% annual data capture was required for each site and year. For each year, the lowest, highest and median values together with the 25th and 75th percentile values (box) are shown. The number of sites included varies from 26 (NO 26) in 1994 to 59 (55) in 2018, the total number of sites being 209 (205). A total of 1326 (1271) annual values were included. The subplot shows the development of the annual NO_x emissions in Finland (SYKE, 2019b).

Primary NO_2 emission trend

Despite the considerable NO_x emission reductions, in many larger European cities, the urban traffic/roadside NO_2 concentrations have not decreased as expected or have stabilised or even increased, and NO_2 air quality standards are widely exceeded (e.g. Guerreiro et al., 2014; Henschel et al., 2015; Grange et al., 2017). This discrepancy has been attributed largely to the increasing usage of diesel vehicles in Europe and the increase in directly emitted tailpipe NO_2.

Already in the early 2000s, Carslaw and Beevers (2004) and Carslaw (2005) suggested that the detected increase in the ambient NO_2/NO_x concentration ratio in London is related to the increase in the NO_2/NO_x ratio in vehicular exhaust, especially in this London case, due to the increasing number of buses and cars fitted with catalytic diesel particulate filters (CDPF). These devices oxidise carbon monoxide and hydrocarbons and generate NO_2 to aid in the emissions control of diesel particulate. Since then, the increase in the urban NO_2/NO_x concentration ratio and the underlying causes of the phenomenon have been widely studied (Keuken et al., 2009; **Paper II**; Carslaw et al., 2011; Mavroidis and Chaloulakou, 2011; Keuken et al., 2012; Kurtenbach et al., 2012; Melkonyan and Kuttler, 2012; Carslaw and Rhys-Tyler, 2013; O'Driscoll et al., 2016; Carslaw et al., 2016; Degraeuwe et al., 2017; Wild et al., 2017; Olstrup et al., 2018; Casquero-Vera et al., 2019). Nowadays, it is well-established that the proportion of primary NO_2 (i.e. the NO_2/NO_x ratio) in diesel vehicle exhaust has increased over the past decade because of exhaust gas after-treatment technologies (CDPF and others).

Additionally, it has long been known (and addressed in, e.g. emission inventories; e.g. Ntziachristos et al., 2016) that the on-road real-driving NO_x emissions of vehicles – especially those of diesel vehicles – differ from the standardised approval emission tests. This discrepancy rose to the spotlight in 2015 when Volkswagen's "diesel defeat devices" were exposed (BMVI, 2016). In certain vehicles (belonging to the emission classes Euro 5 or Euro 6), the manufacturer had installed a specific engine control software that recognises if the vehicle follows a type approval test cycle in lab conditions (NEDC) and accordingly switches to a low-NO_x emission strategy. In real-life road operations, these vehicles run in a different mode, resulting in higher NO_x emissions. However, it quickly emerged that the problem was not limited just to Volkswagen, but most manufacturers had been "optimising" the performance of their vehicles to pass the type approval tests. Permissive testing procedures at the EU level and defective emissions control strategies (so-called "lawful defeat devices") were found to legally allow higher NO_x emissions on the road than in a laboratory setting (BMVI, 2016).

It should be noted that, by now, the EU has already adopted several measures to improve the type approval emission testing; e.g. real driving emissions (RDE) measurements of NO_x (but not NO_2) and particle number (PN) by portable emission measuring systems (PEMS) gradually became compulsory for new car models, starting from September 2017; also, an improved laboratory test cycle (worldwide harmonised light vehicle test procedure – WLTP) replaced the NEDC as of 2017.

Also, in Finland, the number of diesel passenger cars began to grow rapidly in the mid-2000s due to the new CO_2 emission–based tax for passenger cars. In **Paper I**, we showed that the ambient NO_2/NO_x ratio was increasing at urban and suburban sites in the mid-1990s and early 2000s. To see the further development, the observed NO_2/NO_x concentration ratios are reproduced here, but they now include all Finnish monitoring stations up to the year 2018 (Figure 9). All five calculated percentiles of the annual NO_2/NO_x ratios displayed a statistically significant increasing trend (OLS, *t*-test; $p<0.05$) for the whole 1994–2018 period, but of the latter years (2007–2018), only the 25th percentile displayed an increasing trend ($p=0.04$). The summary of all monitoring data suggests that after 2007, the NO_2/NO_x ratio continued to increase at roadsides (with heavy traffic and high NO emission), albeit at a clearly slower pace (Figure 9).

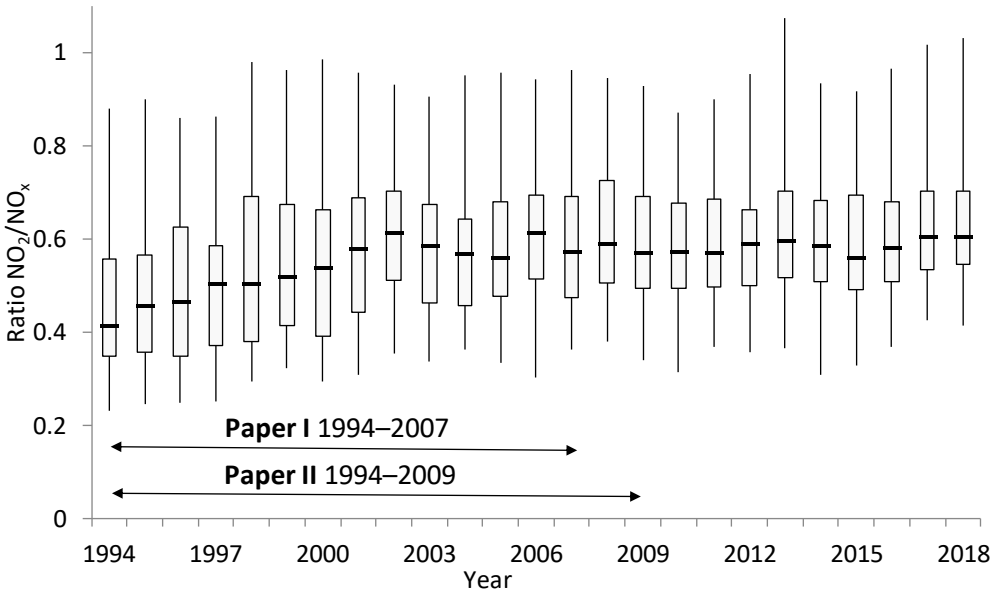

Figure 9. Distribution of annual NO_2/NO_x ratios calculated from NO_2 (in ppbv) and NO (in ppbv) concentrations measured at the Finnish monitoring sites in 1994−2018. At least a 75% annual data capture was required for each site and year. For each year, the lowest, highest and median values together with the 25th and 75th percentile values (box) are shown. The number of sites varies from 24 in 1994 to 54 in 2018, the total number of sites being 203. A total of 1257 annual ratios were included.

The steepest growth of the NO_2/NO_x ratio occurred in the first decade of the whole study period (1994–2004). During this period, the passenger car fleet in Finland was dominated by petrol-fuelled vehicles (92% and 88% of the car fleet in 1994 and 2004, respectively) and by the increasing fraction of cars with three-way catalysts (TWCs). Petrol cars emitted/emit very little, if any, tailpipe NO_2 (less than 5% of total NO_x) and TWC controlled NO (and HC and CO) very efficiently. So, vehicles' NO emissions declined systematically, while secondary NO_2 (formation from $NO+O_3$) and regional background concentrations declined less or not at all, resulting in an increasing NO_2/NO_x concentration ratio in urban areas. In general, the situation was comparable to the Töölö case presented in **Paper II**.

Instead, the data from Mannerheimintie (**Paper II**) span over the period of the most intense diesel penetration, and thus, the total oxidant model calculation is supplemented here with new data up to 2015, when O_3 monitoring at Mannerheimintie ended. Table 3 and Figure 10 summarise the updated results of the primary NO_2 emission fraction calculated with the total oxidant model (see **Paper II**).

Table 3. Annual regression results of $[O_x]_{local} = c[NO_x]_{local} + d$ (see **Paper II**) at the Mannerheimintie site in 2005–2015 (SE = standard error)

							diesel share %	
year	c	SE.	d	SE.	r	n	passenger car fleet	1st registrations
2005	0.151	0.002	2	0.1	0.78	4162	12.5	17
2006	0.173	0.003	0.3	0.2	0.72	2953	13.3	20.3
2007	0.169	0.002	2.3	0.1	0.78	4216	14.5	28.5
2008	0.206	0.002	1.4	0.2	0.81	4212	17.1	49.6
2009	0.21	0.002	2.1	0.1	0.85	4045	18.7	46.3
2010	0.153	0.003	3.5	0.2	0.66	4060	20.3	41.8
2011	0.161	0.002	2.1	0.1	0.73	4083	21.8	42.1
2012	0.134	0.002	2.1	0.1	0.71	3947	23.1	38.7
2013	0.153	0.003	1.4	0.2	0.65	4333	24.1	37.3
2014	0.154	0.003	1.1	0.2	0.63	3918	25.1	39
2015	0.187	0.003	3.2	0.1	0.68	4213	26	35.7

It turns out that the rise in the primary NO_2 emission fraction – calculated with the total oxidant model – was already reversed in 2010, and since then, it has varied between 15% and 19% at the Mannerheimintie site (Table 3). Correspondingly, since 2010, the contribution of the conversion from NO to NO_2 has been larger (51–56% of the total NO_2 concentration) than the primary NO_2 fraction (28–34%). The contribution of the regional background to this urban NO_2 concentration was 14–19% (Figure 10). So, the anticipated future development, that the primary NO_2 emissions will make an increasingly important contribution to the ambient NO_2 concentrations (**Paper II**), has not realised during these six years at this study site.

On the other hand, the number of new registrations of diesel passenger cars has become a steady decrease (24% in 2018) since the peak year 2008 (50%) (Table 3). The share of diesel cars of the total car fleet is still steadily growing; diesel engines last longer than petrol engines, and almost 60% of the imported used cars (total of 45 000) were diesel cars in 2018 (AuT, 2018).

Obviously, the magnitude and time development of the primary NO_2 emission and its contribution to the ambient NO_2 concentrations at roadsides is highly dependent on the country/city and road-specific vehicle fleets. However, based on this updated data, it seems that in Finland, the development of air quality in terms of NO_2 has remained positive despite the (temporarily) accelerated diesel penetration. Ambient NO_2 concentrations are decreasing (Figure 8), and the NO_2/NO_x ratio has stabilised (Figure 9).

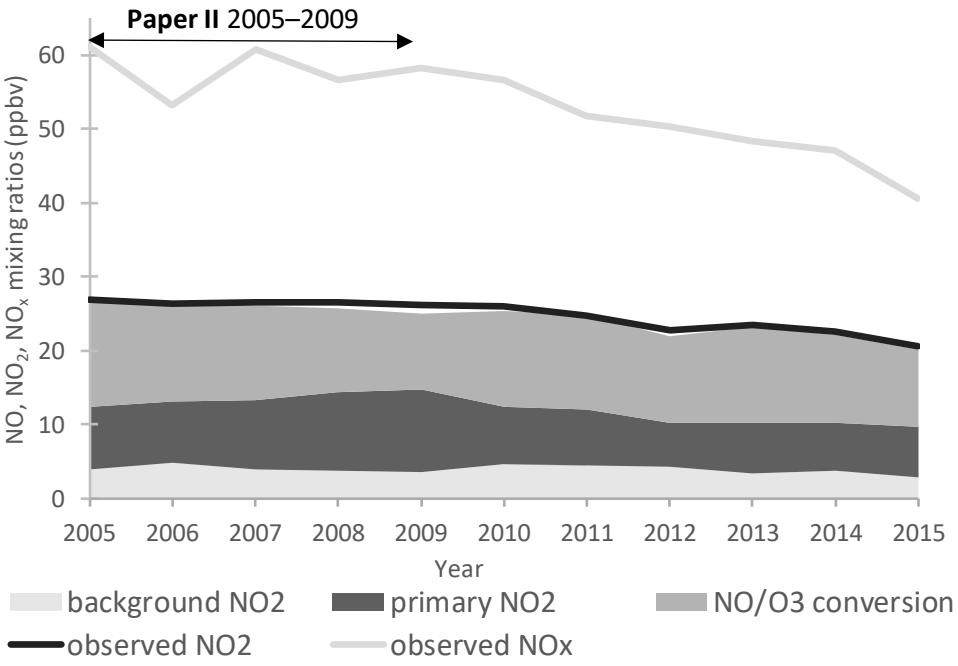

Figure 10. Annual NO_2 budgets during weekday hours between 5:00 and 21:00 at Mannerheimintie, 2005–2015.

Similar results come from the rest of Europe, too. Grange et al. (2017) show that from around 2010, the NO_2/NO_x ratio at most roadside locations across Europe have stabilised. Degraeuwe et al. (2017) conclude that the absolute level of traffic NO_x emissions is more relevant for the NO_2 concentration in urban street canyons than the NO_2 fraction in the total NO_x emissions. Carslaw et al. (2019) found that the primary and absolute NO_2 emissions of diesel cars vary a lot depending on the year of the manufacture (Euro status), used emission control techniques, the vehicle "family" manufacturer and mileage. Carslaw et al. (2019) conclude that the importance of primary NO_2 from vehicles has been decreasing in recent years.

4.3 Carbon monoxide (CO) trends

A reduction of CO emissions and concentrations has not encountered problems similar to NO_2. The strong and uniform ambient air concentration reductions of CO (-3% to -7%/yr) at the six studied urban monitoring sites can be related to the realised reductions in road traffic emissions. In Finland, the urban CO concentration levels are nowadays below 300 µg/m^3, and CO is no longer monitored in cities (Figure 11).

Similar temporal behaviour, i.e. marked declines of CO, were also detected in Europe in 2002−2011 (Guerreiro et al., 2014). Nowadays, CO is only a very localised and infrequent air quality problem in Europe. This can be considered another example of the successful implementation of air pollution control

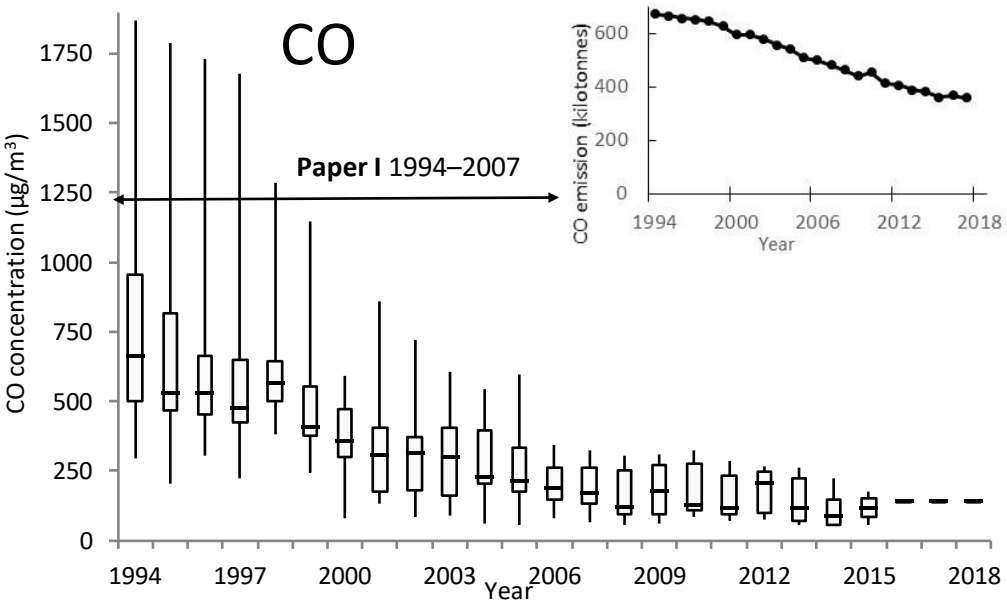

Figure 11. Distribution of annual mean concentrations of CO registered at the Finnish monitoring sites in 1994−2018. At least a 75% annual data capture was required for each site and year. For each year, the lowest, highest and median values together with the 25th and 75th percentile values (box) are shown. The number of sites included varies from 9 in 1994 to 17 in 2002, and after that, it follows a gradual decrease to 4 sites in 2015 and one site (Pallas) since then. A total of 261 annual values were included. The subplot shows the development of the annual CO emissions in Finland (SYKE, 2019a).

Long-term rural background measurements of CO were not available, but international studies combining emission inventories, surface observations, satellite data and modelling suggest widespread decreasing trends in the 2000s across Western Europe, eastern USA (Yoon and Pozzer, 2014) and East Asia (Zheng at al., 2018), mostly due to the changes in anthropogenic emissions.

4.4 Ozone (O_3) trends

Surface-level O_3 concentrations, especially in urban areas, are closely linked to the NO_x emissions and concentrations. Once released into the atmosphere, both NO and NO_2 join in complicated atmospheric photooxidation reaction chains. The simplest of them, the one producing O_3, the photostationary state of the NO_x–O_3 cycle, is fast and important, especially in urban NO_x-rich environments. More generally, O_3 production takes place via the O_3–VOC–NO_x system, which also involves CO and inorganic radicals like hydroxyl, hydroperoxyl and nitrate radicals (e.g. Seinfeld and Pandis 1998; Monks et al., 2015). These chains of reactions can be long, complex and non-linear. Meanwhile, the ozone and its precursors can be transported throughout the lower atmosphere on regional, intercontinental and hemispheric scales (Monks et al., 2015). As a result, an emission reduction of one component is not necessarily reflected as a parallel reduction of ozone ambient concentrations.

Anthropogenic emissions of the major ozone precursors (i.e. NO_x, NMVOCs and CO) have decreased during the past 20 years in Finland as well as in Europe and North America (e.g. Monks et al., 2015). On the other hand, global emission trends vary greatly from region to

region, and while emissions are declining in Europe and North America, the global trend may be stagnant (NO_x) or even rising (NMVOCs) (Miyazaki et al., 2017; Huang et al., 2017).

Ozone concentration trends remain challenging for air pollution control. In Europe, for example, both positive and negative (generally weak) trends have been documented. Guerreiro et al. (2014) presented an overview and an analysis of ozone trends in Europe (AirBase data) in 2002–2011. They found that 80% of the sites (both urban and rural) did not have a statistically significant trend for the studied metric (93.15th percentile of a maximum daily 8 hour mean); 18% of the stations registered a statistically significant decreasing trend, while 2% registered a significant increasing trend.

Yan et al. (2018) report significant ozone enhancements (0.20–0.59 µg/m^3/yr) for the annual means over the European suburban and urban stations (AirBase data) during 1995–2012. For European background sites (EMEP), Yan at al. (2018) report a decreasing trend (-0.9 µg/m^3/yr) in the 95th percentile ozone concentrations (especially at noon), while the 5th percentile ozone concentrations increased with a trend of 0.3 µg/m^3/yr during 1995–2014. Klingsberg et al. (2017) found decreasing summer daytime trends (slopes for the 75th–98th percentiles ranging from -0.2 to -1 µg/m^3/yr) and increasing summer nighttime and winter daytime and nighttime ozone trends at northern European background sites (EMEP) during 1990–2015. Olstrup et al. (2018) found increasing O_3 concentrations at urban background sites in Stockholm, Gothenburg and Malmö during 1990–2015. Hellén et al. (2015) found no ozone trend at Pallas/ Sammaltunturi during 1994–2013. Of the nine studied NMVOCs, only one (ethyne) had a statistically significant decreasing trend.

Fleming et al. (2018) conclude that Europe and North America in particular (both urban and non-urban) are characterised by reduced exposure to peak levels of ozone related to photochemical episodes over the 2000–2014 period. The short-term mid-high and long-term high ozone metrics exhibited more mixed trends. Furthermore, Fleming et al. (2018) conclude that in Europe, the trend results for non-urban and urban stations are broadly similar.

Similar miscellaneous ozone trends were reported in **Paper I**, too. The concentration time series of O_3 were studied from 9 rural background sites and two urban/suburban traffic sites. Increasing and decreasing trends of ozone mean levels were equally common, although the only three statistically significant trends were increasing (Helsinki Töölö, Vantaa Tikkurila and Espoo Luukki). On the other hand, the predominantly increasing trends of the monthly calculated 95th percentiles (**Paper I**) were detected, four being statistically significant, i.e. Raja-Jooseppi, Pallas/Sammaltunturi, Helsinki Töölö and Vantaa Tikkurila.

Figure 12 displays the 95th and 5th percentiles of summertime (March–August) ozone concentrations from all Finnish ozone monitoring sites calculated on an annual basis from 1994 to 2018. Trends, if any, are vague, but some patterns can be extracted.

The increase in summertime ozone peak levels documented in **Paper I** have not continued since 2007, but rather, Figure 12 indicates decreasing peak ozone concentrations for most sites – both urban and non-urban – since the top year 2006. In spring and summer 2006, Finland was affected by two major LRT episodes lasting several days (see **Paper V**), which are clearly reflected in these peak ozone concentrations. For example, the all-time (since 1987) hourly

ozone record (195 µg/m^3) of Finnish monitoring stations was registered on 5 May 2006, at the Virolahti site.

The decrease of episodic ozone peak levels in rural areas of Europe have been attributed to regional pollution emission controls applied to the VOC and NO_x and the following reductions in photochemical ozone formation (Monks et al., 2015 and references therein). On the other hand, in the high-NO_x environments of major European cities, the ozone levels are increasing due to locally decreasing NO emissions and following reductions in ozone scavenging by NO (Monks et al., 2015 and references therein). This latter development is no longer evident in this Finnish data; peak levels (as well as mean levels) of ozone increased at the sites next to the busiest roads in the 1990s (see the red lines in Figure 12) but have since been rather stable and have quite closely followed the interannual variation found in the surrounding urban/suburban and rural areas. The increase in lower-level concentrations (Yan et al., 2018) is not as apparent (Figure 12) in this Finnish material.

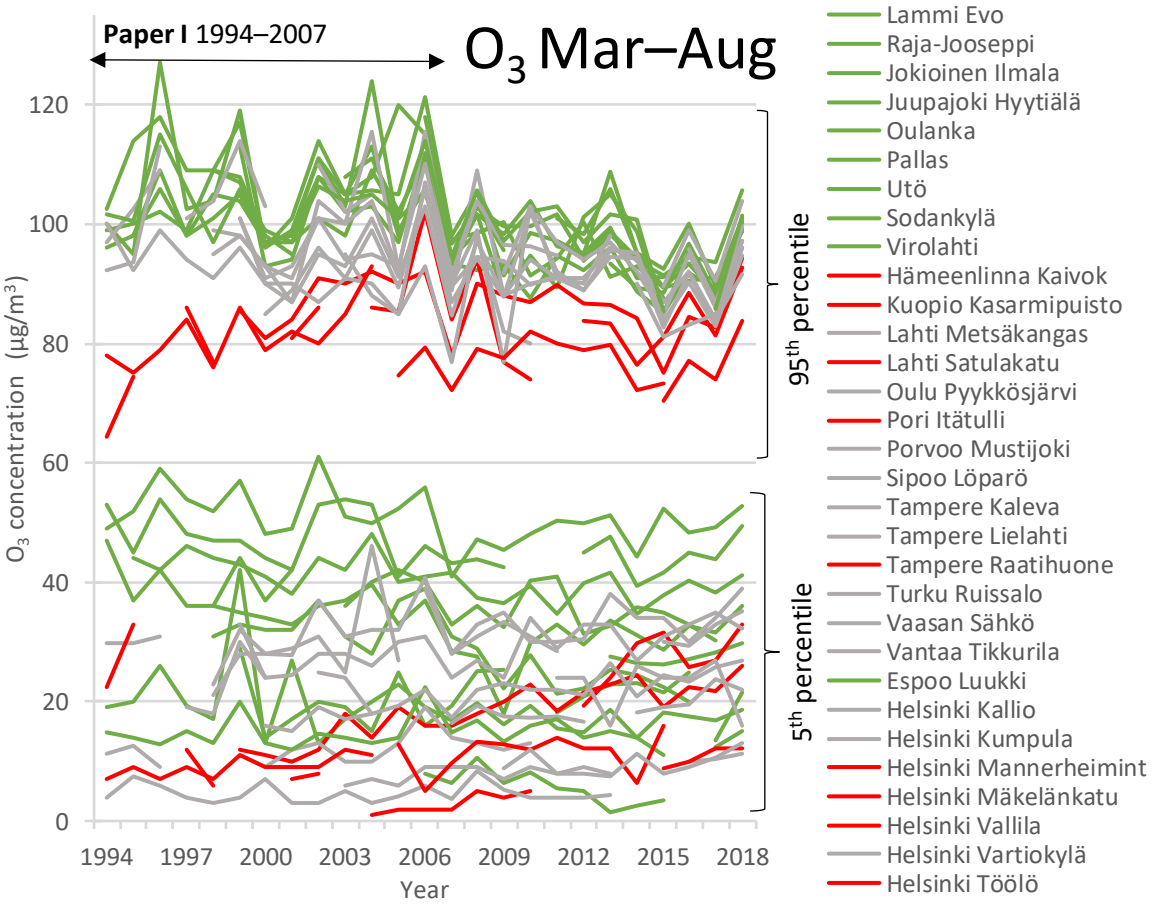

Figure 12. The summer period's (March–August) 5th and 95th percentiles of hourly O_3 concentrations at Finnish monitoring sites 1994–2018. The green lines are rural stations; the grey lines are urban, suburban or industrial stations and red roadside sites.

4.5 PM_{10} particle mass trends

In Finland, elevated PM_{10} concentrations are typically detected near busy roads in springtime (Kukkonen et al., 1999; Pohjola et al., 2002; **Paper IV**; Teinilä et al., 2019). In

Paper IV, it was shown that during the 1998–2003 study period in 20 Finnish cities, the annual peak concentrations occurred very concurrently. Further, it was shown that PM_{10} concentrations started to increase in the first half of March (a week later in northern cities) concurrently with the snowmelt and the low rainfall period. The highest concentrations occurred in urban areas with high traffic volume.

In Finnish studies, urban (road) dust has been identified to be mainly mineral matter in the coarse mode (aerodynamic diameter between 2.5 and 10 µm) (Hosiokangas et al., 1999; Pakkanen et al., 2001; Kupiainen and Tervahattu 2004; Sillanpää et al., 2006). The source of road dust and factors influencing the source strength have been studied both in laboratory tests (Räisänen et al., 2003; Kupiainen et al., 2003; Kupiainen et al., 2005; Räisänen et al., 2005; Tervahattu et al., 2006), near-road measurements (Kupiainen and Tervahattu 2002; Kupiainen et al., 2016), on-road/mobile measurements (Pirjola et al. 2009; Kupiainen and Pirjola 2011; Kupiainen et al., 2016) and by modelling (e.g. Stojiljkovic et al., 2019). Generally, these studies showed that the interactions between studded tyres, traction sanding and pavement aggregate are the major underlying factors behind the production of road dust emissions. Recent study (Kupiainen et al., 2016) suggests that the pavement wear associated with the use of studded tyres contributes most to high ambient PM_{10} concentrations, while the use of traction sanding has a lesser impact. The resulting ambient PM_{10} concentrations depend, obviously, on the traffic amounts, vehicle fleet, road maintenance activities and meteorological factors.

In addition to the spring dust period, **Paper IV** highlighted the PM_{10} episodes that were irregular in time but spatially wide-ranging and concluded that they are related to long-range transport rather than to local sources. Niemi et al. (2009) summarised the frequency and origin of fine particle episodes in Southern Finland; episodes occur several times per year, and they most often originate in Eastern Europe. Starting from the early 2000s, the characteristics and/or sources of the major LRT PM episodes in Finland have become identified in detailed case studies. In September 2001, the dust plumes from the Kazakhstan Ryn-Peski desert mixed with Estonian and Russian oil-shale industry emissions and spread over coastal areas of the Baltic Sea (Sofiev et al., 2003; Hongisto and Sofiev, 2004; Tervahattu et al., 2004). The most serious LRT episodes, though, are related to biomass burning events in 2002 (Niemi et al., 2004; Sillanpää et al., 2005; Niemi et al., 2005; Aarnio et al., 2008), in 2006 (Saarikoski et al., 2007; Saarnio et al., 2010; **Paper V**; Makkonen et al., 2010) and in 2010 (Portin et al., 2012; Mielonen et al., 2012; Leino et al., 2014). In addition to these, wildfire episodes were reported in 2004 (Niemi et al., 2006; Saarikoski et al., 2008), in 2007 (Niemi et al., 2009), in 2008 (Hyvärinen et al., 2011) and in 2009 (Timonen et al., 2010).

These wildfire episodes typically occurred in spring (March–May) and late summer (July–September), and they originated from Eastern/Central Europe and the western part of Russia. The episodes were strongest in Southern Finland, but some of them were detected in Northern Finland, too (e.g. Leino et al., 2014), and further in the High Artic (Stohl et al., 2007). In episode cases, the first alarm typically came from the elevated concentrations of PM mass detected with the continuous monitors. During LRT episodes, the particle mass size distribution was dominated by fine particles (<2.5 µm) rather than by the coarse fraction. In some PM episode cases, however, PM_{10} served as a feasible LRT episode indicator, too (e.g. **Paper V**, Makra et al., 2011). Globally, wildfires release huge amounts of primary organic aerosol (POA) but also photochemically active organic gases (VOCs) and black/elemental carbon (e.g. Andreae, 2019), all contributing to (aged) PM mass. Depending on the trajectory of the polluted air mass, the

aerosol could be a mixture of biomass burning (agricultural/forest) and fossil/industrial emissions like trace metals, resuspended persistent organic pollutants, gaseous mercury and radionuclides (e.g. **Paper V**; **Paper III**; Paatero et al., 2009).

Somewhat surprisingly, the latest reported episodic long-range transport of particles was different from those described above. In Helsinki on 25 May 2011, the ash plume from the eruption in Grimsvötn, Iceland, enhanced PM_{10} mass concentrations up to several tens of $\mu g/m^3$ (Kerminen et al., 2011).

PM mass recorded at any monitoring site is a mixture of primary or secondary, natural or anthropogenic, fossil or biogenic, and local or far away emission/source, which makes PM pollution particularly difficult to control. So, it's not surprising that PM_{10} concentration trends in Finland and elsewhere in Europe are not decreasing in any systematic way.

In **Paper I**, 12 PM_{10} time series of monthly means and monthly 95^{th} percentiles were investigated for potential trends. No nationwide convergent development was found, but instead, both increasing and decreasing trends were identified. This result is not a surprise as all studied time series were from urban/suburban/industrial monitoring sites and given the pronounced contribution of local street dust as a source of ambient PM_{10} particles. Similar partly mixed trend results of PM have been reported elsewhere in Europe, too (Guerreiro et al., 2014; Colette et al., 2011).

In Finland, the springtime street dust raises a lot of public concern and has been identified as one of our major air quality problems; it was also addressed in the National Air Pollution Control Programme (NAPCP, 2019). In this thesis, an attempt is made to extract the spring dust trends by summarising the recent seasonal PM_{10} monitoring results in Finland (Figure 13). Years were divided to three seasons: Feb–May (representing the spring dust period), Jun–Sept (wildfires) and Oct–Jan (other).

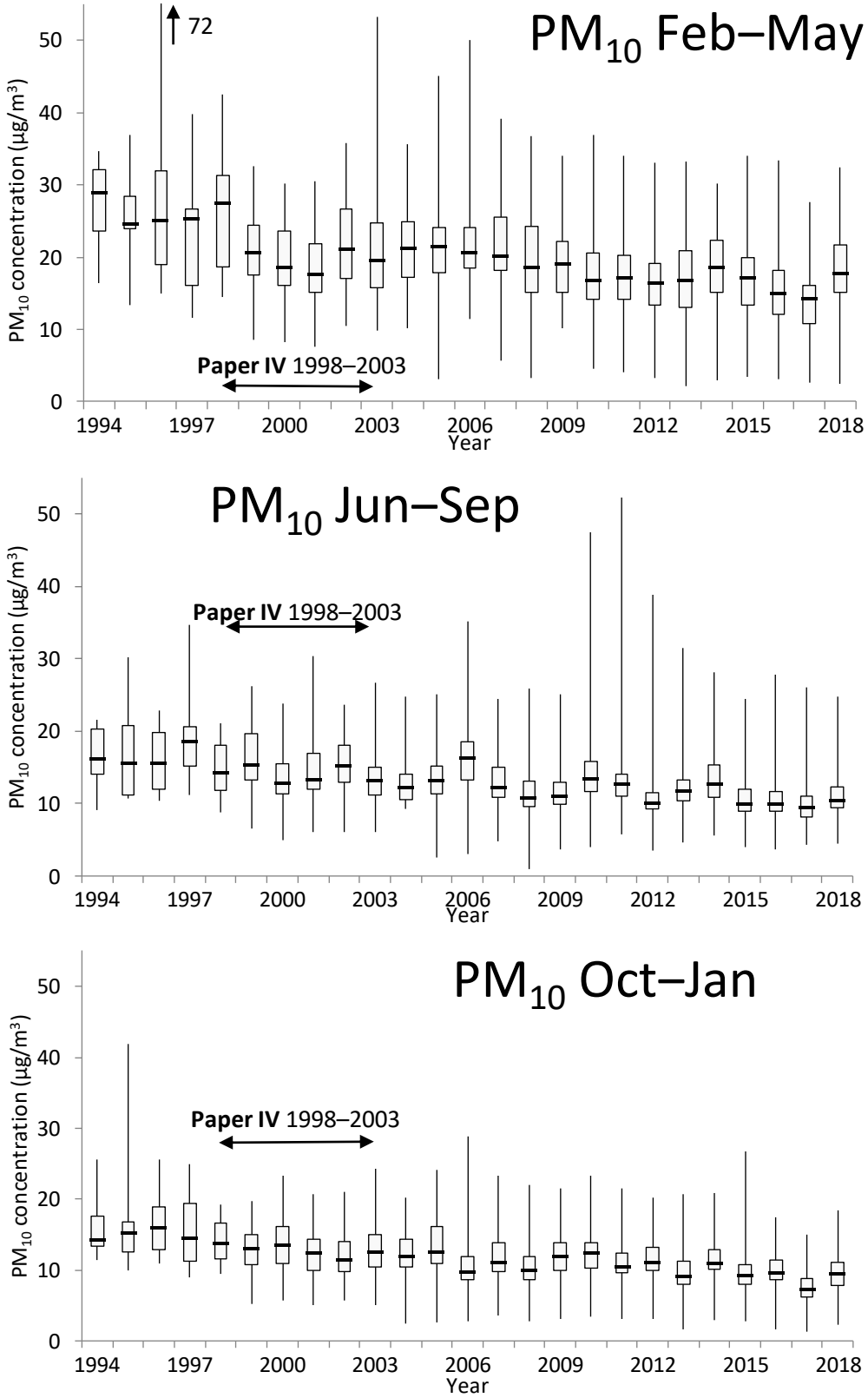

Figure 13. Distribution of seasonal mean concentrations of PM_{10} measured at the Finnish monitoring sites in 1994−2018. At least a 75% seasonal data capture was required for each site and year. For each year, the lowest, highest and median values together with the 25th and 75th percentile values (box) are shown. The number of sites included increased from 9 in 1994 to 60 in 2007, and after that, it has been steady. A total of 1115, 1120 and 1194 seasonal values were included for Feb–May, Jun–Sep and Oct–Jan, respectively. The total number of sites was 171.

It should be noted that in 2017, the updated correction factors for PM continuous monitors (see Waldén et al., 2017) were released and recommended for use. Of around 60 instruments in use in 2017, 32 adopted a correction factor which reduced the measurement result compared to the one used previously. At the median level, the reduction percents were between -30% and -1%. Nine instruments were corrected with a factor that increased the result (8–26%), and the coefficients for twenty devices were not changed or the information was not provided. So, PM results for 2017 onwards are not necessarily comparable to previous years, and they are not included in the following trend analysis.

A quick look at Figure 13 suggests that PM_{10} concentrations have generally been decreasing and that the decrease was steeper at the beginning of the study period. During the first 10 years, the monitoring network expanded strongly (from 10 to 60 sites). At the beginning, the new sites were typically opened at the most polluted roadside locations, which provide highly localised data, especially when it comes to street dust. At the lowest tail of the concentration distribution, the start of PM_{10} monitoring at the remote sites at Pallas and Raja-Jooseppi in 2007 is clearly visible. These kinds of changes in the network may cause some bias in the aggregated data. Since 2007, the network has been roughly stable, and the trend estimates more representative.

For an exact picture of the trends, linear fits to the time series of each percentile were performed over the whole 1994–2016 period and separately over the last ten years, 2007–2016. Table 4 summarises the trend statistics.

Table 4. Trend results of the seasonal mean concentrations of PM_{10} (slopes and their *p*-values; two-tailed t-test, percent change); significance level of at least 5% is bolded

		1994–2016			2007–2016		
		slope	*p*-value	%	slope	*p*-value	%
Feb–May	highest	-0.485	0.103		**-0.615**	**0.014**	**-36**
	75th percentile	**-0.497**	**0.000**	**-37**	**-0.577**	**0.010**	**-53**
	median	**-0.459**	**0.000**	**-40**	**-0.358**	**0.017**	**-41**
	25th percentile	**-0.354**	**0.000**	**-38**	**-0.438**	**0.007**	**-59**
	lowest	**-0.564**	**0.000**	**-88**	-0.397	0.115	
June–Sept	highest	+0.421	0.093		-0.160	0.896	
	75th percentile	**-0.381**	**0.000**	**-42**	-0.209	0.243	
	median	**-0.265**	**0.000**	**-36**	-0.143	0.333	
	25th percentile	**-0.171**	**0.000**	**-28**	-0.134	0.225	
	lowest	**-0.297**	**0.000**	**-71**	+0.130	0.422	
Oct–Jan	highest	-0.283	0.062		-0.194	0.499	
	75th percentile	**-0.308**	**0.000**	**-38**	**-0.259**	**0.034**	**-42**
	median	**-0.249**	**0.000**	**-37**	-0.197	0.100	
	25th percentile	**-0.178**	**0.000**	**-32**	-0.133	0.199	
	lowest	**-0.391**	**0.000**	**-93**	**-0.136**	**0.043**	**-87**

Indeed, when the whole study period is considered for all seasons, all concentration levels except the highest exhibit a s.s. decreasing trend. In contrast, in the latter part of the study period, only the spring season exhibits systematically decreasing trends (all concentration levels except the lowest).

This suggests that, to some extent, the local abatement measures (e.g. reducing traffic amounts, changes in the car fleet, road maintenance activities) have been successful, and the springtime street dust levels have been reduced. However, the springtime concentration levels of PM_{10} are still one and a half times higher than in other seasons on average. In spring, the daily mean of 50 µg/m^3 is exceeded frequently, not only in the biggest cities but also in small towns of 20 000 people. At most, there are about 20–30 exceedances/site/year, so the European PM_{10} norm (daily mean should not exceed 50 µg/m^3 more than 35 five times per year) is not exceeded. Although the European air quality norm is not being violated, street dust remains a persistent flaw in our otherwise good air quality.

4.6 Persistent organic pollutants (POPs) trends

In **Paper III**, long-term atmospheric monitoring data of persistent organic pollutants (POPs) were assembled from a rural site in Southern Sweden, Råö, and the Pallas/Matorova site in Northern Finland. The concentration levels, congener profiles and seasonal and temporal trends (1994–2011) were evaluated to assess the status of POPs in the Scandinavian background atmosphere.

Polycyclic aromatic hydrocarbons (PAHs)

In 2007, globally, the biggest sources of PAHs (i.e. PAH-16) were residential/commercial biomass burning (60.5%), transportation (14.8%) and open-field biomass burning (agricultural waste burning, deforestation and wildfire) (13.6%) (Shen et al., 2013). About 80% of the transportation emissions were in the form of light molecular weight naphthalene, while residential fuel consumption, industrial emissions and nonorganised waste burning contributed more high molecular weight carcinogenic PAHs (6% of total PAH emissions, eight congeners starting from benz(a)anthracene) (Shen et al., 2013). South and East Asia contributed half of the total global PAH emissions. From 1995 to 2008, the global PAH emissions decreased by 15%, and significant emission reductions are expected to continue until 2030 (Shen et al., 2013).

Considerable differences in PAH source profiles and the time development of emissions varied a lot due to energy structure, development status and vegetation cover. According to Shen et al. (2013), in developed countries (like Europe), the PAH emissions peaked in the early 1970s and decreased gradually since, primarily due to the introduction of emission mitigation technologies and the subsequent decline in the PAH emissions from on-road motor vehicles. Meanwhile, only slow decreases in PAH emissions occurred in the residential and commercial sources.

Finnish PAH-4 emissions (the four indicator compounds benzo(a)pyrene, benzo(b)fluoranthene, benzo(k)fluoranthene and indeno(1,2,3cd)pyrene reported under the UNECE LRTAP) increased from 7 tonnes to 11 tonnes between 1990 and 2010. Since then, the PAH-4 emissions have fluctuated around 10 tonnes/year with no clear trend (SYKE, 2019b).

In Finland, the fuel wood consumption in the residential sector has increased by 23% between 1993 and 2017 (LUKE, 2019). Residential wood combustion has been identified as the major emission source of (primary) fine particles and black carbon (e.g. Savolahti et al.,

2016; NAPCP, 2019). And finally, residential wood combustion has been shown to be a significant source of airborne fine particles ($PM_{2.5}$) (Saarnio et al., 2012) and PAHs (Hellén et al., 2008; 2017) in urban and suburban areas, especially in wintertime.

In light of the considerations above, the trends of atmospheric background PAH concentrations in **Paper III** are understandable. Our data comprised 12 PAH congeners consisting of those with three to six aromatic rings. The low molecular weight congeners with two aromatic rings, including naphthalene, were not included in the chemical speciation due to methodological reasons. Therefore, it is not expected that the reduction in European/Finnish traffic emissions will be reflected in this trend analysis, but rather, they will bring out the evolution of the use of biomass fuel in the residential sector and/or wild/agricultural fires.

Of the 12 studied PAH compounds, only two at Råö and three at Pallas exhibited s.s. decreasing trends. At Råö, the three- and four-ring anthracene and benz(a)anthracene decreased, while at Pallas, three-, five- and six-ring fluoranthene, benzo(b)fluoranthene and indeno(123cd)pyrene decreased. Most PAH time series had negative regression slopes, but trends were not statistically significant. Reasonably, these weak or non-existent decreasing trends of PAHs can be linked to the only slowly decreasing regional and long-range transported emissions of biomass burning in the residential sector and/or wild/agricultural fires.

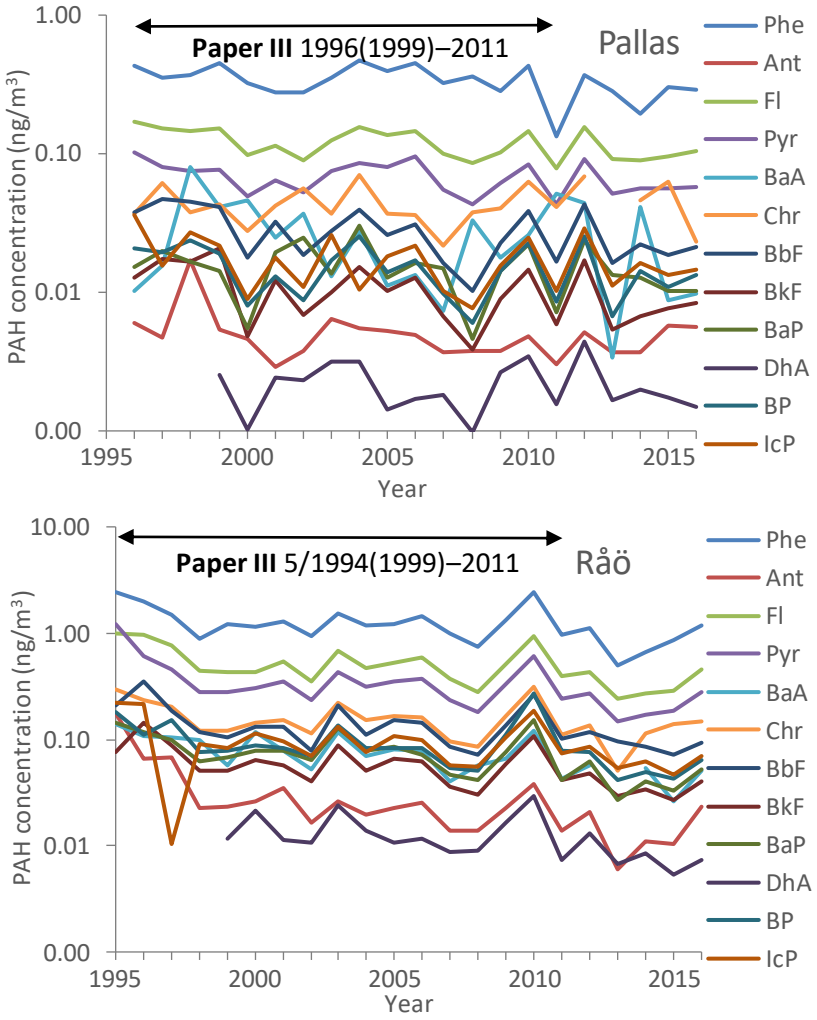

Figure 14. Annual means of 12 PAH compounds at Pallas and Råö in 1995–2016.

In a recent study, Yu at al. (2018) analysed the long-term trends (1992–2015) of selected PAHs (phenanthrene, pyrene and benzo(a)pyrene) at three arctic/subarctic sites, i.e. Alert, Canada; Zeppelin, Svalbard and Pallas, Finland. In line with the findings of **Paper III**, a significant decline in these PAHs was not observed. Forest fires were identified as an important contributing source.

At Råö, closer to the European and Scandinavian emissions sources, the concentrations of PAHs were 3–9 times higher than at the remote Pallas site. Yu et al. (2018) also found that the decrease in PAH concentrations continued when going farther north from Pallas (Pallas > Zeppelin > Alert).

Polychlorinated biphenyls (PCBs) and organochlorine pesticides (OCPs)

Paper III reported declining trends of atmospheric concentrations for the PCBs, HCHs, chlordanes and DDTs at Råö and Pallas. These declines were a very prominent feature in this material; of the studied 28 time series, all but one showed a s.s. decreasing trend. In a recent paper, Kalina et al. (2019) published long-term trends (1996–2016/2018) of PCBs and HCHs based on the very same but extended data from Råö and Pallas. For PCBs and p,p'-DDE, the trends (annual changes per year) were in good agreement with the findings of **Paper III**. For α-HCH, annual changes were -10% and -9% and for γ-HCH, they were -11% and -12% at Råö and Pallas, respectively (Kalina et al., 2019). These rates of changes are almost twice as high as given in **Paper III**. The differences are most likely related to the different transformations applied to the original data. Kalina et al. (2019) fitted the linear trend to log-transformed data accompanied by the Theil–Sen estimator and the Mann-Kendall test.

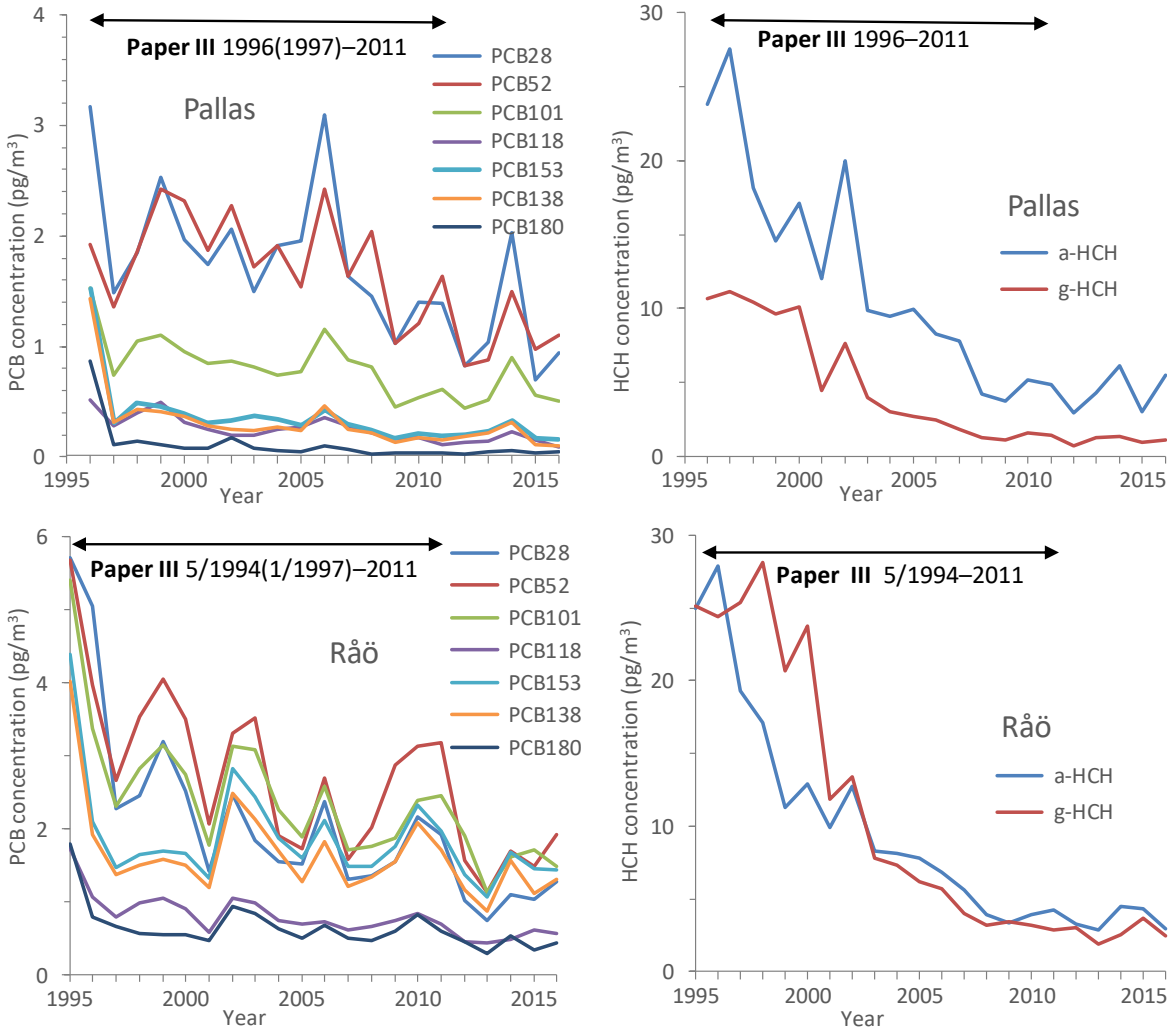

Figure 15. Annual means of PCBs and HCHs at Pallas and Råö in 1995/1996–2016.

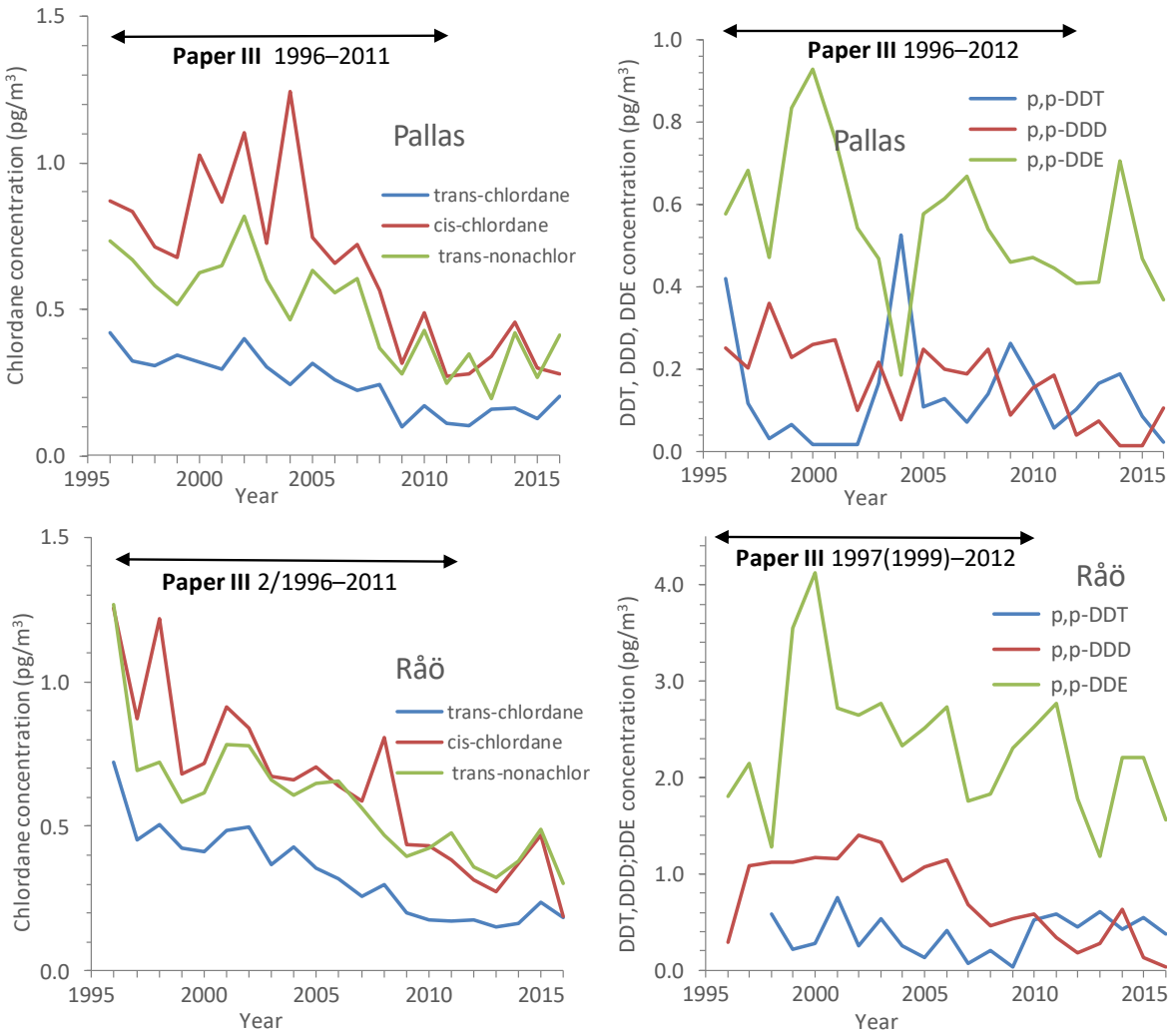

Figure 16. Annual means of chlordanes and DDT and its residues at Pallas and Råö in 1996–2016.

Nevertheless, these studies (**Paper III** and the references therein; Kalina et al., 2019) show large decreases in the atmospheric concentrations of PCB and OCPs in the Nordic atmosphere. PCBs, DDT and chlordanes belonged to the first set and HCHs to the second set of the controlled POPs by the UN Stockholm Convention in 2001 and 2009, respectively. This global treaty and the preceding national and regional regulations (since the late 1970s) banning intentional production, use, import and export have thus been successful in achieving improvements to the atmospheric environment. However, the projections suggest that the most long-lived compounds will persist in the atmospheric cycle beyond 2030 (**Paper III**).

5 Conclusions

Of the 176 analysed long-term time series in the original papers, 51% showed a statistically significant downward trend (**Paper I;** years 1994–2007 and **Paper III,** years 1994–2011). The decrease in concentrations was most common for CO, SO_4^{2-}, POPs (other than PAHs), NO_x, SO_2 and NO_2, i.e. 100%, 100%, 96%, 70%, 68% and 50% of the studied time series decreased, respectively. PM_{10} yielded both decreasing (38%) and increasing (21%) trends. O_3 exhibited only increasing trends (32%), and PAHs, NO_3^- and NH_4^+ were rather characterised by the lack of any uniform trends.

The assessment of the extended material presented in this thesis largely confirmed the above summarised development. The decrease of SO_2 and SO_4^{2-} concentrations have continued, and nowadays, elevated SO_2 concentrations are detected at a handful of industrial monitoring sites, while in Finnish background areas, the highest SO_2 concentrations are detected in northeastern Lapland under the influence of the ongoing and still partly obscure emissions in the Kola Peninsula. Urban CO concentrations have declined to such an extent that monitoring has been discontinued. Atmospheric concentrations of PCBs, HCHs and chlordanes have substantially decreased. NO concentrations have declined, and so have NO_2 concentrations, albeit slower than could be expected based on national NO_x emissions or parallel NO concentrations. There are indications that springtime street dust (PM_{10}) levels have declined over the last 10 years. Since 2006, the peak ozone concentrations have declined. Contrary to these predominantly decreasing trends, the limited available long-term data of PAHs suggest that no widespread decrease in concentrations has occurred.

This thesis demonstrates that internationally launched and nationally implemented regulatory controls have had an important role in improving air quality in Finland. The pollutants subject to long-term ambitious international abatement strategies (like SO_2, PCBs and OCPs) have decreased the most. Also, NO_x emission control has been succesful, but the outcome is a bit more complex. The emission regulations (both stationary and mobile sources) target the total NO_x emissions (which have been reduced successfully), while NO_2 is targeted in the ambient air standards.

The increasing penetration of diesel cars with relatively high (or unknown) primary NO_2 emissions may have been one contributing factor for why urban roadside NO_2 concentrations have not decreased as expected. However, the recent studies from European roadsides suggest that the still-decreasing absolute total NO_x emissions are compensating for the relative increase in primary NO_2 emissions, and the importance of primary NO_2 from vehicles has been decreasing in recent years. The newly adopted improved type approval tests may further reduce emissions – or at least clarify the situation.

In Finland, in terms of EU air quality norms for NO_2, the only problematic areas have been certain busy street canyon sites in Helsinki, which have been below the limit value since 2016. However, our relatively old car fleet and the increased import of old diesel cars cause uncertainty for future development.

A very different type of traffic-related air pollution is springtime street dust due to the use of studded tyres and manifested as elevated concentrations of PM_{10}. This thesis suggests that

springtime PM_{10} concentrations are on the decline. This could mean that the local abatement measures (e.g. reducing traffic amounts, changes in the car fleet, road maintenance activities) have been in the right direction, and the springtime street dust levels have been reduced. However, every spring, strong (even on a European scale) dust episodes occur, not only in the biggest cities but also in the small towns. So even though the European air quality norm is not being violated, street dust remains a persistent flaw in our otherwise good air quality.

In Finland, the ozone peak levels have been declining since 2006. A similar development has been detected in Europe and North America, and it is related to decreasing anthropogenic precursor emissions of NO_x and VOCs. For Finland, high background concentrations are more problematic, the reduction of which would require international and even hemispheric cooperation.

The available long-term background data of PAH concentrations suggest that no widespread decrease in concentrations has occurred. This is not necessarily surprising as the major global sources are small-scale solid fuel combustion and wildfires. Efforts to reduce these emissions have been relatively limited or non-existent so far.

Increasing wood burning and an increasing number of diesel cars are examples of cases when policies or economic controls to address one environmental issue (climate change) have had unintended consequences on another (air pollution).

References

Aarnio, P., Martikainen, J., Hussein, T., Vehkamäki, H., Sogacheva, L., Kulmala, M., 2008. Analysis and evaluation of selected PM pollution episodes in the Helsinki Metropolitan Area in 2002. Atmos. Environ., 42, 3992–4005.

Aas, W., Mortier, A., Bowersox, V., Cherian, R., Faluvegi, G., Fagerli, H., Hand, J., Klimont, Z., Galy-Lacaux, C., Lehmann, C.M.B., Myhre Lund, C., Myhre, G., Olivié, D., Sato, K., Quaas, J., Rao, P.S.P., Schulz, M., Shindell, D., Skeie, R.B., Stein, A., Takemura, T., Tsyro, S., Vet, R., Xu, X., 2019. Global and regional trends of atmospheric sulfur. Scientific Reports 9:953.

Akaike, H., 1973. Information theory as an extension of the maximum likelihood principle. In: Petrov, B.N., Csaki, F. (Eds.), Second International Symposium on Information Theory, Akademiai Kiado, Budapest pp. 267–281.

Andreae, M.O., 2019. Emission of trace gases and aerosols from biomass burning – an updated assessment, Atmos. Chem. Phys., 19, 8523–8546.

Anttila, P., Alaviippola, B., Salmi, T., 2003. Air quality in Finland–monitoring results in relation to the guideline and limit values and comparisons with European concentration levels. Publications on Air quality No. 33. Finnish Meteorological Institute. (In Finnish with an English abstract)

AuT, 2018. Share of diesel cars in new registrations and car fleet. The Finnish Information Centre of Automobile Sector, viewed 28 August 2018, <http://www.aut.fi/en/statistics/long-term_statistics/share_of_diesel_cars>.

BMVI, 2016. Report by the "Volkswagen" Commission of Inquiry. Investigations and administrative measures with regard to Volkswagen, results of the field investigation of the Federal Motor Transport Authority into unlawful defeat devices in diesel vehicles, and conclusions. Federal Ministry of Transport and Digital Infrastructure (BMVI), viewed 1 October 2019, <https://www.bmvi.de/SharedDocs/EN/publications/bericht-untersuchungskommission-volkswagen.pdf?__blob=publicationFile>.

Brockwell, P.J., Davis, R.A., 2002. Introduction to Time Series and Forecasting, Second Edition, Springer-Verlag, New York, Inc.

Carslaw, D., 2005. Evidence of an increasing NO_2/NO_x emissions ratio from road traffic emissions. Atmos. Environ., 39, 4793–4802.

Carslaw, D.C., Beevers, S.D., 2004. Investigating the potential importance of primary NO_2 emissions in a street canyon. Atmos. Environ., 38, 3585–3594.

Carslaw, D.C., Beevers, S.D., Tate, J.E., Westmoreland, E.J., Williams, M.L., 2011. Recent evidence concerning higher NOx emissions from passenger cars and light duty vehicles. Atmos. Environ., 45 (39), 7053v7063.

Carslaw, D.C., Farren, N.J., Vaughan, A.R., Drysdale, W.S., Young, S., Lee, J.D., 2019. The diminishing importance of nitrogen dioxide emissions from road vehicle exhaust. Atmos. Environ., X 1, 100002.

Carslaw, D.C., Murrels, T.P., Andersson, J., Keenan, M., 2016. Have vehicle emissions of primary NO_2 peaked? Faraday Discussions, 189, 439–454.

Carslaw, D.C., Rhys-Tyler, G., 2013. New insights from comprehensive on-road measurements of NO_x, NO_2 and NH_3 from vehicle emission remote sensing in London, UK. Atmos. Environ., 81, 339–347.

Casquero-Vera, J.A., Lyamani, H., Titos, G. Borrás, E., Olmo, J.F., Alados-Arboledas, L., 2019. Impact of primary NO_2 emissions at different urban sites exceeding the European NO_2 standard limit. Sci. Total Environ., 646, 1117–1125.

Colette, A., Aas, W., Banin, L., Braban, C. F., Ferm, M., González Ortiz, A., Ilyin, I., Mar, K., Pandolfi, M., Putaud, J.-P., Shatalov, V., Solberg, S., Spindler, G., Tarasova, O., Vana, M., Adani, M., Almodovar, P., Berton, E., Bessagnet, B., Bohlin-Nizzetto, P., Boruvkova, J., Breivik, K., Briganti, G., Cappelletti, A., Cuvelier, K., Derwent, R., D'Isidoro, M., Fagerli, H., Funk, C., Garcia Vivanco, M., Haeuber, R., Hueglin, C., Jenkins, S., Kerr, J., de Leeuw, F., Lynch, J., Manders, A., Mircea, M., Pay, M.T., Pritula, D., Querol, X., Raffort, V., Reiss, I., Roustan, Y., Sauvage, S., Scavo, K., Simpson, D., Smith, R.I., Tang, Y.S., Theobald, M.,

Tørseth, K., Tsyro, S., van Pul, A., Vidic, S., Wallasch, M., Wind, P., 2016. Air pollution trends in the EMEP region between 1990 and 2012. EMEP/CCC-Report 1/2016.

Colette, A., Granier, C., Hodnebrog, Ø., Jakobs, H., Maurizi, A., Nyiri, A., Bessagnet, B., D'Angiola, A., D'Isidoro, M., Gauss, M., Meleux, F., Memmesheimer, M., Mieville, A., Rouïl, L., Russo, F., Solberg, S., Stordal, F., Tampieri, F., 2011. Air quality trends in Europe over the past decade: a first multi-model assessment, Atmos. Chem. Phys., 11, 11657–11678.

Crippa, M., Janssens-Maenhout, G., Dentener, F., Guizzardi, D., Sindelarova, K., Muntean, M., Van Dingenen, R., Granier, C., 2016. Forty years of improvements in European air quality: regional policy-industry interactions with global impacts. Atmos. Chem. Phys., 16, 3825–3841.

EU, 2004. Directive 2004/107/EC of the European Parliament and of the Council of 15 December 2004 relating to arsenic, cadmium, mercury, nickel and polycyclic aromatic hydrocarbons in ambient air.

EU, 2008. Directive 2008/50/EC of the European Parliament and of the Council of 21 May 2008 on ambient air quality and cleaner air for Europe.

EU, 2016. Directive 2016/802 of the European Parliament and of the Council of 11 May 2016 relating to a reduction in the sulphur content of certain liquid fuels.

Degraeuwe, B., Thunis, P., Clappier, A., Weiss, M., Lefebvre, W., Janssen, S., Vranck, S., 2017. Impact of passenger car NO_x emissions on urban NO_2 pollution – Scenario analysis for 8 European cities. Atmos. Environ., 171, 330–337.

EEA, 2018. Air quality in Europe −2018 report. EEA Report 12/2018. 83pp.

Fleming, Z.L., Doherty, R.M., von Schneidemesser, E., Malley, C.S., Cooper, O.R., Pinto, J.P., Colette, A., Xu, X., Simpson, D., Schultz, M.G., Lefohn, A.S., Hamad, S., Moolla, R., Solberg, S., Feng, Z., 2018. Tropospheric Ozone Assessment Report: Present-day ozone distribution and trends relevant to human health. Elementa: Science of the Anthropocene, 6(1), p.12.

Grange, S.K., Lewis, A.C., Moller, S.J., Carslaw, D.C., 2017. Lower vehicular primary emissions of NO_2 in Europe than assumed in policy projections. Nature Geoscience 10, 914–918.

Grennfelt, P., Engleryd, A., Forsius, M., Hov, Ø., Rohde, H., Cowling, E., 2020. Acid rain and air pollution: 50 years of progress in environmental science and policy. Ambio. 49, 849–864.

Guerreiro, C.B.B., Foltescu, V., de Leeuw, F., 2014. Air quality status and trends in Europe. Atmos. Environ., 98, 376–384.

Hamilton, J.D., 1994. Time Series Analysis. Princeton University Press, New Jersey.

Hellén, H., Hakola, H., Haaparanta, S., Pietarila, H., Kauhaniemi, M., 2008. Influence of residential wood burning on local air quality. Sci. Total Environ., 393, 283–290.

Hellén, H., Kouznetsov, R., Anttila, P., Hakola, H., 2015. Increasing influence of easterly air masses on NMHC concentrations at the Pallas-Sodankylä GAW station. Boreal Env. Res., 20, 542–552.

Hellén, H., Kangas, L., Kousa, A., Vestenius, M., Teinilä, K., Karppinen, A., Kukkonen, J., Niemi, J.V., 2017. Evaluation of the impact of wood combustion on benzo[a]pyrene (BaP) concentrations; ambient measurements and dispersion modeling in Helsinki, Finland. Atmos. Chem. Phys., 17, 3475–3487.

Henschel, S., Querol, X., Atkinson, R., Pandolfi, M., Zeka, A., Le Tertre, A., Analitis, A., Katsouyanni, K., Chanel, O., Pascal, M., Bouland, C., Haluza, D., Medina, S., Goodman, P.G., 2013. Ambient air SO_2 patterns in 6 European cities. Atmos. Environ., 79, 236–247.

Henschel, S., Le Tertre, A., Atkinson, R.W., Querol, X., Pandolfi, M., Zeka, A., Haluza, D., Analitis, A., Katsouyanni, K., Bouland, C., Pascal, M., Medina, S., Goodman, P.G., 2015. Trends of nitrogen oxides in ambient air in nine European cities between 1999 and 2010 Atmos. Environ., 117, 234–241.

Hongisto, M., Sofiev, M., 2004. Long-range transport of dust to the Baltic Sea Region. Int. J. Environ. Pollut., 22(1–2), 72–86.

Hosiokangas, J., Ruuskanen, J., Pekkanen, J., 1999. Effects of soil dust episodes and mixed fuel sources on source apportionment of PM_{10} particles in Kuopio, Finland. Atmos. Environ., 33, 3821–3829.

Huang, G., Brook, R., Crippa, M., Janssens-Maenhout, G., Schieberle, C., Dore, C., Guizzardi, D., Muntean, M., Schaaf, E., Friedrich, R., 2017. Speciation of anthropogenic emissions of non-methane volatile organic compounds: a global gridded data set for 1970–2012. Atmos. Chem. Phys., 17, 7683–7701.

Hurvich, C.M., Tsai, C.L., 1989. Regression and time series model selection in small samples. Biometrika, 76, 297–307.

Huutoniemi, K., Estlander, A., Hahkala, M., Hämekoski, K., Kulmala, A., Lahdes, R., Laukkanen, T., (Eds.). 2006. Savuntarkastajista päästökauppiasiin. Suomen ilmansuojelun historiaa. Ilmansuojeluyhdistys ry. Gummerus, Jyväskylä.

Hyvärinen, A.-P., Kolmonen, P., Kerminen, V.-M., Virkkula, A., Leskinen, A., Komppula, M., Hatakka, J., Burkhart, J., Stohl, A., Aalto, P., Kulmala, M., Lehtinen, K.E.J., Viisanen, Y., Lihavainen, H., 2011. Aerosol black carbon at five background measurement sites over Finland, a gateway to the Arctic. Atmos. Environ., 45, 4042–4050.

Ialongo, I., Hakkarainen, J., Kivi, R., Anttila, P., Krotkov, N.A., Yang, K., Li, C., Tukiainen, S., Hassinen, S., Tamminen, J., 2015. Validation of satellite SO_2 observations in northern Finland during the Icelandic Holuhraun fissure eruption. Atmos. Meas. Tech. Discuss., 8, 599–621.

IMO, 2008. Revised MARPOL Annex VI of the International Convention for the Prevention of Air Pollution from Ships. International Maritime Organization, viewed 9 September 2020 <http://www.imo.org/en/KnowledgeCentre/IndexofIMOResolutions/Marine-Environment-Protection-Committee-(MEPC)/Documents/MEPC.176(58).pdf>

Joffre, S.M., Laurila, T., Hakola, H., Lindfors, V., Konttinen, S., Taalas, P., 1990. On the effects of meteorological factors on air pollution concentrations and depositions in Finland. In: Kauppi, P., Anttila, P., Kenttämies, K., (eds.). Acidification in Finland, Springer-Verlag, Berlin, pp.43–94.

Jones, A.M., Harrison, R.M., 2011. Temporal trends in sulphate concentrations at European sites and relationships to sulphur dioxide. Atmos. Environ., 45, 873–882.

Kalina, J., White, K.B., Scheringer, M., Přibylová, P., Kukučka, P., Audy, O., Klánová, J., 2019. Comparability of long-term temporal trends of POPs from co-located active and passive air monitoring networks in Europe. Environmental Science, Processes and Impacts, 21, 1132.

Karl, M., Jonson, J. E., Uppstu, A., Aulinger, A., Prank, M., Sofiev, M., Jalkanen, J.-P., Johansson, L., Quante, M., and Matthias, V.: Effects of ship emissions on air quality in the Baltic Sea region simulated with three different chemistry transport models, Atmos. Chem. Phys., 19, 7019–7053.

Karlsson, V., Pyy, K., Saari, H., 2007. Measurement uncertainty of sulphur and nitrogen containing inorganic compounds by 1-stage and 2-stage filter-pack methods. Water Air Soil Pollut., 182, 395–405.

Karlsson, P.E., Klingbeg, J., Engardt, M., Andersson, C., Langner, J., Pihl Karlsson, G., Pleijel, H., 2017. Past, present and future concentrations of ground-level ozone and potential impacts on ecosystems and human health in northern Europe. Sci. Total Environ., 576, 22–35.

Kauppi, P., Anttila, P., Kenttämies, K., (Eds.), 1990. Acidification in Finland. Springer Verlag, 1237 p.

Kerminen, V.-M., Niemi, J.V., Timonen, H., Aurela, M., Frey, A., Carbone, S., Saarikoski, S., Teinilä, K., Hakkarainen, J., Tamminen, J., Vira, J., Prank, M., Sofiev, M., Hillamo, R., 2011. Characterization of a volcanic ash episode in southern Finland caused by the Grimsvötn eruption in Iceland in May 2011. Atmos. Chem. Phys., 11, 12227–12239.

Keuken, M., Roemer, M., van den Elshout, S., 2009. Trend analysis of urban NO_2 concentrations and the importance of direct NO_2 emissions versus ozone/NO_x equilibrium. Atmos. Environ., 43, 4780–4783.

Keuken, M.P., Roemer, M.G.M., Zandveld, P., Verbeek, R.P., Velders, G.J.M., 2012. Trends in primary NO_2 and exhaust PM emissions from road traffic for the period 2000–2020 and

implications for air quality and health in the Netherlands. Atmos. Environ., 54, 313–319.

Kukkonen, J., Salmi, T., Saari, H., Konttinen, M., Kartastenpää, R., 1999. Review of urban air quality in Finland. Boreal Env. Res., 4, 55–65.

Kupiainen, K., Pirjola, P., 2011. Vehicle non-exhaust emissions from the tyre-road interface – effect of stud properties, traction sanding and resuspension. Atmos. Environ., 45, 4141–4146.

Kupiainen, K., Ritola, R., Stojiljkovic, A., Pirjola, L., Malinen, A., Niemi, J., 2016. Contribution of mineral dust sources to street side ambient and suspension PM_{10} samples. Atmos. Environ., 147, 178–189.

Kupiainen, K., Tervahattu, H., Räisänen, M., 2003. Experimental studies about the impact of traction sand on urban road dust composition. The Sci. Total Environ., 308, 175–184.

Kupiainen, K., Tervahattu, H., 2004. The effect of traction sanding on urban suspended particles in Finland. Environ. Monit. Assess., 93, 287–300.

Kupiainen K.J., Tervahattu H., Räisänen M., Mäkelä T., Aurela M., Hillamo R., 2005. Size and composition of airborne particles from pavement wear, tires, and traction sanding. Environ. Sci. Technol., 39, 699–706.

Kurtenbach, R., Kleffmann, J., Niedojadlo, A., Wiesen, P., 2012. Primary NO_2 emissions and their impact on air quality in traffic environments in Germany. Environmental Sciences Europe, 24:21.

Kyllönen, K., Vestenius, M., Anttila, P., Makkonen, U., Aurela, M., Wängberg, I., Nerentorp Mastromonaco, M., Hakola, H., 2020. Trends and source apportionment of atmospheric heavy metals at a subarctic site during 1996–2018. Atmos. Environ., 236, (2020) 117644, <doi.org/10.1016/j.atmosenv.2020.117644>.

Kyrö, E.-M., Väänänen, R., Kerminen, V.-M., Virkkula, A., Petäjä, T., Asmi, A., Dal Maso, M., Nieminen, T., Juhola, S., Shcherbinin, A., Riipinen, I., Lehtipalo, K., Keronen, P., Aalto, P.P., Hari, P., Kulmala, M., 2014. Trends in new particle formation in eastern Lapland, Finland: effect of decreasing sulfur emissions from Kola Peninsula. Atmos. Chem. Phys., 14, 4383–4396.

Leino, K., Riuttanen, L., Nieminen, T., Dal Maso, M., Väänänen, R., Pohja, T., Keronen, P., Järvi, L., Aalto, P.P., Virkkula, A., Kerminen, V.-M., Petäjä, T., Kulmala, M., 2014. Biomass-burning smoke episodes in Finland from Eastern European wildfires. Boreal Env. Res., 19 (suppl. B), 275–292.

LUKE, 2019. Residential firewood consumption, Natural Resources Institute Finland, viewed 3 January 2020, <http://statdb.luke.fi/PXWeb/pxweb/fi/LUKE>.

Makra, L., Matyasovszky, I., Guba, Z., Karatzas, K., Anttila, P., 2011. Monitoring the long-range transport effects on urban PM_{10} levels using 3D clusters of backward trajectories. Atmos. Environ., 45, 2630–2641.

Miyazaki, K., Eskes, H., Sudo, K., Boersma, K.F., Bowman, K., Kanaya, Y., 2017. Decadal changes in global surface NO_x emissions from multi-constituent satellite data assimilation, Atmos. Chem. Phys., 17, 807–837.

Monks, P.S., Archibald, A.T., Colette, A., Cooper, O., Coyle, M., Derwent, R., Fowler, D., Granier, C., Law, K.S., Mills, G.E., Stevenson, D.S., Tarasova, O., Thouret, V., von Schneidemesser, E., Sommariva, R., Wild, O., Williams, M.L., 2015. Tropospheric ozone and its precursors from the urban to the global scale from air quality to short-lived climate forcer. Atmos. Chem. Phys., 15, 8889–8973.

Makkonen, U., 2014. Measurements of inorganic ions and their precursor gases in ambient air. Finnish Meteorological Institute Contributions, 110, 59 pp.

Makkonen, U., Hellén, H., Anttila, P., Ferm, M., 2010. Size distribution and chemical composition of airborne particles in south-eastern Finland during different seasons and wildfire episodes in 2006. Sci. Total Environ., 408, 644–651.

Mavroidis, I., Chaloulakou, A., 2011. Long-term trends of primary and secondary NO_2 production in the Athens area. Variation of the NO_2/NO_x ratio. Atmos. Environ., 45, 38, 6872–6879.

Melkonyan, A., Kuttler, W., 2012. Long-term analysis of NO, NO_2 and O_3 concentrations in North Rhine-Westphalia, Germany. Atmos. Environ., 60, 316–326.

Mielonen, T., Portin, H., Komppula, M., Leskinen, A., Tamminen, J., Ialongo, I., Hakkarainen, J., Lehtinen, K.E.J., Arola, A., 2012. Biomass burning aerosols observed in eastern Finland during the Russian wildfires in summer 2010 — Part 2: Remote sensing. Atmos. Environ., 47, 279–287.

NAPCP, 2019. National Air Pollution Control Programme 2030. Publications of the Ministry of the Environment, 14, 96 p.

Niemi, J.V., Tervahattu, H., Vehkamäki, H., Kulmala, M., Koskentalo, T., Sillanpää, M., Rantamäki, M., 2004. Characterization and source identification of a fine particulate episode in Finland. Atmos. Environ., 38, 5003–5012.

Niemi, J.V., Tervahattu, H., Vehkamäki, H., Martikainen, J., Laakso, L., Kulmala, M., Aarnio, P., Koskentalo, T., Sillanpää, M., Makkonen, U., 2005. Characterization of aerosol particle episodes in Finland caused by wildfires in Eastern Europe. Atmos. Chem. Phys., 5, 2299–2310.

Niemi, J.V., Saarikoski, S., Tervahattu, H., Mäkelä, T., Hillamo, R., Vehkamäki, H., Sogacheva, L., Kulmala, M., 2006. Changes in background aerosol composition in Finland during polluted and clean periods studied by TEM/EDX individual particle analysis. Atmos. Chem. Phys., 6, 5049–5066.

Niemi, J.V., Saarikoski, S., Aurela, M., Tervahattu, H., Hillamo, R., Westphal, D.L., Aarnio, P., Koskentalo, T., Makkonen, U., Vehkamäki, H., Kulmala, M., 2009. Long-range transport episodes of fine particles in southern Finland during 1999–2007. Atmos. Environ., 43, 1255–1264.

Nieminen, T., Asmi, A., Dal Maso, M., Aalto, P., Keronen, P., Petäjä, T., Kulmala, M., Kerminen, V.-M., 2014. Trends in atmospheric new-particle formation: 16 years of observations in a boreal-forest environment. Boreal Env. Res., 19 (suppl. B), 191–214.

O'Driscoll, R., ApSimon, H.M., Oxley, T., Molden, N., Stettler, M.E.J., Thiyagarajah, A., 2016. A Portable Emissions Measurement System (PEMS) study of NO_x and primary NO_2 emissions from Euro 6 diesel passenger cars and comparison with COPERT emission factors. Atmos. Environ., 145, 81–91.

Olstrup, H., Forsberg, B., Orru, H., Nguyen, H., Molnár, P., Johansson, C., 2018. Trends in air pollutants and health impacts in three Swedish cities over the past three decades. Atmos. Chem. Phys., 18, 15705–15723.

Paatero, J., Vesterbacka, K., Makkonen, U., Kyllönen, K., Hellén, H., Hatakka, J., Anttila, P., 2009. Resuspension of radionuclides into the atmosphere due to forest fires. Journal of Radioanalytical and Nuclear Chemistry, 282, 473–476.

Pakkanen, T., Loukkola, K., Korhonen, C., Aurela, M., Mäkelä, T., Hillamo, R., Aarnio, P., Koskentalo, T., Kousa, A., Maenhaut, W., 2001. Sources and chemical composition of atmospheric fine and coarse particles in the Helsinki area. Atmos. Environ., 35, 5381–5391.

Pirjola, L., Kupiainen, K.J., Perhoniemi, P., Tervahattu, H., Vesala, H., 2009. Non-exhaust emission measurement system of the mobile laboratory SNIFFER. Atmos. Environ., 43, 4703−4713.

Pohjola, M., Kousa, A., Kukkonen, J., Härkönen, J., Karppinen, A., Aarnio, P., Koskentalo, T., 2002. The spatial and temporal variation of measured urban PM_{10} and $PM_{2.5}$ in the Helsinki metropolitan area. Water, Air and Soil Pollution: Focus 2(5–6), 189–201.

Portin, H., Mielonen, T., Leskinen, A., Arola, A., Pärjälä E., Romakkaniemi, S., Laaksonen, A., Lehtinen, K.E.J., Komppula, M., 2012. Biomass burning aerosols observed in Eastern Finland during the Russian wildfires in summer 2010 – Part 1: In-situ aerosol characterization. Atmos. Environ., 47, 269–278.

Prank, M., Sofiev, M., Denier van der Gon, H.A.C., Kaasik, M., Ruuskanen, T.M., Kukkonen, J., 2010. A refinement of the emission data for Kola Peninsula based on inverse dispersion modelling, Atmos. Chem. Phys., 10, 10849–10865.

Rafaj, P., Amann, M., Siri, J., Wuester, H., 2014. Changes in European greenhouse gas and air pollutant emissions 1960–2010: decomposition of determining factors. Climatic Change 124, 477–504.

Riuttanen, L., Hulkkonen, M., Dal Maso, M., Junninen, H., Kulmala, M., 2013. Trajectory analysis of atmospheric transport of fine particles, SO_2, NO_x and O_3 to the SMEAR II station in Finland in 1996–2008. Atmos. Chem. Phys., 13, 2153–2164.

Ruoho-Airola, T., 2004. Temporal and regional patterns of atmospheric components affecting acidification in Finland. Finnish Meteorological Institute, Contributions 44.

Ruoho-Airola, T., Anttila, P., Hakola, H., Ryyppö, T., Tuovinen, J.-P., 2015. Trends in the bulk deposition and atmospheric concentration of air pollutants in the Finnish Integrated Monitoring catchment Pallas during 1992–2012. Boreal Env. Res., 20, 553–569.

Räisänen, M., Kupiainen, K., Tervahattu, H., 2003. The effect of mineralogy, texture and mechanical properties of anti-skid and asphalt aggregates on urban dust. Bulletin of Engineering, Geology and the Environment 62, 359–368.

Räisänen, M., Kupiainen, K., Tervahattu, H., 2005. The Effect of mineralogy, texture and mechanical properties of anti-skid and asphalt aggregates on urban dust, Stages II and III. Bulletin of Engineering Geology and the Environment 64, 247–256.

Saarnio, K., Aurela, M., Timonen, H., Saarikoski, S., Teinilä, K., Mäkelä, T., Sofiev, M., Koskinen, J., Aalto, P.P., Kulmala, M., Kukkonen, J., Hillamo, R. 2010. Chemical composition of fine particles in fresh smoke plumes from boreal wild-land fires in Europe. Sci. Total Environ., 408, 2527–2542.

Saarnio, K., Niemi, J.V., Saarikoski, S., Aurela, M., Timonen, H., Teinilä, K., Myllynen, M., Frey, A., Lamberg, H., Jokiniemi, J., Hillamo, R., 2012. Using monosaccharide anhydrides to estimate the impact of wood combustion on fine particles in the Helsinki Metropolitan Area. Boreal Env. Res., 17, 163–183.

Saarikoski, S., Sillanpää, M., Saarnio, K., Hillamo, R., Pennanen, A., Salonen R., 2008. Impact of biomass combustion on urban fine particulate matter in Central and Northern Europe. Water Air Soil Pollut., 191, 265–77.

Saarikoski S., Sillanpää M., Sofiev M., Timonen H., Saarnio K., Teinilä K., Karppinen A., Kukkonen J., Hillamo R., 2007. Chemical composition of aerosols during a major biomass burning episode over Northern Europe in spring 2006: Experimental and modeling assessment. Atmos. Environ., 41, 3577–3589.

Salmi, T., Määttä, A., Anttila, P., Ruoho-Airola, T., Amnell, T., 2002. Detecting trends of annual values of atmospheric pollutants by the Mann-Kendall test and Sen's slope estimates – the Excel template application MAKESENS. Finnish Meteorological Institute, Publications on Air Quality No. 31.

Savolahti, M., Karvosenoja, N., Tissari, J., Kupiainen, K., Sippula, O., Jokiniemi, J., 2016. Black carbon and fine particle emissions in Finnish residential wood combustion: emission projections, reduction measures and the impact of combustion practices. Atmos. Environ., 140, 495–505.

Seinfeld, J.H., Pandis, S.N., 1998. Atmospheric chemistry and physics. From air pollution to climate change. John Wiley and Sons. New York. 1326 p.

Shen, H., Huang, Y., Wang, R., Zhu, D., Li, W., Shen, G., Wang, B., Zhang, Y., Chen, Y., Lu, Y., Chen, H., Li, T., Sun, K., Li, B., Liu, W., Liu, J., Tao, S., 2013. Global atmospheric emissions of polycyclic aromatic hydrocarbons from 1960 to 2008 and future predictions. Environ. Sci. Technol., 47, 6415– 6424.

Sillanpää, M., Saarikoski, S., Hillamo, R., Pennanen, A., Makkonen, U., Spolnik, Z., Van Grieken, R., Koskentalo, T., Salonen, R.O., 2005. Chemical composition, mass size distribution and source analysis of long-range transported wildfire smokes in Helsinki. Sci. Total Environ., 350, 119–135.

Sillanpää, M., Hillamo, R., Saarikoski, S., Frey, A., Pennanen, A., Makkonen, U., Spolnik, Z., Van Grieken, R., Braniš, M., Brunekreef, B., Chalbot, M.-C., Kuhlbusch, T., Sunyer, J., Kerminen, V.-M., Kulmala, M. & Salonen, R.O., 2006. Chemical composition and mass closure of particulate matter at six urban sites in Europe. Atmos. Environ., 40S2, 212–223.

Sofiev, M., Kaasik, M., Hongisto, M., 2003. Model simulations of the alkaline dust distribution from Estonian sources over the Baltic Sea Basin. Water Air Soil Pollut., 146, 211–223.

Stohl, A., Berg, T., Burkhart, J.F., Fjæraa, A.M., Forster, C., Herber, A., Hov, Ø., Lunder, C., McMillan, W.W., Oltmans, S., Shiobara, M., Simpson, D., Solberg, S., Stebel, K., Ström J., Tørseth, K., Treffeisen, R., Virkkunen, K., Yttri, K.E., 2007. Arctic smoke – record high air pollution levels in the European Arctic due to agricultural fires in Eastern Europe. Atmos. Chem. Phys., 7, 511–534.

Stojiljkovic, A., Kauhaniemi, M., Kukkonen, J., Kupiainen, K., Karppinen, A., Denby, B.R., Kousa, A., Niemi, J.V., Ketzel, M., 2019. The impact of measures to reduce ambient air PM_{10} concentrations originating from road dust, evaluated for a street canyon in Helsinki. Atmos. Chem. Phys., 19, 11199–11212.

SYKE, 2019a. Emissions of air pollutants in Finland (in Finnish). Finnish Environment Institute, viewed 23 March 2019,

<https://www.ymparisto.fi/fi-FI/Kartat_ja_tilastot/Ilman_epapuhtauksien_paastot>.

SYKE, 2019b. Emissions of air pollutants in Finland (in Finnish). Finnish Environment Institute, viewed 16 September 2019,

<https://www.ymparisto.fi/fi-FI/Kartat_ja_tilastot/Ilman_epapuhtauksien_paastot>.

Teinilä, K., Aurela, M., Niemi, J., Kousa, A., Petäjä, T., Järvi, L., Hillamo, R., Kangas, L., Saarikoski, S., Timonen, H., 2019. Concentration variation of gaseous and particulate pollutants in the Helsinki city centre—observations from a two-year campaign from 2013–2015. Boreal Env. Res., 24, 115–136.

Tervahattu, H., Hongisto, M., Aarnio, P., Kupiainen, K., Sillanpää, M., 2004. Composition and origins of aerosol during a high PM_{10} episode in Finland. Boreal Env. Res., 9, 335–345.

Tervahattu, H., Kupiainen, K.J., Räisänen, M., Mäkelä, T., Hillamo, R., 2006. Generation of urban road dust from anti-skid and asphalt concrete aggregates. Journal of Hazardous Materials, 132, 39–46.

Timonen, H., Aurela, M., Carbone, S., Saarnio, K., Saarikoski, S., Mäkelä, T., Kulmala, M., Kerminen, V.-M., Worsnop, D. R., Hillamo, R., 2010. High time-resolution chemical characterization of the water-soluble fraction of ambient aerosols with PILS-TOC-IC and AMS. Atmos. Meas. Tech., 3, 1063–1074.

Tørseth, K., Aas, W., Breivik, K., Fjæraa, A.M., Fiebig, M., Hjellbrekke, A.G., Lund Myhre, C., Solberg, S., Yttri, K.E., 2012. Introduction to the European Monitoring and Evaluation Programme (EMEP) and observed atmospheric composition change during 1972–2009, Atmos. Chem. Phys., 12, 5447–5481.

UNECE, 1985. Protocol to the 1979 Convention on Long-Range Transboundary Air Pollution on the reduction of sulphur emissions or their transboundary fluxes by at least 30 per cent. United Nations Economic Commission for Europe, Helsinki.

UNECE, 1988. Protocol to the 1979 convention on long-range transboundary air pollution concerning the control of emissions of nitrogen oxides or their transboundary fluxes. United Nations Economic Commission for Europe, Sofia.

Vestreng, V., Myhre, G., Fagerli, H., Reis, S., Tarrasón, L., 2007. Twenty-five years of continuous sulphur dioxide emission reduction in Europe. Atmos. Chem. Phys., 7, 3663–3681.

Waldén, J., 2009. Metrology of gaseous air pollutants. Finnish Meteorological Institute, Contributions 79.

Waldén, J., Bergius, J., Pohjola, V., Laurila, S., Kuronen, P., Wemberg, A., 2008. Field comparison of CO, SO_2, NO, H_2S and O_3 ambient air measurements and field audit 2006 (in Finnish). Finnish Meteorological Institute, Studies No. 2.

Waldén, J., Hillamo, R., Aurela, M., Mäkelä, T., Laurila, S., 2010. Demonstration of the equivalence of $PM_{2.5}$ and PM_{10} measurement methods in Helsinki 2007–2008 (in Finnish). Finnish Meteorological Institute, Studies No. 3.

Waldén, J., Laurila, S., Lusa, K., Kuronen, P., Waldén, T., Anttila, T., 2015. Interlaboratory comparison exercise and field audit 2011 – measurements of CO, SO_2, NO, and O_3 (in Finnish). Finnish Meteorological Institute, Reports 2015:2.

Waldén, J., Talka, M., Pohjola, V., Häkkinen, T., Lusa, K., Sassi, M.-K., Laurila, S., 2004. The field comparison of carbon monoxide, sulphur dioxide and nitrogen monoxide ambient air measurements and a field audit 2002–2003 (in Finnish). Finnish Meteorological Institute, Publications on Air Quality, No. 35.

Waldén, J., Waldén, T., Laurila, S., Hakola, H., 2017. Demonstration of the equivalence of $PM_{2.5}$ and PM_{10} measurement methods in Kuopio 2014–2015. Finnish Meteorological Institute, Reports 2017:1.

Waldén, J., Vestenius, M., 2018.Verification of PM-analyzers for PM_{10} and $PM_{2.5}$ with the PM reference method. Finnish Meteorological Institute, Reports 2018:2.

Wild, R.J., Dubé, W.P., Aikin, K.C., Eilerman, S.J., Neuman, J.A., Peischl, J., Ryerson T.B., Brown, S.S., 2017. On-road measurements of vehicle NO_2/NO_x emission ratios in Denver, Colorado, USA. Atmos. Environ., 148, 182−189.

Yan, Y., Pozzer, A., Ojha, N., Lin, J., Lelieveld, J., 2018. Analysis of European ozone trends in the period 1995–2014. Atmos. Chem. Phys., 18, 5589–5605.

Yoon, J., Pozzer, A., 2014. Model-simulated trend of surface carbon monoxide for the 2001–2010 decade. Atmos. Chem. Phys., 14, 10465–10482.

Yu, Y., Katsoyiannis, A., Bohlin-Nizzetto, P., Brorström-Lundén, E., Ma, J., Zhao, Y., Wu, Z., Tych, W., Mindham, D., Sverko, E., Barresi, E., Dryfhout-Clark, H., Fellin, P., Hung, H., 2019. Polycyclic aromatic hydrocarbons not declining in Arctic air despite global emission reduction. Environ. Sci. Technol., 53, 2375–2382.

Zheng, B., Chevallier, F., Ciais, P., Yin, Y., Deeter, M.N., Worden, H.M., Wang, Y., Zhang, Q., He, K., 2018. Rapid decline in carbon monoxide emissions and export from East Asia between years 2005 and 2016. Environ. Res. Lett., 13, 044007.

Trends of primary and secondary pollutant concentrations in Finland in 1994–2007

I

Atmospheric Environment 44 (2010) 30–41

Contents lists available at ScienceDirect

Atmospheric Environment

journal homepage: www.elsevier.com/locate/atmosenv

Trends of primary and secondary pollutant concentrations in Finland in 1994–2007

Pia Anttila*, Juha-Pekka Tuovinen

Finnish Meteorological Institute, P.O. Box 503, FI-00101 Helsinki, Finland

ARTICLE INFO

Article history:
Received 20 July 2009
Received in revised form
29 September 2009
Accepted 29 September 2009

Keywords:
Long-term trend
Air quality monitoring
Generalized least-squares (GLS) regression
Autoregressive moving average (ARMA) errors

ABSTRACT

The trends in the atmospheric concentrations of the main gaseous and particulate pollutants in urban, industrial and rural environments across Finland were estimated for the period of 1994–2007. The statistical analysis was based on generalized least-squares regression with classical decomposition and autoregressive moving average (ARMA) errors, which was applied to monthly-averaged data. In addition, three alternative methods were tested. Altogether 102 pollutant time series from 42 sites were analyzed. During the study period, the concentrations of SO_2, CO and NO_x declined considerably and widely across Finland. The SO_2 concentrations at urban and industrial sites were approaching background levels. The reductions in NO_x and CO concentrations were comparable to those in national road traffic emissions. A downward trend was detected in half of the NO_2 time series studied, but the reductions were not as large as would be expected on the basis of emission trends, or from NO_x concentrations. For O_3, neither the mean nor peak values showed large changes in background areas, but were increasing in the urban data. For PM_{10}, five of the 12 urban time series showed decreasing mean levels. However, the highest concentrations, typically attributable to the problematic springtime street dust, did not decrease as widely. The reduction of the long-range transported major ions, mainly driven by the large-scale reduction in sulphur emissions, possibly plays a significant part in the decreases in the mean PM_{10} concentrations. It was shown that the handling of the serially-correlated data with the ARMA processes improved the analysis of monthly values. The use of monthly rather than annually-averaged data helped to identify the weakest trends.

1. Introduction

Within European-wide assessments of air quality, Finland and other Nordic countries are repeatedly highlighted as those least affected by local and regional air pollution (e.g. EEA, 2003, 2007). For Finland, there are several obvious reasons behind this position. Firstly, its location in northernmost Europe, separated from the main continent by the Baltic Sea, reduces the transboundary influence of the major European source areas. Secondly, the population of about 5.3 million people spread over 338,000 km^2 limits the size of cities, and makes Finland one of the most sparsely-populated countries in Europe. Thirdly, as a response to the threat of forest and lake acidification in the late 1970s and the 1980s, considerable emission abatement measures were accomplished within energy production and industry in the 1980s, which also improved local-scale air quality. Moreover, the previous decades had already witnessed a widespread introduction of district heating from combined heat and power plants, which together with increasing stack heights evidently had a positive effect on urban air quality.

The concentrations of most air pollutants are low in Finland as compared to many regions in Europe. For example, the occurrences of values over the limit, threshold and target concentrations set by the European Union (EU) are very rare. However, this does not mean that air pollution no longer poses any potential threats. For example, the background concentration of ozone is high, even in the remote northern parts of the country (e.g. Laurila et al., 2004, 2009); in urban areas, including minor towns, local concentrations of particulate matter (PM) may persist at highly elevated levels for weeks during the so-called springtime dust period (Anttila and Salmi, 2006); small-scale wood combustion increases wintertime concentrations of benzo(a)pyrene in residential areas (Hellén et al., 2008); episodic transboundary pollution from wild fires may cause high PM concentrations over large areas, potentially enriched with carcinogenic polycyclic aromatic hydrocarbons (e.g. Anttila et al., 2008; Niemi et al., 2009). Consequently, while the 1980s can be characterized as a decade of successful reduction of sulphur pollution from energy production and industry, in the 1990s and

* Corresponding author.
E-mail address: pia.anttila@fmi.fi (P. Anttila).

1352-2310/$ – see front matter © 2009 Elsevier Ltd. All rights reserved.
doi:10.1016/j.atmosenv.2009.09.041

2000s it has been necessary to focus attention on ozone, its nitrogen precursors (NO, NO_2) and PM, on account of their adverse effects on human health and ecosystems. Since joining the EU in 1995, Finland has followed the emission control framework developed within the EU. Now, more than ten years later, it seems appropriate to evaluate the development of air quality in Finland during this period.

The objective of this study is to quantify trends in the atmospheric concentrations of the main gaseous and particulate pollutants from 1994 to 2007, to briefly compare these with national emission trends and to discuss the effectiveness of emission control measures. Air pollution trends are estimated for NO_2, NO_x ($NO + NO_2$), O_3, SO_2, CO, PM_{10} (particles of less than 10 μm in aerodynamic diameter), SO_4^{2-} (p), NO_3^- (p) + HNO_3 (g) and NH_4^+ (p) + NH_3 (g) concentrations, measured in various locations across Finland. This is the first national trend study that extensively covers both urban and industrial environments as well as the rural background. The statistical analysis is based on an advanced method that evaluates the serial correlation in a time series, but we also test three other statistical techniques for detecting linear trends.

2. Data

The measurement data used in this study were downloaded from the national air quality database maintained by the Finnish Meteorological Institute (FMI). Air quality monitoring data from all Finnish urban, industrial and background networks are collected annually into this database, which contains a total of 30 networks with about 120 permanent measurement sites. The more comprehensive hourly data, measured with common commercial automatic analyzers, are available from this database from 1994, which was taken as the start year of this study.

The networks themselves are responsible for the quality assurance of their measurements. Nationwide field audits of the operations and quality control systems of the networks, completed with field comparison campaigns, were performed by FMI in 2002–2003 and 2006 (Waldén et al., 2004, 2008). In both comparisons, the results of all the networks were very good for O_3, SO_2 and CO, the deviation from the reference data in nearly all cases being less than 8%, which was set as the limit value for an acceptable result. For NO, which is the compound detected by NO_x analyzers, the results of the former comparison were considered satisfactory, with two-thirds of the results lying within the 8% deviation (Waldén et al., 2004), while in the latter there was only one anomalous observation (Waldén et al., 2008).

The PM measurements have not yet been nationally intercompared. The mass concentrations of PM_{10} presented in this study are measured either by the tapered element oscillating microbalance or the beta-attenuation method. Neither of these methods is necessarily fully compatible with the gravimetric methods, nor with each other, due to the unknown losses of semi-volatile compounds. In this study, we did not apply any corrections for these losses, but included in the trend analysis only those sites at which the PM measurement method had remained the same during the whole study period.

Within the database, the stations are qualitatively classified as urban, suburban or rural according to the type of site surroundings, and as traffic, industry or background in relation to the dominant emission source, in accordance with the European Commission decision 2001/752/EC (EC, 2001). A summary of the measurement sites and components included from each site is presented in Table 1.

The monthly and annual means of NO_2, NO_x, O_3, SO_2, CO and PM_{10} were calculated from the hourly data for the years 1994–2007 for all available monitoring stations. A data completeness of 75% was required for an acceptable monthly value. For further processing, only those time series with at least ten years of valid data between 1994 and 2007 were accepted. Single missing monthly values in the middle of time series (up to a maximum of five per year and site) were replaced by the mean of all accepted values for the month and site in question. In two cases (the Jyväskylä Lyseo and Oulu Keskusta stations), the time series were formed from the combination of two subsets of data, resulting from a minor transfer (a couple of hundred metres) of the site location. In these cases, the hourly and daily data were also visually inspected to ensure that there was no stepwise change in the measured concentrations.

In addition to the continuously-analyzed components listed above, analogous monthly time series were compiled from the daily atmospheric concentrations of sulphate (SO_4^{2-} (p)), nitrate (representing the sum of NO_3^- (p) and HNO_3 (g)) and ammonium (the sum of NH_4^+ (p) and NH_3 (g)) measured at three EMEP (European Monitoring and Evaluation Programme) stations: Korppoo Utö, Kuusamo Oulanka and Virolahti. For these sites, SO_2 concentrations measured with the filter pack technique (Leppänen et al., 2005) were also utilized. The data from the EMEP stations were available up to 2006. Altogether 102 pollutant time series from 42 sites passed the validity criteria (Table 1).

3. Statistical methods

Four different methods were used for estimating the linear trend in the concentration time series: (1) Generalized Least-Squares (GLS) regression with classical decomposition and autoregressive moving average (ARMA) errors, applied to monthly data; (2) Ordinary Least-Squares (OLS) regression applied to deseasonalized monthly data; (3) OLS regression applied to annual data; (4) Non-parametric Sen's slope estimation method with the non-parametric Mann–Kendall significance test, applied to annual data. The GLS-ARMA-based method was used as the reference method, with which the other methods were compared. In this statistical model, the autocorrelation typically present in air pollution concentration time series is accounted for by iteratively applying an ARMA-based correlation structure to the residuals of the fitted linear model.

The seasonal decomposition employed for the methods (1) and (2) above was carried out following Brockwell and Davis (2002). Briefly, the monthly time series were deseasonalized by the classical seasonal decomposition, in which a moving average with a 13-month window (with the first and last observations averaged) was first subtracted from the original data. Next, the mean of the monthly deviations thus obtained was subtracted, to ensure that the mean of the seasonal component is zero. The seasonal component was then calculated by averaging the scaled deviations on a monthly basis. Finally, a deseasonalized time series was produced by subtracting this seasonal component from the original data.

The GLS-ARMA-based trend analysis consisted of the following steps; for additional details, see Brockwell and Davis (2002).

(*i*) A first-order OLS regression model was fitted to the deseasonalized data.

(*ii*) The autocorrelation function (ACF) of the resulting residuals (i.e., the noise obtained by subtracting the estimated seasonal and trend components from the original time series) was calculated. If 5% of the values of the sample ACF up to a lag of 40 were outside the bounds $\pm 1.96/\sqrt{n}$ (corresponding to the 95% confidence interval), where n is the number of observations, it was concluded that the residuals were not independent and identically-distributed (i.i.d.) random variables, and an ARMA model was introduced.

Table 1
Characteristics of the measurement sites.

Network	City/municipality station	Station type	Latitude	Longitude	Population in municipality	Time series included								
						NO_2	NO_x	O_3	SO_2	CO	PM_{10}	SO_4^{2-} (p)	NO_3^- ($g+p$)	NH_4^+ ($g+p$)
FMI[a]	Ilomantsi	Rural/background	63.14301	31.04695	6000			x						
	Inari Raja-Jooseppi	Rural/background	68.47701	28.30310	7000			x	x					
	Korppoo Utö	Rural/background	59.77923	21.37395	<1000	x	x	x	x			x	x	x
	Lammi Evo	Rural/background	61.21578	25.13340	6000			x						
	Muonio Sammaltunturi	Rural/background	67.96715	24.11233	2000			x	x					
	Kuusamo Oulanka	Rural/background	66.32170	29.40157	17 000			x	x			x	x	x
	Virolahti	Rural/background	60.52607	27.67136	4000	x	x	x	x			x	x	x
	Ähtäri	Rural/background	62.58855	24.19189	7000	x	x	x	x					
Harjavalta	Harjavalta Kaleva	Suburban/industry	61.31495	22.13671	8000				x					
	Harjavalta Pirkkala	Suburban/industry	61.33169	22.14330					x					
	Harjavalta Torttila	Suburban/industry	61.32931	22.11613					x					
Imatra	Imatra Rautionkylä	Suburban/industry	61.23792	28.87299	30 000	x			x		x			
	Imatra Teppanala	Suburban/industry	61.15322	28.80917							x			
	Imatra Mansikkala	Suburban/background	61.18921	28.77066					x					
	Lappeenranta Lauritsala	Suburban/industry	61.07169	28.26275	59 000	x	x							
	Lappeenranta Tirilä	Suburban/industry	61.05731	28.24555					x					
Jyväskylä	Jyväskylä Lyseo	Urban/traffic	62.24305	25.74321	82 000	x	x		x		x			
Kajaani	Kajaani Keskusta	Urban/background	64.22444	27.73333	36 000	x	x							
Kotka	Kotka Kirjastotalo	Urban/background	60.46550	26.93893	55 000	x	x							
Kouvola	Kouvola Keskusta	Urban/traffic	60.86717	26.70368	31 000	x	x				x			
	Valkeala Lappakoski	Rural/industry	60.92562	26.67530	11 000				x					
Kuopio	Kuopio Kasarmipuisto	Urban/background	62.89374	27.67010	88 000					x				
Lahti	Lahti Kisapuisto	Urban/background	60.98781	25.64954	98 000	x	x							
	Lahti Vesku	Urban/traffic	60.98389	25.66218		x	x			x				
Oulu	Oulu Keskusta	Urban/traffic	65.00997	25.47132	126 000	x	x			x	x			
	Oulu Pyyköjärvi	Suburban/background	65.04338	25.49790		x	x				x			
	Oulu Nokela	Suburban/industry	64.99466	25.47902					x					
Pietarsaari	Pietarsaari Bottenviksvägen	Urban/traffic	63.67912	22.71837	19 000				x					
Pori	Pori Lampaluoto	Rural/background	61.63648	21.51125	76 000				x					
Neste Oil	Porvoo Mustijoki	Rural/industry	60.36005	25.56605	47 000	x	x		x					
Rauma	Rauma Sinisaari	Suburban/industry	61.12407	21.49343	37 000				x					
Seinäjoki	Seinäjoki Vapaudentie	Urban/traffic	62.78752	22.83432	32 000	x	x							
Tampere	Tampere Lielahti	Suburban/industry	61.52834	23.68503	201 000	x								
Turku	Raisio Keskusta	Urban/traffic	60.48622	22.17112	23 000	x	x				x			
	Raisio Kaanaa	Suburban/industry	60.46928	22.10890					x					
	Turku Kauppatori	Urban/traffic	60.45122	22.26748	174 000	x	x				x			
Varkaus	Varkaus Pääterveysasema	Suburban/industry	62.32958	27.88931	23 000						x			
YTV[b]	Espoo Luukki	Rural/background	60.31349	24.68937	242 000	x	x	x	x					
	Helsinki Töölö	Urban/traffic	60.18539	24.91648	578 000	x	x	x		x	x			
	Helsinki Vallila	Urban/traffic	60.19367	24.96395		x	x		x	x	x			
	Vantaa Tikkurila	Suburban/traffic	60.28696	25.04080	196 000	x	x	x		x	x			

[a] Finnish Meteorological Institute.
[b] Helsinki Metropolitan Area Council.

(*iii*) The optimal ARMA(p, q) model to represent the residuals was selected. The order of the model (i.e., the p and q for the autoregressive and moving-average process, respectively) was determined based on the bias-corrected version of the information criterion of Akaike (AICC) (Hurvich and Tsai, 1989). The model producing the lowest AICC value for the combinations of $p \leq 12$ and $q \leq 12$ was selected (with 12 as an arbitrary choice).

(*iv*) The parameters of the selected ARMA(p, q) process were estimated, together with the coefficients of linear regression, by maximizing the Gaussian likelihood.

(*v*) The maximum likelihood estimation was repeated with the residuals from the updated regression parameters until the parameter values stabilized, providing the final estimates of trend and error structure.

The OLS-based method (2) applied in this study corresponds to step (*i*) above, and is otherwise analogous to the GLS-ARMA method described above, but the autocorrelation of the time series still present after the elimination of trend and seasonality is not accounted for in any way. In the annual OLS method (3), the first-order model was fitted directly to the annually-averaged concentration data.

The analyses described above were conducted with ITSM 2000-V.7.3 (Professional) software (Copyright, 1999, B and D Enterprises Inc. 1 Oct 2005).

The fourth alternative trend analysis option considered in this study was based on non-parametric techniques. The slope of the linear trend was estimated with Sen's method (Sen, 1968), and the Mann–Kendall test was used to evaluate whether the slope estimate is statistically different from zero (Gilbert, 1987; Sirois, 1998). This two-phase method is applicable to a monotonically-increasing or decreasing trend within a time series in the absence of any seasonal variation or other cycles. In practice, this analysis was carried out using the Microsoft Excel template MAKESENS (Salmi et al., 2002) developed at the FMI (available at www.fmi.fi/organization/contacts_25.html). In MAKESENS applications, the most common way to eliminate the seasonal variation has been to limit the analysis to annually-averaged data or to time series of a specific month or season of the year (Ruoho-Airola et al., 2003; Laurila et al., 2004; Tsutsumi et al., 2006; Derwent et al., 2007; Quinn et al., 2007; Berg et al., 2008; Viana et al., 2008; Hole et al., 2009). In this study, MAKESENS was applied to annually-averaged data, thus eliminating seasonal variation, and it was further assumed that no other serial correlation, other than the monotonic trend, exists in the annual time series.

4. Results and discussion

4.1. Nitrogen oxides and ozone

We first discuss the results of the trend analysis carried out with the GLS-ARMA method, which is the reference method of this study. For NO_2 and NO_x concentrations, a decreasing trend was found for all except two rural background sites (Korppoo Utö and Virolahti) and one urban background site (Kotka Kirjastotalo) (Table 2). In half of the 22 NO_2 time series studied, the negative trend was statistically significant ($P < 0.05$). The majority of significant trends (8/11) occurred at urban or suburban traffic and background stations. Of the three remaining stations with significant trend, one was suburban industrial station (Imatra Rautionkylä) and two were rural background stations (Espoo Luukki and Ähtäri). The annual reductions varied between 1.1% and 4.3%. However, in most cases the reduction was within 1–2%, which is less than the reduction in annual NO_x emissions in Finland (−2.1% for total NO_x and −4.3% for road traffic NO_x, Table 3).

For NO_x concentrations, statistically significant negative trends were even more frequent (14/20) than for NO_2; only four rural and two urban background sites did not show a significant downward trend (Table 2). The average annual reductions in NO_x concentrations were also clearly higher than for NO_2, varying within 2.1–5.8% yr^{-1} and typically within 3–4% yr^{-1}. This corresponds well to the reductions in national road vehicle emissions (Table 3). The NO_x trends were also comparable to those detected at five urban stations in the UK in 1993–2006, at which the decreases in NO_x concentration varied within 2.8–4.3% yr^{-1} (Jenkin, 2008).

The time series of NO_2 and NO_x are characterized by a strong seasonal variation, which is captured by the classical decomposition applied as part of the statistical analysis. This is illustrated for three sites in Fig. 1, which shows the original monthly mean time series of NO_2 and NO_x together with the time series obtained from the GLS-ARMA procedure. Of these sites, Oulu Keskusta and Turku Kauppatori are located in urban city centres, while Espoo Luukki is a rural background site on the outskirts of the Helsinki metropolitan area, about 20 km north of central Helsinki. NO_x has its highest concentrations during the coldest and darkest months (November–February), and a minimum in midsummer. NO_2 concentrations also show a minimum in midsummer, but the maximum occurs during the more photochemically-active spring months (Fig. 1).

The more steeply decreasing NO_x trends compared to NO_2 (Table 2 and Fig. 1) suggest that the proportion of NO_2 in NO_x in ambient air has increased. Indeed, this is a general pattern at the urban traffic sites studied, at which high local NO emissions result in a low NO_2-to-NO_x concentration ratio. However, the same development is also visible at many suburban (background or industrial) sites with moderate NO_2/NO_x ratios (Fig. 2). At the rural sites, there is no similar increase in the NO_2/NO_x ratio, which is close to unity, due to the absence of local NO_x emissions and the oxidation of NO in the aged air masses.

Table 3
Estimates of NO_x, CO and SO_2 emissions in Finland (compiled from FEI, 2008; VTT, 2008).

Pollutant	Source	Annual emission Gg yr^{-1}			Change % yr^{-1}
		1994	2000	2006	1994–2006
NO_x	Total	263	210	193	−2.1
	Road traffic	111	78	53	−4.3
CO	Total	606	610	511	−1.1
	Road Traffic	400	333	218	−3.4
SO_2	Total	114	76	85	−2.2

Table 2
Results of the trend analysis of the monthly mean NO_2 and NO_x concentrations based on the GLS-ARMA method. Standard error is shown in parentheses. The yearly changes are shown with their 95% confidence intervals. Statistically significant ($P < 0.05$) trends are shown in bold text.

City/municipality station	Station type	Start	No. of months	NO_2				NO_x			
				ARMA *p,q*	Intercept, μg m^{-3}	Slope, μg m^{-3} $month^{-1}$	Change, % yr^{-1}	ARMA *p,q*	Intercept, μg m^{-3}	Slope, μg m^{-3} $month^{-1}$	Change, % yr^{-1}
Korppoo Utö	Rural/background	Aug-94[a]	161	0,2	5 (0)	0.002 (0.004)	0.5 ± 2.2	1,0	5 (1)	0.01 (0.01)	1.7 ± 3.9
Virolahti	Rural/background	Mar-97[a]	130	2,1	5 (0)	0.003 (0.005)	0.7 ± 2.4	2,1	5 (0)	0.01 (0.01)	1.4 ± 2.3
Ähtäri	Rural/background	Jun-97[a]	127	7,1	3 (0)	−0.003 (0.001)	**−1.4 ± 1.0**	2,0	3 (0)	−0.00 (0.01)	−1.6 ± 4.8
Imatra Rautionkylä	Suburban/industry	Jan-94	168	0,1	12 (0)	−0.022 (0.005)	**−2.1 ± 0.9**				
Lappeenranta Lauritsala	Suburban/industry	Jan-98	120	2,1	14 (0)	−0.013 (0.007)	−1.1 ± 1.1	1,0	28 (1)	−0.08 (0.02)	**−3.3 ± 1.7**
Jyväskylä Lyseo	Urban/traffic	Jan-94	168	1,0	26 (1)	−0.062 (0.010)	**−2.8 ± 0.9**	4,2	60 (3)	−0.25 (0.03)	**−5.1 ± 1.3**
Kajaani Keskusta	Urban/background	Jan-97[b]	132	1,11	20 (2)	−0.013 (0.026)	−0.8 ± 3.0	3,2	30 (2)	−0.04 (0.03)	−1.4 ± 2.5
Kotka Kirjastotalo	Urban/background	Jan-97[c]	132	0,10	13 (2)	0.000 (0.024)	0.0 ± 4.3	3,0	19 (1)	0.00 (0.02)	0.0 ± 2.7
Kouvola Keskusta	Urban/traffic	Jan-94	144	5,2	27 (3)	−0.036 (0.036)	−1.6 ± 3.2	3,3	59 (2)	−0.16 (0.02)	**−3.3 ± 1.0**
Lahti Kisapuisto	Urban/background	Jan-95[d]	156	2,3	24 (1)	−0.087 (0.011)	**−4.3 ± 1.1**	3,1	56 (3)	−0.27 (0.03)	**−5.8 ± 1.4**
Lahti Vesku	Urban/traffic	Jan-94	168	8,2	34 (2)	−0.026 (0.022)	−0.9 ± 1.5	3,3	135 (5)	−0.40 (0.05)	**−3.5 ± 0.9**
Oulu Keskusta	Urban/traffic	Jan-94	168	3,2	35 (1)	−0.055 (0.013)	**−1.9 ± 0.9**	1,1	112 (5)	−0.35 (0.05)	**−3.7 ± 1.1**
Oulu Pyykösjärvi	Suburban/ background	Jan-94	168	0,1	14 (0)	−0.010 (0.005)	**−0.9 ± 0.9**	0,1	26 (1)	−0.05 (0.01)	**−2.3 ± 1.1**
Porvoo Mustijoki	Rural/industry	Jan-94	168	2,6	10 (1)	−0.005 (0.008)	−0.6 ± 1.9	2,2	14 (1)	−0.01 (0.01)	−0.8 ± 1.6
Seinäjoki Vapaudentie	Urban/traffic	Jan-94	168	5,2	20 (1)	−0.009 (0.013)	−0.6 ± 1.6	10,1	50 (1)	−0.10 (0.01)	**−2.4 ± 0.6**
Tampere Lielahti	Suburban/industry	Jan-94	132	3,3	12 (1)	−0.001 (0.008)	−0.1 ± 1.6				
Raisio Keskusta	Urban/traffic	Jan-97[b]	132	1,1	26 (2)	−0.065 (0.028)	**−3.0 ± 2.5**	0,1	70 (3)	−0.23 (0.04)	**−3.9 ± 1.2**
Turku Kauppatori	Urban/traffic	Jan-94	168	6,1	40 (0)	−0.060 (0.003)	**−1.8 ± 0.2**	0,3	86 (4)	−0.27 (0.04)	**−3.8 ± 1.1**
Espoo Luukki	Rural/background	Jan-94	168	1,0	8 (0)	−0.011 (0.005)	**−1.6 ± 1.4**	1,0	10 (1)	−0.02 (0.01)	**−2.3 ± 1.4**
Helsinki Töölö	Urban/traffic	Jan-94	132	4,4	40 (0)	−0.042 (0.003)	**−1.3 ± 0.2**	4,4	156 (2)	−0.60 (0.03)	**−4.6 ± 0.5**
Helsinki Vallila	Urban/traffic	Jan-94	168	2,3	31 (1)	−0.028 (0.009)	**−1.1 ± 0.7**	2,3	72 (3)	−0.19 (0.03)	**−3.2 ± 0.9**
Vantaa Tikkurila	Suburban/traffic	Jan-96	144	2,3	30 (1)	−0.006 (0.010)	−0.2 ± 0.8	2,3	90 (3)	−0.16 (0.03)	**−2.1 ± 0.9**

[a] NO_x started Jan-98; 120 months.
[b] NO_x started Feb-97; 131 months.
[c] NO_x started Feb-98; 119 months.
[d] NO_x started Nov-94; 158 months.

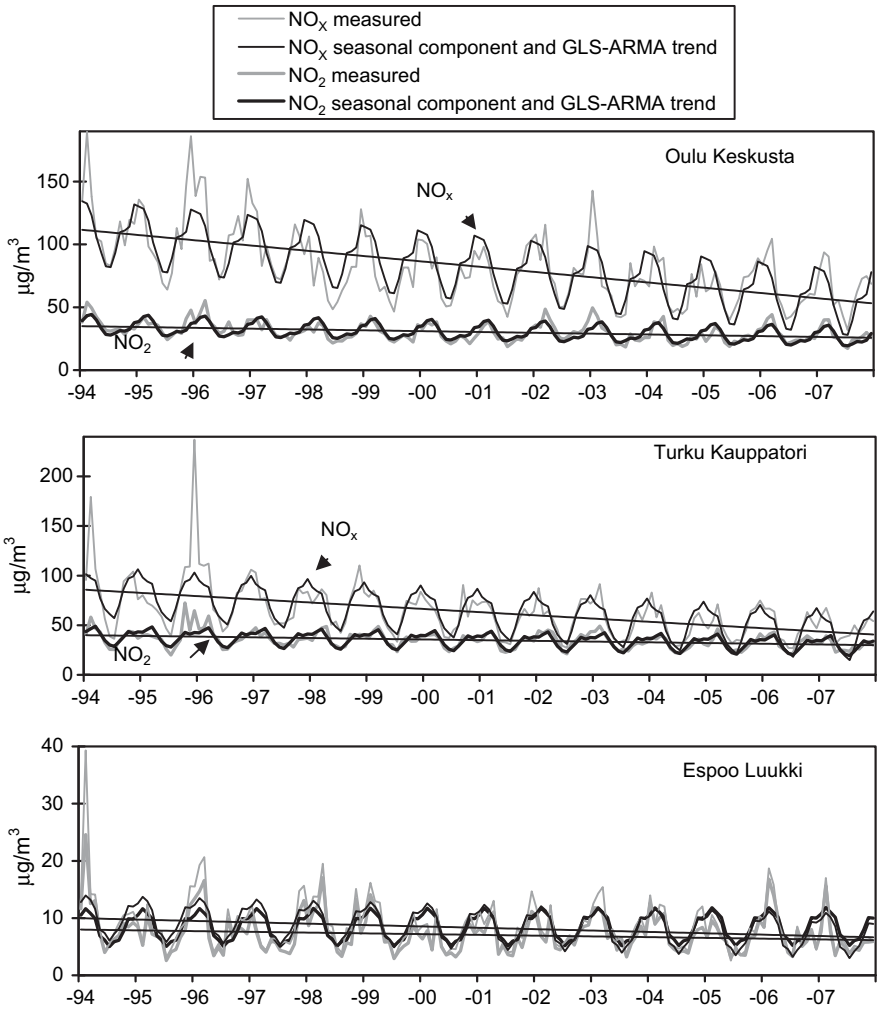

Fig. 1. Monthly mean NO_x and NO_2 concentrations at three measurement sites in 1994–2007. The black lines indicate the seasonal component combined with the GLS-ARMA-estimated trend.

The pattern of much smaller negative or even increasing trends of NO_2 compared to NO_x in traffic-intense environments has been attributed to the increased NO_2/NO_x ratio in vehicular exhaust (Carslaw, 2005; Hueglin et al., 2006). The emissions of diesel vehicles contain higher proportions of NO_2 in NO_x, and it has been proposed that the increasing number of diesel cars, together with the particulate filters and oxidation catalysts employed in modern diesel engines, is the probable cause for the smaller decreases,

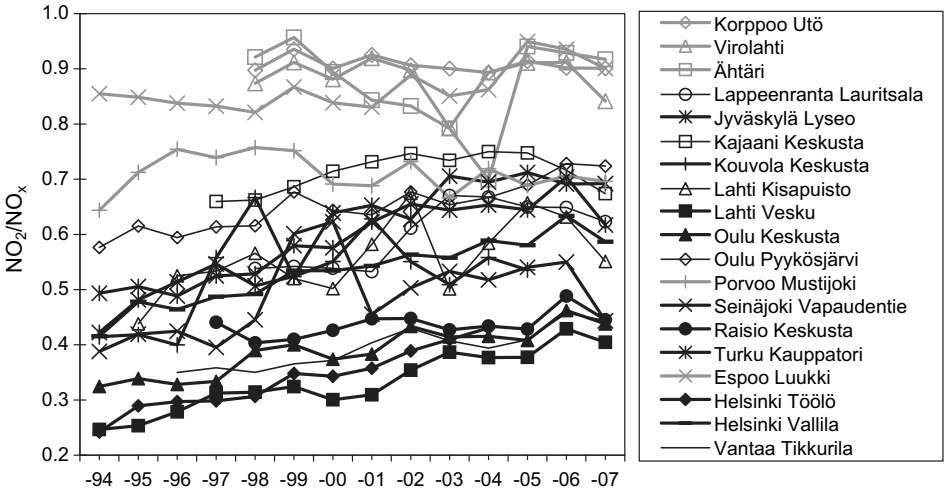

Fig. 2. Annual means of the NO_2/NO_x concentration ratios calculated from the measured monthly means at each site. The urban traffic sites are denoted with thick black lines, rural sites with grey lines and others with thin black lines.

stabilization or even increase of NO_2 concentrations detected in roadside environments (Carslaw and Beevers, 2004; Alvarez et al., 2008). In Finland, the fraction of diesel-powered passenger cars has increased from around 7% in 1994 to 14% in 2007 (AuT, 2009), so the higher NO_2/NO_x ratio in diesel exhaust may partly explain the weaker downward trends of NO_2.

Another important factor contributing to the changes in the atmospheric NO_2-to-NO_x ratio is the atmospheric equilibrium between NO, NO_2 and O_3 (e.g. Keuken et al., 2009). The urban levels of O_3 are controlled by NO_x emissions, as O_3 is effectively depleted by the NO emitted locally. If the oxidation process of NO to NO_2 is limited by the availability of O_3, a decline in NO concentrations does not necessarily lead to a similar decline in NO_2 concentrations.

The temporal development of the mean O_3 concentrations was markedly different from that of nitrogen oxides, as increasing and decreasing trends were equally common (Table 4). Moreover, the only statistically significant ($P < 0.05$) trends estimated with GLS-ARMA were the increases at the three sites located within the Helsinki metropolitan area (Helsinki Töölö, Vantaa Tikkurila and Espoo Luukki). These three sites also show the lowest mean O_3 concentrations of the sites considered (see the intercepts in Table 4), due to the local NO_x emissions.

The rest of the O_3 monitoring sites considered here are located in more remote rural background areas. These sites exhibit mixed and statistically insignificant O_3 trends. The O_3 concentrations at these sites show a clear seasonal variation, with a maximum in April (Fig. 3) and an increase in the mean annual concentration from about 60 μg m^{-3} at 60 °N to about 70 μg m^{-3} at 70 °N. Korppoo Utö is a maritime site on an outer island in the Gulf of Finland and thus O_3 concentrations observed there follow a slightly different seasonal pattern (Laurila, 1999). The three more urban-influenced sites in the Helsinki area also have a spring maximum; however, this maximum tends to extend further into the summer months (Fig. 3).

As a whole, the climate in Finland does not favour photochemical O_3 production, and episodes of high O_3 concentrations are exceptional. In these data covering 14 years and 11 sites, the hourly mean of 180 μg m^{-3}, which is the EU threshold value for informing the public, has been exceeded only during three episodes: in summer 1996 at Lammi Evo, in May 2004 at Vantaa Tikkurila and Espoo Luukki, and in May 2006 at Virolahti.

Similar to our trend estimates, Jenkin (2008) reported increasing annual O_3 trends of 1.6–3.7% yr^{-1} for five urban sites in the UK in 1993–2006. On the other hand, the peak concentrations were decreasing at these sites. This pattern, i.e., reductions in the highest concentrations and increasing or stable mean levels in rural and remote areas, is a common finding in Europe (Brönnimann et al., 2002; Laurila et al., 2004; Derwent et al., 2007; EEA, 2009). To identify the possible trends in peak O_3 concentrations in the present data set, we performed an analogous GLS-ARMA analysis for the monthly 95th percentiles in March–June, the period corresponding to the highest monthly means (Fig. 3). At the rural background sites, statistically significant ($P < 0.05$) trends were only detected for two northern stations (Table 4). At the other background sites, there were no clear trends, which is in accordance with Laurila et al. (2004), who did not find any significant trends for the 99th percentiles of hourly daytime concentrations in May–July during 1989–2001. At the urban traffic sites Helsinki Töölö and Vantaa Tikkurila, the high end of the O_3 distribution also proved to be increasing during 1994–2007 (Table 4).

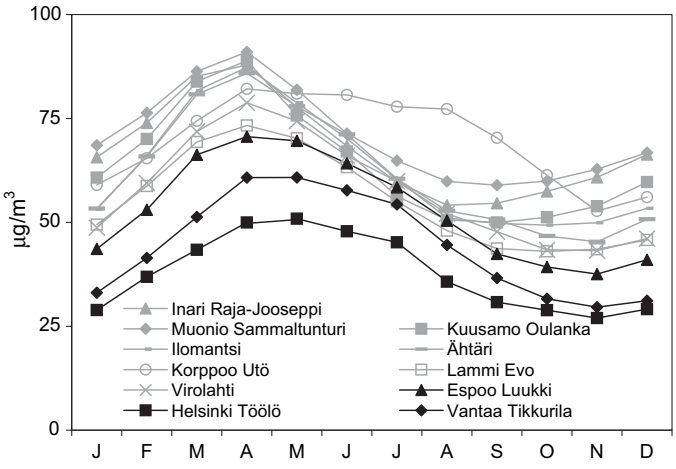

Fig. 3. Monthly mean O_3 concentrations at all measurement sites. The urban-influenced sites are denoted by black lines and the rural sites by grey lines.

Even though the reductions in NO_2 concentrations have not been as strong as would be expected on the basis of emission trends, many downward trends in NO_2 concentrations were detected in this study. This positive development is mostly due to the increased use of three-way catalytic converters in petrol-powered cars. In 2007, as much as 20% of the Finnish petrol car fleet was still without these converters, but in a few years this emission reduction potential will be exhausted (Mäkelä et al., 2008). Moreover, in 2008 Finland adopted a new CO_2-based car tax for passenger cars, which caused an immediate increase (from 29% to 50%) in diesel car sales compared to the previous year (AuT, 2009). The decrease in NO_2 concentrations in the next few years is thus not obvious, due to the completion of the transition to petrol cars with catalytic converters and the accelerating adoption of diesel cars.

Table 4
Results of the trend analysis of the monthly means and the monthly 95th percentiles (March–June) of hourly O_3 concentrations based on the GLS-ARMA method. Standard error is shown in parentheses. The yearly changes are shown with their 95% confidence intervals. Statistically significant ($P < 0.05$) trends are shown in bold text.

City/municipality station	Station type	Start	No. of months	Mean				95th percentile
				ARMA p,q	Intercept, μg m^{-3}	Slope, μg m^{-3} $month^{-1}$	Change, % yr^{-1}	Change, % yr^{-1}
Ilomantsi	Rural/background	Jan-98	120	4,7	65 (2)	−0.036 (0.028)	−0.7 ± 1.0	−0.6 ± 1.4
Inari Raja-Jooseppi	Rural/background	Jan-94	168	1,0	70 (1)	−0.022 (0.012)	−0.4 ± 0.4	**0.1 ± 0.1**
Korppoo Utö	Rural/background	Jan-94	168	1,1	69 (2)	0.004 (0.021)	0.1 ± 0.7	0.3 ± 0.7
Lammi Evo	Rural/background	Feb-95	155	2,0	54 (2)	0.014 (0.025)	0.3 ± 1.1	−0.1 ± 0.3
Muonio Sammaltunturi	Rural/background	Mar-94	166	1,1	71 (2)	−0.005 (0.017)	−0.1 ± 0.6	**0.4 ± 0.2**
Kuusamo Oulanka	Rural/background	Jan-94	168	2,2	65 (2)	−0.012 (0.016)	−0.2 ± 0.6	0.2 ± 0.4
Virolahti	Rural/background	Jan-94	168	1,1	56 (3)	0.017 (0.028)	0.4 ± 1.2	0.4 ± 0.9
Ähtäri	Rural/background	Jun-97	127	1,0	63 (2)	−0.018 (0.023)	−0.3 ± 0.9	0.1 ± 0.2
Espoo Luukki	Rural/background	Jan-94	168	5,1	53 (0)	0.009 (0.003)	**0.2 ± 0.2**	0.1 ± 0.3
Helsinki Töölö	Urban/traffic	Jan-94	132	6,5	33 (0)	0.067 (0.006)	**2.4 ± 0.5**	**1.1 ± 0.7**
Vantaa Tikkurila	Suburban/traffic	Jan-94	168	6,2	43 (0)	0.023 (0.003)	**0.7 ± 0.2**	**0.4 ± 0.2**

Table 5
Results of the trend analysis of the monthly mean SO_2 concentrations based on the GLS-ARMA method. Standard error is shown in parentheses. The yearly changes are shown with their 95% confidence intervals. Statistically significant ($P < 0.05$) trends are shown in bold text.

City/municipality station	Station type	Start	No. of months	ARMA *p,q*	Intercept, μg m^{-3}	Slope, μg m^{-3} $month^{-1}$	Change, % yr^{-1}
Inari Raja-Jooseppi	Rural/background	Jan-98	120	1,0	2.4 (0.2)	−0.011 (0.003)	**−5.7 ± 3.2**
Korppoo Utö	Rural/background	Jan-94	168	1,0	1.5 (0.2)	−0.005 (0.002)	**−4.2 ± 2.5**
Muonio Sammaltunturi	Rural/background	Jan-98	120	0,10	1.2 (0.2)	−0.005 (0.003)	−5.0 ± 5.5
Kuusamo Oulanka	Rural/background	Jan-94	168	0,12	1.2 (0.1)	−0.004 (0.001)	**−3.9 ± 1.8**
Virolahti	Rural/background	Jan-94	168	1,0	2.7 (0.3)	−0.011 (0.003)	**−4.7 ± 2.6**
Ähtäri	Rural/background	Jun-97	127	0,1	0.8 (0.1)	−0.002 (0.001)	**−3.4 ± 3.1**
Harjavalta Kaleva	Suburban/industry	Feb-94	167	0,10	8.1 (1.8)	−0.017 (0.019)	−2.6 ± 5.5
Harjavalta Pirkkala	Suburban/industry	Feb-94	167	1,12	4.9 (1.3)	−0.019 (0.013)	−4.6 ± 6.3
Harjavalta Torttila	Suburban/industry	Feb-94	167	7,4	7.7 (1.6)	−0.032 (0.016)	**−5.1 ± 4.8**
Imatra Rautionkylä	Suburban/industry	Feb-94	167	0,1	3.6 (0.3)	−0.012 (0.003)	**−4.0 ± 1.9**
Imatra Mansikkala	Suburban/background	Jan-98	168	0,4	2.4 (0.3)	−0.008 (0.004)	**−3.8 ± 3.9**
Lappeenranta Tirilä	Suburban/industry	Jan-94	168	0,1	3.3 (0.2)	−0.008 (0.002)	**−2.8 ± 1.5**
Jyväskylä Lyseo	Urban/traffic	Jan-94	168	4,8	3.6 (0.4)	−0.018 (0.004)	**−5.9 ± 2.9**
Valkeala Lappakoski	Rural/industry	Jan-94	144	3,2	1.1 (0.4)	0.005 (0.005)	6.0 ± 10.5
Oulu Nokela	Suburban/industry	Jan-94	168	1,1	2.5 (0.3)	−0.003 (0.003)	−1.4 ± 2.9
Pietarsaari Bottenviksvägen	Urban/traffic	Jan-97	133	1,0	2.9 (0.2)	−0.012 (0.003)	**−4.9 ± 2.1**
Pori Lampaluoto	Rural/background	Jan-94	144	1,0	2.4 (0.3)	−0.016 (0.003)	**−8.0 ± 3.2**
Porvoo Mustijoki	Rural/industry	Jan-94	168	9,4	2.8 (0.3)	−0.008 (0.003)	**−3.2 ± 2.3**
Rauma Sinisaari	Suburban/industry	Jan-94	168	3,0	7.6 (0.8)	−0.035 (0.008)	**−5.6 ± 2.6**
Raisio Kaanaa	Suburban/industry	Jan-94	168	3,2	3.9 (0.4)	−0.004 (0.004)	−1.3 ± 2.2
Espoo Luukki	Rural/background	Jan-94	168	2,1	2.1 (0.3)	−0.005 (0.003)	−2.6 ± 3.3
Helsinki Vallila	Urban/traffic	Jan-94	168	0,1	5.3 (0.3)	−0.013 (0.003)	**−2.9 ± 1.4**

4.2. Sulphur dioxide and carbon monoxide

Atmospheric SO_2 concentrations have declined quite uniformly in 1994–2007; of the 22 SO_2 time series studied, only one industrial measurement site showed an increasing (but statistically insignificant) trend (Table 5).

At the remote rural background sites, relatively high decreases (up to −5.7% yr^{-1}) were detected (Table 5). Of these stations, Inari Raja-Jooseppi and Muonio Sammaltunturi are located in northern Finland, an area affected by the industrial emissions in the Kola Peninsula (e.g. Tuovinen et al., 1993). Korppoo Utö is located in the southern outer archipelago, and Virolahti is in the south-eastern border area, only 160 km from the metropolis of St Petersburg. The fact that the relative reductions in SO_2 concentrations at these sites are larger than the average reduction rate of national SO_2 emissions (about −2.2% yr^{-1}, Table 3) probably reflects the air pollution abatement measures adopted in neighbouring countries and other European source areas. Overall, we can conclude that the decline of SO_2 concentrations in Finnish background areas, which already started in the 1980s (Ruoho-Airola et al., 2003), has continued in the 2000s.

Urban and industrial SO_2 concentrations have also declined, and are currently approaching the background levels. Even at the beginning of the study period, the lowest urban and industrial SO_2 concentrations were already very close to the background levels and shared the same seasonal variation (Fig. 4a and b): the highest concentrations occur in December–February, when the emissions from energy production are at their highest level, while the removal and transformation processes are then at their weakest. A few sites showed higher concentrations and an irregular (Harjavalta Torttila and Rauma Sinisaari) or anomalous seasonal variation (Harjavalta Kaleva, with a maximum in May–June) (Fig. 4c), suggesting that individual local industrial sources controlled the observed SO_2 concentrations. All (except one) of the SO_2 time series converged to about 2–3 μg m^{-3} at the end of the time series.

In urban areas, motor vehicles have a strong influence on ambient CO concentrations, but this pollutant is efficiently removed by three-way catalytic converters. As a result, road traffic emissions in Finland have lessened by 3.4% yr^{-1} during the study period (Table 3). The concentration reductions at the six urban monitoring stations available for this study have also been substantial, annual reductions varying between 2.9% and 7.0% (Table 6). Kuebler et al. (2001) and Zamboni et al. (2009) reported similar downward trends of urban and suburban CO concentrations in Switzerland and Italy, respectively, and concluded that these correlate well with the road traffic emission reductions in these countries.

As a whole, the primary pollutants SO_2 and CO exhibit the largest relative reductions of all the components studied here. Their atmospheric concentrations have decreased strongly during the past two decades also in many parts of Europe (EEA, 2007). While SO_2 and CO nowadays play a lesser role as air pollutants, these compounds are still of importance, due to their climatic effects, CO producing indirect radiative forcing and SO_2 being the precursor of sulphate aerosols.

4.3. Particulate matter

Of the 12 time series of monthly mean PM_{10} concentrations studied, nine showed decreasing trends, of which five were statistically significant ($P < 0.05$) (Table 7). However, three increasing trends were also detected: the traffic-dominated sites in Kouvola (statistically insignificant) and Raisio (significant), and the industrial site in Varkaus (insignificant). The prevalence of decreasing trends would initially suggest that the emission reduction efforts for PM_{10} have had some limited success.

In Finland, the direct primary PM_{10} emissions of anthropogenic origin, i.e., from energy production, industry, traffic and agriculture, have only been estimated since 2000. The estimates have varied within the range 45–57 Gg (in 2000–2007) without a clear trend (FEI, 2008). We consider this time series too short to be linked to the detected trends in ambient PM_{10} concentrations. The interpretation is further complicated by the fact that the majority of our PM_{10} measurement sites are strongly influenced by traffic, in which case the non-exhaust emissions may constitute a more significant contributor to the PM_{10} concentrations than those related to exhaust emissions. In Finnish conditions, the road dust raised by vehicles can make up a considerable portion of the airborne PM_{10}. Dust formation is enhanced by the common use of studded tyres and gravelling as an antiskid treatment. Dust raised by traffic emerges especially as high short-term concentration peaks during the snowmelt period in spring in dry conditions (e.g. Anttila and Salmi, 2006).

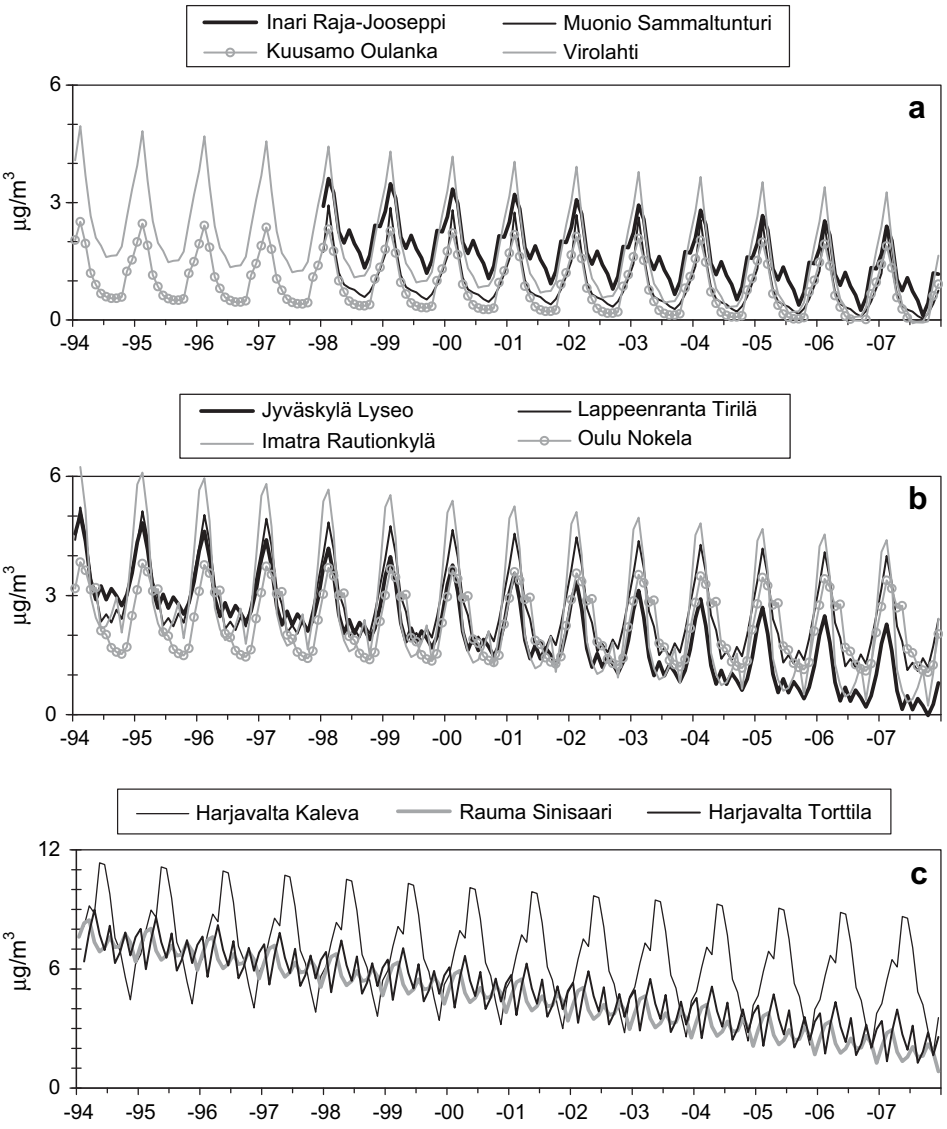

Fig. 4. The GLS-ARMA-smoothed monthly SO_2 time series (seasonal component and estimated trend) at selected rural background (a) and urban sites (b and c).

The role of road dust during the PM_{10} concentration peak is clearly depicted in the present data, too. At the majority of the sites studied, the monthly mean peaked in April, but in south-western Finland (Raisio and Turku) it already occurred in March. On the other hand, the Imatra Teppanala industrial station showed a different kind of seasonal cycle and the lowest seasonal amplitude of all sites, suggesting a different source contribution, probably with a significant industrial component (Fig. 5).

To study whether the highest concentrations, mainly attributable to street dust, have decreased, we conducted an analogous trend analysis for the monthly 95th percentiles of the hourly PM_{10} concentrations in February–May (Table 7, Fig. 5). Compared to the mean values, in most cases the peak concentrations either decreased less or the slope turned positive or the increasing trend strengthened. Four statistically significant trends were detected for both increases and decreases. Thus, in terms of air pollution abatement, the results of this analysis are less favourable than those for the monthly means. Our results suggest that the measures taken to reduce the yearly street dust problem have not in general been successful. In any case, the reduction of street dust does not serve as

Table 6
Results of the trend analysis of the monthly mean CO concentrations based on the GLS-ARMA method. Standard error is shown in parentheses. The yearly changes are shown with their 95% confidence intervals. Statistically significant ($P < 0.05$) trends are shown in bold text.

City station	Station type	Start	No. of months	ARMA p,q	Intercept, mg m^{-3}	Slope, mg m^{-3} $month^{-1}$	Change, % yr^{-1}
Kuopio Kasarmipuisto	Urban/background	Jan-94	124	2,4	0.31 (0.03)	−0.0015 (0.0004)	**−5.8 ± 2.9**
Lahti Vesku	Urban/traffic	Jan-94	168	3,3	0.55 (0.07)	−0.0015 (0.0007)	**−3.3 ± 3.0**
Oulu Keskusta	Urban/traffic	Jan-94	168	3,5	0.97 (0.11)	−0.0057 (0.0010)	**−7.0 ± 2.4**
Helsinki Töölö	Urban/traffic	Jan-94	132	0,9	0.98 (0.04)	−0.0043 (0.0005)	**−5.3 ± 1.2**
Helsinki Vallila	Urban/traffic	Jan-94	132	1,0	0.46 (0.03)	−0.0011 (0.0003)	**−2.9 ± 1.7**
Vantaa Tikkurila	Suburban/traffic	Mar-96	142	3,6	0.66 (0.05)	−0.0021 (0.0006)	**−3.7 ± 2.3**

Table 7
Results of the trend analysis of the monthly means and the monthly 95th percentiles (February–May) of hourly PM_{10} concentrations based on the GLS-ARMA method. Standard error is shown in parentheses. The yearly changes are shown with their 95% confidence intervals. Statistically significant ($P < 0.05$) trends are shown in bold text.

City station	Station type	Start	No. of months	Mean				95th percentile
				ARMA *p,q*	Intercept, μg m^{-3}	Slope, μg m^{-3} $month^{-1}$	Change, % yr^{-1}	Change, % yr^{-1}
Imatra Rautionkylä	Suburban/industry	Apr-95	141	2,1	13.9 (0.5)	−0.006 (0.007)	−0.5 ± 1.1	0.0 ± 1.9
Imatra Teppanala	Suburban/industry	Jan-96	144	2,2	19.8 (1.1)	−0.046 (0.013)	**−2.8 ± 1.6**	**−2.1 ± 1.4**
Jyväskylä Lyseo	Urban/traffic	Jan-94	156	1,0	15.3 (0.9)	−0.011 (0.009)	−0.9 ± 1.5	−0.7 ± 2.0
Kouvola Keskusta	Urban/traffic	Jan-94	144	2,5	18.5 (1.2)	0.024 (0.014)	1.6 ± 1.8	0.2 ± 2.3
Oulu Keskusta	Urban/traffic	Feb-94	167	1,0	20.9 (0.6)	−0.009 (0.006)	−0.5 ± 0.7	**−1.0 ± 1.0**
Oulu Pyykösjärvi	Suburban/background	Jan-94	168	2,2	13.1 (0.4)	−0.008 (0.004)	**−0.7 ± 0.7**	**1.4 ± 1.3**
Raisio Keskusta	Urban/traffic	Jul-96	138	2,2	12.5 (0.5)	0.021 (0.006)	**2.0 ± 1.1**	**4.2 ± 0.8**
Turku Kauppatori	Urban/traffic	Jul-96	139	0,1	20.1 (0.8)	−0.027 (0.010)	**−1.6 ± 1.2**	**−1.1 ± 0.6**
Varkaus Pääterveysas.	Suburban/industry	Jan-98	120	4,2	10.8 (0.3)	0.007 (0.004)	0.8 ± 0.9	**2.6 ± 1.4**
Helsinki Töölö	Urban/traffic	Jan-94	132	4,2	28.1 (1.0)	−0.054 (0.013)	**−2.3 ± 1.1**	**−1.9 ± 0.6**
Helsinki Vallila	Urban/traffic	Jan-97	132	0,12	21.3 (0.8)	−0.020 (0.010)	**−1.1 ± 1.1**	0.3 ± 1.0
Vantaa Tikkurila	Suburban/traffic	Jan-98	120	0,12	21.0 (0.6)	−0.005 (0.009)	−0.3 ± 1.0	**1.3 ± 1.6**

a plausible explanation for the decreasing trends in mean PM_{10} concentrations found in this study.

The secondary sulphate and nitrate aerosols are among the main contributors to PM_{10} (e.g. Harrison et al., 2008). At the three rural background sites from which such data were available, the sulphate and nitrate trends were similar to those of the corresponding primary compounds SO_2 and NO_x (Tables 2, 5 and 8). Significant decreasing trends were detected for SO_4^{2-} (p), which was also the case for SO_2, while neither NO_x nor NO_3^- ($g + p$) showed a statistically significant trend at these sites; there was no trend in the monthly mean NH_4^+ ($g + p$) concentrations, either (Table 8).

Despite the small changes in NO_3^- and NH_4^+ concentrations, the SO_4^{2-} concentrations and their trends were large enough at all three sites to produce a statistically significant decreasing trend in the combined mass concentration of SO_4^{2-}, NO_3^- and NH_4^+. The annual decreases of this sum concentration were $-1.6 \pm 0.6\%$ yr^{-1}, $-1.6 \pm 1.4\%$ yr^{-1} and $-2.3 \pm 1.0\%$ yr^{-1} at Korppoo Utö, Oulanka and Virolahti, respectively.

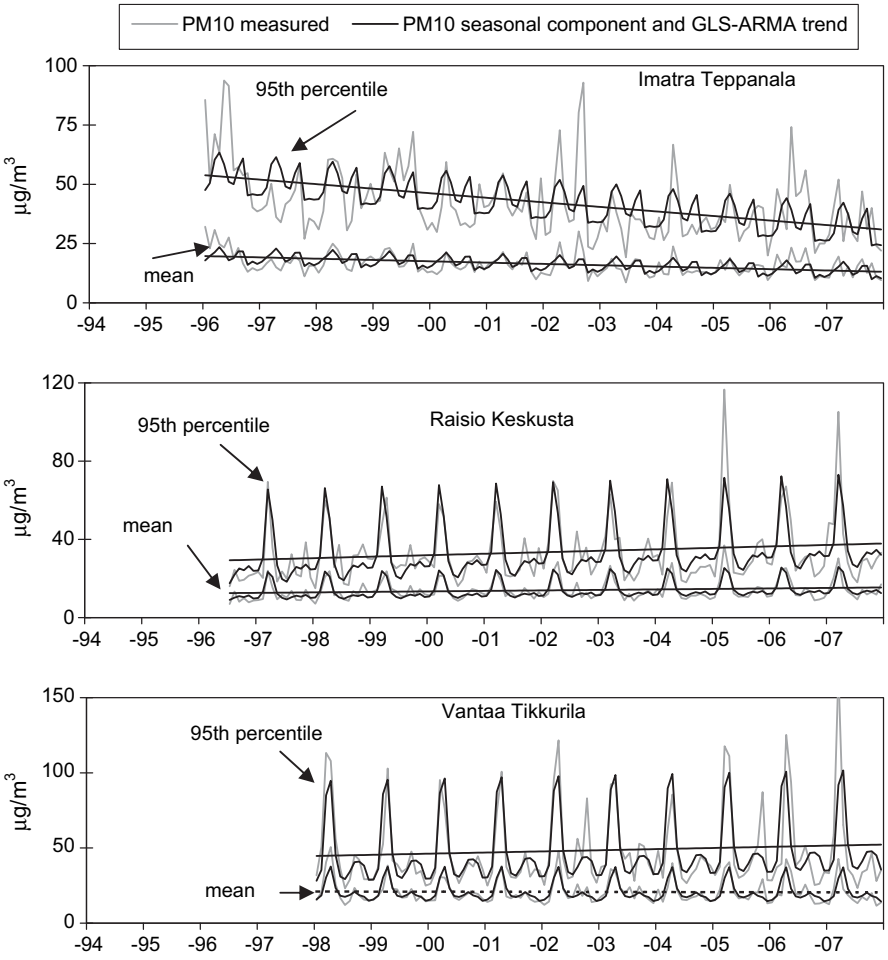

Fig. 5. Monthly means and the monthly 95th percentiles of the hourly PM_{10} concentrations at three measurement sites (grey lines). The black lines indicate the seasonal component with the GLS-ARMA-estimated trend. A solid straight line indicates a statistically significant trend and a dotted line an insignificant trend.

Table 8
Results of the trend analysis of the monthly mean SO_4^{2-} (p), NO_3^- ($g + p$) and NH_4^+ ($g + p$) concentrations based on the GLS-ARMA method. Standard error is shown in parentheses. The yearly changes are shown with their 95% confidence intervals. Statistically significant ($P < 0.05$) trends are shown in bold text. All sites are of rural/background type and each time series for 1994–2006 consists of 156 months.

Municipality station	ARMA p,q	Intercept, μg m^{-3}	Slope, μg m^{-3} month^{-1}	Change, % yr^{-1}
SO_4^{2-} (p)				
Korppoo Utö	1,0	2.6 (0.1)	−0.006 (0.001)	**−2.8 ± 0.9**
Kuusamo Oulanka	2,2	1.4 (0.1)	−0.002 (0.001)	**−1.7 ± 1.7**
Virolahti	1,0	3.0 (0.1)	−0.008 (0.001)	**−3.2 ± 0.8**
NO_3^- ($g + p$)				
Korppoo Utö	9,2	1.8 (0.1)	−0.000 (0.001)	−0.0 ± 1.3
Kuusamo Oulanka	1,0	0.3 (0.0)	0.000 (0.000)	0.0 ± 0.0
Virolahti	3,0	1.3 (0.1)	0.000 (0.001)	0.0 ± 1.8
NH_4^+ ($g + p$)				
Korppoo Utö	2,2	0.7 (0.0)	−0.000 (0.000)	−0.0 ± 0.0
Kuusamo Oulanka	2,2	0.2 (0.0)	0.000 (0.000)	0.0 ± 0.0
Virolahti	1,9	1.1 (0.2)	−0.001 (0.002)	−1.1 ± 4.3

The combined concentration of the three main inorganic ions at Utö, Oulanka and Virolahti were 5.1 μg m^{-3}, 1.9 μg m^{-3} and 5.4 μg m^{-3}, respectively (representing the sum of the intercepts of the trend lines in 1994, Table 8). These are not negligible in magnitude compared with the PM_{10} concentration at the sites with the lowest concentrations considered in this study (10–15 μg m^{-3}). Thus it is possible that the reduction in the long-range transported major ions, which is mainly driven by the large-scale reduction in sulphur emissions, plays a significant part in the decreasing PM_{10} mean levels, even though the stations measuring PM_{10} are located in urban areas. Indeed, when we subtract the $SO_4^{2-} + NO_3^- + NH_4^+$ concentration measured at Virolahti and Oulanka from the PM_{10} concentration at the nearest urban stations of Imatra Rautionkylä and Oulu Pyykösjärvi, respectively, the decreasing trends in the residual time series weaken markedly. At Imatra Rautionkylä −0.5% yr^{-1} changes to a (statistically insignificant) increase of 0.6 ± 1.4% yr^{-1}, while at Oulu Pyykösjärvi the negative trend is reduced from −0.7% yr^{-1} to −0.3 ± 0.9% yr^{-1}.

4.4. Comparison between the different trend analysis methods

The results of the comparison of the different trend analysis methods are summarized in Table 9, which presents the annual change in the time series estimated with the four methods described in Section 3. The GLS-ARMA and OLS methods predict close-to-equal slopes; in 64 out of 93 cases the differences were less than 10%. The poorest match between the GLS-ARMA and OLS slopes occurred for O_3, for which only 1/4 of the estimated slopes were within ±10%. While the magnitudes of the slopes were quite comparable, the statistical significance of the trends varied a lot between the methods. The OLS method indicated a significant trend much more frequently than GLS-ARMA for the monthly deseasonalized time series (except for CO). Due to the unaccounted residual serial correlation, the estimates of the standard error in the OLS analysis were underestimated, which lead to a biased interpretation of the precision of the parameter estimates. The most frequently overestimated significance was also that of the O_3 concentration trend. The poorest agreement between the GLS-ARMA and OLS-based trends of O_3 reflects the complicated autocorrelative structure involved in the time series of this compound, which is not adequately captured by the classical decomposition.

The simplest trend analysis method employed in this study, i.e., OLS applied to annual mean concentrations, yielded slopes similar to GLS-ARMA; in 58 out of 93 cases the slopes were within ±10% of those estimated by GLS-ARMA. Especially the trends of NO_x were identified accurately with OLS; in 17 out of 20 cases the slopes were within ±10%, and in all cases the significance estimates were consistent with GLS-ARMA in terms of the $P = 0.05$ limit. As a whole, however, the annual OLS method identified fewer significant trends than GLS-ARMA (or OLS with monthly data). This result supports the presumption that annual averaging removes most of the serial correlation in the air pollution time series, so that standard errors can be estimated without any significant bias. On the other hand, the small number of data points (from 10 to 14), together with the only moderate trends, limits the capability of the annual OLS to detect significant trends.

The non-parametric MAKESENS-based (MKS) predictions for the trends differed most from those estimated with GLS-ARMA; only 33 out of 93 cases were within ±10%. However, considering the widely-differing methodological approaches involved, this may be considered a robust result. The predicted significances were more consistent with respect to the $P = 0.05$ limit than was the case for OLS, but slightly worse than for the annual OLS. The majority of the differences were due to underestimation by MKS (i.e., fewer significant trends), but some opposite cases occurred as well. The best agreement with the GLS-ARMA method was in this case too found for NO_x; almost half of the slopes were within ±10%, and the statistical significance rating by MSK was fully consistent with that by GLS-ARMA.

The trend analysis based on the GLS-ARMA method detected 10–20% more cases with significant trends than did the OLS and MKS methods applied to annual data. The handling of serial correlation with the ARMA processes improves the analysis of monthly values and makes it possible to increase the effective number of degrees of freedom. In this way the characteristics of the original data are more thoroughly utilized in the trend analysis. As a whole, the comparison of different methods shows that serial correlation should be taken into account in trend estimation when using monthly time series of air pollutant concentrations, and as such gives a good motivation for the GLS-ARMA model applied in this study.

5. Conclusions

The statistical trend analysis carried out in this study indicates that the concentrations of the primary pollutants SO_2 and CO have declined considerably in Finland during the study period 1994–2007. In remote rural background areas, downward linear SO_2 trends of up to −5.7% yr^{-1} were detected. The high relative reductions reflect the efficient air pollution abatement measures, most probably also those taken in neighbouring countries and other European source areas. Urban and industrial SO_2 concentrations have also declined and currently approach background levels. For CO, concentration reductions at the six urban monitoring stations available for this study have been substantial, and are comparable to the reductions of emissions from road traffic.

For the secondary pollutants O_3 and NO_2, the progress in air quality improvement has been limited. In background areas, the mean O_3 concentration did not decrease at any site, while for the springtime peak concentration an increasing trend was detected at the two northernmost sites. Within the Helsinki metropolitan area (the only urban O_3 data available), the concentrations increased. While the downward NO_x trends were frequent and strong, corresponding to the successful reduction of direct NO emissions from petrol cars, for NO_2 the downward trends detected in urban areas were clearly fewer and weaker. This may be partly due to the increased proportion of diesel-powered passenger cars and their higher direct NO_2 emissions. Another explanation lies in changes in the atmospheric NO_x–O_3 equilibrium.

Table 9
Linear trends estimated with different statistical methods from monthly or annual mean concentrations (μg m^{-3} yr^{-1}, CO:mg m^{-3} yr^{-1}). Statistically significant ($P < 0.05$) results are shown in bold text. GLS = Generalized Least-Squares regression with classical decomposition and ARMA errors, applied to monthly data; OLS = Ordinary Least-Squares regression applied to deseasonalized monthly data; OLSa = OLS regression applied to annual data; MKS = Sen's slope estimation method with the Mann–Kendall significance test, applied to annual data.

City/municipality station	NO_2				NO_x				O_3				SO_2				CO				PM_{10}			
	GLS	OLS	OLSa	MKS	GLS	OLS	OLSa	MKS	GLS	OLS	OLSa	MKS	GLS	OLS	OLSa	MKS	GLS	OLS	OLSa	MKS	GLS	OLS	OLSa	MKS
Ilomantsi									−0.43	**−0.42**	−0.42	−0.30												
Inari Raja-Jooseppi									−0.27	**−0.28**	**−0.28**	**−0.25**	**−0.14**	**−0.13**	**−0.13**	**−0.14**								
Korppoo Utö	0.03	0.03	0.03	−0.01	0.1	**0.1**	0.1	0.0	0.05	0.00	−0.01	−0.03	**−0.06**	**−0.06**	**−0.06**	**−0.04**								
Lammi Evo									0.17	**0.19**	0.17	−0.09												
Muonio Sammaltunturi									−0.05	**−0.04**	−0.03	−0.04	−0.06	−0.04	−0.04	−0.05								
Kuusamo Oulanka									−0.15	**−0.18**	−0.18	−0.14	**−0.05**	**−0.05**	**−0.05**	**−0.05**								
Virolahti	0.04	0.03	0.05	0.06	0.1	**0.1**	0.1	0.1	0.20	**0.13**	0.12	0.23	**−0.13**	**−0.12**	**−0.12**	**−0.11**								
Ähtäri	**−0.04**	−0.05	−0.06	−0.08	−0.1	0.0	0.0	−0.1	−0.22	**−0.17**	−0.10	−0.18	**−0.03**	−0.03	−0.03	−0.04								
Harjavalta Kaleva													−0.21	**−0.20**	−0.23	0.05								
Harjavalta Pirkkala													−0.23	**−0.13**	−0.14	−0.10								
Harjavalta Torttila													**−0.39**	**−0.27**	−0.28	−0.15								
Imatra Rautionkylä	**−0.26**	**−0.26**	**−0.26**	**−0.25**									**−0.14**	**−0.14**	**−0.13**	**−0.13**					−0.07	**−0.07**	−0.06	−0.05
Imatra Teppanala																					**−0.55**	**−0.48**	**−0.47**	**−0.39**
Imatra Mansikkala													**−0.09**	**−0.10**	**−0.10**	**−0.13**								
Lappeenranta Lauritsala	−0.16	**−0.15**	−0.15	−0.14	**−0.9**	**−0.9**	**−0.9**	**−0.8**																
Lappeenranta Tirilä													**−0.09**	**−0.09**	**−0.09**	**−0.11**								
Jyväskylä Lyseo	**−0.75**	**−0.73**	**−0.73**	**−0.66**	**−3.0**	**−3.0**	**−3.0**	**−2.7**					**−0.21**	**−0.20**	**−0.20**	**−0.21**					−0.14	**−0.14**	−0.13	−0.09
Kajaani Keskusta	−0.15	**−0.06**	−0.06	−0.23	−0.4	**−0.3**	−0.2	−0.3																
Kotka Kirjastotalo	0.00	**−0.07**	−0.08	−0.03	0.0	0.0	0.0	0.0																
Kouvola Keskusta	−0.43	**−0.36**	−0.35	−0.45	**−2.0**	**−2.0**	**−1.9**	**−2.0**													0.29	**0.29**	0.28	0.27
Valkeala Lappakoski													0.07	**0.06**	0.06	0.04								
Kuopio Kasarmipuisto																	**−0.018**	−0.017	**−0.016**	−0.016				
Lahti Kisapuisto	**−1.04**	**−1.02**	**−1.02**	**−1.04**	**−3.2**	**−3.3**	**−3.2**	**−3.3**																
Lahti Vesku	−0.31	**−0.22**	−0.22	−0.23	**−4.8**	**−4.6**	**−4.6**	**−4.8**									**−0.018**	−0.017	**−0.017**	**−0.022**				
Oulu Keskusta	**−0.66**	**−0.67**	**−0.66**	**−0.61**	**−4.1**	**−4.0**	**−4.0**	**−3.7**									**−0.068**	**−0.067**	**−0.067**	**−0.060**	−0.11	**−0.11**	−0.13	−0.17
Oulu Pyyköjärvi	**−0.12**	**−0.12**	**−0.12**	**−0.09**	**−0.6**	**−0.6**	**−0.6**	**−0.6**													**−0.09**	**−0.09**	**−0.09**	−0.10
Oulu Nokela													−0.04	−0.01	−0.01	0.02								
Pietarsaari Bottenviksvägen													**−0.14**	**−0.15**	**−0.15**	**−0.10**								
Pori Lampaluoto													**−0.19**	**−0.19**	**−0.19**	**−0.18**								
Porvoo Mustijoki	−0.06	**−0.06**	−0.06	−0.06	−0.1	**−0.1**	−0.1	−0.1					**−0.09**	**−0.09**	**−0.10**	**−0.10**								
Rauma Sinisaari													**−0.43**	**−0.47**	**−0.47**	**−0.40**								
Seinäjoki Vapaudentie	−0.11	**−0.08**	−0.08	−0.10	**−1.2**	**−1.1**	**−1.1**	**−0.8**																
Tampere Lielahti	−0.01	−0.01	−0.01	0.01																				
Raisio Keskusta	**−0.79**	**−0.85**	**−0.86**	**−0.94**	**−2.8**	**−2.8**	**−2.7**	**−3.0**													**0.25**	**0.25**	**0.22**	**0.21**
Raisio Kaanaa													−0.05	**−0.05**	−0.05	−0.05								
Turku Kauppatori	**−0.72**	**−0.71**	**−0.71**	**−0.74**	**−3.3**	**−3.2**	**−3.2**	**−3.1**													**−0.33**	**−0.33**	**−0.36**	−0.38
Varkaus Pääterveysasema																					0.09	**0.09**	0.09	**0.09**
Espoo Luukki	**−0.14**	**−0.13**	−0.13	−0.15	**−0.2**	**−0.2**	**−0.2**	**−0.2**	**0.11**	**0.13**	0.12	0.23	−0.05	**−0.05**	−0.05	−0.02								
Helsinki Töölö	**−0.51**	**−0.56**	**−0.55**	**−0.57**	**−7.2**	**−7.8**	**−7.7**	**−6.9**	**0.80**	**0.88**	**0.88**	**0.91**					**−0.052**	**−0.051**	**−0.051**	**−0.060**	**−0.65**	**−0.65**	**−0.65**	**−0.57**
Helsinki Vallila	**−0.33**	**−0.34**	**−0.34**	**−0.34**	**−2.3**	**−2.3**	**−2.2**	**−1.8**					**−0.15**	**−0.16**	**−0.16**	**−0.14**	**−0.013**	−0.014	**−0.014**	−0.015	**−0.24**	**−0.25**	−0.25	**−0.24**
Vantaa Tikkurila	−0.07	−0.04	−0.04	−0.14	**−1.9**	**−1.9**	**−1.9**	**−2.3**	**0.28**	**0.30**	**0.29**	0.27					**−0.025**	−0.020	**−0.019**	**−0.025**	−0.05	**−0.10**	−0.09	−0.10

Even though the reductions of NO_2 concentrations have not been as strong as would be expected on the basis of emission trends, a downward trend was detected in half of the NO_2 time series studied. However, it is not obvious that this development will continue in the future, due to the completion of the transition to petrol cars with catalytic converters and the accelerating adoption of diesel cars.

For PM_{10}, five of the 12 urban time series studied showed a decreasing trend. This might suggest that emission reduction measures have been successful. However, the highest concentrations, which typically are attributable to the springtime street dust produced by studded tyres and gravelling, are not decreasing as widely. The measures taken to reduce this annually-occurring air pollution problem have not in general been successful. Instead, it is possible that the reduction in the long-range transported major ions, which is mainly driven by the large-scale reduction of sulphur emissions, has played a significant part in the decreases detected in the mean PM_{10} concentrations.

The trends were analyzed with the advanced GLS-ARMA method, which was compared with some commonly-used methods. It was shown that the handling of the serial correlation present in the time series with the ARMA processes improved the analysis of monthly values. Furthermore, the use of monthly rather than annually-averaged data was beneficial to the identification of the weakest trends, in particular.

References

Alvarez, R., Weilenmann, M., Favez, J.-Y., 2008. Evidence of increased mass fraction of NO_2 within real-world NO_x emissions of modern light vehicles – derived from a reliable online measuring method. Atmospheric Environment 42, 4699–4707.

Anttila, P., Makkonen, U., Hellén, H., Kyllönen, K., Leppänen, S., Saari, H., Hakola, H., 2008. Impact of the open biomass fires in spring and summer of 2006 on the chemical composition of background air in south-eastern Finland. Atmospheric Environment 42, 6472–6486.

Anttila, P., Salmi, T., 2006. Characterizing temporal and spatial patterns of urban PM_{10} using six years of Finnish monitoring data. Boreal Environment Research 11, 463–479.

AuT, 2009. The Finnish Information Centre of Automobile Sector. http://www.autoalantiedotuskeskus.fi/ (21 January 2009).

Berg, T., Aas, W., Pacyna, J., Uggerud, H.T., Vadset, M., 2008. Atmospheric trace metal concentrations at Norwegian background sites during 25 years and its relation to European emissions. Atmospheric Environment 42, 7494–7501.

Brockwell, P.J., Davis, R.A., 2002. Introduction to Time Series and Forecasting, second ed. Springer-Verlag New York, Inc.

Brönnimann, S., Buchmann, B., Wanner, H., 2002. Trends in near-surface ozone concentrations in Switzerland: the 1990s. Atmospheric Environment 36, 2841–2852.

Carslaw, D., 2005. Evidence of an increasing NO_2/NO_x emissions ratio from road traffic emissions. Atmospheric Environment 39, 4793–4802.

Carslaw, D.C., Beevers, S.D., 2004. Investigating the potential importance of primary NO_2 emissions in a street canyon. Atmospheric Environment 38, 3585–3594.

Derwent, R.G., Simmonds, P.G., Manning, A.J., Spain, T.G., 2007. Trends over a 20-year period from 1987 to 2007 in surface ozone at the atmospheric research station, Mace Head, Ireland. Atmospheric Environment 39, 9091–9098.

EC, 2001. Commission decision of 17 October 2001 amending the annexes to council decision 97/101/EC establishing a reciprocal exchange of information and data from networks and individual stations measuring ambient air pollution within the Member States. Official Journal L282 44, 69–76.

EEA, 2003. Air Pollution in Europe 1990–2000. Topic report 4/2003. European Environment Agency, Copenhagen, 84 pp.

EEA, 2007. Air Pollution in Europe 1990–2004. Report 2/2007. European Environment Agency, Copenhagen, 79 pp.

EEA, 2009. Assessment of Ground-Level Ozone within the EEA Member Countries, with Focus on Long-Term Trends. Technical Report 7/2009. European Environment Agency, Copenhagen, 52 pp.

FEI, 2008. Air Pollutant Emissions in Finland 1990–2006, Informative Inventory Report to the Secretariat of the UNECE Convention on Long-Range Transboundary Air Pollution. Finnish Environment Institute, Helsinki, Finland, 164 pp. Available from: <www.ymparisto.fi/download.asp?contentid=81835&;lan=fi>.

Gilbert, R.O., 1987. Statistical Methods for Environmental Pollution Monitoring. Van Nostrand Reinhold, New York.

Harrison, R.M., Stedman, J., Derwent, D., 2008. New directions: why are PM_{10} concentrations in Europe not falling? Atmospheric Environment 42, 603–606.

Hellén, H., Hakola, H., Haaparanta, S., Pietarila, H., Kauhaniemi, M., 2008. Influence of residential wood burning on local air quality. Science of the Total Environment 393, 283–290.

Hole, L.R., Christensen, J.H., Ruoho-Airola, T., Tørseth, K., Ginzburg, V., Glowacki, P., 2009. Past and future trends in concentrations of sulphur and nitrogen compounds in the Arctic. Atmospheric Environment 43, 928–939.

Hueglin, C., Buchmann, B., Weber, R.O., 2006. Long-term observation of real-world road traffic emission factors on a motorway in Switzerland. Atmospheric Environment 40, 3696–3709.

Hurvich, C.M., Tsai, C.L., 1989. Regression and time series model selection in small samples. Biometrika 76, 297–307.

Jenkin, M.E., 2008. Trends in ozone concentration distributions in the UK since 1990: local, regional and global influences. Atmospheric Environment 42, 5434–5445.

Keuken, M., Roemer, M., van den Elshout, S., 2009. Trend analysis of urban NO_2 concentrations and the importance of direct NO_2 emissions versus ozone/NO_x equilibrium. Atmospheric Environment 43, 4780–4783.

Kuebler, J., van den Bergh, H., Russell, A.G., 2001. Long-term trends of primary and secondary pollutant concentrations in Switzerland and their response to emission controls and economic changes. Atmospheric Environment 35, 1351–1363.

Laurila, T., 1999. Observational study of transport and photochemical formation of ozone over northern Europe. Journal of Geophysical Research 104, 26235–26243.

Laurila, T., Tuovinen, J.-P., Tarvainen, V., Simpson, D., 2004. Trends and scenarios of ground-level ozone concentrations in Finland. Boreal Environment Research 9, 167–184.

Laurila, T., Tuovinen, J.-P., Hatakka, J., 2009. Ozone concentration variations observed in northern Finland in relation to photochemical, transport and cloud processes. Boreal Environment Research 14, 550–558.

Leppänen, S., Anttila, P., Lättilä, H., Makkonen, U., 2005. Long-term comparison of filter method and sensitive analyser in monitoring of sulphur dioxide. Atmospheric Environment 39, 2683–2693.

Mäkelä, K., Laurikko, J., Kanner, H., 2008. Road Traffic Exhaust Gas Emissions in Finland, LIISA 2007 Calculation Software (In Finnish). Report VTT-R-05607-08. VTT Technical Research Centre of Finland, Helsinki, 48 pp.

Niemi, J.V., Saarikoski, S., Aurela, M., Tervahattu, H., Hillamo, R., Westphal, D.L., Aarnio, P., Koskentalo, T., Makkonen, U., Vehkamäki, H., Kulmala, M., 2009. Long-range transport episodes of fine particles in southern Finland during 1999–2007. Atmospheric Environment 43, 1255–1264.

Quinn, P.K., Shaw, G., Andrews, E., Dutton, E.G., Ruoho-Airola, T., Gong, S.L., 2007. Arctic haze: current trends and knowledge gaps. Tellus 59B, 99–114.

Ruoho-Airola, T., Anttila, P., Salmi, T., 2003. Airborne sulfur and nitrogen in Finland – trends and exposure in relation to air transport sector. Journal of Environmental Monitoring 6, 1–11.

Salmi, T., Määttä, A., Anttila, P., Ruoho-Airola, T., Amnell, T., 2002. Detecting Trends of Annual Values of Atmospheric Pollutants by the Mann-Kendall Test and Sen's Slope Estimates – the Excel Template Application MAKESENS. Publications on Air Quality No. 31. Finnish Meteorological Institute, Helsinki, 35 pp.

Sen, P.K., 1968. Estimates of the regression coefficient based on Kendall's tau. Journal of the American Statistical Association 63, 1379–1389.

Sirois, A., 1998. A brief and biased overview of time-series analysis or how to find that evasive trend. Annex E. WMO/GAW Report No. 133. In: WMO/EMEP Workshop on Advanced Statistical Methods and Their Application to Air Quality Data Sets, Helsinki, 14–18 September 1998. World Meteorological Organization, Geneva, Switzerland.

Tsutsumi, Y., Mori, K., Ikegami, M., Tashiro, T., Tsuboi, K., 2006. Long-term trends of greenhouse gases in regional and background events observed during 1998–2004 at Yonagunijima located to the east of the Asian continent. Atmospheric Environment 40, 5868–5879.

Tuovinen, J.-P., Laurila, T., Lättilä, H., Ryaboshapko, A., Brukhanov, P., Korolev, S., 1993. Impact of the sulphur dioxide sources in the Kola Peninsula on air quality in northernmost Europe. Atmospheric Environment 27A, 1379–1395.

Viana, M., Pandolfi, M., Minguillon, M.C., Querol, X., Alastuey, A., Monfort, E., Celades, I., 2008. Inter-comparison of receptor models for PM source apportionment: case study in an industrial area. Atmospheric Environment 42, 3820–3832.

VTT, 2008. LIPASTO Calculation System for Traffic Emissions and Energy Consumption. VTT Technical Research Centre of Finland. http://lipasto.vtt.fi/indexe.htm.

Waldén, J., Talka, M., Pohjola, V., Häkkinen, T., Lusa, K., Sassi, M.-K., Laurila, S., 2004. The Field Comparison of Carbon Monoxide, Sulphur Dioxide and Nitrogen Monoxide Ambient Air Measurements and a Field Audit 2002–2003 (In Finnish). Publications on Air Quality No. 35. Finnish Meteorological Institute, Helsinki, 49 pp.

Waldén, J., Bergius, J., Pohjola, V., Laurila, S., Kuronen, P., Wemberg, A., 2008. Field Comparison of CO, SO_2, NO, H_2S and O_3 Ambient Air Measurements and Field Audit 2006 (In Finnish). Studies No. 2. Finnish Meteorological Institute, Helsinki, 71 pp.

Zamboni, G., Capobianco, M., Daminelli, E., 2009. Estimation of road vehicle exhaust emissions from 1992 to 2010 and comparison with air quality measurements in Genoa, Italy. Atmospheric Environment 43, 1086–1092.

II

Primary NO_2 emissions and their role in the development on NO_2 concentrations in a traffic environment

Atmospheric Environment 45 (2011) 986–992

Contents lists available at ScienceDirect

Atmospheric Environment

journal homepage: www.elsevier.com/locate/atmosenv

Primary NO_2 emissions and their role in the development of NO_2 concentrations in a traffic environment

Pia Anttila [a,*], Juha-Pekka Tuovinen [a], Jarkko V. Niemi [b,c]

[a] Finnish Meteorological Institute, P.O. Box 503, FI-00101 Helsinki, Finland
[b] HSY Helsinki Region Environmental Services Authority, P.O. Box 100, FI-00066 HSY, Finland
[c] Department of Environmental Sciences, P.O. Box 65, FI-00014 University of Helsinki, Finland

ARTICLE INFO

Article history:
Received 23 July 2010
Received in revised form
28 October 2010
Accepted 29 October 2010

Keywords:
Nitrogen oxides
Vehicle exhaust emissions
Urban NO_2 concentrations
$NO–NO_2–O_3$ equilibrium
Total oxidant model
Limit values
Helsinki
Finland

ABSTRACT

An assessment of the formation of NO_2 concentrations in heavily traffic-influenced environments in Helsinki, Finland was carried out. The proportion of primary NO_2 emissions from road traffic was estimated using a statistical model for the relationship between the mixing ratios of nitrogen oxides ($NO + NO_2$) and total oxidant ($O_3 + NO_2$) measured in 1994–2009. Based on this analysis, a quantitative estimate was derived for the relative importance of the primary NO_2 emissions, ambient $NO–NO_2–O_3$ equilibrium and background concentrations in the observed NO_2 concentrations. The proportion of primary NO_2 in the vehicular NO_x emissions increased from below 10% in the 1990s to about 20% in 2009, with a more distinctive increase during the most recent years. This development was related to the changes in the proportion of diesel-powered passenger cars in Finland. Between 1994 and 2004, the photochemical NO-to-NO_2 conversion comprised on average 51% of the mean NO_2 concentration, while the primary NO_2 emissions contributed 31%. The role of the primary NO_2 emissions was limited by the steeply-decreasing total NO_x emissions. More recent data (2005–2009) yielded higher primary NO_2 emission fractions (15–21%), with a clearly increasing trend. As a result, the contribution of chemical conversion steadily decreased from 54% in 2005 to 43% in 2009, while that of the primary NO_2 emissions increased from 32 to 44%. In order not to exceed in future the annual limit of NO_2 concentration, set by the European Union, in the busiest street canyons in downtown Helsinki, the primary NO_2 emissions need to be addressed alongside the total NO_x emissions.

1. Introduction

A limit value for the annual mean NO_2 concentration in the ambient air of 40 $\mu g\,m^{-3}$ came into force in the European Union (EU) at the beginning of 2010 (EC, 2008). In order to meet this target, Europe-wide measures have been taken to reduce the anthropogenic emissions of nitrogen oxides ($NO_x = NO + NO_2$). These measures have resulted in a strong and steady decrease in emissions in Western Europe since 1990, when NO_x emissions were at their highest level (Vestreng et al., 2009). This development has significantly reduced the NO_x concentrations in urban areas during the 1990s and 2000s; however, the NO_2 levels have not decreased at the same rate as those of NO_x (Carslaw, 2005; Hueglin et al., 2006; Carslaw et al., 2007; Zamboni et al., 2009; Anttila and Tuovinen, 2010). Consequently, in spite of successful NO_x emission control in Europe during the past twenty years, present NO_2 concentrations still widely exceed, or are close to, the EU limit value in polluted roadside environments (Carslaw et al., 2007; Chaloulakou et al., 2008; Velders and Diederen, 2009; Pleijel et al., 2009; Zamboni et al., 2009; Mol et al., 2010).

One reason for the slower reduction in urban NO_2 concentrations relates to the increasing proportion of diesel-powered vehicles in national car fleets with their higher primary (i.e. direct) emissions of NO_2. While the primary NO_2 constitutes less than 5% of the total NO_x in the emissions of petrol-fuelled vehicles, this proportion is typically within 10–12% for diesel vehicles not fitted with modern exhaust treatment; for those with particle traps and oxidation catalysts the value is even higher (up to 70%) (e.g. Grice et al., 2009; Alvarez et al., 2008). It has been observed that the unexpectedly small decreases, stabilization or even increases in the NO_2 concentrations in heavily traffic-influenced roadside environments in the UK, Switzerland and Germany, for example, are mainly due to the increasing proportion of primary NO_2 emissions, originating especially from modern diesel-technology vehicles (Carslaw,

* Corresponding author.
E-mail address: pia.anttila@fmi.fi (P. Anttila).

1352-2310/$ – see front matter © 2010 Elsevier Ltd. All rights reserved.
doi:10.1016/j.atmosenv.2010.10.050

2005; Hueglin et al., 2006; Kessler et al., 2006; Carslaw and Carslaw, 2007).

In addition to NO_x emissions and their NO-NO_2 partitioning, urban NO_2 concentrations are controlled by meteorology and chemistry. Meteorological factors, operating on a wide range of spatial scales, determine the dispersion and transport of NO_x emissions and other airborne compounds. Chemical reactions are particularly important for urban concentrations, since the emitted NO is oxidized to NO_2 by O_3 on a timescale of seconds to minutes, while in daylight NO_2 is rapidly photolysed back to NO, regenerating O_3 (e.g. Seinfeld, 1986). Thus a photochemical equilibrium, the so-called photostationary state, is established between NO, NO_2 and O_3, which closely couples the atmospheric behaviour of these compounds. This equilibrium, representing the conversion of the emitted NO to NO_2, has been found to act as the main control on the NO_2 concentration trend observed at an urban background site in the city of Rotterdam in the Netherlands (Keuken et al., 2009). This contrasts with the studies cited above, which highlight the importance of changes in the primary NO_2 emissions.

In Finland also, urban NO_x concentrations have been observed to decrease faster than the NO_2 concentrations (Anttila and Tuovinen, 2010). In a trend study covering the years 1994–2007, this pattern occurred at all nine urban traffic monitoring sites studied, and also at four suburban sites that were less influenced by traffic. Over this period, Finnish NO_x emissions from road traffic decreased by 50%, while urban NO_x concentrations decreased by 40% on average, but urban NO_2 concentrations only decreased by 20% (Anttila and Tuovinen, 2010). Nevertheless, as a result of these reductions, values exceeding the annual limit value of NO_2 set by the EU are nowadays only detected in Helsinki. In smaller cities, no exceedings have been recorded.

At the Mannerheimintie air quality monitoring station, situated on the main street in Helsinki, the annual NO_2 limit value of 40 $\mu g\,m^{-3}$ has been exceeded every year since the start of continuous monitoring at this site, i.e., in 2005–2009 (Niemi et al., 2009; Malkki et al., 2010). Values over the limit have also been detected in year-long measurement campaigns in two other street canyons with heavy traffic in central Helsinki, at Hämeentie (in 2005 and 2009) and at Töölöntulli (in 2006) (Malkki et al., 2010). Based on passive sampling measurements, it has been estimated that the annual limit value has also been exceeded in some other busy street canyons and near the busiest main roads (Malkki et al., 2010).

In order to effectively target the measures to reduce NO_2 concentrations, it is important not only to understand the factors contributing to the observed concentrations in these specifically problematic urban locations, but also to be able to quantify these influences. In this study we examine the formation of NO_2 concentrations in heavily traffic-influenced environments in Helsinki using long-term air quality monitoring data. We particularly explore the role that possible changes in the primary NO_2 emissions, the ambient NO–NO_2–O_3 equilibrium and background pollution play in the observed NO_2 concentration trend, and we provide a quantitative estimate for the relative importance of these components.

2. Data

Hourly-averaged data of ambient NO, NO_2 and O_3 concentrations from three measurement sites located within the Helsinki metropolitan area in Finland were used in this study. The sites include two urban traffic stations in central Helsinki, i.e., Töölö (location 60.18539°N, 24.91648°E; data from 1994–2004) and Mannerheimintie (60.16964°N, 24.93924°E; 2005–2009), while the third one, Luukki in Espoo (60.31349°N, 24.68937°E; 1994–2009), is classified as a rural background station. The Töölö and Mannerheimintie stations are located about 20 km south of the Luukki station.

The Töölö measurement station, which was operational until the end of 2004, was located in a wide crossing area of several streets: Mechelininkatu (25,000 vehicles per weekday in 2004), Topeliuksenkatu (17,000), Linnankoskenkatu (12,000) and Nordenskiöldinkatu (14,000) (Niemi et al., 2009; Lilleberg and Hellman, 2009). The distances between the street edges and the measurement station varied from 2 to 20 m.

The Mannerheimintie measurement station is located at the kerbside of the street canyon of Mannerheimintie, 2 m from the street edge. The street canyon is fairly wide (47 m); there are four lanes for cars and an additional two for trams. The height of the surrounding buildings is about 26 m. The average weekday traffic volume in 2008 was 23,000 vehicles per day (Niemi et al., 2009; Lilleberg and Hellman, 2009). The distance from the nearest junction is 35 m. The traffic volume on the intersection street of this junction (Kaivokatu) in 2008 was 15,000 vehicles per day (Niemi et al., 2009; Lilleberg and Hellman, 2009).

The air quality measurements were performed by the HSY Helsinki Region Environmental Services Authority (former YTV Helsinki Metropolitan Area Council) (Malkki et al., 2010). Ozone was monitored with UV absorption analysers (TEI 49C; MonitorLabs 8810 at Töölö until May 1997). Nitrogen oxides were monitored with chemiluminescence analysers (Horiba APNA 360; Environnement AC30 at Töölö until June 1997 and TEI 42 at Luukki until January 2000). The measurement height was at all sites 4 m.

3. Methods

We studied the relative importance of the primary NO_2 emissions, the NO-NO_2-O_3 equilibrium and background concentrations for the urban NO_2 concentrations by means of the total oxidant method presented by Clapp and Jenkin (2001) and Carslaw and Beevers (2004), and further developed by Keuken et al. (2009).

Clapp and Jenkin (2001) showed that the sum of the O_3 and NO_2 mixing ratios (i.e., the mixing ratio of the total oxidant, $O_x = O_3 + NO_2$) at an urban location can be approximated as being made up of the NO_x-independent regional background contribution and the NO_x-dependent local contribution correlating with the local primary emissions. We express this as a linear regression

$$[O_x]_{urban} = a[NO_x]_{urban} + b, \quad (1)$$

where the square brackets indicate a mixing ratio (in ppbv), and a and b are regression parameters. Carslaw and Beevers (2004) further removed the effect of background pollution by considering the difference in the O_x and NO_x mixing ratios between an urban traffic station and a nearby background station (here denoted by the subscript 'local'), so we can write the regression equation

$$[O_x]_{local} = c[NO_x]_{local} + d, \quad (2)$$

where c is a regression parameter, which provides an estimate of the contribution of primary NO_2 emissions to the NO_x mixing ratio, and the intercept parameter d is expected to be close to zero. The 'local' mixing ratios are defined as

$$\begin{aligned}[O_x]_{local} &= [O_x]_{urban} - [O_x]_{background} \\ &= [O_3]_{urban} + [NO_2]_{urban} - [O_3]_{background} - [NO_2]_{background}\end{aligned} \quad (3)$$

and

$$\begin{aligned}[NO_x]_{local} &= [NO_x]_{urban} - [NO_x]_{background} \\ &= [NO]_{urban} + [NO_2]_{urban} - [NO]_{background} - [NO_2]_{background}\end{aligned} \quad (4)$$

With the primary NO_2 emission coefficient c obtained from the ordinary least-square regression based on Eqs. (2)–(4), we can construct a NO_2 concentration budget similarly to the procedures presented by Keuken et al. (2009), which we formalise in the following. We assume that at each urban site, at each moment i, the NO_2 concentration is composed of three contributions: (1) primary NO_2 emission, (2) conversion from the NO-O_3 reaction and (3) regional background:

$$[NO_2]_{urban,i} = [NO_2]_{primary,i} + [NO_2]_{conversion,i} + [NO_2]_{background,i}, \quad (5)$$

where

$$[NO_2]_{primary,i} = c[NO_x]_{local,i}, \quad (6)$$

$$[NO_2]_{conversion,i} = (1-c)[NO_x]_{local,i} + [NO]_{background,i} - [NO]_{urban,i} \quad (7)$$

and $[NO_2]_{background,i}$ is the NO_2 mixing ratio measured at a background site. The first term of $[NO_2]_{conversion}$ represents the direct emission of NO, which, when summed with the background mixing ratio, would approximate the expected $[NO]_{urban}$ in the absence of any NO-to-NO_2 oxidation. Thus the difference between this sum and the $[NO]_{urban}$ actually measured estimates the contribution from the conversion of NO to NO_2. Equivalently, $[NO_2]_{conversion}$ can be expressed as

$$[NO_2]_{conversion,i} = [O_3]_{background,i} - [O_3]_{urban,i} + d \quad (8)$$

In this study we first regressed each annual set of hourly $[O_x]_{local}$ (defined in Eq. (3)) against the corresponding $[NO_x]_{local}$ data (Eq. (4)). The urban data were taken from the traffic-influenced stations of Töölö and Mannerheimintie, while the observations at the Luukki station provided the regional background concentrations. From this regression we obtained an estimate for the contribution of primary NO_2 emissions to NO_x mixing ratios (i.e., the parameter c in Eq. (2)) on an annual basis for 1994–2004 and 2005–2009 for Töölö and Mannerheimintie, respectively. As we made no assumptions about the development of the primary NO_2 emissions, these c values were used directly in the further analysis. This is in contrast to Keuken et al. (2009), who first fitted a linear trend to the annual estimates. The annual budgets of NO_2 were compiled for Töölö and Mannerheimintie according to Eqs. (5)–(7) using the annually-averaged mixing ratios of NO, NO_2 and NO_x.

4. Results and discussion

4.1. Evaluation of the total oxidant model

As examples of the relationships between $[O_x]_{local}$ and $[NO_x]_{local}$, the linear regressions calculated from the hourly data are shown in Fig. 1 for Töölö in 2003 and 2004, and for Mannerheimintie in 2008 and 2009. In spite of the scatter, the linear relationship between $[O_x]_{local}$ and $[NO_x]_{local}$ is apparent in each dataset. At Töölö, the data points tend to be biased towards the accumulation near the y-axis, i.e., near-zero $[NO_x]_{local}$ values. At both sites, the regression line fails to cross the origo, resulting in significant positive intercepts, which violate the assumptions of the total oxidant model.

By definition, near-zero $[NO_x]_{local}$ values occur when the NO_x concentration at the urban traffic site is close to that detected at the background site. The traffic exhaust emissions are dominated by the rush-hour peaks in the morning and evening; the urban NO_x concentrations largely follow this pattern (Fig. 2a). The difference between the urban and background NO_x concentrations is smallest during the night-time (Fig. 2a). NO_x emissions and the resulting urban NO_x concentrations are also markedly lower during the weekends (Fig. 2b). On the other hand, the proportion of primary NO_2 emission is not expected to have any marked diurnal or weekly variation. Thus, to reduce the number of the rather uninformative near-zero $[NO_x]_{local}$ data points, we removed from further analysis the night-time hours from 22:00 to 4:00 (UTC + 2, start time of the averaging), as well as all data from Saturdays and Sundays.

Excluding the night-time hours can also be justified by the diurnal behaviour of the O_3 concentrations. The background O_3 concentration at Luukki, which is the largest component in $[O_x]_{local}$, typically exhibits a daily maximum and a nightly minimum. The nocturnal decrease is mainly due to O_3 deposition to the ground, with isolation of the lowest layers of the atmosphere from the air above by the nocturnal temperature inversion. In the morning, atmospheric mixing is re-established, resulting in O_3 transport from aloft to the surface. The total oxidant model does not resolve this nocturnal surface sink, which is one reason for the positive intercepts obtained.

The results of the total oxidant model for the data limited to the daytime and weekdays are shown in Fig. 3 and Table 1. The data screening reduced both the scatter and the positive intercepts systematically at both sites. At Töölö, the data screening also increased the slopes slightly (around 10%), while at

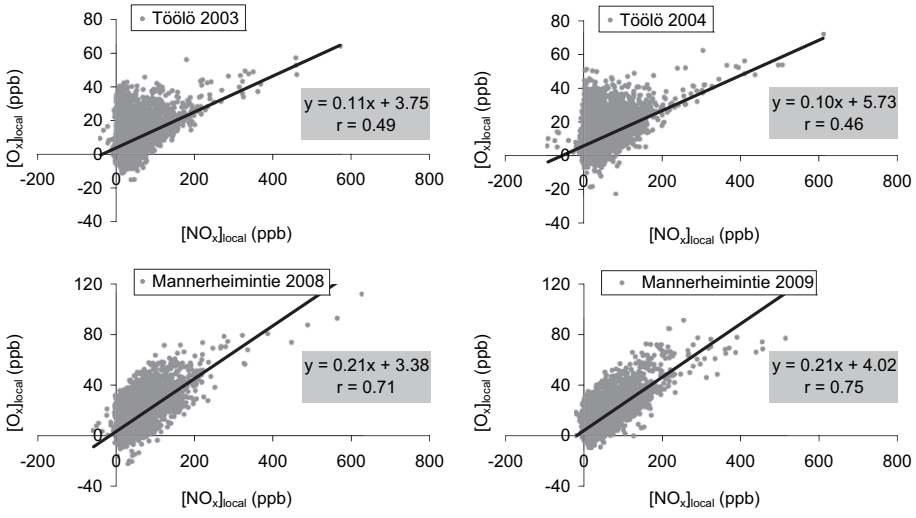

Fig. 1. Linear regressions between $[O_x]_{local}$ and $[NO_x]_{local}$ calculated from the hourly data measured at Töölö in 2003 and 2004 and at Mannerheimintie in 2008 and 2009.

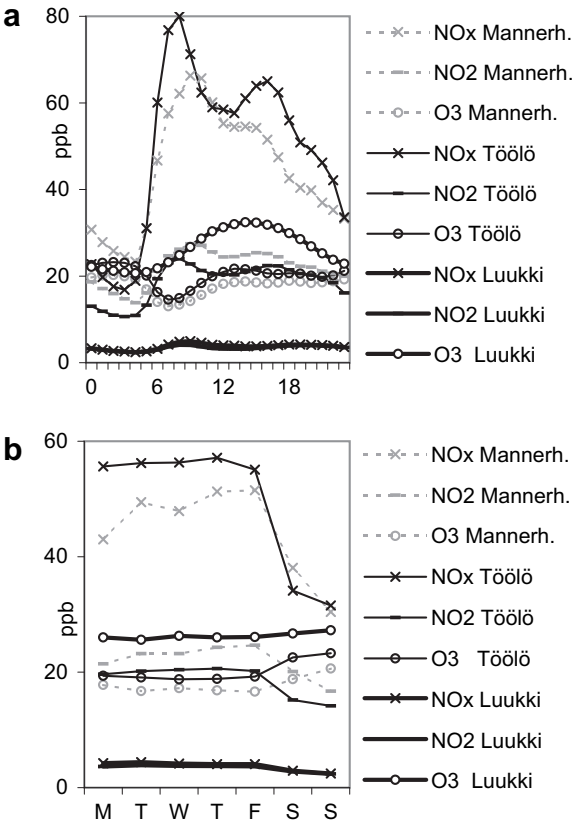

Fig. 2. Mean diurnal (a) and weekly (b) variation of the NO_x, NO_2 and O_3 concentrations at Mannerheimintie and Luukki in 2005–2009 and at Töölö in 2000–2004.

Table 1
Annual regression results of $[O_x]_{local} = c[NO_x]_{local} + d$ at Töölö and Mannerheimintie. s.e. is the standard error of the regression parameter, r is the Pearson correlation coefficient and n is the number of data.

Station	Year	c (s.e.)	d (s.e.)	r	n
Töölö	1994	0.067 (0.001)	0.6 (0.2)	0.64	3907
	1995	0.110 (0.001)	−1.8 (0.2)	0.84	3911
	1996	0.110 (0.001)	−2.4 (0.2)	0.77	4052
	1997	0.089 (0.002)	−0.2 (0.2)	0.62	4106
	1998	0.075 (0.001)	2.3 (0.1)	0.68	4219
	1999	0.085 (0.001)	2.8 (0.1)	0.69	3815
	2000	0.088 (0.002)	2.0 (0.1)	0.66	4171
	2001	0.087 (0.002)	3.2 (0.1)	0.60	4883
	2002	0.108 (0.002)	1.9 (0.2)	0.61	4201
	2003	0.123 (0.002)	1.3 (0.1)	0.68	4119
	2004	0.119 (0.002)	3.5 (0.2)	0.63	4884
Mannerheimintie	2005	0.151 (0.002)	2.0 (0.1)	0.78	4162
	2006	0.173 (0.003)	0.3 (0.2)	0.72	2953
	2007	0.169 (0.002)	2.3 (0.1)	0.78	4216
	2008	0.206 (0.002)	1.4 (0.2)	0.81	4212
	2009	0.210 (0.002)	2.1 (0.1)	0.85	4045

Mannerheimintie the slopes, which estimate the proportion of primary NO_2 emissions, remained practically unchanged.

The residuals of the linear regressions (not shown) do not display a significant dependency on $[NO_x]_{local}$. In some cases (Mannerheimintie in 2007–2009, Töölö in 1999 and 2001), the fit was poorer for the highest concentrations, as is apparent from Fig. 3. However, the elimination of these deviating points had an insignificant effect on the regression slopes. For some annual datasets from Töölö, the residuals tended to be heteroscedastic, with higher variances at low concentrations.

4.2. Development of primary NO_2 emissions

The development of the ambient NO_x and O_3 concentrations measured within the Helsinki metropolitan area, when analyzed

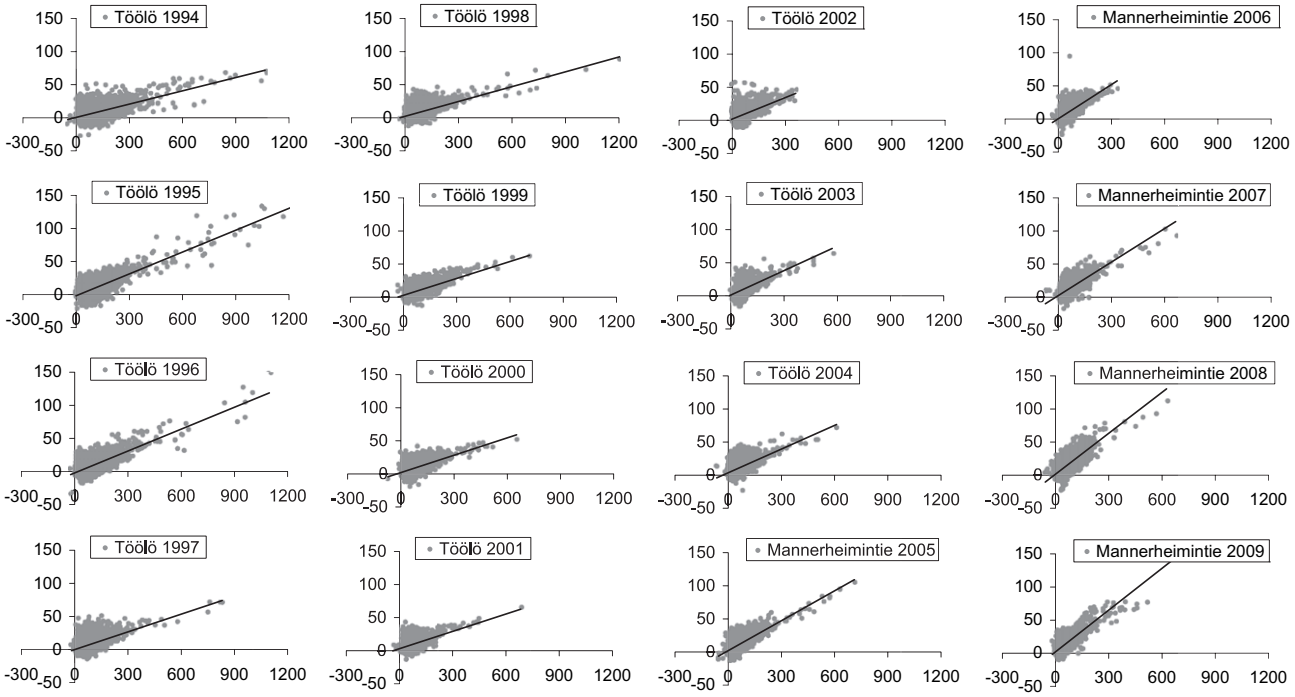

Fig. 3. Scatter plots of hourly $[NO_x]_{local}$ (abscissa, ppb) versus hourly $[O_x]_{local}$ (ordinate, ppb) for the weekday hours between 5:00 and 21:00. The regression equations are presented in Table 1.

with the total oxidant model, suggests that the proportion of primary NO_2 emissions in the total vehicular NO_x emissions has been on the increase, especially during the latter part of the 2000s (Fig. 4a, bars). At the Töölö station, the primary NO_2 fraction varied between 6.7 and 12.3% by volume. The values in 1995 and 1996 (11.0%) appear high, as compared to the trend, but we are unable to explain these anomalies by measurement errors or exceptional frequency distributions of the data (not shown). At Mannerheimintie, the primary NO_2 fraction increased from 15.1 to 21.0% by volume in 2005–2009.

The sources of $[NO_x]_{local}$ and $[O_x]_{local}$ can vary from site to site due to a number of differing factors, such as vehicle fleet composition, local driving conditions, time-lags between the emission and measurement points (caused by different distances and mixing conditions) and background concentrations (Clapp and Jenkin, 2001; Carslaw and Beevers, 2005). It is possible that these factors result in a systematic difference in the O_x–NO_x relationship between Töölö and Mannerheimintie. Thus comparisons of the magnitude of the primary NO_2 fraction between these two sites should be made with caution. However, it is evident that in the first part of the study period the primary NO_2 fraction remained rather stable and that a significant increase occurred after 2006.

The changes in the primary NO_2 fraction in NO_x emissions can be related to the increase of the proportion of diesel-powered passenger cars in Finland. The diesel share of new passenger car registrations was among the lowest in the EU until 2006, when 20% of the new passenger cars in Finland were diesel-powered (Fig. 4a, solid line), while the EU15 average was already as high as 51% (ACEA, 2010). At the beginning of 2008, a new CO_2-emission-based tax for passenger cars was adopted in Finland, which immediately caused a further increase (from 29 to 50%) in the diesel car sales compared to the previous year (AuT, 2010). Thus the western European level of the diesel share in new cars was attained in three years. Accordingly, the diesel share in the total passenger car fleet has increased from 7% in 1995 to 18% in 2009 (AuT, 2010) (Fig. 4a, dashed line), with the steepest increase in 2007–2008. As the average age of Finnish passenger cars is 11 years (AuT, 2010), changes in the total car fleet will be realized only slowly.

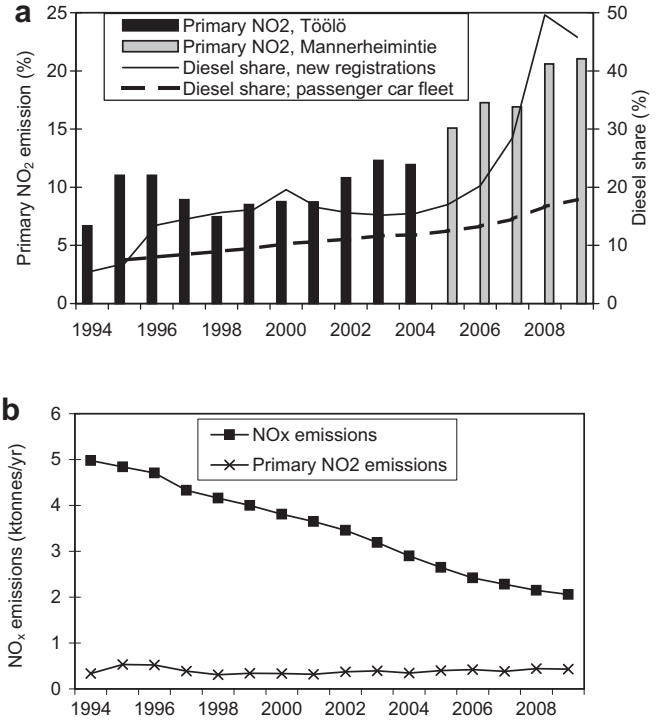

Fig. 4. a) Proportion of the primary NO_2 emissions at Töölö (black bars) and at Mannerheimintie (grey bars). The proportion of diesel vehicles in new passenger car registrations in Finland (continuous line) and in the total passenger car fleet (dashed line) are also shown. b) Total NO_x emissions from road traffic in Helsinki (Mäkelä et al., 2009; Malkki et al., 2010) and the corresponding primary NO_2 emissions.

In an emission inventory for four street canyons and two open roads in the Helsinki metropolitan area, the proportion of primary NO_2 emissions varied within the range 14–16% in 2006 (Kousa and Kauhaniemi, 2008). This is comparable with the estimate of 17% obtained in the present study for Mannerheimintie for the same year (Table 1).

Based on a European-wide TREMOVE emission model, Grice et al. (2009) estimated that the proportion of primary NO_2 emissions from urban road transport in Finland has increased from 4.8% in 1995 to 7.1% in 2005. These values are significantly lower than our estimates, but do show a similar, weakly-increasing trend for this period. For 2010, Grice et al. (2009) predicted the NO_2 fraction for urban roads to be 10.2%, which corresponds to only a slight increase in its trend, while our results indicate that the NO_2 fraction has increased much faster in the latter part of the decade. One possible reason for these differences is that the Europe-wide approach and the assumptions involved in the TREMOVE model may not successfully reflect the rapid changes that have occurred in Finland since the mid-1990s. For example, TREMOVE provides 26, 44 and 53% higher estimates of the NO_x emissions from road transport for 2000, 2005 and 2010, respectively, than the latest national emission inventory for Finland (Mäkelä et al., 2009).

It may be noted that Grice et al. (2009) also estimated the proportion of primary NO_2 emissions using an alternative method, which is based on a chemical model similar to that used in the present study. However, this method produced an inconsistent result for Finland, with a decreasing trend in the primary NO_2 fraction. This can be explained by an inappropriate selection of the measurement stations used in the analysis. Firstly, the station adopted as a background site is located in the city of Helsinki and thus does not provide a regional background reference. Secondly, neither of the two urban sites analyzed by Grice et al. (2009) are located within the most NO_x-polluted city in Finland, i.e., Helsinki.

Our study provides evidence of an increase in the NO_2-to-NO_x ratio in the road traffic NO_x emissions in Helsinki between 1994 and 2009. On the other hand, the magnitude of these emissions has decreased steeply during this period in Helsinki (Mäkelä et al., 2009; Malkki et al., 2010; Fig. 4b). Applying the primary NO_2 fractions estimated above, we can estimate the development of the total primary NO_2 emissions from road traffic in this area (Fig. 4b). These estimates show that the steep decrease in NO_x emissions has largely compensated for the relative increase of primary NO_2 emissions, resulting in a rather steady level for the absolute primary NO_2 emissions from road traffic during the study period.

After 2010, the NO_x emission reduction in Finland is expected to slow down (Mäkelä et al., 2009). At the same time, the diesel share of vehicles will continue to increase, which will lead to a higher proportion of NO_x being emitted as NO_2. In the next few years, it is thus possible that the absolute magnitude of primary NO_2 emissions will also start to rise.

4.3. NO_2 budgets at Töölö and Mannerheimintie

The annual NO_2 budgets calculated as described in Section 3 are shown in Fig. 5. The trend analysis of Anttila and Tuovinen (2010) showed that at Töölö the monthly mean NO_x and NO_2 concentrations decreased by $4.6 \pm 0.5\%$ yr^{-1} and $1.3 \pm 0.2\%$ yr^{-1}, respectively, from 1994 to 2004, while the corresponding O_3 concentration increased by $2.4 \pm 0.5\%$ yr^{-1}. However, no clear-cut conclusions

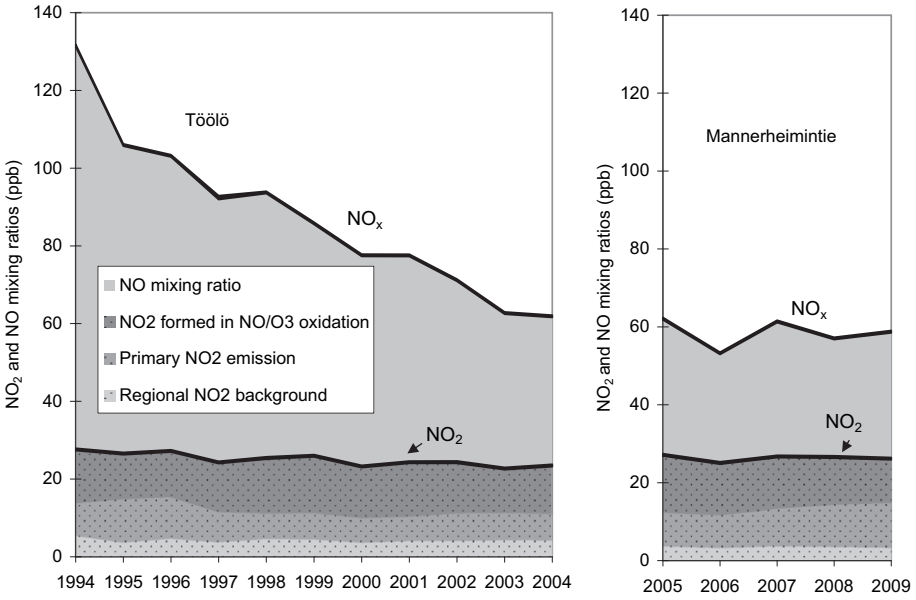

Fig. 5. Annual NO_2 budgets during the weekday hours between 5:00 and 21:00. The dotted areas indicate the different contributions to the NO_2 mixing ratio. The grey area denotes the measured annual mean NO mixing ratio, while the lines indicate the corresponding NO_x and NO_2 mixing ratios.

could be drawn in that study concerning the role of the primary NO_2 emissions and other factors in generating the observed NO_2 trends. The annual NO_2 budgets calculated in the present study show that the photochemical conversion of NO to NO_2 comprised on average 51% (average of the annual percentage contributions varying within 43–56%) of the mean NO_2 concentration at Töölö, while the primary NO_2 emissions contributed 31% (26–42%). The contribution of the regional background to the urban concentration varied within 15–20%, with an average of 18% (Fig. 5). Thus photochemical conversion remained the dominating contributor to the ambient NO_2 concentrations at Töölö throughout the study period there. The role of primary NO_2 emissions was limited by the low primary NO_2 emissions ratios (7–12%) together with the decreasing total NO_x emissions.

At Mannerheimintie, the conversion from NO to NO_2 reduced steadily during the five-year study period, its contribution to the NO_2 mixing ratio decreasing from 14.4 to 11.1 ppb (i.e., from 27.5 to 21.3 $\mu g\,m^{-3}$ at 20 °C), which corresponds to a decrease from 54 to 43%. At the same time, the contribution of primary NO_2 emissions increased from 32 to 44% (from 8.6 to 11.3 ppb, or from 16.5 to 21.6 $\mu g\,m^{-3}$), overtaking the conversion term in 2009. The contribution of the regional background to the urban NO_2 concentration was 13–15% (3.4–3.9 ppb; 6.5–7.5 $\mu g\,m^{-3}$). It should be noted that these mean concentrations are calculated from data limited to daytime hours and weekdays, and are thus not readily comparable to the EU's annual limit value. For example, the annual mean NO_2 concentration in 2009 in the screened dataset was 49.5 $\mu g\,m^{-3}$, while that of the complete dataset was 41.3 $\mu g\,m^{-3}$.

5. Conclusions

Our analysis of air quality monitoring data from two heavily traffic-influenced sites in Helsinki shows that the primary NO_2 emission fractions have increased from below 10% in the 1990s to about 20% in 2009, with a more distinctive increase during the very latest years. This development can be related to the changes in the proportion of diesel-powered passenger cars in Finland.

At the Töölö station, the photochemical conversion of NO to NO_2 comprised 51% of the mean NO_2 concentration, while the contribution of primary NO_2 emissions was 31%, and that of the regional background 18%, when averaged over the period 1994–2004. At this site, which represents the first part of our study period with lower (7–12%) and rather unsystematically varying NO_2 emission fractions, the photochemical conversion remained the dominating contributor to the ambient NO_2 concentrations.

At the Mannerheimintie station, the importance of the chemical conversion from NO to NO_2 has steadily decreased during the five-year study period (2005–2009), from 54 to 43%. At the same time, the share of the primary NO_2 emissions has increased from 32 to 44%, the remaining part consisting of the relatively invariable background term (13–15%). Thus the higher (15–21%) and clearly increasing primary NO_2 emission fraction at this site resulted in a contribution that in 2009 had reached a similar level to that of the NO-to-NO_2 conversion.

At the beginning of the 2010s, the NO_x emissions from road traffic in Finland are expected to stabilize and follow a trend that decreases only slowly. With an increasing NO_2 fraction in emissions, this potentially increases the absolute magnitude of the primary NO_2 emissions. Thus it is possible that these emissions will make an increasingly significant contribution to the ambient NO_2 concentrations. This would make it even more difficult in coming years to attain the EU limit value for NO_2, which is presently exceeded in heavily traffic-influenced environments in Helsinki.

The situation is potentially further exacerbated by the enhanced NO-to-NO_2 oxidation resulting both from the less frequent O_3 limitation and from the increasing hemispheric background O_3 concentration (Monks et al., 2009). Thus, in order to reduce the NO_2 concentrations to below the limit value, the primary NO_2 emissions need to be addressed alongside the total NO_x emissions.

References

ACEA, 2010. EU economic report, March 2010. European Automobile Manufacturers' Association (ACEA), Brussels, Belgium. http://www.acea.be/images/uploads/files/20100311_ER_1003_2010_I_Q1-4.pdf.

Alvarez, R., Weilenmann, M., Favez, J.-Y., 2008. Evidence of increased mass fraction of NO_2 within real-world NO_x emissions of modern light vehicles—derived from a reliable online measuring method. Atmospheric Environment 42, 4699–4707.

Anttila, P., Tuovinen, J.-P., 2010. Trends of primary and secondary pollutant concentrations in Finland in 1994–2007. Atmospheric Environment 44, 30–41.
AuT, 2010. The Finnish Information Centre of Automobile Sector. http://www.autoalantiedotuskeskus.fi/ (21 May 2010).
Carslaw, D., 2005. Evidence of an increasing NO_2/NO_x emissions ratio from road traffic emissions. Atmospheric Environment 39, 4793–4802.
Carslaw, D.C., Beevers, S.D., 2004. Investigating the potential importance of primary NO_2 emissions in a street canyon. Atmospheric Environment 38, 3585–3594.
Carslaw, D.C., Beevers, S.D., 2005. Estimations of road vehicle primary NO_2 exhaust emission fractions using monitoring data in London. Atmospheric Environment 39, 167–177.
Carslaw, D.C., Beevers, S.D., Bell, M.C., 2007. Risks of exceeding the hourly EU limit value for nitrogen dioxide resulting from increased road transport emissions of primary nitrogen dioxide. Atmospheric Environment 41, 2073–2082.
Carslaw, D.C., Carslaw, N., 2007. Detecting and characterizing small changes in urban nitrogen dioxide concentrations. Atmospheric Environment 41, 4723–4733.
Chaloulakou, A., Mavroidis, I., Gavriil, I., 2008. Compliance with the annual NO_2 air quality standard in Athens. Required NO_x levels and expected health implications. Atmospheric Environment 42, 454–465.
Clapp, L.J., Jenkin, M.E., 2001. Analysis of the relationship between ambient levels of O_3, NO_2 and NO as a function of NO_x in the UK. Atmospheric Environment 35, 6391–6405.
EC, 2008. Directive 2008/50/EC of the European Parliament and of the Council of 21 May 2008 on ambient air quality and cleaner air for Europe. Official Journal of the European Union L152, 1–44.
Grice, S., Stedman, J., Kent, A., Hobson, M., Norris, J., Abbott, J., Cooke, S., 2009. Recent trends and projections of primary NO_2 emissions in Europe. Atmospheric Environment 43, 2154–2167.
Hueglin, C., Buchmann, B., Weber, R.O., 2006. Long-term observation of real-world road traffic emission factors on a motorway in Switzerland. Atmospheric Environment 40, 3696–3709.
Kessler, C., Niederau, A., Scholz, W., 2006. Estimation of NO_2/NO_x ratios of traffic emissions in Baden-Württemberg from 1995 to 2005. In: 2nd Conference on Environment & Transport, including 15th Conference on Transport and Air Pollution, Reims, France, 12–14 June 2006. Proceedings no. 107, vol. 2, pp. 101–105. Inrets, Arceuil, France.
Keuken, M., Roemer, M., van den Elshout, S., 2009. Trend analysis of urban NO_2 concentrations and the importance of direct NO_2 emissions versus ozone/NO_x equilibrium. Atmospheric Environment 43, 4780–4783.
Kousa, A., Kauhaniemi, M., 2008. Air Quality in Street Canyon and in Open Road Environments Estimated with Air Quality Models (in Finnish with English abstract). Publications 23/2008. YTV Helsinki Metropolitan Area Council, Helsinki, Finland, ISBN 978-951-798-711-0, 37 pp.
Lilleberg, I., Hellman. T., 2009. Liikenteen kehitys Helsingissä vuonna 2008 (in Finnish). Helsingin kaupunkisuunnitteluviraston liikennesuunnitteluosaston selvityksiä 2009:1, City Planning Department, Helsinki, Finland. ISBN 978-952-223-424-7.
Mäkelä, K., Laurikko, J., Kanner, H., 2009. Road traffic exhaust gas emissions in Finland. LIISA 2008 calculation software (in Finnish with English abstract). Report VTT-R-08700-09, VTT Technical Research Centre, Helsinki, Finland, 45 pp. http://lipasto.vtt.fi/liisa/liisa2008raportti.pdf.
Malkki, M., Niemi, J., Lounasheimo, J., Myllynen, M., Julkunen, A., Loukkola, K., 2010. Air Quality in the Helsinki Metropolitan Area in 2009 (in Finnish with English abstract). Publications 2/2010. Helsinki Region Environmental Services Authority, Helsinki, Finland, ISBN 978-952-6604-03-9, 124 pp.
Mol, W., van Hooydonk, P., de Leeuw, F., 2010. The state of the air quality in 2008 and the European exchange of monitoring information in 2009. ETC/ACC Technical paper 2010/1, European Topic Centre on Air and Climate Change, Bilthoven, The Netherlands, 77 pp.
Monks, P.J., Granier, C., Fuzzi, S., et al., 2009. Atmospheric composition change – global and regional air quality. Atmospheric Environment 43, 5268–5350.
Niemi, J., Malkki, M., Myllynen, M., Lounasheimo, J., Kousa, A., Julkunen, A., Koskentalo, T., 2009. Air Quality in the Helsinki Metropolitan Area in 2008 (in Finnish with English abstract). Publications 15/2009. YTV Helsinki Metropolitan Area Council, Helsinki, Finland, ISBN 978-951-798-749-3, 128 pp.
Pleijel, H., Klingberg, J., Bäck, E., 2009. Characteristics of NO_2 pollution in the city of Gothenburg, south-west Sweden—relation to NO_x and O_3 levels, photochemistry and monitoring location. Water, Air and Soil Pollution: Focus 9, 15–25.
Seinfeld, J.H., 1986. Atmospheric Chemistry and Physics of Air Pollution. John Wiley & Sons, New York, 738 pp.
Velders, G., Diederen, H., 2009. Likelihood of meeting the EU limit values for NO_2 and PM_{10} concentrations in the Netherlands. Atmospheric Environment 43, 3060–3069.
Vestreng, V., Ntziachristos, L., Semb, A., Reis, S., Isaksen, I.S.A., Tarrason, L., 2009. Evolution of NO_x emissions in Europe with focus on road transport control measures. Atmospheric Chemistry and Physics 9, 1503–1520.
Zamboni, G., Capobianco, M., Daminelli, E., 2009. Estimation of road vehicle exhaust emissions from 1992 to 2010 and comparison with air quality measurements in Genoa, Italy. Atmospheric Environment 43, 1086–1092.

Assessment of the spatial and temporal distribution of persistent organic pollutants (POPs) in the Nordic atmosphere

III

Atmospheric Environment 140 (2016) 22–33

Contents lists available at ScienceDirect

Atmospheric Environment

journal homepage: www.elsevier.com/locate/atmosenv

Assessment of the spatial and temporal distribution of persistent organic pollutants (POPs) in the Nordic atmosphere

Pia Anttila [a, *], Eva Brorström-Lundén [b], Katarina Hansson [b], Hannele Hakola [a], Mika Vestenius [a]

[a] Finnish Meteorological Institute, P.O. Box 503, FI-00101 Helsinki, Finland
[b] IVL Swedish Environmental Research Institute, Sweden

HIGHLIGHTS

- The POP levels were generally higher in the south, closer to the original source areas, compared to the north.
- Elevated concentration levels of low-chlorinated PCBs, chlordanes and α-HCH were detected in the north.
- Most of the legacy POPs showed statistically significant decreasing trends varying from 2 to 6% per year.
- The projections suggest that the most long-lived compounds will persist in the atmospheric cycle beyond 2030.

ARTICLE INFO

Article history:
Received 5 January 2016
Received in revised form
20 May 2016
Accepted 23 May 2016
Available online 24 May 2016

Keywords:
PAHs
PCBs
OCP
Air concentrations
Atmospheric transport
Trends
Scandinavia
South-north gradient
Projections

ABSTRACT

Long-term atmospheric monitoring data (1994–2011) of persistent organic pollutants (POPs) were assembled from a rural site in southern Sweden, Råö, and a remote, sub-Arctic site in Finland, Pallas. The concentration levels, congener profiles, seasonal and temporal trends, and projections were evaluated in order to assess the status of POPs in the Scandinavian atmosphere. Our data include atmospheric concentrations of polycyclic aromatic hydrocarbons (PAHs), polychlorinated biphenyls (PCBs) and organochlorine pesticides (OCPs), altogether comprising a selection of 27 different compounds.

The atmospheric POP levels were generally higher in the south, closer to the sources (primary emissions) of the pollutants. The levels of low-chlorinated PCBs and chlordanes were equal at the two sites, and one of the studied POPs, α-HCH, showed higher levels in the north than in the south.

Declining temporal trends in the atmospheric concentrations for the legacy POPs — PCBs (2–4% per year), HCHs (6–7% per year), chlordanes (3–4% per year) and DTTs (2–5% per year) — were identified both along Sweden's west coast and in the sub-Arctic area of northern Finland. Most of PAHs did not show any significant long-term trends.

The future projections for POP concentrations suggest that in Scandinavia, low-chlorinated PCBs and p,p′-DDE will remain in the atmospheric compartment the longest (beyond 2030). HCH's and PCB180 will be depleted from the Nordic atmosphere first, before 2020, whereas chlordanes and rest of the PCBs will be depleted between the years 2020 and 2025. PCBs tend to deplete sooner and chlordanes later from the sub-Arctic compared to the south of Sweden.

This study demonstrates that the international bans on legacy POPs have successfully reduced the concentrations of these particular substances in the Nordic atmosphere. However, the most long-lived compounds may continue in the atmospheric cycle for another couple of decades.

1. Introduction

Persistent organic pollutants, known as POPs, have a great potential for atmospheric long-range transport. Deposition from the atmosphere is an important pathway for these contaminants to environments both far from and close to their source areas, where

* Corresponding author.
E-mail address: pia.anttila@fmi.fi (P. Anttila).

http://dx.doi.org/10.1016/j.atmosenv.2016.05.044
1352-2310/

they may have adverse effects both on ecosystems and humans (UNEP, 2014). That the atmosphere is an important pathway for POPs into the Nordic environment as well as the Arctic areas has been clearly demonstrated both via measurement activities and model exercises.

Many POPs are semi-volatile, and as such, they can be transported in the atmosphere either in the gas or particulate phases. Atmospheric transport, removal and degradation processes (e.g. precipitation scavenging, dry deposition, photolysis and atmospheric oxidation) act differently on gas and particle-bound substances, thereby affecting their potential for long-range transport (e.g. Bidleman, 1988; Lammel et al., 2009). The properties of atmospheric particles may also affect the gas/particle distribution of POPs, e.g. the organic matter contents of aerosols is an important factor affecting the partitioning between the two phases (e.g. Lohman and Lammel, 2004).

Due to their semi-volatility, several POPs are also characterised by an exchange between the atmosphere and environmental surfaces in a way that has been described as the 'grasshopper effect' (Wania and Mackay, 1996). Gas/surface partitioning is a temperature-driven process. Varying temperatures thus enable repeated surface-air exchanges, which can in turn lead to the migration of POPs by air from the warmer, mid-latitude, primary source areas to the cooler, high-latitude regions. During this 'global fractionation and condensation' process (e.g. Wania and Mackay, 1993, 1996; Lammel and Stemmler, 2012), POP mixtures become fractionated as more volatile substances undergo more frequent secondary releases and thus travel further.

Due to the lipophilic and bio-accumulative properties of POPs, they have a great affinity for organic material in soils and vegetation. Prior studies have demonstrated that global surface soils serve as an important reservoir for POPs (e.g. Meijer et al., 2003a; Ockenden et al., 2003; Dalla Valle et al., 2005; Cabrerizo et al., 2011). Thus remobilization of POPs is driven both by changes in temperature and soil organic matter (SOM) content (Cabrerizo et al., 2013).

Also, water surfaces are known to sequester atmospheric POPs by enhanced air–water diffusive fluxes driven by phytoplankton uptake and organic carbon settling fluxes (Berrojalbiz et al., 2011; Galbán-Malagón et al. 2012, 2013a, 2013b; Nizzetto et al. 2012).

Several of the substances included in the POP group have been used as industrial chemicals or as pesticides, but the majority of the direct production and use (primary emissions) are nowadays banned or have restricted use. However, as a result of their persistence they are still present in the environment and society and are emitted via various diffuse sources. Unintentional releases due to combustion (polycyclic aromatic hydrocarbons PAHs) and inappropriate waste management of decommissioned products (PCBs and organochlorine pesticides OCPs) still continue.

As emissions and atmospheric concentrations of the restricted POPs decline, reservoirs that have accumulated in oceans, on land and in snow/ice can become secondary sources of POPs released into the atmosphere (Bidleman et al., 1995; Stemmler and Lammel, 2009; Ma et al., 2011; Becker et al., 2012; Bidleman et al., 2015). The profile of POPs in the air at any given location is a combination of local and regional primary and secondary emissions and meteorological conditions coupled with transport from more distant regions, mainly through the air.

Long-term air monitoring is a powerful tool for following up on present levels and temporal trends and for assessing atmospheric transport processes and the pathways of POPs, e.g. to remote areas. Data from national monitoring programmes are reported and used within EMEP (Co-operative programme for monitoring and evaluating the long-range transmission of air pollutants in Europe) and AMAP (Arctic Monitoring Assessment Programme) to support international strategies and protocols. Long-term measurements are also used to identify source areas and to obtain information on developing follow-up policies to reduce emissions.

Here, the levels and time trends of POPs in the Nordic atmosphere are presented. Our data include selected polycyclic aromatic hydrocarbons (PAHs), polychlorinated biphenyls (PCBs) and organochlorine pesticides (OCPs), altogether comprising a selection of 27 different compounds that were measured between 1994 and 2011 at two Scandinavian air-quality monitoring stations, Råö and Pallas. Our methods include advanced time series analyses of this unique monitoring data, comparisons of seasonal variations and congener profiles as well as long-term trend analyses. Our goal is to define the status of POPs in the Scandinavian atmosphere with reference to the current distribution and possible sources.

2. Material and methods

2.1. Measurement sites

Råö (until 2002 Rörvik) (57.3937, 11.9142) is a background monitoring station for air pollutants within the EMEP network. It is located close to the shoreline along the west coast of southern Sweden, approximately 35 km south of Gothenburg (Fig. 1). The area has a mild coastal climate with an average monthly mean temperature in January-February of about 0 °C, in July 19 °C and a yearly mean of 9 °C (Gothenburg, SMHI Opendata, 2003–2012).

The Pallas area is located 170 km north of the Arctic Circle (Fig. 1). Pallas is actually an acronym for a collection of several research sites representing contrasting ecosystems. From the very beginning, in 1996, POP measurements have been carried out at the Matorova site (68.00, 24.23). Matorova lies at an elevation of 340 m a.s.l. and is on the top of a hill covered by coniferous forest (Lohila et al., 2015). The monthly mean temperature in January is about −14 °C, in July 14 °C and the yearly mean is −1 °C (Matorova/Kenttärova FMI, 2003–2012).

In terms of POPs, both sites serve as background sites, but Råö, which is located a thousand kilometres further south than Pallas, is more exposed to the potential on-going primary emissions from local and mid/low-latitude sources. Pallas is closer to the accumulated reservoirs of the Arctic ecosystems and potentially more influenced by the remobilised secondary emissions.

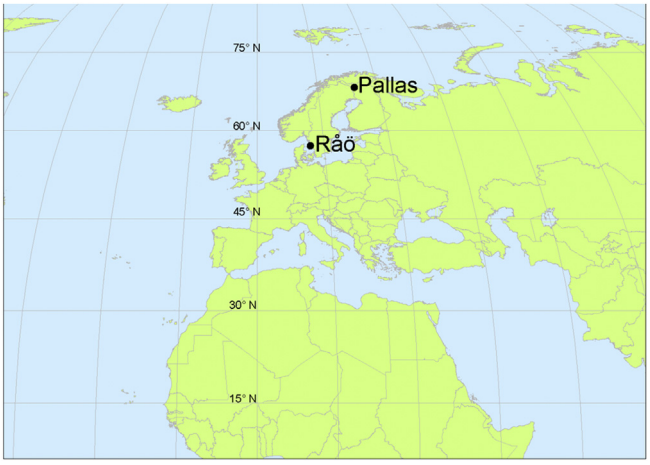

Fig. 1. Location of the sites.

2.2. Sampling and analyses

In the beginning, the sampling programme included one weekly sample per month, and the sampling was undertaken simultaneously at both sites. At Råö the sampling was extended to continuous weekly sampling in 2001, and all samples were analysed (2001–2004) or combined to two week samples (2004–2009). The weekly samples have been collected and combined to represent one month at both sites since 2009. Both the sampling and analysis methods have followed the same procudures during the whole measurement period 1996–2012.

POPs in the air were collected using a high-volume air sampler with a flow rate of approximately 25 m^3/h and 4000 m^3 weekly sample volume. A glass fibre filter was used to trap the particles followed by an adsorbent of polyurethane foam (PUF) to collect compounds in the gas phase. Both fractions (gas + particle) of each weekly sample were combined for analysis.

For the analyses, the Quality Assurance/Quality control (QA/QC) program follow the procedures according to laboratory accreditation (SS-EN ISO/IEC 17025:2005). The laboratory frequently participate in inter-laboratory comparisons e.g. AMAP/EMEP/NCP air monitoring inter-laboratory study (Schlabach et al., 2012) and Northern Contaminants Interlaboratory Quality Assurance Program (NCP III – PHASE 7) (Tkatcheva et al., 2013). Both the sampling and analysis methods have followed the same procudures during the whole measurement period 1996–2012.

More details of the sampling, QA/QC and analytical procedures are described in the Supplementary Information (S1).

2.3. Data analysis methods

The original data sets were homogenised to a continuous monthly time series, i.e. one weekly sample per month was taken as representative for the monthly mean and the weekly/bi-weekly samplings were averaged to obtain a monthly mean. Due to a high number of missing or below-detection limit values, dibenz(*ah*) anthracene data until the year 1999 were rejected from further analysis at both sites; likewise, chlordanes data until the year 1996 was rejected at Råö. After these rejections, the validity rates (missing values and values below detection limits excluded) were over 90% at Råö and over 80% at Pallas (see Tables 1 and 2).

For the trend analyses, the time series were further completed by replacing the missing values with the mean for the previous and subsequent monthly concentrations and values below the detection limit with the half of the detection limit.

In this study, a linear regression model was adopted to calculate the long-term trends of the concentration time series. All of the time series were first visually inspected for non-linearities that obviously could not be explained in a satisfactory manner by the linear regression model. Some of the time series had anomalously high values during the first months/years of the study period, thus suggesting rather an exponential decay. Typically, this initial steep decline levelled off to a moderate rate of change. In these cases, the linear model was fitted only to the latter, even part of the time series. Due to obvious non-linear behaviour, the first 20 months of data on PCB28 at Råö, and first 12 months of data on PCB138, PCB153 and PCB180 at Pallas were rejected from the trend analysis. Similarly, the first year of p,p′-DDT and the three first years of p,p′-DDE at Råö were rejected due to non-linearity problems. p,p′-DDD was not included in the trend analysis at all.

Then the monthly time series were deseasonalized as follows. First, the 13-month moving average (first and last observations averaged) was subtracted from the original monthly observation. The seasonal component thus obtained was normalised to zero by subtracting the residual mean. The seasonal component was then calculated by averaging the normalised deviations on a monthly basis. Relative seasonal components are presented in the supplementary information (S2) for all components.

The trends of the monthly time series were estimated with Generalized Least-Squares (GLS) regression with classical decomposition (additive) and autoregressive moving average (ARMA) errors. Briefly, first a linear regression was fitted on the deseasonalized monthly time series. The optimal error structure (ARMA (p,q)) of the residuals of the fitted linear model was selected. This error structure was then added to the regression model and the GLS estimators were calculated. The coefficients of the linear model and the parameters of the selected ARMA process were estimated by maximizing the Gaussian likelihood. The ML estimation was repeated with the residuals from the updated regression parameters until the parameter values stabilized, providing the final estimates of trend and error structure.

We followed the approach described by Brockwell and Davis (2002). Anttila and Tuovinen (2010) provide more details on the procedure and also compare this method to three other trend analysis methods applied to atmospheric concentration time series.

Using the statistically significant best fit trend lines, we also calculated the future projections obtain estimates on the near-future developments under unaltered assumptions. These projections are rough estimates of future developments assuming that the driving forces for change, such as emissions and climate change rates, remain relatively similar to the originally regressed time period. The projections are here used to compare the developments of POP loads between the two study sites. Care should be taken when using the absolute forecasts or making generalisations based on these results to other environments.

3. Results

Here we present the results for the different substance groups supported by selected graphic examples. All of the trend statistics for Råö and Pallas are summarised in Tables 1 and 2, respectively, where the individual substances included in this data evaluation are also shown. All data on the atmospheric concentrations can be found in the Swedish air data base (http://ivl.se/). The entire set of graphs are presented in the Supplementary Information: seasonal variations, S2; distributions of monthly concentrations, S3; observed time series and fitted seasonal and trend components, S4; and, projections, S5.

3.1. Polycyclic aromatic hydrocarbons (PAHs)

At Råö, the concentrations of PAHs were typically 3–9 times higher than at Pallas. In 2011, the annual mean of the sum of the twelve PAHs ($\sum$PAHs) was 2100 ± 1800 pg/m^3 and 400 ± 350 pg/m^3 at Råö and Pallas, respectively. This difference is obviously the result of the closer proximity of Råö to the major European and Scandinavian PAH sources compared to the more remote Pallas site.

The PAH concentration profiles (Fig. 2: compilation of the 2007–2011 data) at the two sites are similar; at both sites the most volatile PAHs (except anthracene) had the highest concentrations (Fig. 2).

The PAHs in the atmosphere may undergo chemical reactions with atmospheric oxidants, i.e. OH, NO_3/NO_2 and O_3 which may take place both in the gas and particle phases (Keyte et al., 2013). During atmospheric transport, relative compositions of PAH mixtures may be modified by reactions with these oxidants. We investigated whether the remote Pallas site would exhibit a different PAH profile (PAH/$\sum$PAH) than the southern Råö site (Fig. 3). The differences between the relative PAH content at Råö and Pallas were small, but mostly statistically significant (Fig. 3).

Table 1
Results of the trend analyses at Råö between 1994 and 2011. A valid percentage is when missing data and values below the detection limit were excluded. Standard errors for the regression parameters are shown in parenthesis. Trend values (slopes) significantly different (at 95% confidence level) than zero are shown in bold. For the percentage change per annum, the 95% confidence limits are also shown.

Råö	Time period	Valid %	Intercept pg m^{-3}	Slope pg m^{-3} $month^{-1}$	Change % $year^{-1}$
Phenanthrene	5/1994–12/2011	99	1500 (180)	−1.7(1.5)	−1.3 ± 2.3
Anthracene	5/1994–12/2011	99	72 (16)	**−0.33 (0.13)**	**−5.5 ± 4.1**
Fluoranthene	5/1994–12/2011	99	700 (80)	−1.2 (0.6)	−2.1 ± 2.1
Pyrene	5/1994–12/2011	99	560 (90)	−1.5 (0.8)	−3.3 ± 3.2
Benz(*a*)anthracene	5/1994–12/2011	99	110 (4)	**−0.21 (0.04)**	**−2.4 ± 0.8**
Chrysene	5/1994–12/2011	99	180 (26)	−0.17 (0.21)	−1.1 ± 2.7
Benzo(*b*)fluoranthene	5/1994–12/2011	98	180 (30)	−0.30 (0.22)	−2.0 ± 2.9
Benzo(*k*)fluoranthene	5/1994–12/2011	98	78 (12)	−0.13 (0.10)	−2.0 ± 2.9
Benzo(*a*)pyrene	5/1994–12/2011	97	96 (15)	−0.12 (0.12)	−1.6 ± 2.9
Dibenz(*ah*)anthracene	1/1999–12/2011	94	14 (4)	−0.002 (0.04)	−0.2 ± 7.6
Benzo(*ghi*)perylene	5/1994–12/2011	97	100 (21)	+0.01 (0.17)	0.2 ± 4.0
Indeno(123*cd*)pyrene	5/1994–12/2011	92	120 (25)	−0.14 (0.21)	−1.4 ± 4.0
PCB28	1/1997–12/2011	99	2.5 (0.2)	**−0.05 (0.002)**	**−2.5 ± 2.1**
PCB52	5/1994–12/2011	99	4.0 (0.4)	**−0.009 (0.003)**	**−2.7 ± 1.7**
PCB101	5/1994–12/2011	99	4.0 (0.3)	**−0.011 (0.002)**	**−3.4 ± 1.5**
PCB118	5/1994–12/2011	99	1.3 (0.1)	**−0.004 (0.001)**	**−3.3 ± 1.4**
PCB153	5/1994–12/2011	99	2.9 (0.4)	**−0.007 (0.003)**	**−3.0 ± 2.5**
PCB138	5/1994–12/2011	99	2.8 (0.4)	**−0.008 (0.003)**	**−3.3 ± 2.6**
PCB180	5/1994–12/2011	99	1.4 (0.3)	**−0.05 (0.002)**	**−4.4 ± 4.0**
α-HCH	5/1994–12/2011	99	24.9 (2.0)	**−0.120 (0.016)**	**−5.8 ± 1.5**
γ-HCH	5/1994–12/2011	98	33.5 (2.8)	**−0.179 (0.023)**	**−6.4 ± 1.6**
trans-chlordane	2/1996–12/2011	99	0.58 (0.03)	**−0.0022 (0.0002)**	**−4.5 ± 1.0**
cis-chlordane	2/1996–12/2011	98	1.07 (0.07)	**−0.0035 (0.0007)**	**−3.9 ± 1.5**
trans-nonachlor	2/1996–12/2011	99	0.90 (0.07)	**−0.0026 (0.0006)**	**−3.5 ± 1.6**
p,p′-DDT	1/1997–12/2012	96	1.38 (0.16)	**−0.054 (0.0014)**	**−4.7 ± 2.4**
p,p′-DDD	10/1998–12/2012	95	na	na	na
p,p′-DDE	1/1999–12/2012	95	3.34 (0.27)	**−0.0089 (0.0027)**	**−3.2 ± 1.9**

Table 2
Results of the trend analyses at Pallas between 1996 and 2011. A valid percentage is when missing data and values below the detection limit were excluded. Standard errors for the regression parameters are shown in parenthesis. Trend values (slopes) significantly different (at 95% confidence level) than zero are shown in bold. For the percentage change per annum, the 95% confidence limits are also shown.

Pallas	Time period	No of months	Valid %	Intercept pg m^{-3}	Slope pg m^{-3} $month^{-1}$	Change % $year^{-1}$
Phenanthrene	1/1996–12/2011	192	100	400 (40)	−0.50 (0.36)	−1.5 ± 2.1
Anthracene	1/1996–12/2011	192	99	6 (2)	−0.02 (0.02)	−4.4 ± 6.1
Fluoranthene	1/1996–12/2011	192	99	150 (13)	**−0.27 (0.11)**	**−2.2 ± 1.8**
Pyrene	1/1996–12/2011	192	100	81 (8)	−0.11 (0.07)	−1.8 ± 2.0
Benz(*a*)anthracene	1/1996–12/2011	192	94	33 (9)	−0.5 (0.08)	−1.9 ± 5.8
Chrysene	1/1996–12/2011	192	97	43 (7)	−0.01 (0.06)	−0.2 ± 3.2
Benzo(*b*)fluoranthene	1/1996–12/2011	192	99	40 (5)	**−0.11 (0.5)**	**−3.3 ± 2.7**
Benzo(*k*)fluoranthene	1/1996–12/2011	192	99	15 (3)	−0.04 (0.02)	−3.6 ± 3.7
Benzo(*a*)pyrene	1/1996–12/2011	192	94	17 (4)	−0.02 (0.03)	−1.5 ± 4.5
Dibenz(*ah*)anthracene	1/1999–12/2011	156	83	na	na	na
Benzo(*ghi*)perylene	1/1996–12/2011	192	88	18 (3)	−0.04 (0.03)	−2.4 ± 3.6
Indeno(123*cd*)pyrene	1/1996–12/2011	192	81	24 (3)	**−0.07 (0.03)**	**−3.4 ± 2.8**
PCB28	1/1996–12/2011	192	100	2.4 (0.2)	**−0.056 (0.0022)**	**−2.8 ± 2.1**
PCB52	1/1996–12/2011	192	100	2.1 (0.2)	−0.0028 (0.0015)	−1.6 ± 1.6
PCB101	1/1996–12/2011	192	99	1.2 (0.1)	**−0.0036 (0.0011)**	**−3.5 ± 2.0**
PCB118	1/1996–12/2011	192	99	0.44 (0.04)	**−0.0016 (0.0004)**	**−4.3 ± 2.0**
PCB153	1/1997–12/2011	180	99	0.44 (0.03)	**−0.0013 (0.0003)**	**−3.6 ± 1.5**
PCB138	1/1997–12/2011	180	99	0.39 (0.03)	**−0.0013 (0.0003)**	**−3.8 ± 1.6**
PCB180	1/1997–12/2011	180	94	0.13 (0.01)	**−0.0006 (0.0001)**	**−5.5 ± 1.0**
α-HCH	1/1996–12/2011	192	99	23.4 (1.5)	**−0.11 (0.01)**	**−5.8 ± 1.3**
γ-HCH	1/1996–12/2011	192	99	11.3 (0.8)	**−0.063 (0.007)**	**−6.7 ± 1.6**
trans-chlordane	1/1996–12/2011	192	99	0.41 (0.02)	**−0.0014 (0.0002)**	**−4.1 ± 1.1**
cis-chlordane	1/1996–12/2011	192	99	1.00 (0.09)	**−0.0028 (0.0008)**	**−3.3 ± 1.9**
trans-nonachlor	1/1996–12/2011	192	99	0.75 (0.07)	**−0.0021 (0.0006)**	**−3.4 ± 1.8**
p,p′-DDT	1/1996–12/2012	204	91	0.28 (0.03)	**−0.0008 (0.0002)**	**−3.5 ± 1.8**
p,p′-DDD	1/2003–12/2012	120	84	na	na	na
p,p′-DDE	1/1996–12/2012	204	99	0.70 (0.07)	**−0.0013 (0.0006)**	**−2.2 ± 2.1**

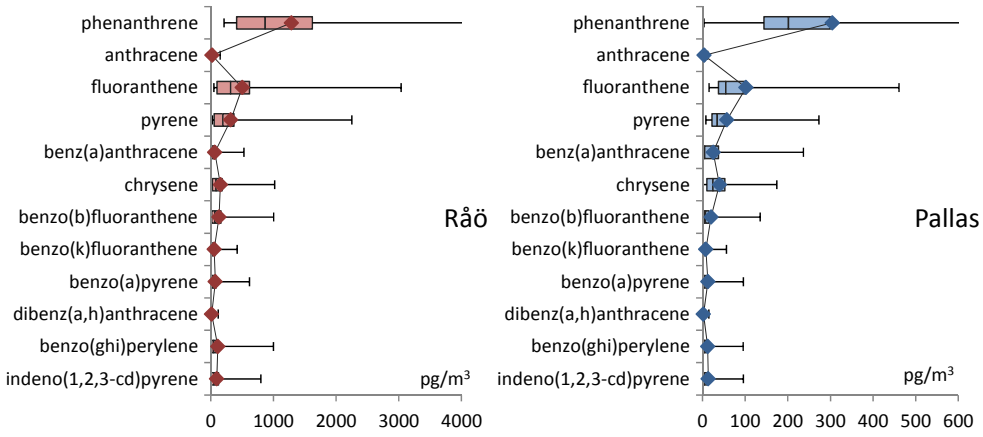

Fig. 2. Distributions of the average monthly PAH concentrations between 2007 and 2011 at Råö and Pallas. Minimum, first quartile, median, third quartile and maximum levels are shown. The means are denoted with diamonds and connected with a line.

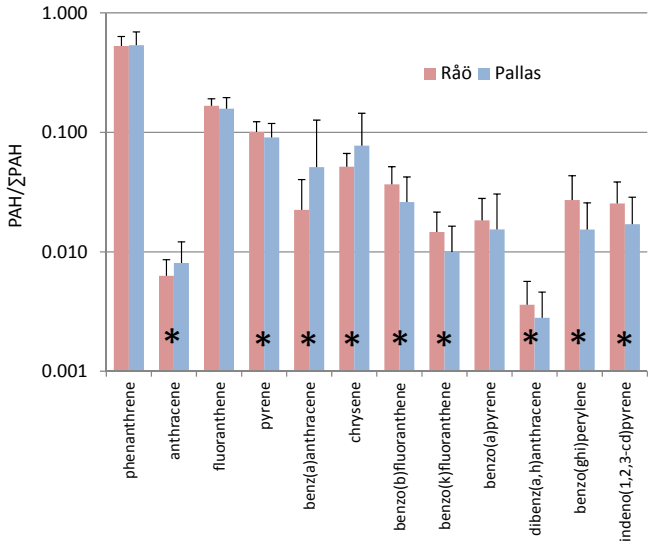

Fig. 3. Relative average contribution of each individual PAH to the sum of the 12 PAHs for the years 2007–2011 at Råö and Pallas. The error bars are standard deviations of the ratios. The stars indicate significant differences of the ratio PAH/sumPAH between the two sites (at $p < 0.05$, two tailed *t*-test for the difference of means, $n = 60$).

The PAHs with three or four aromatic rings (up to chrysene) tended to be relatively more abundant at the remote Pallas site, while the heavier PAHs with five or six rings (from benzo(*b*)fluoranthene onward) had a higher relative contribution at the more polluted Råö site (Fig. 3). A similar principal pattern occurred both during the summer and winter time (not shown).

All PAHs at both sites had the highest concentrations in the winter months, which then steeply decreased in April (Råö) and March (Pallas) (Fig. 4). Concentrations started to increase again in October (Råö) and November (Pallas). This behaviour could be connected to the higher emission rates and ineffective atmospheric photochemical loss in wintertime. For example, at Pallas the increase in insolation after the winter solstice (which ends in the middle of January) is steep towards the summer solstice, starting in the beginning of June, which could explain the decrease in PAH concentrations. This behaviour is quite similar for both volatile and non-volatile PAHs, so we concluded that primary emissions, long-range transport and atmospheric removal processes control the PAH concentrations at both sites.

Most PAHs did not have any significant long-term trends (Tables 1 and 2; S4), which could be related to the ongoing and not decreasing emissions in the major source areas. However, the individual PAHs behaved rather differently. At Råö, anthracene and benzo(a) anthracene did decrease by −5.5% per year and −2.4% per year, respectively. At Pallas, fluoranthene, benzo(*b*)fluoranthene and indeno (1,2,3-cd)pyrene decreased by −2.2% per year, −3.3% per year and −3.4% per year, respectively. At both sites, benzo(*a*) pyrene decreased by 1–2 per cent per year, but this trend was not statistically significant (Tables 1 and 2).

3.2. Polychlorinated biphenyls PCBs

PCB concentrations were higher at Råö than at Pallas. For example, in 2011 the annual means of the ∑PCB (sum of the seven PCBs) were 12.5 ± 7.5 pg/m^3 and 4.1 ± 3.4 pg/m^3 at Råö and Pallas, respectively. Compared to the concentration levels detected in 2005 at Arctic sites in Canada (Alert), Iceland (Storhofdi) and Zeppelin (Svalbard, Norway), the concentrations at Råö were clearly higher (twice as high) while those at Pallas were equal or lower (see Hung et al., 2016).

The PCB profiles differed between Råö and Pallas (Fig. 5a,b), and the concentration ratio for Råö/Pallas increased systematically from 1 to 19 when going from the most volatile and low-chlorinated PCB28 (tri-CB) to the high-chlorinated PCB180 (hepta-CB) (Fig. 5c).

So, low chlorinated and most volatile PCB congeners make up a greater proportion of the measured PCBs at Pallas than at Råö. Latitudinal fractionation of atmospheric concentrations of the low molecular PCBs along the North Western Europe has been reported since the 1990's (Ockenden et al., 1998; Agrell et al., 1999; Meijer et al., 2003b; Schuster et al., 2010). These studies concluded that latitudinal fractionation in this region is driven by primary (diffusive) emissions and the higher long-range transport potentials of the more volatile PCBs.

It would be expected that moving over from primary emissions to secondary emissions (re-volatilisation from surfaces) would be reflected in the resulting atmospheric PCB mixtures (e.g. Schuster et al., 2010; Li et al., 2010,; Lammel and Stemmler, 2012). The time development of the fractionation the PCB congeners (PCB/∑PCB) at Råö and Pallas, 1995–2011, is presented in Fig. 6. After the first years of measurements, the relative abundances of PCB congeners have remained essentially stable, and no systematic change in the fractionation pattern can be detected (Fig. 6). This result suggests that primary diffusive emissions still are dominating, especially at Pallas. This result is in line with the findings by

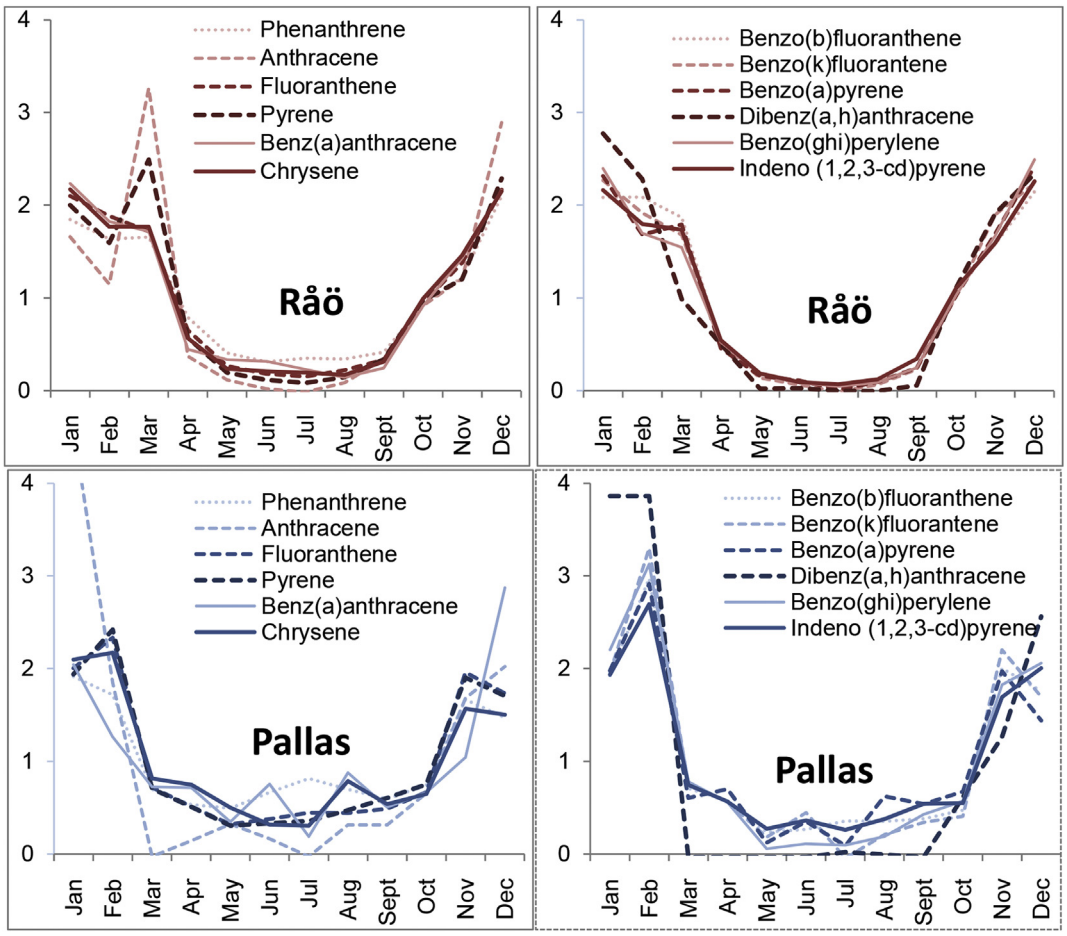

Fig. 4. The relative seasonal components of the PAH compounds at Råö and Pallas (normalised to the centre of the aggregation period).

Schuster et al. (2010).

The more volatile PCBs in particular displayed also a regular seasonal cycling with summer maxima (S2), suggesting a significant diffusive fraction. Only PCB180 at Pallas displayed a deviant spring (March) maximum (S2).

In April–May 2006, smoke plumes from agricultural fires in Eastern Europe swept over most of the European Arctic (e.g. Stohl et al., 2007; Eckhardt et al., 2007) and Scandinavia (Anttila et al., 2008; Makkonen et al., 2010; Targino et al., 2013), causing elevated PCB levels, among other problems. Interestingly, we detected an abnormal spring maximum in April 2006 for most of the PCBs at Pallas, too (Fig. 7; S4). For low-chlorinated PCBs, this long-range transported pollution episode caused smaller peaks than the corresponding regular summer peaks, while for the medium-chlorinated and more highly chlorinated PCBs (PCB138; 153; 180) this and other irregular LRT episodes seemed to exceed the summer maxima. As a whole, at both sites the atmospheric concentrations of PCBs seem to be controlled by seasonal volatilisation and by the irregular LRT episodes.

All fourteen PCB time series exhibited a decreasing linear trend (only PCB52 at Pallas was not significant), typically 2–4% per year (the first exponentially decreasing months excluded) (Tables 1 and 2). The rates of decline were similar at the both sites and for all congeners, especially at Pallas, where the congener mixture maintained essentially unchanged throughout the decline period (see Fig. 6).

The decreasing PCB trends in the Arctic, North America and Europe have also been identified in several other studies (e.g. Hung et al., 2010, 2016; Kong et al., 2014). Hung et al. (2016) also detected, via the so-called digital filtration method, that some of the PCB decline at Pallas seems to have slowed down and concentrations have dropped to a low level in recent years. This kind of change is indiscernible, by default, with our analysis method. As a whole, the internationally implemented production, use and emission restrictions have been successful in reducing the amount of PCBs circulating via the atmospheric pathways at these two sites.

Using regression analysis, we calculated the concentration projections for the future. The currently equal PCB28 concentrations at Råö and Pallas are also declining at the same rate and concentrations are projected to reach a level of zero by the mid-2030s (S5). In general, according to these projections the more chlorinated PCBs will be depleted from the atmospheric compartment sooner: PCB180 already by the end of the 2010s and PCB101, 118, 138 and 153 sometime in the 2020s. Note, that in practice the PCBs (which mostly have a strong seasonal variation with summer maxima) will first be depleted in winter time while the summer maxima will continue to be detectable for a longer period of time.

3.3. Organochlorine pesticides OCPs

3.3.1. Hexachlorocyclohexanes

In 2011, the annual means for α-HCH and γ-HCH were 4.2 ± 1.0 pg/m^3 and 2.9 ± 1.2 pg/m^3 at Råö and 4.9 ± 1.3 pg/m^3 and 1.5 ± 0.9 pg/m^3 at Pallas, respectively. Evidently, the 2011 annual mean of α-HCH at Pallas was higher than at Råö; and this was also the case during the period 2007–2011 (Råö 4.2 ± 1.5 pg/m^3; Pallas

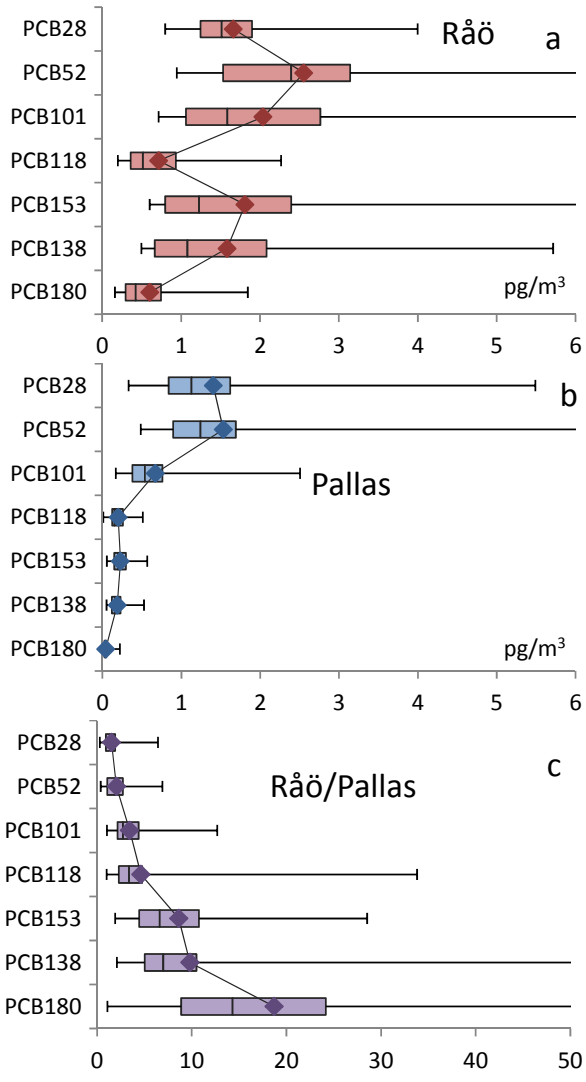

Fig. 5. Distributions (min, 1st quartile, median, mean, 3rd quartile, max) of the monthly PCB concentrations for the years 2007–2011 at Råö (a) and Pallas (b). Distribution of the monthly Råö/Pallas ratio (c).

5.2 ± 2.0 pg/m^3; p = 0.004) (S3). We also calculated the long term GLS-ARMA trend for the monthly α-HCH ratio between Råö and Pallas. This ratio Pallas/Råö has been 1.3 ± 0.5 with no significant trend (not shown) since the start of the parallel measurement in 1996. α-HCH is the only substance in this study that shows higher concentrations at Pallas than Råö. For comparison, at Zeppelin in the high Arctic the annual averages in 2011 were 6.3 pg/m^3 and 0.89 pg/m^3 for α-HCH and γ-HCH, respectively (data from http://ebas.nilu.no/). Thus, atmospheric α-HCH shows an increasing concentration gradient from south to north, while γ-HCH shows a more common spatial gradient with higher concentrations in the south.

The use and production of technical HCH (mainly α-HCH) was banned earlier than γ-HCH (lindane); consequently, γ-HCH has a higher risk for atmospheric emissions (primary or secondary) in the original consumption areas, and Råö is more exposed due to its closer proximity to the original production and use areas in other parts of Europe.

Air–sea exchange studies have shown that α-HCH strongly partition into cold water, resulting in an accumulation of α-HCH in the northern oceans (e.g. Iwata et al., 1993; Bidleman et al., 1995; Jantunen and Bidleman, 1996; Li et al., 1998). Due to declining primary emissions and atmospheric concentrations, the storage levels in oceans have changed from being a sink to a source. Researchers now believe that this secondary emission is the major contributor to the observed atmospheric concentrations of HCHs, especially in the Arctic regions (e.g. Wu et al., 2010; Wöhrnschimmel et al., 2012; Bidleman et al., 2015).

At both Råö and Pallas, HCHs have a regular seasonal variation with high concentrations during summer (S2), indicating volatilisation, i.e. diffusive emissions. The enhanced summer re-volatilisation of HCHs from the global reservoirs most likely controls the HCH concentrations at both sites.

During the period 1994–2011, the α-HCH concentrations decreased at the same rate (5.8% per year) (Tables 1 and 2) with the constant concentration ratio, 1.3 at the two sites (Fig. 8). With this decline rate, α-HCH is projected to be eliminated from the atmosphere sometime in the 2010's (S5).

The adopted γ-HCH (lindane) restrictions after the mid-90s are clearly reflected in the concentration time series (Fig. 8). The long-term concentrations decreased by 6.4 ± 1.6 and 6.8 ± 1.6 per cent a

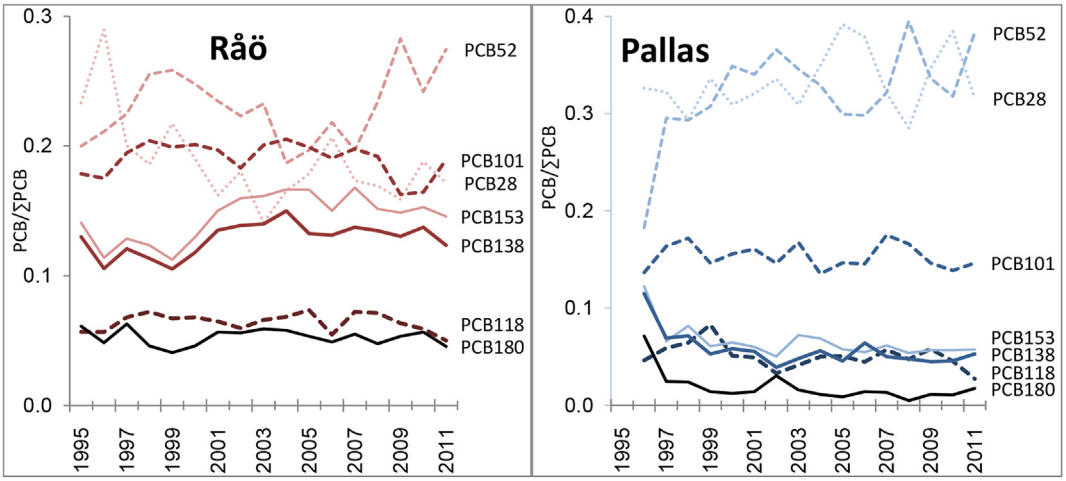

Fig. 6. Annual means of the PCB congener fractions at Råö and Pallas, 1995–2011.

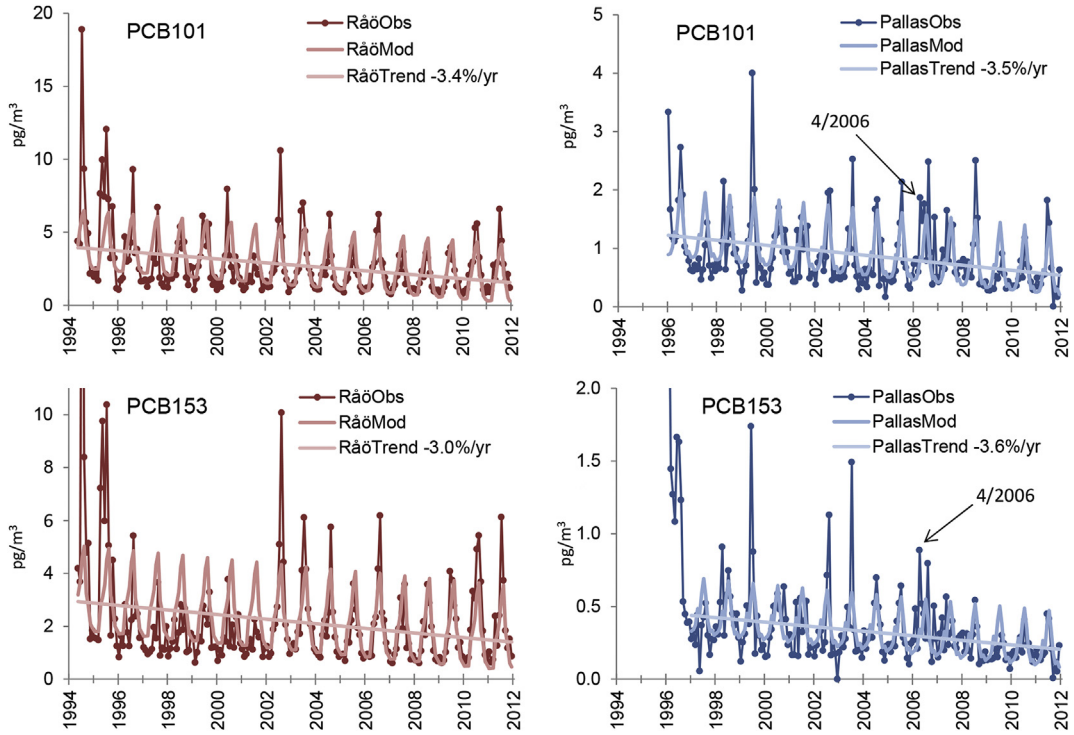

Fig. 7. The observed time series (Obs) for PCB101 and PCB153 at Råö and Pallas. The modelled seasonal and GLS-ARMA components (Mod) as well as the trend line (Trend) are shown. In the legend, the percentage change per annum is given for the statistically significant trends.

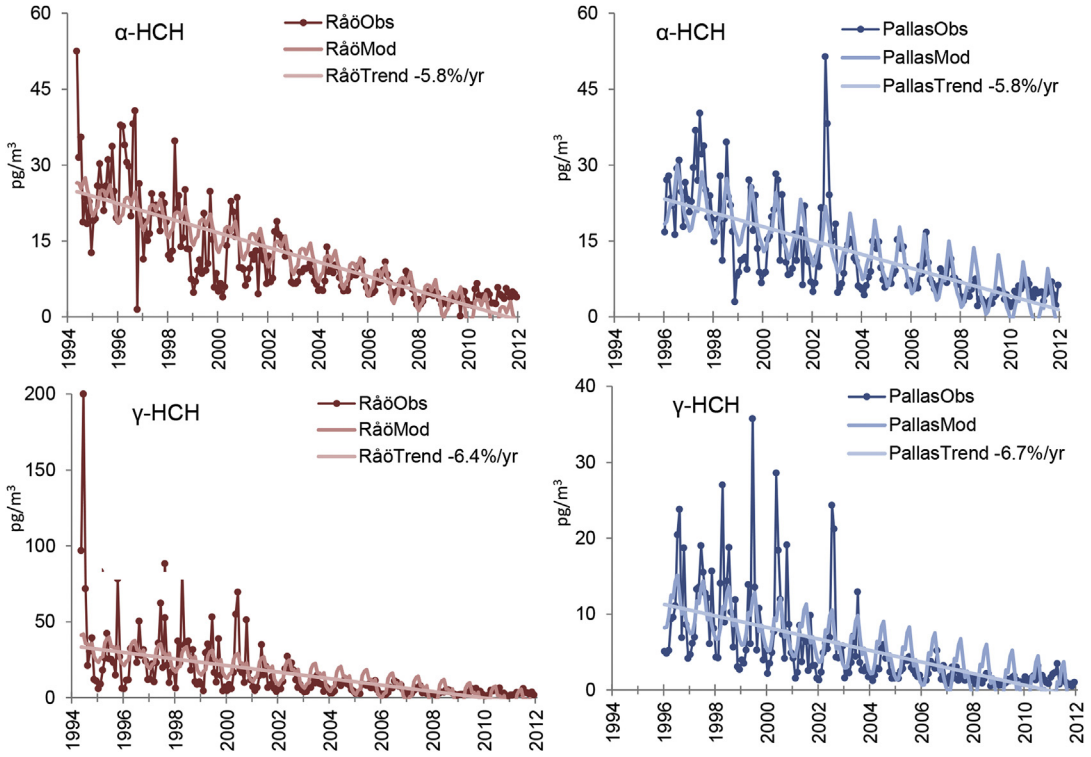

Fig. 8. The observed time series (Obs) for HCHs at Råö (red) and Pallas (blue). The modelled seasonal and GLS-ARMA components (Mod) as well as the trend line (Trend) are shown. In the legend, the percentage change per annum is given for the statistically significant trends. (For interpretation of the references to colour in this figure legend, the reader is referred to the web version of this article.)

year at Råö and Pallas, respectively, which are the largest decline rates in this study.

With this high rate of change (over 6% per year), the projected γ-HCH concentrations will be declining towards a concentration of

close to zero already in the 2010s (S5). Note, however, that visual assessments (S3) might suggest that the strong decreasing trends for HCHs have been levelling off in the past couple of years, a pattern that our linear model is unable to discern.

3.3.2. Chlordanes

The concentrations of the three studied chlordane isomers were slightly higher at Råö than at Pallas with the Råö/Pallas ratios (2007–2011) being 1.6, 1.2 (not significant, $p = 0.2525$) and 1.4 for *trans*-chlordane, *cis*-chlordane and *trans*-nonachlor, respectively (S3). The most abundant isomer was *cis*-chlordane.

Due to the production and use restrictions, in general chlordanes display overall decreasing trends of 3.3–4.5% per year (Fig. 9). Interestingly, at both sites prior to 2003 all three isomers (but mostly *trans*-chlordane) tended to display periods of elevated concentrations that are not consistent with the overall trend. These periods could be related to the long-range transport of fresh chlordane emissions, e.g. from ongoing (and peaking) production and usage in China (Wang et al., 2013).

The levels of *cis*-chlordane and *trans*-nonachlor were highest during the summer months, while the *trans*-chlordane levels had a summer minimum (S2). The summertime decrease in atmospheric *trans*-chlordane level in the Arctic could be due to its greater photochemical reactivity (Oehme, 1991; Halsall et al., 1998; Hung et al., 2002; Becker et al., 2012), or to an increased contribution of microbially-weathered *trans*-chlordane from secondary sources (Bidleman et al., 2015).

The main constituents of technical chlordane are *trans*-chlordane (TC) and *cis*-chlordane (CC), with the TC/CC ratio typically being 1.1–1.3 (Buchert et al., 1989; Patton et al., 1991). Thus, in fresh emissions *trans*-chlordane is more abundant than *cis*-chlordane, but this ratio will change over time as *trans*-chlordane becomes more degradable in the environment. Declining trends in the ratios of *trans*-chlordane to *cis*-chlordane (TC/CC) have previously been detected and might well indicate a shift from primary sources to more aged secondary sources (Bidleman et al., 2002; Becker et al., 2012).

The TC/CC ratios in this study, expressed as the fraction $F_{TC} = TC/(TC + CC)$, were generally higher at Råö than at Pallas; but both sites showed a distinctive seasonal variation with respect to the

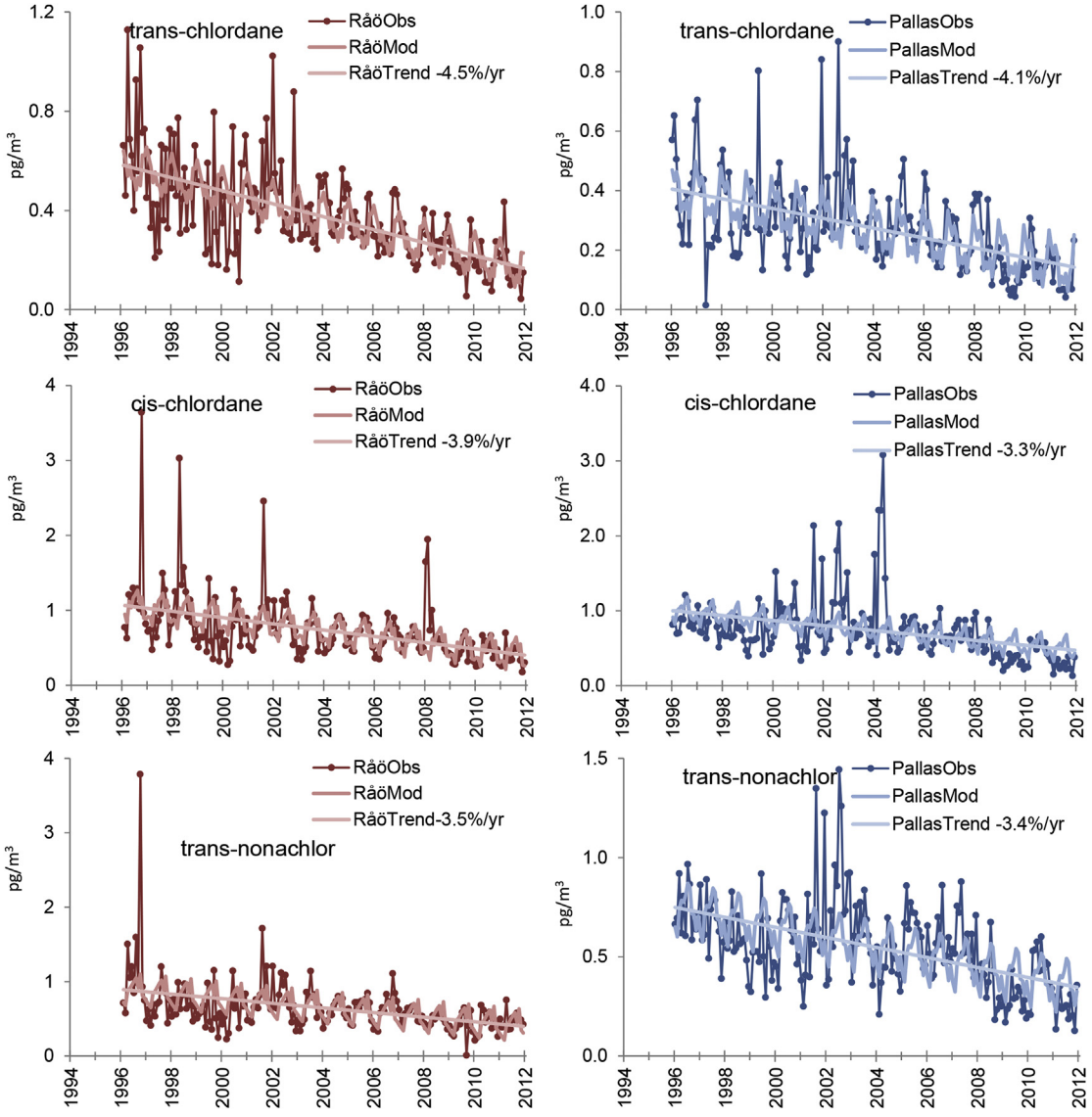

Fig. 9. The observed time series (Obs) for chlordanes at Råö and Pallas. The modelled seasonal and GLS-ARMA components (Mod) as well as the trend line (Trend) are shown. In the legend, the percentage change per annum is given for the statistically significant trends.

wintertime maxima and summertime minima. We also discovered a very weak (c. −1% per year), but significant, declining long-term trend for F_{TC} (Fig. 10) at both sites. The F_{TC} time series at Pallas are similar to the ones recorded for Alert, Canada between 1994 and 2000, as presented by Bidleman et al. (2015).

Our findings suggest that Råö generally could be more influenced by a relatively fresh chlordane source, as exemplified on two occasions: November 2002 and January 2004 (TC/CC > 1). The summertime decrease in *trans*-chlordane compared to *cis*-chlordane was equal at both sites. The long-term total loss of TC seems to be a slow process (e.g. the half-life of F_{TC} is 50 years).

The projections for chlordanes suggest that *trans*-chlordane, the most degradable isomer, will be depleted from the Nordic atmosphere first, sometime in the 2020s, with *cis*-chlordane and *trans*-nonachlor being depleted some years later (S5). Chlordanes will be depleted at Råö before Pallas (S5).

3.3.3. *p,p′-DDT, p,p′-DDD and p,p′-DDE*

In 2011, the annual means for p,p′-DDT, p,p′-DDD and p,p′-DDE were 0.33 ± 0.24 pg/m^3, 0.58 ± 0.26 pg/m^3 and 2.8 ± 1.4 pg/m^3, respectively, at Råö. They were 0.22 ± 0.23 pg/m^3, 0.06 ± 0.03 pg/m^3 and 0.49 ± 0.35 pg/m^3, respectively, at Pallas. During the five-year period from 2007 to 2011 (S3), the mean concentrations at Råö were 2–4 times higher than at Pallas (the ratios were 2.9, 1.6 and 4.2 for p,p′-DDT, p,p′-DDD and p,p′-DDE, respectively). The ratios (p,p′-DDD + p,p′-DDE)/p,p′-DDT were 4.8 and 3.8 at Råö and Pallas, i.e. the concentrations of the degradation products of DDT were four to five times higher at both sites. p,p′-DDE was the most abundant metabolite.

The time series for DDTs were problematic to adjust with respect to linear trends (Fig. 11). The p,p′-DDD time series had no systematic seasonal variation and displayed both high and low concentration periods lasting for an uneven number of years. Linear regression was not attempted for p,p′-DDD. Also, p,p′-DDT and p,p′-DDE behaved more irregularly than other OCPs, but satisfactory linear models could be fitted to the shortened time series (Fig. 11). Of the DDT residues, only p,p′-DDE had a relatively consistent seasonal variation at both sites with the late autumn maximum and summertime minimum (S2), which also is in contrast with the other OCPs.

The more erratic behaviour of DDT residues may be due to the ongoing primary emissions and because DDTs are among the least volatile and most particle bound of the OCPs, which limits their ability to become well mixed on a regional scale.

For p,p′-DDT and p,p′-DDE, this adjusted analysis resulted in statistically significant decreasing trends (2–5% per year) at both sites, and the projections (S5) suggest that these compounds will be eliminated from the atmospheric cycle first at Råö, by the late 2010s (DDT) or early 2030s (DDE), and at Pallas ten years later.

4. Conclusions

The monitoring of POPs in the Nordic atmosphere confirms the fact that the atmosphere is also an important pathway for these contaminants into the Nordic environment in more remote areas. There are, however, spatial and temporal variations among substances and substance groups, which differ in the south and north of Scandinavia. The POP levels were generally higher in the south, closer to the original source areas in the mid-latitudes, compared to the sub-Arctic north. However, the levels of low-chlorinated PCBs and chlordanes were equal at the two sites, and α-HCH showed higher levels in the north than south.

Declining temporal trends in the atmospheric concentrations for the legacy POPs — PCBs, HCHs, chlordanes and DDTs — were identified both along the Swedish west coast and in the sub-Arctic area of northern Finland. On the other hand, most PAHs did not show any significant long-term trends.

The future projections for POPs concentrations suggest that in Scandinavia, low-chlorinated PCBs and p,p′-DDE will remain in the atmospheric compartment the longest (beyond 2030), while HCHs and PCB180 will be depleted from the Nordic atmosphere first, already before 2020. PCBs tend to be depleted sooner and chlordanes later from the sub-Arctic area of Pallas than from Råö, in southern Sweden.

The observed atmospheric POP levels and their distribution in the Nordic atmosphere are a result of both primary and secondary emission sources and of transport, transformation and deposition processes, which depend on the chemical and physical properties of the individual POPs, as well as by meteorological conditions, including LRT events.

In summary for the different substance groups:

- The PCB levels were higher in the south closer to source areas. The distribution of the congeners differed between south and north, with a higher share of low-chlorinated PCBs in northern Finland compared the south of Sweden. The relative abundances of PCB congeners have remained relatively unchanged since the late 1990's. The atmospheric concentrations of PCBs seem to be largely controlled by seasonal volatilisation at both sites. However, at Pallas irregular LRT episodes were identified by an increased amount of high-chlorinated PCBs. All of the PCBs except one (PCB52 at Pallas) had a significant decreasing trend

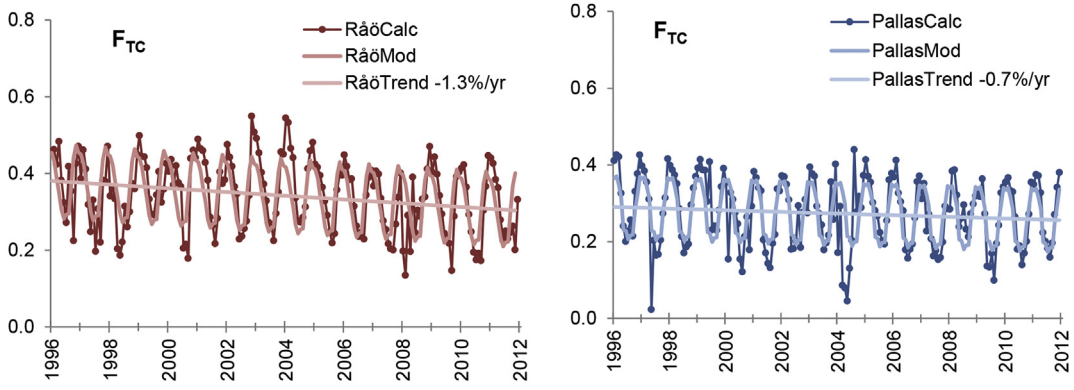

Fig. 10. The calculated (Calc) F_{TC}s (F_{TC} = TC/(TC + CC)) at Råö and Pallas in the years 1996–2011. The modelled F_{TC}'s seasonal and GLS-ARMA components (Mod) as well as the trend line (Trend) are shown.

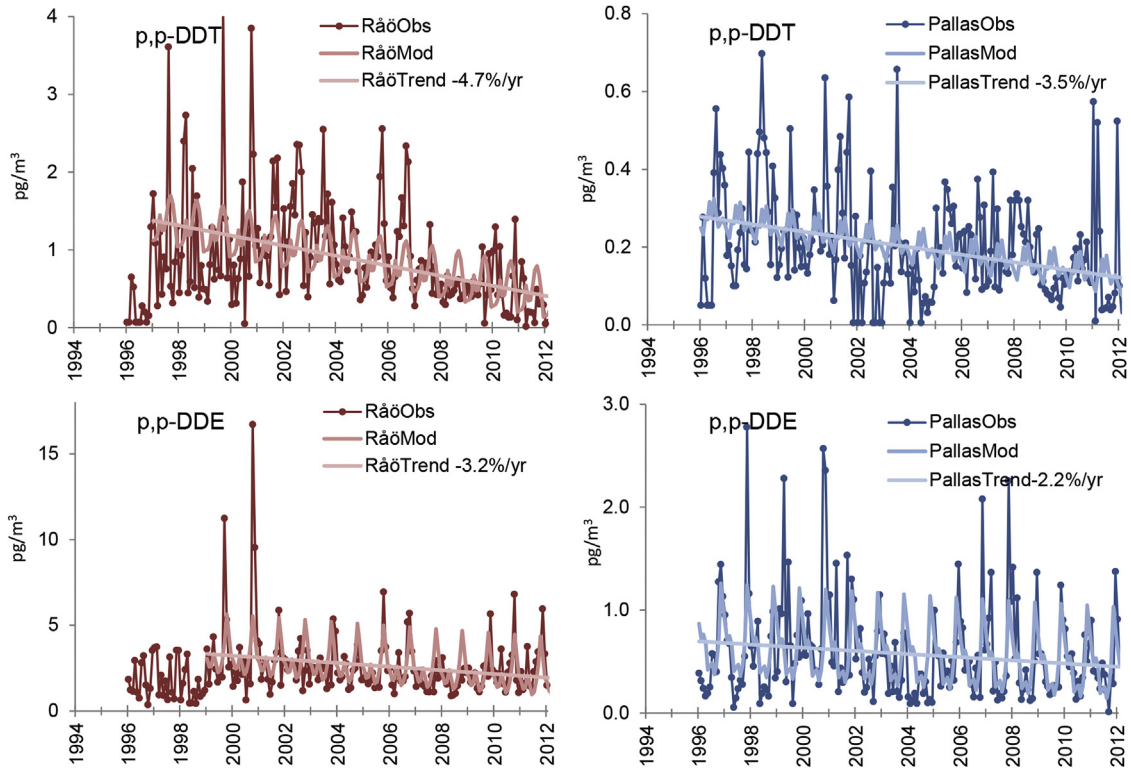

Fig. 11. The observed time series (Obs) for p,p′-DDT and p,p′-DDE at Råö and Pallas. The modelled seasonal and GLS-ARMA components (Mod) as well as the trend line (Trend) are shown. In the legend, the percentage change per annum is given for the statistically significant trends.

from 1994 to 2011, typically 2–4% per year. With these decline rates, the higher chlorinated PCBs will be depleted from the atmosphere by the end of the 2010s or 2020s, while the low-chlorinated PCBs will be depleted in the 2030s or later.

- α-HCH concentration was 30% higher at Pallas than at Råö, and this ratio has been unchanged throughout the whole study period. Thus, atmospheric α-HCH shows an increasing concentration gradient from south to north, while γ-HCH shows a more common spatial gradient with higher concentrations in the south. HCH concentrations have decreased quite rapidly between 1994 and 2011 (6–7% per year) at both sites.
- The concentrations of *trans*-chlordane and *trans*–nonachlor were slightly higher at Råö, while *cis*-chlordane concentrations were on the same level at both sites, which suggests that chlordanes are relatively evenly distributed in the Nordic atmosphere. Chlordanes show a decreasing trend from 1994 to 2011 (3.3–4.5% per year). The projections for chlordanes suggest that the most degradable *trans*-chlordane will be depleted from the Nordic atmosphere by around 2020, and *cis*-chlordane and *trans*-nonachlor a couple of years later. Chlordanes will be depleted from the southern Scandinavian atmosphere first.
- DDTs behaved more irregularly than other OCPs in terms of seasonal variation and long-term trends. The more erratic behaviour of DDT residues may be because of ongoing primary emissions and because DDTs are among the least volatile of OCPs, which limits their ability to become well mixed on a regional scale. However, we discovered a statistically significant decreasing trend from 1994 to 2011 (2–5% per year) for p,p′-DDT and p,p′-DDE. The projections suggest that DDTs will be removed from the atmospheric cycle first at Råö in the late 2010s (DDT) and early 2030s (DDE) and at Pallas ten years later. PAH levels were higher in southern Sweden than in the remote parts of northern Finland, with a winter maxima being recorded at both locations. Most PAHs did not have any significant long-term time trends. Ongoing primary emissions, atmospheric removal processes and long-range transport most likely control the PAH concentrations at the Nordic background areas.

Acknowledgements

The authors want to thank Ann Sjöblom from the IVL Swedish Environmental Research Institute for her analytical work and John Munthe at the IVL Swedish Environmental Research Institute for his comments on the manuscript as well as the Swedish Environmental Protection Agency for its financial support.

Supplementary information

Supplementary information related to this article can be found at http://dx.doi.org/10.1016/j.atmosenv.2016.05.044.

References

Agrell, C., Okla, L., Larsson, P., Backe, C., Wania, F., 1999. Evidence of latitudinal fractionation of polychlorinated biphenyl congeners along the Baltic Sea Region. Environ. Sci. Technol. 37, 454–461.

Anttila, P., Makkonen, U., Hellén, H., Pyy, K., Leppänen, S., Saari, H., Hakola, H., 2008. Impact of the open biomass fires in spring and summer of 2006 on the chemical composition of background air in south-eastern Finland. Atmos. Environ. 42, 6472–6486. http://dx.doi.org/10.1016/j.atmosenv.2008.04.020.

Anttila, P., Tuovinen, J.-P., 2010. Trends of primary and secondary pollutant concentrations in Finland in 1994–2007. Atmos. Environ. 44, 30–41.

Becker, S., Halsall, C.J., Tych, W., Kallenborn, R., Schlabach, M., Manø, S., 2012. Changing sources and environmental factors reduce the rates of decline of organochlorine pesticides in the Arctic atmosphere. Atmos. Chem. Phys. 12, 4033–4044.

Berrojalbiz, N., Dachs, J., Del Vento, S., Ojeda, M.J., Valle, M.C., Castro-Jiménez, J., Mariani, G., Wollgast, J., Hanke, G., 2011. Persistent organic pollutants in Mediterranean seawater and processes affecting their accumulation in plankton. Environ. Sci. Technol. 45, 4315–4322.

Bidleman, T., 1988. Atmospheric processes: wet and dry deposition of organic compounds are controlled by their vapour-particle partitioning. Environ. Sci. Technol. 22, 361–367.
Bidleman, T.F., Jantunen, L.M., Falconer, R.L., Barrie, L.A., Fellin, P., 1995. Decline of hexachlorocyclohexane in the Arctic atmosphere and reversal of air-sea gas exchange. Geophys. Res. Lett. 22, 219–222.
Bidleman, T.F., Jantunen, L.M., Helm, P., Brorström-Lundén, E., Juntto, S., 2002. Chlordane enantiomers and temporal trends of chlordane isomers in Arctic air. Environ. Sci. Technol. 36, 539–545.
Bidleman, T.F., Jantunen, L.M., Hung, H., Ma, J., Stern, G.A., Rosenberg, B., Racine, J., 2015. Annual cycles of organochlorine pesticide enantiomers in Arctic air suggest changing sources and pathways. Atmos. Chem. Phys. 15, 1411–1420.
Brockwell, P.J., Davis, R.A., 2002. Introduction to Time Series and Forecasting, second ed. Springer-Verlag, New York, Inc.
Buchert, H., Class, T., Ballschmiter, K., 1989. High resolution gas chromatography of technical chlordane with electron capture- and mass selective detection. Fresenius' Z. für Anal. Chem. 333 (3), 211–217.
Cabrerizo, A., Dachs, J., Jones, K.C., Barceló, D., 2011. Soil–air exchange controls on background atmospheric concentrations of organochlorine pesticides. Atmos. Chem. Phys. 11, 12799–12811.
Cabrerizo, A., Dachs, J., Barceló, D., Jones, K.C., 2013. Climatic and biogeochemical controls on the remobilization and reservoirs of persistent organic pollutants in Antarctica. Environ. Sci. Technol. 47, 4299–4306.
Dalla Valle, M., Jurado, E., Dachs, J., Sweetman, A.J., Jones, K.C., 2005. The maximum reservoir capacity of soils for persistent organic pollutants: implications for global cycling. Environ. Pollut. 134, 153–164.
Eckhardt, S., Breivik, K., Manø, S., Stohl, A., 2007. Record high peaks in PCB concentrations in the Arctic atmosphere due to long-range transport of biomass burning emissions. Atmos. Chem. Phys. 7, 4527–4536.
Galbán-Malagón, C., Berrojalbiz, N., Ojeda, M.J., Dachs, J., 2012. The oceanic biological pump modulates the atmospheric transport of persistent organic pollutants to the Arctic. Nat. Commun. 3, 862. http://dx.doi.org/10.1038/ncomms1858.
Galbán-Malagón, C., Berrojalbiz, N., Gioia, R., Dachs, J., 2013a. The degradative and biological pumps controls on the atmospheric deposition and sequestration of hexachlorocyclohexanes and hexachlorobenzene in the North Atlantic and Arctic Oceans. Environ. Sci. Technol. 47, 7195–7203.
Galbán-Malagón, C., Del Vento, S., Cabrerizo, A., Dachs, J., 2013b. Factors affecting the atmospheric occurrence and deposition of polychlorinated biphenyls in the Southern Ocean. Atmos. Chem. Phys. 13, 12029–12041.
Halsall, C.J., Bailey, R., Stern, G.A., Barrie, L.A., Fellin, P., Muir, D.C.G., Rosenberg, B., Rovinsky, F., Kononov, E., Pastukhov, B., 1998. Multi-year observations of organohalogen pesticides in the Arctic atmosphere. Environ. Pollut. 102, 51–62.
Hung, H., Halsall, C.J., Blanchard, P., Li, H.H., Fellin, P., Stern, G., Rosenberg, B., 2002. Temporal trends of organochlorine pesticides in the Canadian Arctic atmosphere. Environ. Sci. Technol. 36, 862–868.
Hung, H., Kallenborn, R., Breivik, K., Su, Y., Brorström-Lundén, E., Olafsdottir, K., Thorlacius, J.M., Leppänen, S., Bossi, R., Skov, H., Manø, S., Patton, G.W., Stern, G., Sverko, E., Fellin, P., 2010. Atmospheric monitoring of organic pollutants in the Arctic under the Arctic Monitoring and Assessment Programme (AMAP): 1993-2006. Sci. Total Environ. 408, 2854–2873.
Hung, H., Katsoyiannis, A.A., Brorström-Lundén, E., Olafsdottird, K., Aas, W., Breivik, K., Bohlin-Nizzetto, P., Sigurdsson, A., Hakola, H., Bossi, R., Skov, H., Sverko, E., Barresi, E., Fellin, P., Wilson, S., 2016. Temporal trends of persistent organic pollutants (POPs) in Arctic air: 20 years of monitoring under the Arctic Monitoring and Assessment Programme (AMAP). Environ. Pollut. http://dx.doi.org/10.1016/j.envpol.2016.01.079.
Iwata, H., Tanabe, S., Sakai, N., Tatsukawa, R.D., 1993. Distribution of persistent organochlorine pollutants in the oceanic air and surface seawater and the role of ocean on their global transport and fate. Environ. Sci. Technol. 27, 1080–1098.
Jantunen, L.M., Bidleman, T., 1996. Air water gas exchange of hexachlorocyclohexanes (HCHs) and the enantiomers of α-HCH in arctic regions. J. Geophys. Res. 101 (D22), 28837–28846.
Keyte, I.J., Harrison, R.M., Lammel, G., 2013. Chemical reactivity and long-range transport potential of polycyclic aromatic hydrocarbons -a review. Chem. Soc. Rev. 42, 9333–9392.
Kong, D., MacLeod, M., Hung, H., Cousins, I.T., 2014. Statistical analysis of long-term monitoring data for persistent organic pollutants in the atmosphere at 20 monitoring stations broadly indicates declining concentrations. Environ. Sci. Technol. 48, 12492–12499.
Lammel, G., Sehili, A.M., Bond, T.C., Feichter, J., Grassl, H., 2009. Gas/particle partitioning and global distribution of polycyclic aromatic hydrocarbons – a modelling approach. Chemosphere 76, 98–106.
Lammel, G., Stemmler, I., 2012. Fractionation and current time trends of PCB congeners: evolvement of distributions 1950-2010 studied using a global atmosphere-ocean general circulation model. Atmos. Chem. Phys. 12, 7199–7213.
Li, Y.F., Bidleman, T.F., Barrie, L.A., McConnell, L.L., 1998. Global hexachlorocyclohexane use trends and their impact on the arctic atmospheric environment. Geophys. Res. Lett. 25, 39–41.
Li, Y.F., Harner, T., Liu, L., Zhang, Z., Ren, N.Q., Jia, H., Ma, J., Sverko, E., 2010. Polychlorinated biphenyls in global air and surface soil: distributions, air-soil exchange, and fractionation effect. Environ. Sci. Technol. 44, 2784–2790.
Lohila, A., Penttilä, T., Jortikka, S., Aalto, T., Anttila, P., Asmi, E., Aurela, M., Hatakka, J., Hellén, H., Henttonen, H., Hänninen, P., Kilkki, J., Kyllönen, K., Laurila, T., Lepistö, A., Lihavainen, H., Makkonen, U., Paatero, J., Rask, M., Sutinen, R., Tuovinen, J.-P., Vuorenmaa, J., Viisanen, Y., 2015. Preface to the special issue on integrated research of atmosphere, ecosystems and environment at Pallas. Boreal Environ. Res. 20, 431–454.
Lohman, R., Lammel, G., 2004. Adsorptive and absorptive contributions to the gas-particle partitioning of polycyclic aromatic hydrocarbons: state of knowledge and recommended parametrization for modeling. Environ. Sci. Technol. 38, 3793–3803.
Ma, J., Hung, H., Tian, C., Kallenborn, R., 2011. Revolatilization of persistent organic pollutants in the Arctic induced by climate change. Nat. Clim. Change 1, 255–260.
Makkonen, U., Hellén, H., Anttila, P., Ferm, M., 2010. Size distribution and chemical composition of airborne particles in south-eastern Finland during different seasons and wildfire episodes in 2006. Sci. Total Environ. 408, 644–651.
Meijer, S.N., Ockenden, W.A., Sweetman, A., Breivik, K., Grimalt, J.O., Jones, K.C., 2003a. Global distribution and budget of PCBs and HCB in background surface soils: implications for sources and environmental processes. Environ. Sci. Technol. 37, 667–672.
Meijer, S.N., Ockenden, W.A., Steinnes, E., Corrigan, B.P., Jones, K.C., 2003b. Spatial and temporal trends of POPs in Norwegian and UK background air: implications for global cycling. Environ. Sci. Technol. 37, 454–461.
Nizzetto, L., Gioia, R., Li, J., Borgå, K., Pomati, F., Bettinetti, R., Dachs, J., Jones, K.C., 2012. Biological pump control of the fate and distribution of hydrophobic organic pollutants in water and plankton. Environ. Sci. Technol. 46, 3204–3211.
Ockenden, W.A., Sweetman, A.J., Prest, H.F., Steinnes, E., Jones, K.C., 1998. Toward an understanding of the global atmospheric distribution of persistent organic pollutants: the use of semipermeable membrane devices as time-integrated passive samplers. Environ. Sci. Technol. 32, 2795–2803.
Ockenden, W., Breivik, K., Meijer, S., Stiennes, E., Sweetman, A., Jones, K., 2003. The global re-cycling of persistent organic pollutants is strongly retarded by soils. Environ. Pollut. 121, 75–80.
Oehme, M., 1991. Further evidence for long range air transport of polychlorinated aromatics and pesticides from North America and Eurasia to the Arctic. Ambio 20, 293–297.
Patton, G.W., Walla, M.D., Bidleman, T.F., Barrie, L.A., 1991. Polycyclic aromatic and organochlorine compounds in the atmosphere of Northern Ellesmere Island, Canada. J. Geophys. Res. 96, 10867–10877.
Schlabach, M., Farag-Clement, R., Hung, H., Kallenborn, R., Su, Y., Aas, W., 2012. AMAP/EMEP/NCP Inter-laboratory Study for POP Analysis 2010. EMEP/CCC-Report 7/2011. Norwegian Institute for Air Research, Kjeller, Norway.
Schuster, J.K., Gioia, R., Breivik, K., Steinnes, E., Scheringer, M., Jones, K.C., 2010. Trends in European background air reflect reductions in primary emissions of PCBs and PBDEs. Environ. Sci. Technol. 44, 6760–6766.
Stemmler, I., Lammel, G., 2009. Cycling of DDT in the global environment 1950–2002: world ocean returns the pollutant. Geophys. Res. Lett. 40, 1373–1378.
Stohl, A., Berg, T., Burkhart, J.F., Fjæraa, A.M., Forster, C., Herber, A., Hov, Ø., Lunder, C., McMillan, W.W., Oltmans, S., Shiobara, M., Simpson, D., Solberg, S., Stebel, K., Ström, J., Tørseth, K., Treffeisen, R., Virkkunen, K., Yttri, K.E., 2007. Arctic smoke – record high air pollution levels in the European Arctic due to agricultural fires in Eastern Europe. Atmos. Chem. Phys. 7, 511–534.
Targino, A.C., Krecl, P., Johansson, C., Swietlicki, E., Massling, A., Coraiola, G.C., Lihavainen, H., 2013. Deterioration of air quality across Sweden due to transboundary agricultural burning emissions. Boreal Environ. Res. 18, 19–36.
Tkatcheva, V., Ali, B., Reiner, E., 2013. Northern Contaminants Interlaboratory Quality Assurance Program, (NCP III-Phase 7. Northern Contaminants Program, Ottawa.
UNEP, 2014. Stockholm Convention, United Nations Environment Programme, Geneva. Available at: http://chm.pops.int/TheConvention/Overview/tabid/3351/ (last access 05.03.15.).
Wang, Q., Zhao, L., Fang, X., Xu, J., Li, Y.-F., Shi, Y., Hu, J., 2013. Gridded usage inventories of chlordane in China. Front. Environ. Sci. Eng. 7, 10–18.
Wania, F., Mackay, D., 1993. Global fractionation and cold condensation of low volatility organochlorine compounds in Polar Regions. Ambio 22, 10–18.
Wania, F., Mackay, D., 1996. Tracking the distribution of persistent organic pollutants. Environ. Sci. Technol. 30, 390A–397A.
Wu, X., Lam, J.W.C., Xia, C., Kang, H., Sun, L., Xie, Z., Lam, P.K.S., 2010. Atmospheric HCH concentrations over the marine boundary layer from Shanghai, China to the Arctic Ocean: role of human activity and climate change. Environ. Sci. Technol. 44, 8422–8428.
Wöhrnschimmel, H., Tay, P., von Waldow, H., Hung, H., Li, Y.F., MacLeod, M., Hungerbuhler, K., 2012. Comparative assessment of the global fate of α- and β-hexachlorocyclohexane before and after phase-out. Environ. Sci. Technol. 46, 2047–2254.

Characterizing temporal and spatial patterns of urban PM_{10} using six years of Finnish monitoring data

IV

BOREAL ENVIRONMENT RESEARCH 11: 463–479 ISSN 1239-6095
Helsinki 29 November 2006

Characterizing temporal and spatial patterns of urban PM_{10} using six years of Finnish monitoring data

Pia Anttila and Timo Salmi

Finnish Meteorological Institute, Air Quality Research, P.O. Box 503, FI-00101 Helsinki, Finland

Received 20 Feb. 2006, accepted 30 May 2006 (Editor in charge of this article: Veli-Matti Kerminen)

Anttila, P. & Salmi, T. 2006: Characterizing temporal and spatial patterns of urban PM_{10} using six years of Finnish monitoring data. *Boreal Env. Res.* 11: 463–479.

Data from the Finnish Meteorological Institute's Air Quality Monitoring Data Management System (ILSE) for 1998–2003 were used to examine the temporal and spatial patterns of urban PM_{10} in Finland. Long term means of PM_{10} at 24 Finnish urban stations vary between 11 and 24 μg m^{-3}. The seasonal variation of PM_{10} at all stations was dominated by the spring maximum. A strong influence of traffic on the urban PM_{10} concentrations is shown. However the highly synchronized day-to-day variation at a variety of sites across the country highlights the role of large scale weather patterns also in the formation of spring episodes. Every year, most often in August, September and October, there were also 1–5 irregular regional PM_{10} episodes, lasting from one day to six days and most likely caused by long-range transported particles. During these regional events, the PM_{10} concentrations may well reach the typical spring peak concentration levels.

Introduction

In its recent review the World Health Organization confirmed the causal relationship between particulate matter (PM) exposure and health effects (WHO 2003). The present information shows that fine particles are strongly associated with mortality and cardio-pulmonary diseases. There is evidence that also coarse particles promote respiratory illnesses, but their effect on mortality is less clear. Epidemiological studies on large populations have been unable to identify a threshold concentration below which ambient PM has no effect on health (WHO 2003). It is estimated that in the European Union 55% of the urban population in 2002 was exposed to concentrations of particulate matter exceeding those of the EU limit values set for the protection of human health (European Environment Agency 2005).

Atmospheric particulate matter is a mixture of solid and aqueous species originating from anthropogenic and natural sources. Due to the large number of sources, PM may present diverse physical and chemical patterns in different areas. In addition to the emissions, both climatology (temperature, humidity, radiation, precipitation scavenging, re-circulation *vs.* dispersion of air masses) and geography (topography, soil cover, proximity of arid zones or the coast) have effect on the ambient PM characteristics in a given region. Therefore, wide variations in PM levels and characteristics may be expected when considering regions with different climatological and geographical patterns.

Here we present a broad, national-level summary of the spatial and temporal patterns of PM_{10} in Finland. Although PM_{10} is not a specific indicator for human health impacts, it represents the

overall thoracic fraction of the ambient particles and as such forms an inevitable part of human exposure.

At present in about 50 cities in Finland there are over a hundred fixed monitoring stations, equipped with on-line ambient air quality monitors. These sites are managed and operated by local bodies that also carry out regular assessments of air quality based on the needs of each territory. Whereas the routine monitoring data from e.g. the Helsinki metropolitan area have nowadays become highly exploited in combination with extended measurement and modeling research projects, the vast majority of these long term data have remained scientifically undiscovered. Especially integrated assessments aiming at broad national level have been very few and have mainly been focused on the establishment of the exceedances of the air quality guideline and limit values (Kukkonen *et al*. 1999, Pietarila *et al*. 2000, Anttila *et al*. 2003).

The Finnish long term PM_{10} monitoring data with the high time resolution and capture and encompassing different sized cities in different parts of the country make up a worthy data set for the establishment of this national PM_{10} summary.

Material and methods

The mass concentrations of PM_{10} presented in this paper were obtained with automatic analyzers using either the tapered element oscillating microbalance (TEOM) or the beta-attenuation method (Table 1). In the TEOM instrument particles are collected on an oscillating filter whose frequency changes as the mass loading of the filter increases. In these instruments, the aerosol stream towards the filter is typically heated to 50 °C to prevent moisture from affecting the mass measurements. The beta-attenuation analyzer is based on the measurement of the reduction in the intensity of beta particles passing through a dust-laden filter. The filter material or the air flow is not usually heated. The manufacturer provides calibration foils against which the performance of the instrument can be checked and adjusted. In both methods the particle size selection is determined by the inlet geometry and the flow rate used so flow calibration is an essential part of the routine maintenance of the instruments.

The data obtained by these automatic analyzers are not necessarily fully equivalent with those from direct gravimetric methods (or with each other), the unknown loss of semi-volatile species being an important cause of differences. To quantify these errors in the Finnish climatic conditions a field intercomparison was arranged in Helsinki (station Helsinki2 of this study) in autumn 2000 and winter/spring 2001 (http://www.fmi.fi/kuvat/FINal_PM_Report.pdf). Two beta-attenuation instruments and a TEOM instrument were compared with the reference samplers according to the European Standard EN12341. Based on the results of this comparison it was concluded that the equivalency of both these methods with the reference method was good enough and no correction factors were needed. These conclusions were proposed for all public monitoring networks in Finland.

However, the PM_{10} measurements of all local networks in Finland have not yet been systematically intercompared. The first field intercomparison campaign of the public monitoring networks (directed at gaseous compounds) was carried out in 2002 and 2003 (Walden *et al*. 2004). In this context also a field audit of the operation and quality control of the measurement stations was conducted. Almost all the networks have documented quality assurance procedures and orderly maintenance practices together with obviously functional data acquisition, transfer and processing methods. However, the methods and procedures often differ significantly between the networks. In the case of PM_{10} this lack of national harmonization creates a potential for discrepancies, which cannot be fully ruled out here.

PM_{10} data were extracted from the Finnish Meteorological Institute's Air Quality Monitoring Data Management System (ILSE), a database which aggregates all national monitoring results from local networks. Those PM_{10} measurement sites with a minimum annual data capture of 75% during at least four years between 1998 and 2003 were used. Altogether 25 sites in 20 cities in different parts of the country met these criteria (Table 1 and Fig. 1). In the past the PM_{10} data in the ILSE database were reported relative to

Table 1. Overview of the PM_{10} monitoring sites.

Place	Station name	Network	Population	Type of the measurement site	Nearest street		NO_x[1] median ($\mu g\ m^{-3}$)	PM_{10} measurements 1998–2003		
					Distance (m)	Traffic flow (vehicles day^{-1})		Capture (%)	Height (m)	Instrument
Turku	Kauppatori	Turku	175000	urban/traffic	4	6000	53	98	3.5	Eberline FH62IN
Raisio	Keskusta	Turku	23000	urban/traffic	18	4500	46	98	3	Eberline FH62IN
Naantali	Keskusta	Turku	14000	urban/traffic	6	n/a[2]	27	82	3	TEOM 1400A
Pori	Itätulli	Pori	76000	urban/traffic	3	n/a[2]	45	82	4	Eberline FH62IR
Lohja	Nahkurintori	Lohja	36000	urban/background	4	2500	23	99	3	TEOM 1400A[4]
Hämeenlinna	Raatihuoneenkatu	Hämeenlinna	47000	urban/traffic	30	8500	48	63	3	TEOM 1400
Jyväskylä	Lyseo	Jyväskylä	82000	urban/traffic	25	12000	25	65	3.5	TEOM 1400A
Helsinki1	Töölö	YTV	560000	urban/traffic	2	25000	95	99	4.5	TEOM 1400AB
Helsinki2	Vallila	YTV	560000	urban/traffic	12	13000	45	98	4.5	Eberline FH 62IR
Helsinki3	Kallio	YTV	560000	urban/background	80	7700	31	82	4	Eberline FH62IR
Espoo1	Leppävaara	YTV	224000	suburban/traffic	30	14500	48	99	4.5	TEOM 1400AB
Espoo2	Luukki	YTV	224000	rural/background	800	4900	6	80	7[3]	Eberline FH 62 IR
Vantaa	Tikkurila	YTV	184000	suburban/traffic	8	14500	69	97	4	TEOM 1400AB
Lappeenranta	Keskusta	Imatra	59000	urban/traffic	25	24000	34	60	3	Eberline FH62IR
Imatra1	Rautionkylä	Imatra	30000	suburban/industry	350	10000	14	95	8	Eberline FH62IN[4]
Imatra2	Mansikkala	Imatra	30000	suburban/background	100	8000	19	65	3	Eberline FH62IR[4]
Kotka	Kirjastotalo	Kotka	55000	urban/background	40	6400	15	65	13	Eberline FH62IR
Kouvola	Keskusta	Kouvola	31000	urban/traffic	30	10000	41	87	4	TEOM 1400
Varkaus	Pääterveysasema	Varkaus	23000	suburban/industry	20	5500	11	96	6	TEOM 1400A
Oulu1	Keskusta	Oulu	126000	urban/traffic	5	7000	63	95	4	TEOM 1400
Oulu2	Pyykösjärvi	Oulu	126000	suburban/background	n/a[2]	n/a[2]	14	97	4	TEOM 1400
Kajaani	Keskusta	Kajaani	36000	urban/traffic	6	13800	23	99	2	TEOM 1400A
Kokkola	Keskusta	Kokkola	36000	urban/traffic	15	3000	24	95	4	TEOM 1400A[5]
Pietarsaari	Bottenviksvägen	Pietarsaari	19000	urban/traffic	10	3600	21	81	3	TEOM 1400
Kuopio	Keskusta	Kuopio	88000	urban/background	50	11800	19	77	4	TEOM 1400A

[1]whole period median of the parallel NO_x measurement as NO_2.
[2]not available.
[3]height changed to 4.5 meters 24 January 2000.
[4]instrument was changed to ThermoESMAndersen FH 62IN/R 1 January 2003.
[5]instrument was changed to Eberline FH 62IR 11 July 2002

Fig. 1. Locations of the stations. Division of the stations into four geographical regions is denoted with lines.

20 °C; now all historical data have been revised to local temperatures which is also the format used here.

The classification of the sites is based on the European Communities exchange of information decision (EC 2001). All except one (Espoo2) of the stations are located in urban or suburban surroundings. Espoo2 is located in the countryside about 20 km northwest from Helsinki and represents rural surroundings. The majority of the stations (16) are classified as traffic stations, with seven and two classified as background and industry stations, respectively. These nine background or industry stations are here referred to as non-traffic stations (Table 1).

The data were grouped into four broad geographical regions; southwestern Finland, the Helsinki metropolitan area, southeastern Finland and northern Finland (Fig. 1). The four groups were adjusted to nearly equal size to enhance the clarity of the graphical displays of data. This grouping is used in the text and figures unless stated otherwise.

All measuring sites included in this study had collocated NO_x measurements with the conventional chemiluminescent method (*see* the field comparison results in Walden *et al*. 2004). These NO_x concentrations in 1998–2003 were also retrieved from the ILSE database (the whole-period median is given in Table 1). Temperature, precipitation and depth of snow cover data from Turku, Helsinki, Lappeenranta and Oulu airport synoptic stations, i.e. one station from each of the four geographical groups, were retrieved from the database of the Finnish Meteorological Institute. These weather data were utilized to compare the seasonal variation of PM_{10} concentrations in different parts of the country.

Results and discussion

Annual variations

At each station the annual median PM_{10} concentrations spanned a relatively narrow range (Fig. 2). The station-specific difference in the highest and lowest annual median concentration was typically only 2–4 μg m^{-3}, and with no common trend. From station to station the concentrations differed more. The total-period median of PM_{10} varied by a factor of two between the lowest three, Varkaus, Kajaani and Espoo2 (9 μg m^{-3}), and the highest, Helsinki1 (20 μg m^{-3}). The non-traffic stations tended to have lower concentrations than the traffic stations, however these categories overlap. The rural background station Espoo2 has distinguishably lower concentrations than the rest of the stations in the Helsinki metropolitan area.

Traffic-induced dust has been reported to be a substantial source of elevated PM_{10} concentrations at Finnish urban sites especially in spring (e.g. Hosiokangas *et al*. 1999, 2004, Vallius *et al*. 2000, Pakkanen *et al*. 2001, Pohjola *et al*.

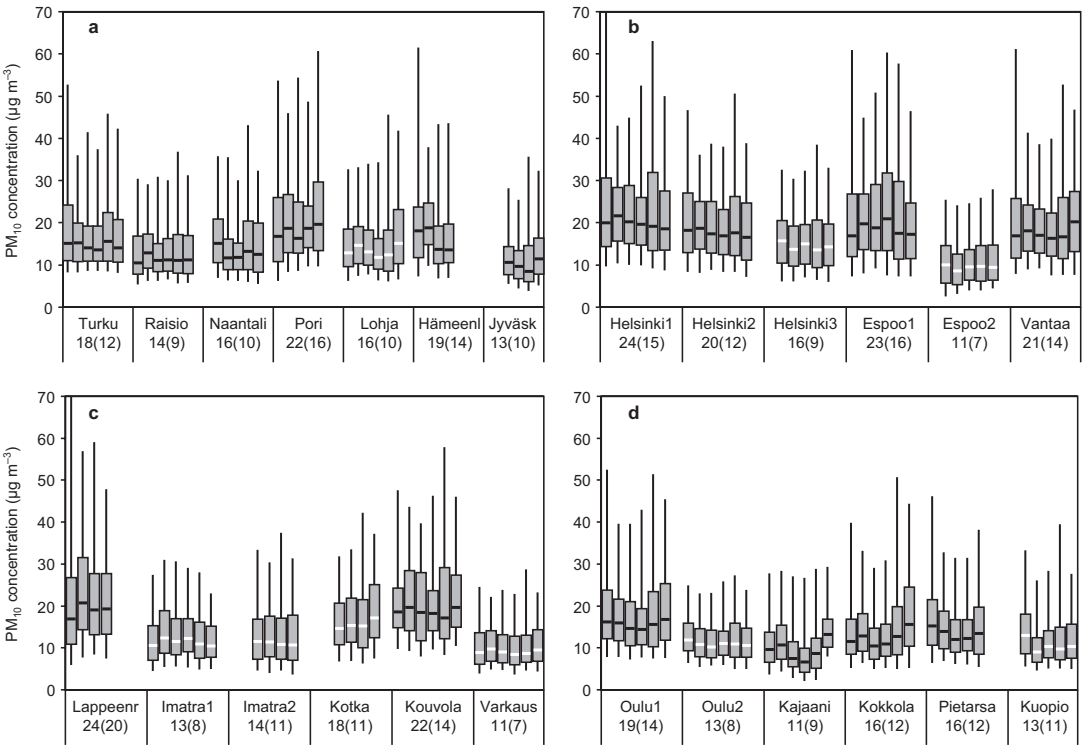

Fig. 2. Annual distribution of 24-hr average PM_{10} concentrations from 1998 to 2003 at the 25 stations in Finland. (**a**) Southwestern Finland, (**b**) the Helsinki metropolitan area, (**c**) southeastern Finland, and (**d**) northern Finland. Values for the 5th, 25th, 50th (median), 75th and 95th percentiles are shown. At the non-traffic stations the medians are denoted with white horizontal lines. The total means (1998–2003) and standard deviations (in μg m^{-3}) are shown at the bottom of each set of plots.

2002, Laakso *et al*. 2003, Kukkonen *et al*. 2005). However, the long-term mean concentrations of PM_{10} seemed not to be extremely sensitive to the very unequal traffic volumes contributing at the stations (Table 1). While the PM_{10} total-period median varied by a factor of two between the lowest and highest in this material, NO_x concentration varied by a factor of 15 between the lowest (rural Espoo2) and highest (Helsinki1) (*see* Table 1). This indicates that the long term PM_{10} concentration is less sensitive to the local traffic sources than is the NO_x concentration.

Van Dingenen *et al*. (2004) used the 5th percentile values of PM_{10} at the rural and near city background sites to derive a European continental background PM_{10} concentration 7.0 ± 4.1 μg m^{-3}. The use of the 5th percentile values was justified by the fact that in their extensive compilation of data the 5th percentile values of rural and near city background sites were similar to the annual average concentrations observed at natural background sites (i.e. Norwegian and Swedish EMEP sites, with distances from large pollution sources over 50 km). The mean 5th percentile values of the nine non-traffic stations here yielded an average of 5.2 ± 1.2 μg m^{-3} suggesting a lower background concentration for Finland than the European continental value given by Van Dingenen *et al*. (2004). Note that these background values are not purely natural by definition, but are affected by long-range transported particles.

As a whole the Finnish concentration levels were consistent with those obtained in European city or near-city data compilations (Lazaridis 2001, Van Dingenen *et al*. 2004, Querol *et al*. 2004). Heal *et al*. (2005) found the urban background annual mean concentration in central Edinburgh to be 15.5 μg m^{-3} (in 1999–2000). Harrison *et al*. (2001) found 26 μg m^{-3} as an

annual mean (1997–1998) for the urban background, 36.5 μg m^{-3} for a busy street canyon (Marylebone road) in London, and 16.8 μg m^{-3} and 19.5 μg m^{-3} at two rural sites in the UK. Three-year urban background data from Birmingham gave an annual mean of 22.5 μg m^{-3} (Harrison *et al.* 2001). Gehrig and Buchman (2003) reported 22.5–35.9 μg m^{-3} as long-term means (1998–2001) for urban/suburban stations in five cities in Switzerland, and 20.7 μg m^{-3} for a lowland rural site. Gomišček *et al.* (2004) reported PM_{10} annual means of 26 to 31 μg m^{-3} (1999–2000) for three urban sites in Vienna, Linz and Graz and 21 μg m^{-3} for a rural site in Austria. Rodríguez *et al.* (2003) reported PM_{10} annual means of 46 and 49 μg m^{-3} (year 2000) for two urban street canyons (L'Hospitalet and Sagrera), 59 μg m^{-3} for an industrial urban site (S. Andreau) in northeastern Spain, and 17 μg m^{-3} for a rural site (1998–2000). Chaloulakou *et al.* (2003) reported an annual mean PM_{10} concentration of 75.5 μg m^{-3} (1999–2000) for downtown Athens. These examples from the cities in different parts of Europe show that long-term means exceeding 30 μg m^{-3} are quite typical in urban environments and 15–20 μg m^{-3} are frequently given as rural long-term means. The Finnish concentrations tended to settle in the lower end of the European concentration range.

Seasonal variation

A highly synchronized temporal pattern could be seen not only within each geographical subgroup but also countrywide (Fig. 3). The overarching feature of the PM_{10} concentrations was the sharp maximum in March–April. This spring maximum was highest at the traffic stations but also present at the urban non-traffic stations. The concentrations started to increase already when temperature was well below zero, but reached their peak when temperature approached zero.

Numerous Finnish studies have shown that traffic-induced resuspension is the predominant source of coarse particles and forms a pronounced contribution also to the PM_{10} at urban traffic-influenced sites (e.g. Hosiokangas *et al.* 1999, 2004, Vallius *et al.* 2000, Pakkanen *et al.* 2001, Pohjola *et al.* 2002, Laakso *et al.* 2003, Kukkonen *et al.* 2005). Other identified contributors to PM_{10} in these studies are motor vehicle exhaust, wood combustion, long-range transport and sea salt. While the major role of the traffic related dust in the PM_{10} concentrations is widely accepted, the proportions of geological dust, traction sand, wear of asphalt enhanced by studded tires or even wear of break linings in road dust are not yet quantified (e.g. Kuhns *et al.* 2003, Kupiainen and Tervahattu 2004, Sternbeck *et al.* 2004). However, a commonly accepted hypothesis is that during winter the particles from different sources are accumulated onto road surfaces and shoulders and then resuspended by traffic-induced turbulence during favorable meteorological conditions.

During the study period (as in Finland generally), March–May was the period with least rain (Fig. 4). The elevated concentrations of PM_{10} coincided with this extended period of relatively low rainfall amounts. The PM_{10} concentrations settled down before the more rainy summer season started, so the dryness itself hardly was the ultimate cause of the concentration rise. On the other hand, the elevation of PM_{10} concentrations began quite concurrently with the onset of snowmelt period in the first half of March at the southern coast and a week or two later inland. So the concentration increase at these traffic stations occured well before the soils in general had become uncovered from snow. This may well be due to the fact that roads, and even entire city centers, are kept clear from snow and weather conditions conducive to melting the winter snow pack readily enhanced the particle resuspension from the roads.

Omstedt *et al.* (2005) managed to reproduce the spring peak in a street canyon and in a highway in Stockholm by modeling the road surface moisture and the dust layer growth on the road surface during the wet autumn/winter period and its rapid decrease due to resuspension in early spring when evaporation rates increase due to higher solar radiation and higher temperatures. The high number of cars with studded tires and the winter sanding of the streets were additional factors contributing to the development of the spring peak.

In Finland the use of studded tires is allowed from 1 November up to the week after the Easter

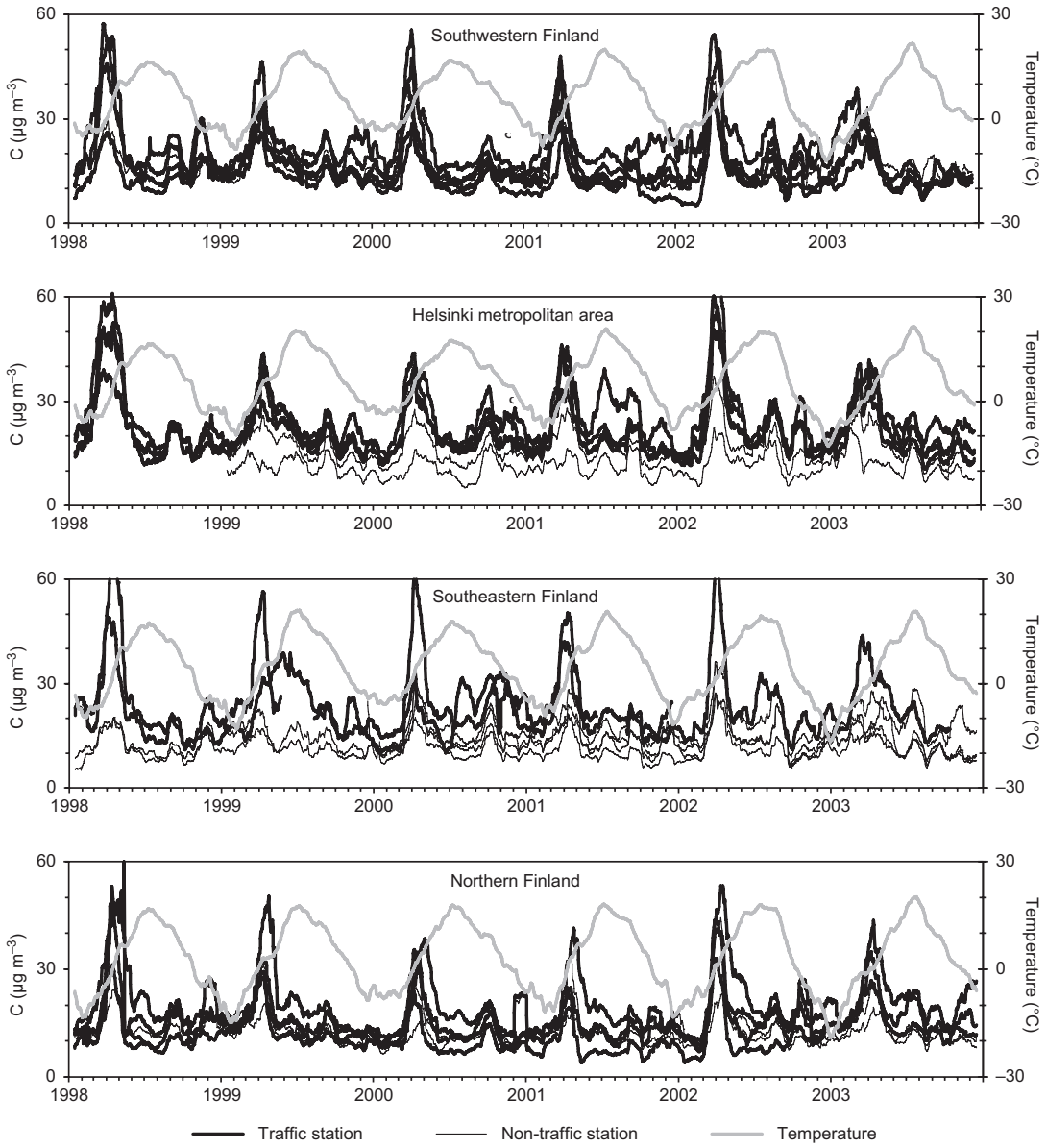

Fig. 3. Monthly running means of the daily PM_{10} concentrations (black lines) and daily mean temperatures in 1998–2003. Meteorological data are from Turku, Helsinki, Lappeenranta and Oulu airport synoptic stations.

Monday, the date of which varied between 8 April and 1 May during this study period. However the autumnal start of the usage of studded tires and/or the start of winter sanding did not instantly cause a large scale suspension of particles from the roads (Fig. 4). This can be due to the higher relative humidity and more frequent rain/snowfall events during the winter months which limit the suspension and rather enhance the accumulation of particles on road surfaces. Only the springtime dry period with higher temperatures, radiation and evaporation enables the effective suspension.

Figure 5 gives an impression of the magnitude of the spring peak at each station compared to the mean concentration of the rest of the year. Here we aggregated the baseline year from the June to January PM_{10} concentration; February

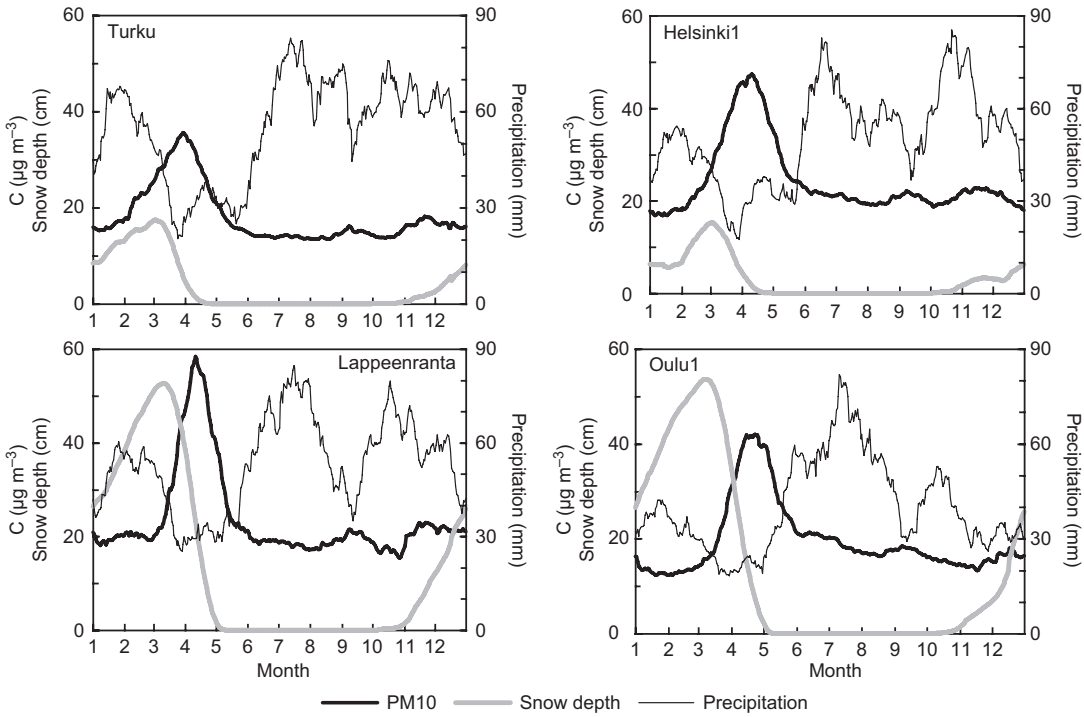

Fig. 4. Seasonal variations of the PM_{10} concentration and snow depth and precipitation averaged over years 1998–2003. PM_{10} concentrations and snow depths were first filtered with monthly running mean and precipitation with monthly running sum.

and May were excluded as transition months, and the spring peak was compiled of the March–April mean concentrations. These were clearly correlated; a high baseline concentration implied a high spring peak, with the long-term mean of the spring peak about twice as high as the rest of the year ($n = 25$, $r = 0.91$, $p < 0.0001$). This suggests that the spring peak is strongly connected to the stations' year-round source/sources which tend to strengthen/discharge during the spring months. At the non-traffic stations the PM_{10} concentrations tended to rise relatively less than at the traffic stations. For example Kotka in the southeastern coast was characterized by a high baseline concentration and a low spring peak. Of the non-traffic stations Kuopio in central Finland, for example, had a relatively high spring peak as compared with its baseline. However, also at the rural Espoo2 the March–April concentrations were about 30% higher than during the rest of the year.

The annual cycle of PM_{10} in Finnish cities differs much from the one observed e.g. in central Europe, where elevated concentrations occur during the winter season and are due to meteorological effects; frequent inversions in winter and good vertical mixing during summer (Gehrig and Buchmann 2003, Gomišček *et al*. 2004). In the Mediterranean region the restrained mesoscale circulations with slow scavenging potential favor the aging of air masses during summer causing subsequent summer elevation of PM_{10} (Rodríguez *et al*. 2003).

The highly synchronized temporal pattern of PM_{10} at a variety of sites across the country (Fig. 3) highlights the role of large scale weather patterns in the formation of PM_{10} episodes in Finland too.

The widespread moderate secondary rises of PM_{10} concentrations in the latter half of the year (*see* Fig. 3) further point toward synoptic scale meteorology. These latter episodes varied in magnitude and timing from year to year more than the spring maximum. For example in 1998 there were simultaneous concentration elevations at almost all stations in September and again at

the turn of November–December, as well as at the turn of September–October in 2000, in September in 2001, in August in 2002, and in July in 2003. We will focus more in these non-spring episodes later in this article.

Day-of-week pattern

The influence of the human activities and traffic flows were clearly seen (Table 2) in the weekly pattern of the PM_{10} concentrations. Traffic intensities are lower during weekends, especially on Sundays when opening hours of shops are regulated, a fact that may be meaningful in city centers.

When calculated for the total period 1998–2003 all stations showed significantly lower concentrations during Sundays than during weekdays, the difference varying between 10% and 30%. Also all non-traffic stations showed this difference. However, seasonally this pattern showed more variation. During the spring period all stations except rural Espoo2 exhibited significantly lower concentrations on Sundays than on weekdays while in the autumn period this was true at only about half of the stations. Thus in spring the lower traffic on Sundays also systematically reduced the PM_{10} concentrations, while in the autumn period equivalent reduction in traffic flows produced no significant reduction in PM_{10} at several sites. This suggests that in the development of the generally lower autumn concentrations the role of traffic is no more so overwhelming. However during the summer period with equally low level of the PM_{10} concentrations the Sunday reduction of the concentrations was yet again more prevalent (even without studded tires and traction sanding). This implies that in the autumn period some additional source disturbs the strong connection between the traffic and PM_{10}. This pattern was most systematic in the southeastern group and almost absent in the northern group.

The influence of the local traffic flows was clearly seen also on the diurnal cycle of PM_{10} concentrations (Fig. 6). The urban city centers Helsinki1, Lappeenranta and Oulu1 experienced the strong morning congestion peak at about 08:00 during weekdays. During the off-peak

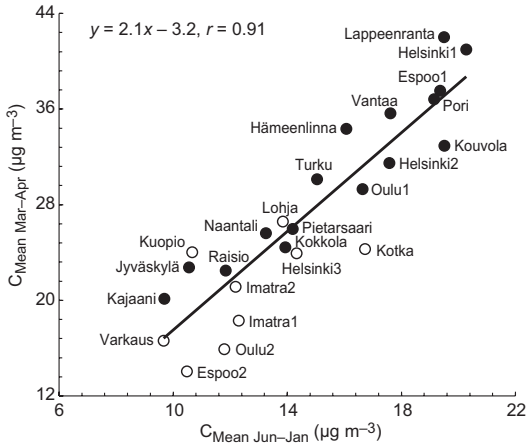

Fig. 5. Relationship (scatter plot and linear regression) between the mean June–January PM_{10} concentrations and the mean March–April concentration at each station in 1998–2003. Open circles are non-traffic stations.

midday hours the concentrations developed more smoothly, and the afternoon rush hour was not reflected as strongly as the morning one maybe due to the typically better atmospheric mixing conditions in the afternoons. The smaller towns Jyväskylä, Pietarsaari and Naantali had concomitant but weaker morning peaks and finally at the small town suburban stations the morning peak was hardly visible. At the rural station Espoo2, the direct weekday morning peak was missing and Sunday differed only slightly from the weekday daily cycle. At urban stations on Sundays, a morning minimum took place and was followed by slow increase during the day. Interestingly the Sunday night concentrations at urban traffic stations were systematically higher than those on weekday nights. Evidently the more intensive nightlife increased concentrations, the effect of which was further strengthened by the decreased mixing of the stable nighttime atmosphere.

The Sunday early morning minimum concentrations are evidently least affected by traffic and other human activities following weekly and diurnal cycles. As such they may give information on the contributions of other PM_{10} sources, such as windblown dust, sea spray, wildfires and anthropogenic secondary particles. Early Sunday morning mean concentrations varied between 7–16 μg m^{-3} (Table 3). Interestingly the Sunday minimums tended to be slightly lower at the

northern stations; all stations north of Jyväskylä and Varkaus had Sunday minimums below 10 μg m^{-3} while in the south only the rural and suburban background stations Espoo2 and Imatra2 had concentrations this low. This may reflect the longer distance and subsequently smaller influence of the southern long range transported pollution to the northern stations. The weekly and diurnally non-cyclic proportions of PM_{10} concentrations represented by the Sunday minimum encompassed on average two thirds of the long-term mean of the PM_{10} (Table 3). The lowest non-cyclic relative proportion was detected at the northern urban traffic station Oulu1 (48%) and highest at the eastern suburban industry station Imatra1 (83%).

Spatial variation

High spatial variability is often associated with the PM_{10} concentrations due to the potential effects of the very localized, sporadic particle suspension in the vicinity of the monitors and short atmospheric lifetime. The spatial distribution of the PM_{10} concentrations was addressed by analyzing the correlation (Pearson r) of the daily values between the different sites. The correlation between the stations declined linearly with the distance between them (Fig. 7a). The list of highest correlations (Table 4) was dominated by the dense network of the Helsinki metropolitan area, but was completed with other closely-spaced (~20 km) station pairs and also

Table 2. Statistically significant differences between the average Sunday and weekday (average Tuesday–Thursday) PM_{10} concentrations. Non-traffic stations are set in italics.

	Difference between Sunday and weekday (%)				
Station	All	Winter	Spring	Summer	Autumn
Southwestern					
Turku	–22***	–29**	–21***	–25***	
Raisio	–19***	–21**	–18***	–23***	–17*
Naantali	–15***		–13*	–24***	
Pori	–24***		–30***	–25***	–19*
Lohja	*–17****	*–18**	*–21****	*–19***	
Hämeenlinna	–20***	–16*	–25**	–16*	
Jyväskylä	–25***	–21**	–29**	–20*	–25**
Helsinki metropolitan area					
Helsinki1	–27***	–32***	–26***	–29***	–23***
Helsinki2	–24***	–23***	–24***	–29***	–19*
Helsinki3	*–26****	*–24****	*–28****	*–31****	
Espoo1	–29***	–25***	–29***	–35***	–26***
Espoo2	*–13***			*–21**	
Vantaa	–25***	–26***	–26***	–25***	–21**
Southeastern					
Lappeenranta	–28***	–21*	–40**	–23**	
Imatra1	*–15****	*–15**	*–15**	*–22****	
Imatra2	*–21****	*–23**	*–30**		
Kotka	*–22****		*–22**	*–25***	
Kouvola	–10**		–19**		
Varkaus	*–12****	*–8**	*–20***	*–15***	
Northern					
Oulu1	–30***	–21***	–32***	–34***	–30***
Oulu2	*–21****	*–22***	*–17***	*–22****	*–25****
Kajaani	–20***	–17**	–20**	–26***	–17*
Kokkola	–28***	–21**	–32***	–28***	–30***
Pietarsaari	–23***	–12*	–19*	–29***	–30***
Kuopio	*–20****		*–21***	*–24****	*–16**

Nonparametric Wilcoxon signed rank test: *$p < 0.01$, **$p < 0.001$, ***$p < 0.0001$.

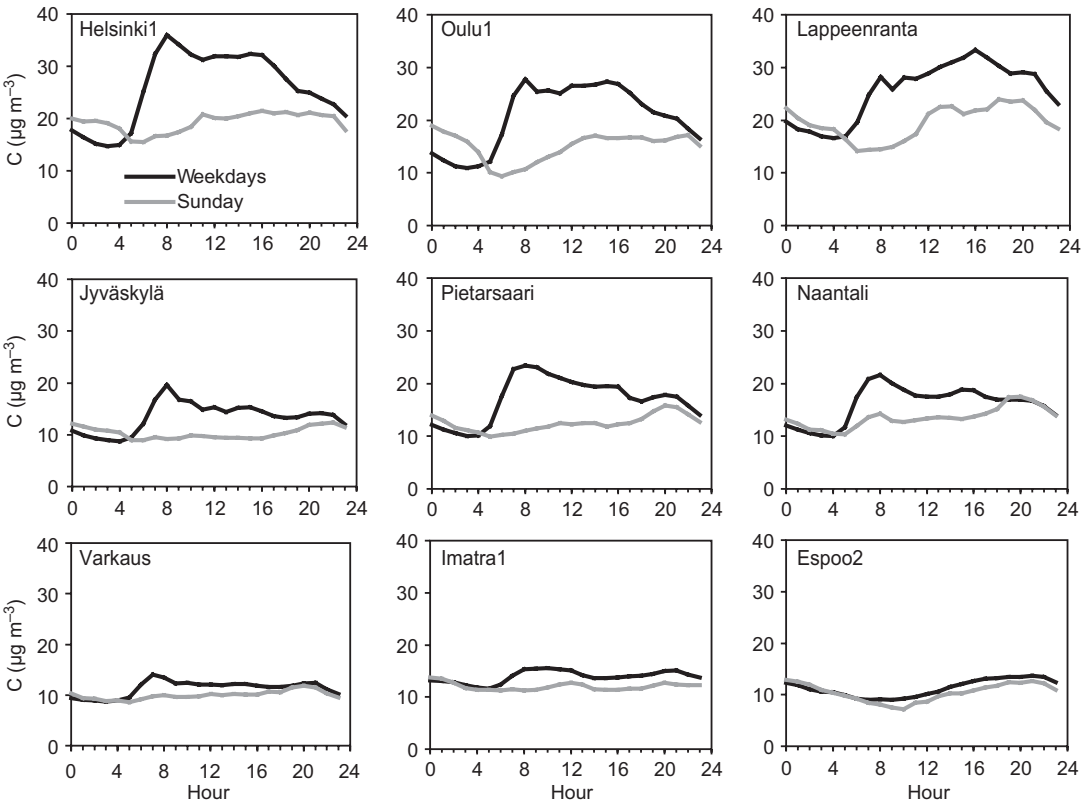

Fig. 6. Average diurnal variation of PM_{10} at selected stations during weekdays (Monday–Friday) (black lines) and Sundays (grey lines) compiled from years 1998–2003.

with a couple of reasonably distant station pairs as Kuopio and Jyväskylä (distance 122 km) or Imatra2 and Varkaus (135 km). The two stations in Oulu with a distance of 4 km and $r = 0.76$ settled only narrowly outside this list. Instead Espoo2 — the only station classified as rural — had outstandingly different behavior than the other stations (*see* Fig. 7a, square symbol) with its poor correlation with especially traffic-stations (squares with dots). Actually it correlated best ($r = 0.77$) with the non-traffic Kotka station at a distance of 123 km eastwards and also with the non-traffic stations of Imatra and Varkaus. So not only the distance but also the type of station affected the correlation between the stations. This suggests that the correlation between the urban traffic stations is based on similar source profiles whose strength varies in time following the common weather conditions.

Another possible explanation for the detected fairly high correlations between urban stations located even as far as 100 km from each other would be the long range transported particles. However the correlations were highest in spring (Fig. 7b) during the period with highly elevated concentrations caused by road dust suspension, which endorses the role of common weather patterns as the primary cause of the correlation. The poorest correlations i.e. the most locally varying PM_{10} concentrations were detected during the winter season (Fig. 7b).

Comparison of our results with the other European studies is complicated due to the more variable European terrains which distracts the simple distance dependence of correlations detected here. However, the extremely high correlations of PM_{10} between distant urban stations reported from e.g. the Swiss basin (Dübendorf and Payerne; distance 160 km; $r = 0.87$; data from 1998–2001 (Gehrig and Buchman 2003) were not present in the Finnish data. This may indicate a higher influence of local sources as compared with the long range transported particles in Finland.

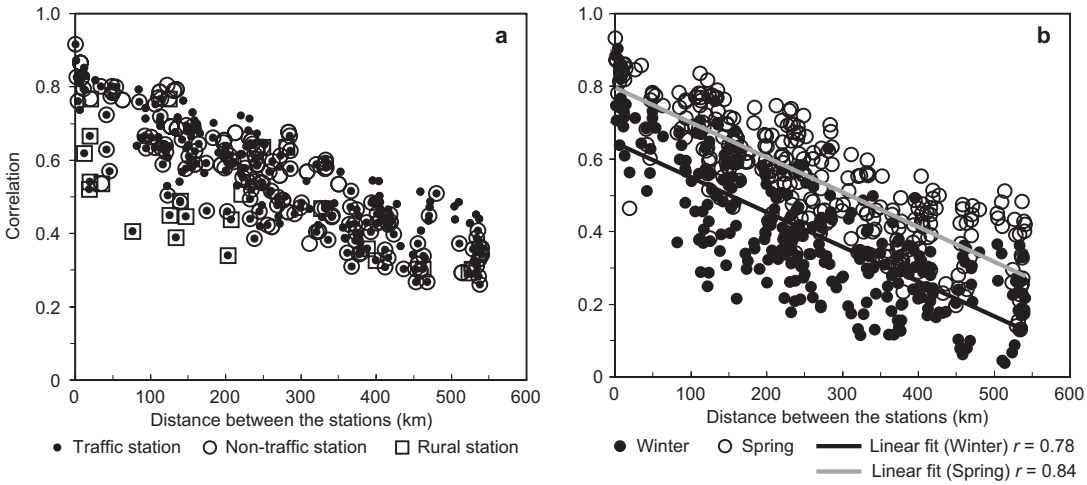

Fig. 7. Correlation (Pearson *r*) of the daily values of PM_{10} between the sites against their distance in 1998–2003. (**a**) All station pairs segregated by station type (note that each mark in the plot is generated as a combination of type marks of the paired stations), and (**b**) all urban station pairs (i.e. Espoo2 removed) segregated by season.

Table 3. Minimum concentrations of the diurnal distributions calculated from Sundays in years 1998–2003 at each station.

Station	Minimum of the Sunday distribution (μg m^{-3})	Proportion of the Sunday minimum of the total period mean (%)
Southwestern		
Turku	11.8	64
Raisio	10.0	72
Naantali	10.4	67
Pori	11.0	49
Lohja	11.6	72
Hämeenlinna	12.4	64
Jyväskylä	8.9	70
Helsinki metropolitan area		
Helsinki1	15.5	64
Helsinki2	13.4	66
Helsinki3	10.5	64
Espoo1	14.0	61
Espoo2	7.2	64
Vantaa	14.1	67
Southeastern		
Lappeenranta	14.1	59
Imatra1	11.2	83
Imatra2	8.9	63
Kotka	11.9	66
Kouvola	15.7	72
Varkaus	8.6	78
Northern		
Oulu1	9.4	48
Oulu2	8.6	69
Kajaani	7.0	61
Kokkola	9.4	60
Pietarsaari	9.9	62
Kuopio	9.3	70

Regional episodes

The repeated coincident elevated PM_{10} concentrations throughout the country were visible in the smoothed time series (Fig. 3). An episodic day for PM_{10} at a site was defined as a day on which the observed 24-hour average concentration exceeded the 90th percentile of all data of the site during 1998–2003. Further a regional

Table 4. Highest correlations of the daily values of PM_{10} between the sites; all measurements 1998–2003.

Station *vs.* station	Pearson *r*	Distance (km)
Helsinki2/Helsinki3	0.91	1
Helsinki1/Helsinki2	0.87	2
Imatra1/Imatra2	0.86	8
Helsinki2/Vantaa	0.85	12
Raisio/Naantali	0.84	8
Helsinki1/Helsinki3	0.83	3
Helsinki2/Espoo1	0.83	7
Espoo1/Vantaa	0.83	15
Helsinki1/Vantaa	0.83	13
Helsinki3/Espoo1	0.82	9
Kokkola/Pietarsaari	0.82	27
Helsinki1/Espoo1	0.81	7
Lohja/Helsinki2	0.8	50
Lappeenranta/Imatra2	0.8	35
Jyväskylä/Kuopio	0.8	122
Turku/Naantali	0.79	13
Hämeenlinna/Vantaa	0.79	85
Helsinki3/Vantaa	0.79	11
Imatra2/Varkaus	0.79	135

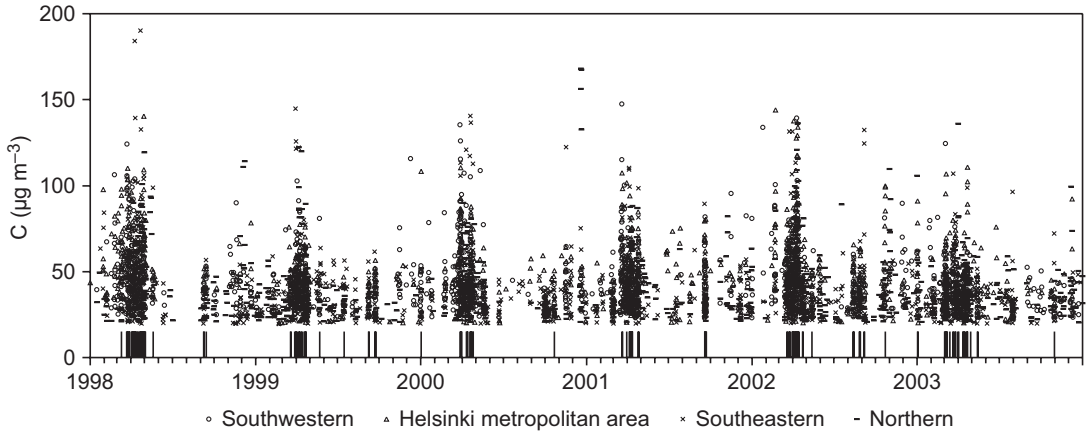

Fig. 8. Time series plot of the episodic day PM_{10} concentrations at each station in 1998–2003. Regional episodic days are indicated with black vertical markers on the abscissa.

episodic day was chosen to be a day when at least half of the measuring stations were observing an episodic day.

The PM_{10} episodic days tended to be grouped in dense clusters as a function of time; most regularly appearing were the March–April episodes (Fig. 8). Of the 2191 days of the total study period, altogether 148 (6.7%) days were regional PM_{10} episode days. Since about half of the episodes of each station occured in March–April (varying from 33% in Espoo2 to 72% in Hämeenlinna) the spring time co-occurrence was hardly a surprise.

More interestingly, every year there were also 1–5 non-spring irregular regional episodes lasting from one day to six days which cannot directly be connected to local dust but might rather be connected to the long range transport. These non-spring episodes typically occured in August, September and October. Only winterly regional episodes were related to New Year's Eves in 2000 and 2003. The winter months were characterized by dispersed occurrence of high concentrations while midsummer (June) was characterized by an absence of high concentrations. Perhaps the poor wintertime mixing conditions give rise to very local concentration development with increased influence of specific local sources such as small scale wood combustion. These low level inversions are most typical in the north. In this respect it is worth noticing that the highest concentrations during winter months were most frequent at northern sites Oulu2 and Kokkola (not shown).

The sources of a pair of the widespread autumn episodes of PM have been identified. Tervahattu *et al*. (2004) and Hongisto and Sofiev (2004) studied the sources and development of the PM_{10} episode on 17–23 September 2001. This episode was shown to be composed of soil dust particles raised by wind in the Kazakhstan Ryn Peski desert and mixed with the anthropogenic particle emission from Estonian and Russian oil-shale burning industries. The data here show that this episode was recorded throughout the country; on 19 September all 25 stations recorded daily PM_{10} concentrations which belonged to the highest tenth of the data at each station i.e. fully comparable to the spring dust episodes in magnitude. An almost equally widespread autumn episode was recorded on 14 September 1998 when 16 of the 17 stations working that day recorded the episode (*see* Fig. 8).

Hongisto and Sofiev (2004) further showed in their long term model simulation that the most important source of natural LRT dust in Scandinavia is the desert area near the Caspian Sea, whose influence is about an order of magnitude higher than that of the Sahara desert. LRT pollution episodes originating from the Caspian Sea region were shown to be most frequent during March; however severe episodes were estimated to be extremely rare.

Niemi *et al*. (2005) reported three fine particle LRT episodes in late summer 2002 (12–15 and 26–28 August and 5–6 September). These fine particle episodes were identified to be enhanced

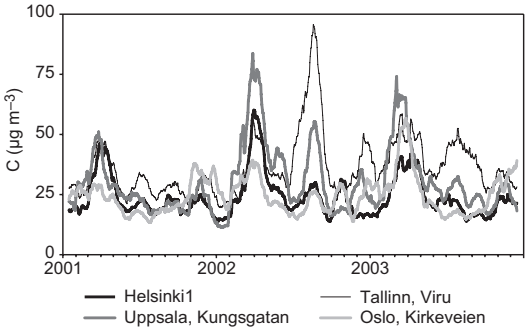

Fig. 9. Monthly running means of PM_{10} at Tallinn, Helsinki, Oslo and Uppsala 2001–2003.

by the forest fires and agricultural field burning in eastern Europe. Also here these fine particle episode days came forward as regional PM_{10} episode days.

These repeated widespread autumn episodes which occured during the period with no specific additional nationwide source or specifically difficult mixing conditions can plausibly be connected to the long range transport. On the other hand equally possible are the LRT-events of PM_{10} during the spring months with frequent co-occurrence of episodes, however the overwhelming influence of traffic-induced road dust may mask this LRT fraction during the spring months.

Niemi *et al*. (2004) identified sources of the fine particle LRT episode on 17–22 March 2002 over large areas of Finland. During this episode most of the PM_{10} particle mass was in the $PM_{2.5}$ size range with high sulphate, ammonium and nitrate concentrations (Niemi *et al*. 2004). Agricultural field burning in the Baltic countries, Belarus, Ukraine and Russia was shown to be a major source of the elevated fine particle concentrations. This fine particle episode coincided with the annual coarse fraction spring episode so its possible contribution to the PM_{10} concentrations at the sites included in this study could not be separated. However, perhaps coincidently, 19–20 March were also regional episode days for PM_{10}; 78% and 95% of stations recorded an episodic day.

Comparison with Oslo, Uppsala and Tallinn

Road dust reinforced by studded tires and small-scale residential wood combustion amplified by poor winterly mixing conditions have been identified as typical Scandinavian PM_{10} sources (e.g. Areskoug *et al*. 2004, Forsberg *et al*. 2005, Yttri *et al*. 2005). Comparison of the PM_{10} time series in Helsinki, Olso, Uppsala and Tallinn is given in Fig. 9. Estonian, Norwegian and Swedish raw data were downloaded from EEA's AirBase (http://air-climate.eionet.eu.int/databases/airbase/airview/index_html) and processed identically to the Finnish data. These cities have populations between 200 000–500 000. Traffic volumes are 25 000 vehicles per day in Oslo/Kirkeveien (Lützenkirchen and Lutnæs 2004) and 18 000 vehicles per day in Uppsala/Kungsgatan (Stockholm-Uppsala Air Quality Management Association http://www.slb.mf.stockholm.se). The traffic volume for Tallinn/Viru is not available.

The presence of the spring maximum was obvious in all four cities; however its dominance in the seasonal course of the PM_{10} concentrations varied a lot among these cities. In Helsinki and Uppsala the highest concentrations occured invariably in March–April. In Oslo the early-winter concentrations approached and even exceeded (in 2001) the spring concentrations, whereas Tallinn was characterized with extremely high summer and early autumn concentrations.

In Norway the spring dust is fought against by regulating the use of studded tires. In Oslo during the winter 2000/2001 the use of studded tires was substantially reduced by setting fees which resulted in significant reduction of the PM_{10} concentrations. This taxation charge was dropped for the next two years and was restored in 2004 due to its favorable effect on reducing the PM_{10} concentrations (Lützenkirchen and Lutnæs 2004).

The high winter concentrations — which were practically absent in the Finnish data — in Oslo are commonly connected to small scale fuel wood use in old wood-burning stoves. It has been estimated that as much as 25% of the PM_{10} mass in Oslo comes from wood burning (Yttri *et al*. 2005). The particulate emissions from small scale wood burning were estimated to be 384 tonnes in winter 2001/2002 (Finstad *et al*. 2004). For comparison, the particulate emissions from

small scale wood burning in the Helsinki metropolitan area have been estimated to be about 300 tonnes per year (Haaparanta *et al*. 2003). When calculated both per capita and per land area this yields roughly twice as high fuel-wood related particulate emission density in Oslo than in the Helsinki area. However, meteorology, topography and positioning of the stations relative to the residential areas evidently have a high impact on the concentrations, which makes this comparison only indicative.

The co-occurring summer and autumn episodes in all stations here were usually strongest in Tallinn which suggests its closer vicinity to the source. The total anthropogenic direct particulate emissions in Estonia were rapidly decreasing during the last 15 years and were in 2002 35 000 tonnes (as PM_{10}) as compared e.g. with the Finnish 55 000 tonnes (Vestreng *et al*. 2005). Combustion in power plants, residential combustion and traffic are the major sources of direct PM_{10} emissions in both countries. So the Estonian national direct emissions alone hardly explain these Scandinavian-wide summer episodes, though the fact is that Estonian emissions specifically originate from a couple of enormous point sources in northeastern Estonia (e.g. Treier *et al*. 2004) which indicates potential for episodic plume transportation and successive concentration enhancement. Sofiev *et al*. (2003) calculated that outside the radius of about 200 km from these Estonian sources, their influence on background deposition becomes negligible as compared with that of other sources. Both Tallinn and Helsinki are on the outskirts of this effective range.

A more probable explanation for these simultaneous but north and westwards attenuating episodes is the long-range transport from continental Europe and Asia. For example, the already mentioned fine particle episodes in August 2002 originating from forest fires in East Europe (Niemi *et al*. 2005) emerged here as a PM_{10} peak expanding over most of Scandinavia. At that time a long lasting hot and dry high pressure prevailed over Scandinavia, and the northwestern corner of Russia (from the Moscow Region to Sankt Petersburg) suffered from an extremely severe fire season; over ten thousand wildfires in forests and bog lands were registered due to long lasting dryness (Davidenko and Eritsov 2003).

The minimums and maximums in Helsinki and Uppsala followed each other almost perfectly, the only clear deviation was October–December 2002 when first Helsinki (and Oslo) experienced a maximum and Uppsala (and Tallinn) about one month later. The midwinter concentration rise was almost absent in Uppsala and Helsinki but very systematic in Oslo and also in Tallinn.

This non-exhaustive comparison implies that these four northern European cities share the spring peak phenomenon of PM_{10} as well as the long-range transported autumn episodes, however during the winter season the PM_{10} concentrations are more diverse.

Summary and conclusions

Long-term means of PM_{10} at twenty four Finnish urban stations varied between 11–24 $\mu g\ m^{-3}$, the urban centers with high traffic tending to have higher concentrations than the suburban stations or small towns. Year to year variation at each station was very low, typically only 2–4 $\mu g\ m^{-3}$. Several non-traffic stations in small towns were quite comparable in magnitude (Varkaus) and temporal variation (Kotka, Imatra, Varkaus) to the rural background station Espoo2 in the vicinity of Helsinki. The national background concentration was estimated to be about 5 $\mu g\ m^{-3}$, and there was some indication that when traffic influence was eliminated a decreasing trend of PM_{10} from south/southeast to north emerged.

The seasonal variation of PM_{10} at all stations was dominated by the maximum during spring; in March–April the PM_{10} concentrations were about twice as high as during the rest of the year. This spring peak of PM_{10} covered practically the whole snowmelt period, which also was the driest period of the year. In spring also the Sunday concentrations at all urban stations were significantly lower (from the 13% in Naantali to the 40% in Lappeenranta) than the weekday concentrations, which implies a strong effect of traffic on the PM_{10} concentrations. It is plausible that the spring dry period with increasing temperatures, radiation and evaporation enables the effective suspension of the dust accumu-

lated from multiple sources to road surfaces and shoulders and initiates the elevation of PM_{10} concentrations. However the highly synchronized day to day variation at a variety of sites across the country highlights the role of large scale weather patterns also in the formation of spring episodes. Thus they should not be regarded as just sporadic dust eruptions in the vicinity of the monitors.

Every year, most often in August, September and October, there were also 1–5 irregular regional PM_{10} episodes, lasting from one day to six days which most likely originated from long-range transported particles. During these regional events the PM_{10} concentrations may well reach the typical spring peak concentration levels. Similar regional LTR-events are probable also in spring but they get masked behind the overwhelming road influence. Summer was characterized by the lack of episodes and winter by spatially more scattered episodes.

Comparison of the PM_{10} concentrations from Oslo, Uppsala, Tallinn and Helsinki points to largely coincident but unequal spring peaks. Also the partly synchronized summer and autumn episodes may be considered characteristic of this region. During winter the PM_{10} concentrations were most diverse at these cities.

References

Anttila P., Alaviippola B. & Salmi T. 2003. *Air quality in Finland — monitoring results in relation to the guideline and limit values and comparisons with European concentration levels*. Publications on Air quality 33. Finnish Meteorological Institute. [In Finnish with English abstract].

Areskoug H., Johansson C., Alesand T., Hedberg E., Ekengren T., Vesely V., Wideqvist U. & Hansson H.-C. 2004. *Concentrations and sources of PM_{10} and $PM_{2.5}$ in Sweden*. ITM-report 110. Institute of Applied Environmental Research, Stockholm University.

Chaloulakou A., Kassomenos P., Spyrellis N., Demokritou P. & Koutrakis P. 2003. Measurements of PM_{10} and $PM_{2.5}$ particle concentrations in Athens, Greece. *Atmos. Environ*. 37: 649–660.

Davidenko E. & Eritsov A. 2003. The fire season 2002 in Russia. Report of the Aerial Forest Fire Service (Aviale-sookhrana). *International Forest Fire News* 28: 15–17.

EC 2001. Commission Decision (2001/752/EC) of 17 October 2001 amending the Annexes to Council Decision 97/101/EC establishing a reciprocal exchange of information and data from networks and individual stations measuring ambient air pollution within the Member States. *Official Journal of the European Communities* No. L 282/69.

European Environment Agency 2005. *The European environment — state and outlook 2005*. Copenhagen.

Finstad A., Flugsrud K., Haakonsen G. & Aasestad K. 2004. *Vedforbruk, fyringsvaner og svevestøv. Resultater fra Folke- og boligtellingen 2001, Levekårsundesøkelsen 2002 og Undersøkelse om vedforbruk og fyringsvaner i Oslo 2002*. Statistisk sentralbyrå Rapporter 2004/5, Oslo.

Forsberg B., Hansson H.-C., Johansson C., Areskoug H., Persson K. & Järvholm B. 2005. Comparative health impact assessment of local and regional particulate air pollutants in Scandinavia. *Ambio* 34: 11–19.

Gehrig R. & Buchmann B. 2003. Characterizing seasonal variations and spatial distribution of ambient PM_{10} and $PM_{2.5}$ concentrations based on long-term Swiss monitoring data. *Atmos. Environ*. 37: 2571–2580.

Gomišček B., Hauck H., Stopper S. & Preining O. 2004. Spatial and temporal variations of PM_1, $PM_{2.5}$ PM_{10} and particle number concentration during the AUPHEP-project. *Atmos. Environ*. 38: 3917–3934.

Haaparanta S., Myllynen M. & Koskentalo T. 2003. *Small-scale combustion in the Helsinki Metropolitan Area*. Publications of the Helsinki Metropolitan Area Council, B 2003:18. YTV, Helsinki. [In Finnish with English abstract].

Harrison R.M., Yin J., Mark D., Stedman J., Appleby R.S., Booker J. & Moorcroft S. 2001. Studies of the coarse particle (2.5–10 μm) component in UK urban atmospheres. *Atmos. Environ*. 35: 3667–3679

Heal M.R., Hibbs L.R., Agius R.M. & Beverland I.J. 2005. Interpretations of variations in fine, coarse and black smoke particulate matter concentrations in a northern European city. *Atmos. Environ*. 39: 3711–3718.

Hongisto M. & Sofiev M. 2004. Long-range transport of dust to the Baltic Sea Region. *Int. J. Environ. Pollut*. 22: 72–86.

Hosiokangas J., Ruuskanen J. & Pekkanen J. 1999. Effects of soil dust episodes and mixed fuel sources on source apportionment of PM_{10} particles in Kuopio, Finland. *Atmos. Environ*. 33: 3821–3829.

Hosiokangas J., Vallius M., Ruuskanen J., Mirme A. & Pekkanen J. 2004. Resuspended dust episodes as an urban air-quality problem in subarctic regions. *Scand. J. Work. Env. Hea*. 30(S2): 28–35.

Kuhns H., Etyemezian V., Green M., Hendricson K., McGown M., Barton K. & Pitchford M. 2003. Vehicle-based road dust emission measurement — part II: Effect of precipitation, wintertime road sanding, and street sweepers on inferred PM_{10} emission potentials from paved and unpaved roads. *Atmos. Environ*. 37: 4573–4582.

Kukkonen J., Salmi T., Saari H., Konttinen M. & Kartastenpää R. 1999. Review of urban air quality in Finland. *Boreal Env. Res*. 4: 55–65.

Kukkonen J., Pohjola M., Sokhi R.S., Luhana L., Kitwiroon N., Fragkou L., Rantamäki M., Berge E., Ødegaard V.,

Slørdal L.H., Denby B. & Finardi S. 2005. Analysis and evaluation of selected local-scale PM_{10} air pollution episodes in four European cities: Helsinki, London, Milan and Oslo. *Atmos. Environ.* 39: 2759–2773.

Kupiainen K. & Tervahattu H. 2004. The effect of traction sanding on urban suspended particles in Finland. *Environ. Monit. Assess.* 93: 287–300.

Laakso L., Hussein T., Aarnio P., Komppula M., HiltunenV., ViisanenY. & Kulmala M. 2003. Diurnal and annual characteristics of particle mass and number concentrations in urban, rural and arctic environments in Finland. *Atmos. Environ.* 37: 2629–2641.

Lazaridis M. (ed.) 2001. *Measurements of particulate matter in EMEP*. EMEP/CCC/5/2001, Norwegian Institute for Air Research.

Lützenkirchen S. & Lutnæs G. 2004. *Luftkvaliteten i Oslo, Status 2004*. Oslo Kommune, Helse- og velferdsetaten.

Niemi J.V., Tervahattu H., Vehkamäki H., Kulmala M., Koskentalo T., Sillanpää M. & Rantamäki M. 2004. Characterization and source identification of a fine particle episode in Finland. *Atmos. Environ.* 38: 5003–5012.

Niemi J.V., Tervahattu H., Vehkamäki H., Martikainen J., Laakso L., Kulmala M., Aarnio P., Koskentalo T., Sillanpää M. & Makkonen U. 2005. Characterization of aerosol particle episodes in Finland caused by wildfires in Eastern Europe. *Atmos. Chem. Phys.* 5: 2299–2310.

Omstedt G., Bringfelt B. & Johansson C. 2005. A model for vehicle-induced non-tailpipe emissions of particles along Swedish roads. *Atmos. Environ.* 39: 6088–6097.

Pakkanen T., Loukkola K., Korhonen C., Aurela M., Mäkelä T., Hillamo R., Aarnio P., Koskentalo T., Kousa A. & Maenhaut W. 2001. Sources and chemical composition of atmospheric fine and coarse particles in the Helsinki area. *Atmos. Environ.* 35: 5381–5391.

Pietarila H., Salmi T., Saari H. & Pesonen R. 2000. *The preliminary assessment under the EC air quality directives in Finland*. Finnish Meteorological Institute, Helsinki.

Pohjola M., Kousa A., Kukkonen J., Härkönen J., Karppinen A., Aarnio P. & Koskentalo T. 2002. The spatial and temporal variation of measured urban PM_{10} and $PM_{2.5}$ in the Helsinki metropolitan area. *Water, Air and Soil Pollution: Focus* 2(5–6): 189–201.

Querol X., Alastuey A., Ruiz C.R., Artiñano B., Hansson H.C., Harrison R.M., Buringh E., ten Brink H.M., Lutz M., Bruckmann P., Straehl P. & Schneider J. 2004. Speciation and origin of PM_{10} and $PM_{2.5}$ in selected European cities. *Atmos. Environ.* 38: 6547–6555.

Rodríguez S., Querol X., Alastuey A., Viana M.-M. & Mantilla E. 2003. Events affecting levels and seasonal evolution of airborne particulate matter concentrations in the Western Mediterranean. *Environ. Sci. Technol.* 37: 216–222.

Sofiev M., Kaasik M. & Hongisto M. 2003. Model simulations of the alkaline dust distribution from Estonian sources over the Baltic Sea Basin. *Water, Air and Soil Pollution* 146: 211–223.

Sternbeck J., Furusjö E. & Palm A. 2004. *Vägtrafikens bidrag till PM_{10} och metaller vid tätorts- och landsvägskörning*. IVL Rapport B1598. IVL Svenska Miljöinstitutet AB.

Tervahattu H., Hongisto M., Aarnio P., Kupiainen K. & Sillanpää M. 2004. Composition and origins of aerosol during a high PM_{10} episode in Finland. *Boreal Env. Res.* 9: 335–345.

Treier K., Pajuste K. & Frey J. 2004. Recent trends in chemical composition of bulk precipitation at Estonian monitoring stations 1994–2001. *Atmos. Environ.* 38: 7009–7019.

Vallius M., Ruuskanen J., Mirme A. & Pekkanen J. 2000. Concentrations and estimated soot content of PM_{1}, $PM_{2.5}$ and PM_{10} in a subarctic urban atmosphere. *Environ. Sci. Technol.* 34: 1919–1925.

Van Dingenen R., Raes F., Putaud J.-P., Baltensperger U., Charron A., Facchini M.C., Decesari S., Fuzzi S., Gehrig R., Hansson H.-C., Harrison R.M., Hüglin C., Jones A.M., Laj P., Lorbeer G., Maenhaut W., Palmgren F., Querol X., Rodriguez S., Schneider J., ten Brink H., Tunved P., Tørseth K., Wehner B., Weingartner E., Wiedensohler A. & Wåhlin P. 2004. A European aerosol phenomenology, 1: physical characteristics of particulate matter at kerbside, urban, rural and background sites in Europe. *Atmos. Environ.* 38: 2561–2577.

Vestreng V., Breivik K., Adams M., Wagener A., Goodwin J., Rozovskkaya O. & Pacyna J.M. 2005. *Inventory review 2005, Emission data reported to LRTAP convention and NEC directive, Initial review of HMs and POPs*. Technical report MSC-W 1/2005.

Walden J., Talka M., Pohjola V., Häkkinen T., Lusa K., Sassi M.-K. & Laurila S. 2004. *The field comparison of carbon monoxide, sulphur dioxide and nitrogen monoxide ambient air measurements and a field audit 2002–2003*. Publications on Air quality 35. Finnish Meteorological Institute. [In Finnish with English abstract].

WHO 2003. *Health aspects of air pollution with particulate matter, ozone and nitrogen dioxide*. Report on a WHO Working Group, Bonn, Germany, 13–15 January 2003, Copenhagen.

Yttri K., Dye C., Slørdal L. & Braathen O.-A. 2005. Quantification of monosaccharide anhydrides by liquid Chromatography combined with mass spectrometry: Application to aerosol samples from an urban and a suburban site influenced by small-scale wood burning. *J. Air & Waste Manage. Assoc.* 55: 1169–1177.

Impact of the open biomass fires in spring and summer of 2006 on the chemical composition of background air in south-eastern Finland

V

Atmospheric Environment 42 (2008) 6472–6486

Contents lists available at ScienceDirect

Atmospheric Environment

journal homepage: www.elsevier.com/locate/atmosenv

Impact of the open biomass fires in spring and summer of 2006 on the chemical composition of background air in south-eastern Finland

Pia Anttila*, Ulla Makkonen, Heidi Hellén, Katriina Kyllönen, Sirkka Leppänen, Helena Saari, Hannele Hakola

Finnish Meteorological Institute, Air Quality, P.O. Box 503, FI-00101 Helsinki, Finland

ARTICLE INFO

Article history:
Received 10 October 2007
Received in revised form 27 March 2008
Accepted 2 April 2008

Keywords:
Open biomass fires
PM_{10}
Total gaseous mercury
Polycyclic aromatic hydrocarbons
Trace elements

ABSTRACT

In the spring and summer of 2006 the air quality in southern Finland was affected by two major biomass fire smoke episodes. At the Virolahti background station, closest to the eastern fire areas, the episodes lasted altogether several weeks. The high point in spring was 25 April and in summer 13 August. In spring the aerosol detected at Virolahti originated at distances of even hundreds of kilometres to the south and south-east, and consequently was a mixture of material from biomass burning and from other sources (both LRT and local), all of which contributed to the detected elevation of PM_{10} concentrations. The elevated concentrations of trace elements (Cd, Pb, Zn) during the most intense biomass fire episode were associated with other anthropogenic emissions.

In contrast, during August 2006, the PM_{10} at Virolahti was quite exclusively impacted by close (ca. 50–100 km) biomass fire sources. The presumably organic component comprised, at its highest, as much as 90% of the total PM_{10}. In addition to record high PM_{10} and $PM_{2.5}$ concentrations, the concentrations of polycyclic aromatic hydrocarbons were considerably elevated, even reaching values more typical of wintertime urban environments. During the peaks of the episodes in August, the total gaseous mercury concentration in the air was more than double its background value. In general, the trace elements did not exceed their background values.

1. Introduction

Over the past few years, climatic anomalies in temperature and precipitation have resulted in an increase in forest fire events across the boreal Russian Federation. Over 95% of the annually burned forest area of Russia is located in Siberia and the Russian Far East (Wooster and Zhang, 2004), but a large number of fires also occur in the non-intact forests of the more densely populated north-western Russia (Mollicone et al., 2006; Cinnirella and Pirrone, 2006).

The exceptional fire occurrences in continental Eurasia in the 2000s and their regional consequences on atmospheric air quality have also been detected in Finland (Niemi et al., 2004, 2005; Sillanpää et al., 2005). In spring 2006 the record high levels of fine particulate matter in Helsinki were shown to originate from biomass fires in the western part of Russia (Saarikoski et al., 2007). These April–May biomass fire emissions in Eastern Europe were detected as far away as the European Arctic (Stohl et al., 2007). In July–August 2006 southern Finland was again covered by an exceptional smoke plume; by means of the online Finnish modelling system SILAM (http://silam.fmi.fi/) and real-time chemical measurements (Saarikoski et al., 2006), this plume could be tracked back to biomass burning in north-western Russia.

* Corresponding author. Tel.: +358 503686420; fax: +358 919295403.
E-mail address: pia.anttila@fmi.fi (P. Anttila).

1352-2310/$ – see front matter © 2008 Elsevier Ltd. All rights reserved.
doi:10.1016/j.atmosenv.2008.04.020

This study describes the impact of these severe pollution episodes of 2006 on the background air quality in south-eastern Finland, the area of the country that is potentially most threatened by eastern European pollutants, while not being affected by any simultaneous local urban pollution. In addition to results for the conventional gaseous (SO_2, NO_x, O_3) and particulate compounds (major ions and inorganic trace elements in PM_{10}) we also present those for the polycyclic aromatic hydrocarbons (PAHs) and total gaseous mercury (TGM) concentrations measured in these widespread biomass-burning-related smoke plumes.

2. Site and measurements

The study site, Virolahti, lies in the south-eastern corner of Finland (Fig. 1). The site is bounded by the Finnish Russian border 6 km to the east, the Gulf of Finland about 2 km to the south and the E18 highway 5 km to the north. The traffic flow on this highway is about 3000 vehicles per day; frequently, however, long truck queues, even tens of kilometres in extent, form along the road waiting to cross the border into Russia.

The Helsinki metropolitan area (population 1 million) is located 160 km to the west and the Russian metropolis of St. Petersburg (4.7 million) 160 km to the south-east. Across the Gulf of Finland, about 130 km south of Virolahti, several significant particle emission sources, e.g. oil shale utilizing power plants and cement plants (e.g. Tervahattu et al., 2004), are to be found.

This study assembles the ongoing research and pilot measurements at the Virolahti site during the two pollution periods that affected southern Finland in the spring and summer of 2006. Both study periods consisted of 31 days; Period 1 (P1) from 22 April to 22 May 2006 and Period 2 (P2) 1–31 August 2006.

Fig. 1. Location of the Virolahti station.

SO_2 was monitored with a commercial UV fluorescence analyser (TEI43CTL), NO/NO_2 with a chemiluminescence $NO\text{-}NO_2\text{-}NO_x$ analyser (TEI42CTL) and O_3 with a UV absorption analyser (TEI49C). The detection limits were about 0.1 ppbv for SO_2, 0.05 ppbv for NO/NO_2 and 1 ppbv for O_3.

Particulate matter mass (PM_{10}, diameter < 10 μm) was monitored with a beta attenuation analyser (Thermo-ESM-Andersen FH62I-R). One week of PM_{10} data in P2 was rejected due to uncertainties in the flow rate stability, and so on a few occasions the co-located $PM_{2.5}$ ($d < 2.5$ μm) measurements are referred to here instead. Hourly PM_{10} and $PM_{2.5}$ concentrations correlated well: $PM_{2.5} = 0.82 \times PM_{10}$, $r = 0.82$; $n = 545$ (intercept set to zero; two obviously erroneous hourly values of PM_{10} on 25 August rejected as outliers). Thus on average 82% of PM_{10} was composed of fine particles during P2.

Total gaseous mercury (TGM) was measured (P2 only) with a Tekran 2537A mercury vapour analyser. The sampling resolution was 5 min and sample flow 1.5 l min^{-1}. Particulate matter was removed by a 45-mm-diameter Teflon prefilter with 0.2-μm-pore-width. The instrument was calibrated every 24 h using an internal permeation source. Here all analyser data were hourly averaged.

For the chemical analyses, particles $d < 10$ μm were also collected on filters (Teflon, Digitel DPM10/2.3/01 sampling head, flow rate of 38 l min^{-1}, filter change at 8 a.m., weighing at room temperature and humidity). The correlation between the mass measurements with the analyser and the filter collection was good: PM_{10} (analyser) $= 1.12 \times PM_{10}$(filter), $r = 0.97$; $n = 50$ (one outlier, on 25 August, was rejected and the intercept was set to zero). The analyser gave 12% higher results than the filter, which may well be due to the analyser's correction factor being too high (i.e., 31%) for volatile compounds. However, no amendments were applied to the analyser results.

Major ions, trace elements and polycyclic aromatic hydrocarbons (PAHs) were analysed from the filters. Analysis methods (see e.g. Hellén et al., 2008; Jalkanen and Häsänen, 1996), detection limits and uncertainties are summarized in Table 1. Due to limited resources, PAHs were only analysed every third day or so.

All results are presented relative to 20 °C, times are local winter time (UTC + 2 h). As reference material, the hourly concentration data from Virolahti for $PM_{10}/PM_{2.5}$, NO, NO_2, SO_2 and O_3 for the previous two years 2004–2005 were used. The meteorological observations (temperature, precipitation, wind speed and direction) for the study periods were retrieved from the Virolahti weather station, while visibility and relative humidity from the Kotka Haapasaari weather station were used.

3. Data analysis

The potential source areas were studied using the FLEXTRA three-dimensional backward air mass trajectories provided by the Norwegian Institute for Air Research (Stohl et al., 1995; Stohl and Seibert, 1998). The three-day trajectories calculated for a height of 500 m above ground level were used. Each 24 h filter sampling was assumed to integrate four consecutive trajectories, i.e., 12, 18, 0 and 6 UTC.

Table 1
The limits of detection (LOD) and uncertaintities (U) for components analysed from 24 h PM_{10} filters

			Number of values above LOD	
Component	LOD ng m^{-3}	*U* %	P1	P2
Ion chromatograph				
Na^+	0.4	10	31	31
K^+	1.2	17	31	31
Mg^{2+}	0.6	15	31	31
Ca^{2+}	1.0	13	31	31
Cl^-	2.0	13	31	31
NO_3^-	8.8	13	31	31
NH_4^+	0.5	15	31	31
SO_4^{2-}	12	15	31	31
Inductively-coupled plasma mass spectrometry				
Al	0.24	30	31	31
As	0.01	24	31	31
Cd	0.01	25	31	31
Co	0.01	25	31	31
Cr	0.13	30	27	11
Cu	0.01	28	31	31
Fe	0.60	40	31	31
Mn	0.01	25	31	31
Ni	0.08	30	31	31
Pb	0.01	22	31	31
V	0.01	25	31	31
Zn	0.01	25	31	31
Gas chromatograph and a mass spectrometer				
Fluoranthene (FL)	0.13	16	4	1
Pyrene (Pyr)	0.13	19	3	1
Benz(*a*)anthracene (BaA)	0.02	28	6	9
Chrycene/trifenylene (CHR)	0.02	14	7	10
Benzo(*k*,*b*,*j*)fluoranthene (BkbjF)	0.06	19	5	7
Benzo(*a*)pyrene (BaP)	0.03	11	4	9
Indeno(1,2,3-cd)pyrene (IND)	0.02	48	7	11
Dibenz(*a*,*h*)anthracene (DBA)	0.04	26	0	4
Benzo(*g*,*h*,*i*)perylene (BghiP)	0.02	48	6	10

LODs were calculated as three times the standard deviation of blanks. The number of values above detection limit are given for P1 and P2. The total number of samples was 31 in both periods except for PAHs: 8 samples in P1 and 12 in P2, respectively.

The daily fire detections were downloaded from the Web Fire Mapper interface that displays active fires detected by the MODIS Rapid Response System (Justice et al., 2002). To exclude false positive occurrences of fires, only detections with a confidence value higher than 25 were included.

Positive matrix factorization (PMF) was used to study the relationships between the chemical compounds of the samples (Paatero and Tapper, 1994; Paatero, 1997). The daily data from the two periods were factorized separately, both cases consisting of 31 samples and 25 variables (PM_{10}, major ions, trace elements and gases). Missing values were replaced by the median of the measured values, and their accompanying error estimates were set to the absolute maximum value for the whole period. The error estimates were calculated as the sum of absolute and relative errors, where the absolute error was set to 10% of the period median and the relative error to 10% of each measured value. PMF was run with different factor numbers; the results that produced a good fit to the data, as well as being the most reasonably interpretable, were adopted.

4. Results and discussion

4.1. Temporal variation of PM_{10}, $PM_{2.5}$ and meteorological parameters

In P1 the PM_{10} started to increase at 6 a.m. on 25 April and remained at an elevated level until 7 May (Fig. 2a). Between 25 April and 1 May (episode EP1.1) the hourly PM_{10} fluctuated between 20 and 50 μg m^{-3}. On 2 May concentrations started to increase. Between 2 and 4 May (EP1.2) concentrations were very stable, but from 4 May onward concentrations varied over a wide range, reaching maximum values of 100–115 μg m^{-3} (4–7 May; EP1.3).

On 25 April, simultaneously with the PM_{10} increase, the visibility was reduced (Fig. 2b); relative humidity remained at a low level, suggesting that visibility was not restricted by fog (Fig. 2c); the wind started to blow from the easterly sector (Fig. 2e) and remained there until 3 May. From 4 May onward, i.e., at the time of the highest PM_{10} concentrations, the wind direction varied more, northern and southern directions also being common. Especially from 1 to 7 May visibility was severely reduced, in concurrence with low relative humidities and elevated PM_{10} concentrations. At the end of P1, from 20 May onwards, the visibility was even poorer, but the relative humidities then reaching 100% (Fig. 2c) suggest that this was due to fog formation and rain. The daily accumulated precipitation amounts on 19, 20 and 21 May were 1.3, 1.3, and 5.2 mm, respectively. The mean temperature of P1 was 8.6 °C.

In August (P2) the north-easterly wind brought the first plumes of $PM_{2.5}$ on 2 and 3 August (EP2.1) (Fig. 2). After five days of lower concentrations, a week-long period (8–15 August; EP2.2) started on 8 August at 3 p.m. This consisted of seven discernible $PM_{2.5}$ peaks. The highest peaks were 145 μg m^{-3} on 12 August at 7 a.m. and 14 August at 1 a.m. Between the peaks, concentrations dropped to about 10 μg m^{-3}. The last days of EP2.2 were characterized by a light easterly breeze which did not weaken even at night (Fig. 2i and j). On 15 August a humid south-westerly flow (Fig. 2h and j) brought this cyclic period abruptly to a close. On 20–21 August (EP2.3) a light easterly breeze brought the last plumes.

These three episodes EP2.1–2.3 were accompanied by reduced visibility (Fig. 2g). At its worst, the visibility was reduced to 600 m (10 min value) on 21 August. During P2 rain was measured on 3, 15, 18, 28 and 30 August, the precipitation amounts being 8.2, 0.2, 0.1, 20.4 and 5.8 mm, respectively. The mean temperature was 17.5 °C.

4.2. Hourly concentrations

The hourly time series of gaseous NO_x, SO_2 and O_3 revealed no such strong episodic patterns as the PM_{10}/$PM_{2.5}$, and also correlated only poorly with the hourly particulate matter. However, on the afternoon of 5 May, at the time of the highest PM_{10} peaks, the ozone hourly value exceeded 180 μg m^{-3} for 5 h; these were the highest values ever recorded since the start of measurements at Virolahti in 1989.

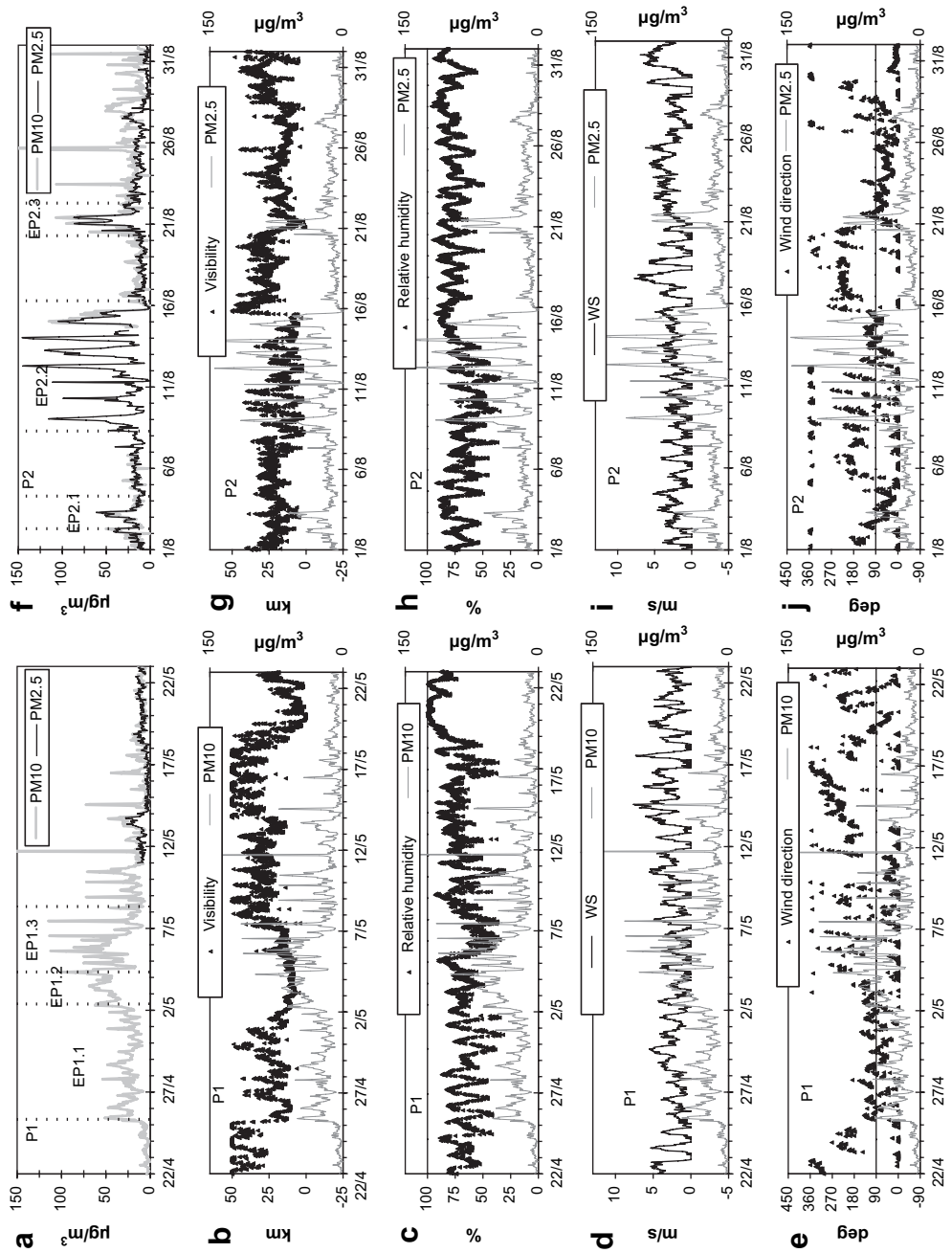

Fig. 2. The hourly concentrations of PM_{10} and $PM_{2.5}$ (a, f), visibility (b, g), relative humidity (c, h), wind speed (d, i) and direction (e, j) during the study periods. The duration of episodes is based on 24 h PM_{10} samplings.

The relationship between the particulate matter and the gaseous compounds were further studied by analyzing the dependence of concentrations on local wind direction. The hourly concentrations were divided into eight clockwise wind direction categories, i.e., north (337.6–22.5°), north-east (22.6–67.5°), etc. based on the hourly wind data from Virolahti. Concentration data with wind speeds less than 0.5 m s^{-1} were excluded. The concentration means of each category were calculated and compared to the equivalent values from the previous 2 years 2004 and 2005, when, as far as we know, the Virolahti station was not affected by major biomass-burning-related anomalies.

The differences between the concentration means were tested by one-way analysis of variance (ANOVA) with year as the independent factor and post hoc Tukey's honest significance difference test for multiple comparisons to determine which pair-wise interactions were significantly different at the $p < 0.05$ level. The original data were log-transformed to meet the normality requirement before ANOVA.

During P1 the highest PM_{10} concentrations were found in the eastern and south-eastern wind sectors, while during P2 the eastern sector had highest $PM_{2.5}$ concentrations (Fig. 3). For all components, the highest concentrations typically are associated in spring with the south-eastern wind sector (Fig. 3). NO_2 concentrations were slightly elevated in both periods: in P1 with winds from the southern quadrants and in P2 rather from the northern quadrants, suggesting an increased influence of Finnish inland sources. On the other hand, the NO concentrations were rather reduced, which indicates that the influence of local sources was minor. Ozone and SO_2 showed no specific patterns in terms of wind direction when compared to the reference periods.

In contrast to the other gaseous components, the hourly peaks of TGM coincided extremely well (Pearson $r = 0.85$; $n = 728$) with those of the $PM_{2.5}$ (Fig. 4a). Besides, for TGM (with no reference data from the earlier years) the highest concentrations were found in the eastern sector (with some peaks in the north-east) (Fig. 4b) in analogy to the behaviour of $PM_{2.5}$ in P2 (Fig. 3). The peaks accompanying the $PM_{2.5}$ suggest that the background concentration of TGM was elevated by the same source as for the particulate matter in this study.

The mercury accumulated in foliage and soils is efficiently liberated to the atmosphere by the heat of a fire (Salt et al., 1998; Grigal, 2003; Friedli et al., 2001, 2003a,b). Peaty soils, in particular, are rich in mercury; concentrations in peat can even be several orders of magnitude higher than those in vegetation (Grigal, 2003). It has been proposed that the proper inclusion of mercury emissions from peatland fires will multiply the earlier estimates of circumboreal mercury emissions by a factor of 15 (Turetsky et al., 2006).

The highest hourly concentrations of TGM were 2.7–2.8 ng m^{-3}, i.e., over twice as high as the period mean. These elevations are clearly higher than the 40% rise from the background level (from 1.4 to 2.0 ng m^{-3}) detected in a smoke plume transported over hundreds of kilometres to the north-eastern U.S.A. from boreal forest fires in Canada (Sigler et al., 2003) or the 45% rises (from 1.05 to 1.52 ng m^{-3}) reported in a short-range transported biomass fire plume in South Africa (Brunke et al., 2001). On the other hand, Friedli et al. (2003b) measured TGM concentrations as high as 7.5 ng m^{-3}, a six-time enhancement over the background, in smoke plumes above large wildfires in temperate forests in the U.S.A.

At the time of the eight highest TGM peaks between 9 and 21 August (see Fig. 4a), the mean mass ratio between the simultaneous hourly maxima of TGM and $PM_{2.5}$ was $(2.1 \pm 0.3) \times 10^{-5}$. This mass ratio falls slightly above the $Hg^0/PM_{2.5}$ best-guess mass ratio range of $(0.5–1.7) \times 10^{-5}$ deduced from Andreae and Merlet (2001) for extratropical forest fire plumes.

These elevated TGM concentrations detected in P2 may therefore well be caused by mercury released by fires from foliage and especially from peaty soils.

4.3. Chemical composition of 24 h PM_{10} samples

The day-to-day variation of the chemical composition of PM_{10} (Fig. 5) points to a couple of partly superimposed source types in P1: NO_3^-, NH_4^+ and SO_4^{2-} (i.e., long-range transported (LRT) secondary inorganic ions) increased sharply on 2 May and stayed elevated for 4–5 days, i.e., covering EP1.2 and part of EP1.3. Crustal dust elements (Al and Fe) peaked on 4–11 May (overlapping EP1.3). This was the time when the wind became more variable, and also northerly winds from inland became common (Fig. 2e). These increased concentrations of Al and Fe may indicate suspension of crustal dust, as this period occurred during the yearly spring dust season (e.g. Anttila and Salmi, 2006).

In P2 the concentrations of the inorganic components were less variable than in P1 and varied independently of PM_{10} (Fig. 5). For PAHs we have discontinuous measurements, which limits conclusions on the day-to-day variation; however, there is a tendency for elevated PAHs during the episodic days of both periods.

One really extreme day of PAH concentrations, 13 August, was captured. The PAH concentrations then (e.g., benzo(*a*)pyrene 1.4 ng m^{-3}) were comparable to wintertime concentrations in a residential area with a high density of wood combustion (Hellén et al., 2008).

Evidently the elevated PM_{10} concentrations in P1 were caused by several sources. To distinguish the impact of biomass fires, we use K^+ as a tracer for biomass combustion sources (e.g. Andreae, 1983). For this the exK^+ (i.e., K^+ corrected for sea salt and crustal dust contributions) in the daily samples was calculated using Na^+ and Al as markers for sea salt and crustal dust, respectively (see e.g. Andreae, 1983). The following compositions were assumed: Na: 31%, K: 1.1%, Al: 0%, and Na: 2.6%, K: 2.9% and Al: 7.7% for sea salt and crustal dust, respectively (Wedepohl, 1995).

In P1 exK^+ was present only between 25 April and 3 May (Fig. 6). The negative values of exK^+ after that date result from the strong increase in Al concentrations (Fig. 5) and the interpretation could be that in this dust episode the K^+/Al default ratio used, 0.38, is too high. The procedure is based on the assumption of constant ratios of elements in the source, which may not necessarily be met, especially in case of the crustal dust. (The calculation

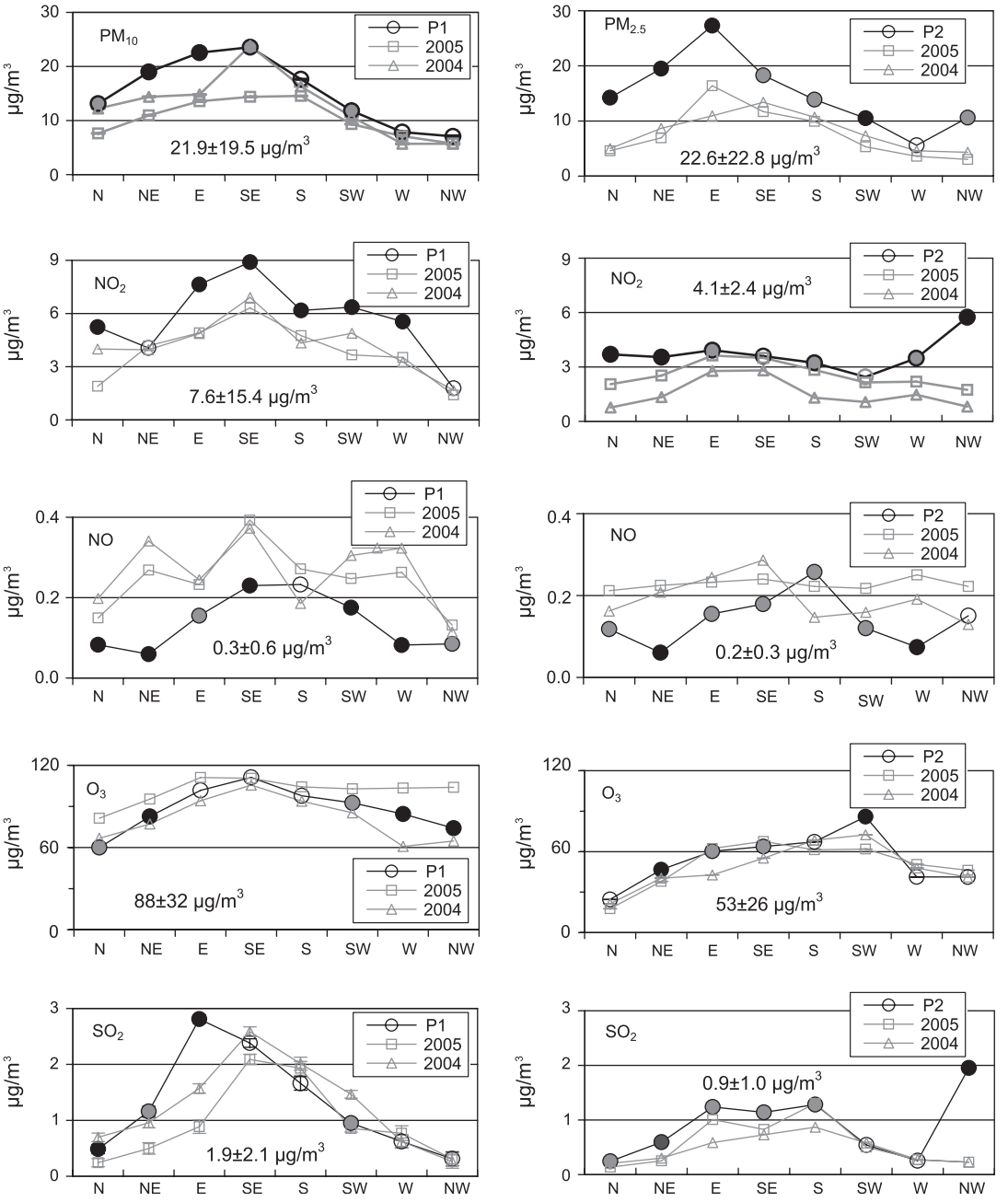

Fig. 3. Averaged hourly mean concentrations of PM_{10}, $PM_{2.5}$, NO_2, NO, O_3 and SO_2 versus wind direction during P1 and P2 and during the equivalent periods in the reference years 2004 and 2005. The mean and standard deviation of each component during the study period is also given in each graph. Black circles: mean concentrations of P1 (or P2) differ statistically significantly (s.s.) from the values of both reference years, 2005 and 2004. Grey circles: mean concentrations of P1(2) differ s.s. from one or the other of the two reference years. Open circles: mean concentrations of P1(2) differ s.s. from neither of the two reference years.

was repeated with Ca^{2+} as the surrogate for crustal dust, which resulted in a slightly narrower range for exK^+, but a very similar temporal variation.)

However, this result suggests that in P1 the biomass fire episode lasted from 25 April to 3 May, i.e., covering EP1.1 and EP1.2. In EP1.2 the secondary inorganic ions increased strongly compared to EP1.1, which may suggest that at this time the biomass fire aerosol was complemented with traditional LRT particles. We thus conclude that in the present study EP1.1 represents the most genuine biomass fire aerosol of P1. During P2 exK^+ was detected most clearly on 8, 12, 13 and 14 August and weakly around 3 and 20 August. These dates coincide satisfactorily with EP2.1, EP2.2 and EP2.3, and suggest that the elevation of PM_{10} during these episodes was related to biomass fires.

To quantify the increase in concentrations of chemical species during episodes, reference data was compiled from the non-episodic days of P1 and P2. The mean

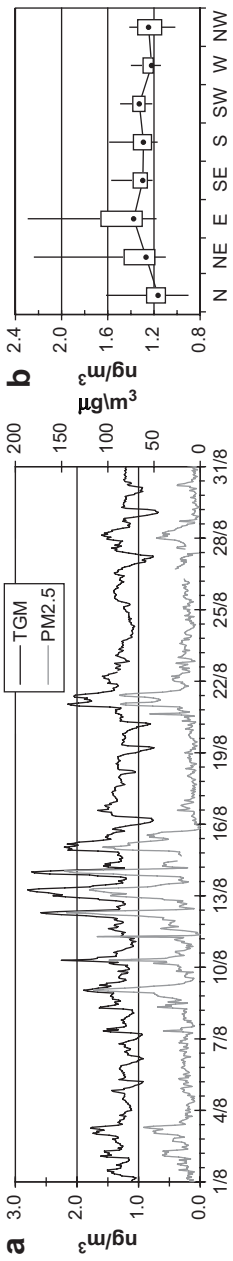

Fig. 4. (a) Hourly averaged time series of TGM (left axis) and $PM_{2.5}$ during P2. (b) Concentration distributions of hourly TGM in P2 in each wind sector. Values for the 5th, 25th, 50th (connected with a line) 75th and 95th percentiles are shown.

concentrations of the reference period and the episodes together with the episode-to-reference concentration ratios are shown in Table 2. Statistically significant elevations ($p < 0.005$, Kruskal Wallis) of concentrations were detected only during EP1.1, EP1.3 and EP2.2 (Table 2). The elevated concentrations present in EP1.2, EP2.1 and EP2.3 were insignificant due to the low number of samples (only two in each) and are not shown.

In the EP1.1 biomass fire episode in addition to K^+, also Ca^{2+}, NO_3^-, Cd, Cu, Mn, Pb and Zn were significantly elevated (Table 2) as well as the gaseous O_3 and SO_2. PAHs also showed very high elevation ratios, but these were mainly not significant due to the low number of data. Instead, during EP1.1 the concentrations of soil elements (Al, Fe), LRT ions (SO_4^{2-} and NH_4^+) and sea salt (Na^+, Mg^{2+}, Cl^-) remained close to their background values.

Of the trace elements, wild forest fires have been estimated to emit considerable amounts of Cu, Mn and Zn (Nriagu, 1989), which elements were enriched in EP1.1 too. In EP1.1 the elemental concentration ratios of Cu, Mn and Zn to K^+ were 0.01, 0.03 and 0.15. For Cu and Mn these are very close to those detected in experimental smoke from smouldering and flaming tropical forest fires (Yamasoe et al., 2000), in smoke plumes from mixed conifer forests in Montana (Ward et al., 2004) and also in experimental surface fires in Scots Pine forests in boreal Central Siberia (Samsonov et al., 2005).

On the other hand, the Zn to K^+ ratio was about ten times higher in EP1.1 than in the above-mentioned forest fire studies; and the highly-enriched Cd and Pb found in this study were not detected at all, or had only low proportions in the biomass fire smokes (Yamasoe et al., 2000; Ward et al., 2004; Samsonov et al., 2005). It is thus highly probable that not even EP1.1 was an undiluted biomass fire aerosol but was contributed to by some other, probably industrial, emissions too.

At the beginning of EP1.1, on 25–26 April, the air masses arrived at Virolahti from the south-east, crossing the intense fire areas south and south-west of St. Petersburg and in the Novgorod region, within a radius of about 500 km (Fig. 7a). One of the trajectories on 25 April also crosses the border areas of Estonia and Russia where oil shale is utilized for energy production. Of the trace metals, Pb, Cd, Zn, Ti and As are accumulated in the fly ash of oil shale (Aunela-Tapola et al., 1998). The anthropogenic emissions along and near the south-eastern coast of the Gulf of Finland could be one explanation for the additional anthropogenic input (e.g. Pb, Cd, Zn, SO_2) detected in the biomass-burning aerosol. However, from 25 April to 3 May, the K^+ concentration in PM_{10} is higher than that of Ca^{2+}, which is rather atypical for, e.g. oil shale emissions. Biomass burning thus remains the major contributor to the PM_{10} aerosol detected at Virolahti on these days.

On 2 May the airstream became more southerly and, after sweeping over the fire areas in the Ukraine and Belarus, crossed an enhanced fire area in the proximity of the Latvian border (Fig. 7a) and also over the industrialized area on the Estonian and Russian border. On 2–3 May (EP1.2) the secondary ions were about three times higher, while the trace elements and gases remained at the same

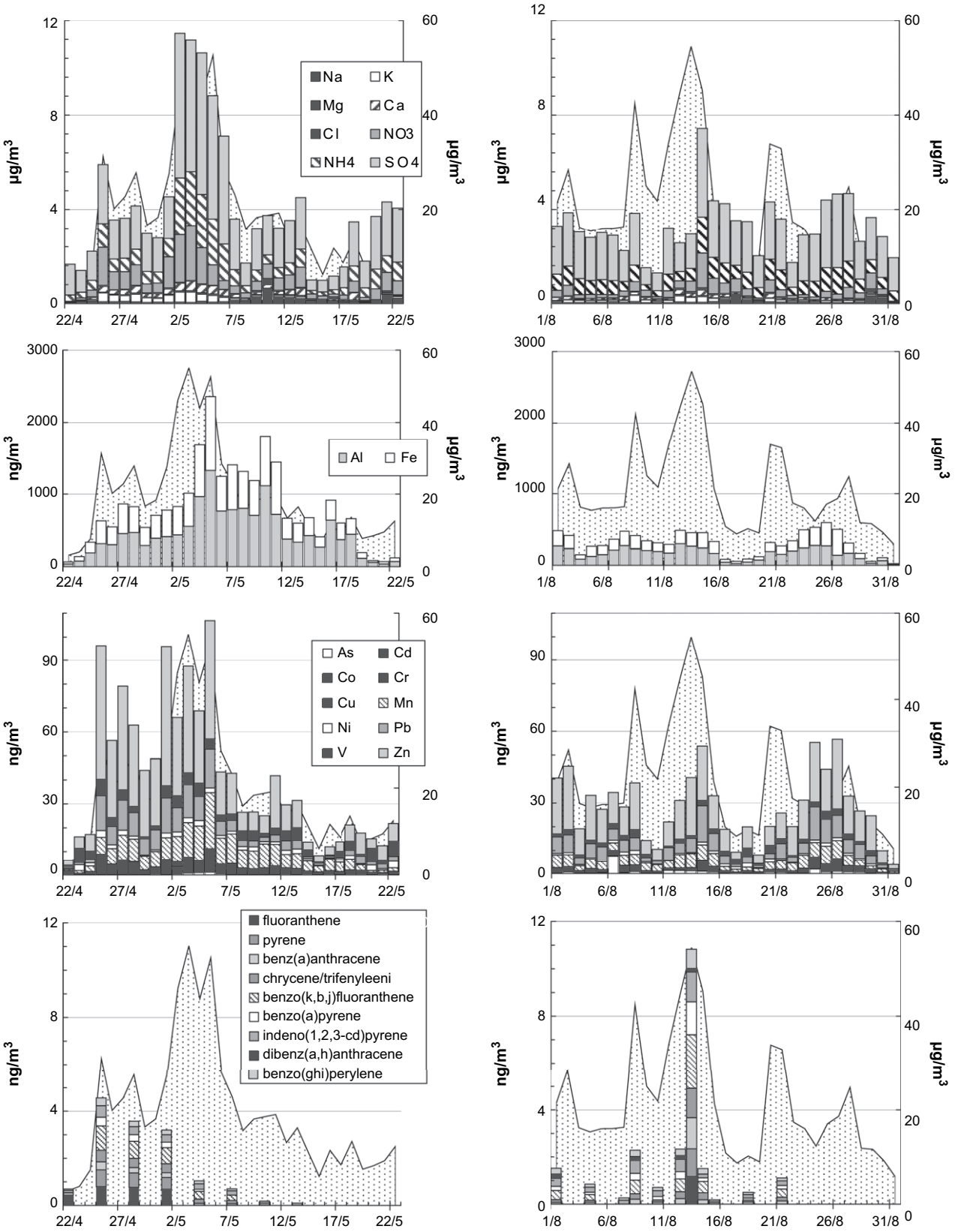

Fig. 5. Daily variation of the chemical composition of PM_{10} during P1 (left panel) and P2 (right panel). In each figure PM_{10} is shown as a dot-filled area with values on the right-hand axis. Chemical components are stacked into daily columns grouped into four groups from top to bottom: major ions, Al and Fe, other trace elements and PAHs.

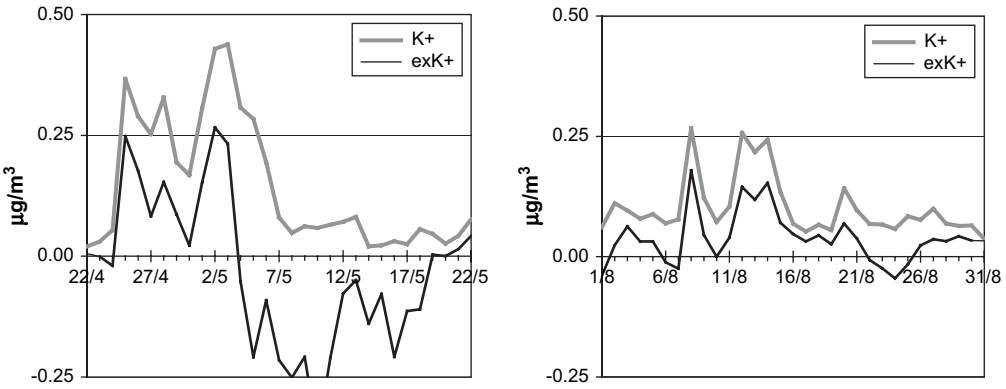

Fig. 6. Daily variation of K^+ and exK^+ in P1 (left) and P2.

elevation levels as in EP1.1. These southern source areas may well be the explanation for the LRT episode (especially as the Ukraine is a major SO_2 emitter) detected along with the biomass-burning aerosol.

On 4–7 May, i.e., EP1.3, during the last and highest PM_{10} peaks, aerosol contained elevated concentrations of LRT ions, trace elements and crustal-related elements (Table 2) and originated largely from regions with no intense fire

Table 2
The 24 h concentrations (mean ± SD and maximum value) during the reference period and the episodes EP1.1, EP1.3 and EP2.2, and the episode-to-reference concentration ratios (ratio) for each species

	Reference[a]		P1						P2		
			EP1.1			EP1.3			EP2.2		
No. of days (PAHs)	37(8)		7(3)			4(2)			8(6)		
Species	Mean ± SD	Max	Mean ± SD	Max	Ratio	Mean ± SD	Max	Ratio	Mean ± SD	Max	Ratio
PM_{10}	12.8 ± 5.0	24.8	23.5 ± 5.5	31.3	**1.8**	37.0 ± 13.7	52.6	**2.9**	36.2 ± 12.5	54.5	**2.8**
Na^+	0.13 ± 0.12	0.52	0.06 ± 0.01	0.08	0.5	0.09 ± 0.04	0.14	0.7	0.05 ± 0.02	0.08	0.4
K^+	0.06 ± 0.02	0.10	0.27 ± 0.07	0.37	**4.7**	0.22 ± 0.10	0.31	**3.7**	0.18 ± 0.08	0.27	**3.1**
Mg^{2+}	0.02 ± 0.02	0.06	0.03 ± 0.01	0.04	1.5	0.04 ± 0.01	0.05	2.0	0.03 ± 0.02	0.06	1.2
Ca^{2+}	0.08 ± 0.07	0.31	0.21 ± 0.05	0.30	**2.5**	0.28 ± 0.10	0.36	**3.4**	0.14 ± 0.06	0.24	1.6
Cl	0.03 ± 0.04	0.24	0.03 ± 0.01	0.05	1.1	0.01 ± 0.01	0.02	0.5	0.04 ± 0.03	0.09	1.6
NO_3^-	0.31 ± 0.22	0.86	0.87 ± 0.45	1.61	**2.8**	0.78 ± 0.56	1.54	2.5	0.50 ± 0.43	1.47	1.6
NH_4^+	0.55 ± 0.24	1.13	0.65 ± 0.19	1.02	1.2	1.62 ± 0.69	2.28	2.9	0.66 ± 0.43	1.55	1.2
SO_4^{2-}	1.72 ± 0.65	3.15	1.81 ± 0.33	2.50	1.1	4.49 ± 1.65	5.99	**2.6**	1.82 ± 1.01	3.75	1.1
Al	255 ± 254	1115	374 ± 74	466	1.5	960 ± 260	1326	**3.8**	220 ± 46	298	0.9
As	0.57 ± 1.23	7.56	0.33 ± 0.07	0.41	0.6	0.77 ± 0.33	1.14	1.4	0.90 ± 0.37	1.34	**1.6**
Cd	0.11 ± 0.09	0.41	0.59 ± 0.15	0.82	**5.4**	0.50 ± 0.24	0.82	**4.6**	0.21 ± 0.10	0.40	1.9
Co	0.09 ± 0.05	0.19	0.15 ± 0.03	0.19	1.7	0.25 ± 0.09	0.38	**2.9**	0.07 ± 0.03	0.10	0.8
Cr	0.72 ± 0.76	3.04	1.11 ± 0.50	1.99	1.5	1.86 ± 0.94	3.25	2.6	0.33 ± 0.22	0.49	0.5
Cu	1.16 ± 0.60	2.57	3.15 ± 1.71	6.20	**2.7**	3.34 ± 1.56	5.58	**2.9**	1.40 ± 1.08	3.47	1.2
Fe	193 ± 178	725	324 ± 61	412	1.7	713 ± 234	1031	**3.7**	164 ± 36	215	0.8
Mn	3.92 ± 2.63	10.2	7.97 ± 1.72	10.43	**2.0**	15.36 ± 5.59	23.47	**3.9**	4.78 ± 1.55	6.88	1.2
Ni	1.11 ± 0.64	2.81	1.57 ± 0.86	2.90	1.4	1.67 ± 0.59	2.35	1.5	0.79 ± 0.52	1.69	0.7
Pb	3.54 ± 2.95	14.0	10.70 ± 3.28	14.73	**3.0**	9.19 ± 5.22	16.18	2.6	5.87 ± 4.3	15.26	1.7
V	2.41 ± 1.64	6.37	3.51 ± 2.05	6.74	1.5	3.71 ± 1.40	5.49	1.5	1.56 ± 0.92	3.39	0.6
Zn	10.5 ± 6.9	29.2	40.0 ± 12.9	58.4	**3.8**	28.8 ± 15.3	49.9	2.7	14.8 ± 7.4	24.5	1.4
FL	0.11 ± 0.13	0.44	0.74 ± 0.06	0.79	6.7	0.06 ± 0.00	<0.13	0.6	0.25 ± 0.45	1.17	2.2
Pyr	0.06 ± 0.00	<0.13	0.61 ± 0.11	0.72	**9.5**	0.06 ± 0.00	<0.13	1.0	0.25 ± 0.45	1.18	3.9
BaA	0.05 ± 0.04	0.09	0.25 ± 0.07	0.34	5.6	0.08 ± 0.01	0.08	1.7	0.34 ± 0.49	1.32	7.4
CHR	0.06 ± 0.05	0.12	0.42 ± 0.06	0.50	6.5	0.16 ± 0.03	0.18	2.5	0.38 ± 0.44	1.26	5.8
BkbjF	0.10 ± 0.14	0.39	0.81 ± 0.19	1.03	8.0	0.27 ± 0.07	0.32	2.7	0.66 ± 0.84	2.29	6.5
BaP	0.05 ± 0.06	0.18	0.30 ± 0.07	0.37	5.6	0.05 ± 0.06	0.09	1.0	0.38 ± 0.5	1.39	7.3
IND	0.14 ± 0.11	0.35	0.38 ± 0.09	0.49	2.8	0.21 ± 0.03	0.23	1.5	0.47 ± 0.43	1.27	3.5
DBA	0.04 ± 0.06	0.17	0.02 ± 0.00	<0.04	0.5	0.02 ± 0.00	<0.04	0.5	0.08 ± 0.07	0.16	2.3
BghiP	0.08 ± 0.08	0.25	0.26 ± 0.07	0.34	3.0	0.11 ± 0.03	0.13	1.3	0.29 ± 0.28	0.81	3.5
TGM	1.23 ± 0.1	1.44				-	-		1.50 ± 0.22	1.87	**1.2**
NO	0.3 ± 0.2	0.7	0.3 ± 0.2	0.6	1.3	0.4 ± 0.2	0.5	1.5	0.2 ± 0.1	0.4	0.9
NO_2	5.1 ± 2.8	15.2	9.2 ± 4.6	16.9	1.8	8.4 ± 3.2	12.4	1.7	5.1 ± 1.6	7.4	1.0
O_3	64 ± 17	105	106 ± 5	113	**1.7**	106 ± 15	126	1.7	51 ± 5	59	0.8
SO_2	0.8 ± 0.6	3.2	3.9 ± 1.4	6.7	**4.6**	2.0 ± 0.8	2.9	2.4	1.2 ± 0.6	1.9	1.4

Trace elements, PAHs and TGM are given in ng m^{-3}, others in µg m^{-3}. In calculation of the means, one-half of the LOD was used for below-LOD values. Bolded ratio entries denote that the mean of the reference period and the episodic period differ statistically significantly ($p < 0.005$ Kruskal-Wallis test).

[a] Reference includes dates 22–24 April, 8–22 May, 1, 4–7, 16–19 and 22–31 August.

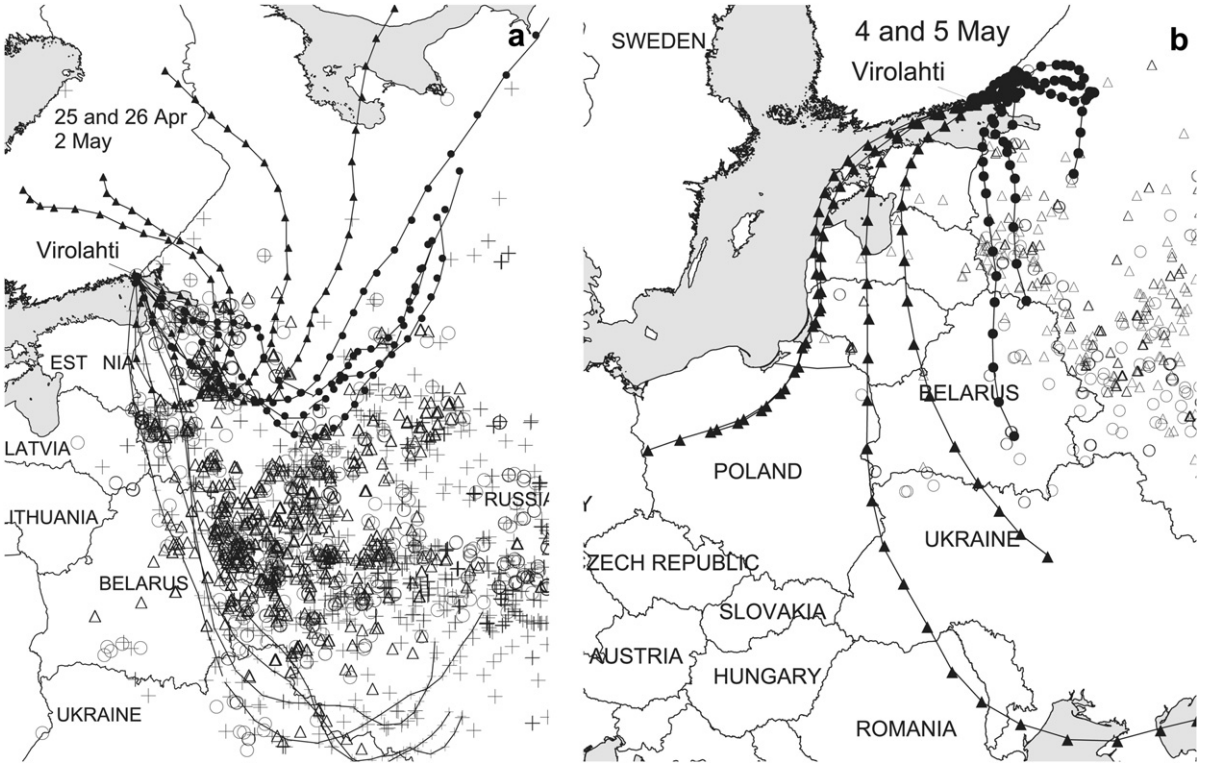

Fig. 7. Three-day backward trajectories arriving at Virolahti on (a) 25 April (lines with triangles), 26 April (circle), 2 May (cross) and (b) 4 May (triangle) and 5 May (circle). Fire detections on each day are denoted with similar but larger open symbols.

areas (Fig. 7b). This period may thus be a combination of polluted air from continental Europe and from across the Gulf of Finland together with the suspension of local dust.

In P2 (EP2.2), of the inorganic components only K^+, As and TGM showed significant increases. Again PAHs showed high but insignificant increases, while no increases were detected e.g. for the secondary ions or crustal dust elements. This suggests that the episode in P2 was more exclusively caused by a single, i.e., biomass fire, source.

In August the biomass-burning plumes arrived at Virolahti from a more easterly direction (covering St. Petersburg and its surrounding areas, but not the industry on the border between Estonia and Russia) and trajectories originated from the sparsely populated north-western Russia (Fig. 8). This main pattern may explain the lower concentration levels and the monotonous temporal pattern of LTR ions and trace elements detected in P2. Also at this time of year, perhaps, anthropogenic emissions were at their lowest, as no heating was needed and the summer holiday season was at its height. Note, however, that on 14 August both the LRT ions and trace metals peaked; this was the day when the southernmost air masses occurred (Fig. 8).

The biomass fire positions also differed from P1. In August the fires were concentrated in latitudes south of Moscow, while there was a practically fireless belt up to St. Petersburg and then again fires around the eastern end of the Gulf of Finland. About twenty fires were detected in the surroundings of Vyborg at distances of 50–100 km from Virolahti during August. With a wind speed of 2.5 m s^{-1}, plumes from these fires could reach Virolahti in a couple of hours and would represent more fresh and and undiluted aerosol. The proximity of the sources may explain the extreme variations detected with the hourly $PM_{2.5}$ analyzer, the close correlation between $PM_{2.5}$ and TGM, and possibly also the large variation detected in PAH concentrations.

A major component of aerosols emitted from biomass burning is organic matter and, to a lesser extent, elemental carbon (e.g. Andreae and Merlet, 2001). Neither organic nor elemental carbon were chemically analysed in this study (except PAHs). To illustrate the time variation of this unidentified fraction (i.e., probably largely organic matter) we calculated the contributions of crustal dust (based on Al), inorganic secondary ions and sea salt (based on Na^+) in the daily PM_{10} samples (cf. the calculation of exK^+ earlier) (Fig. 9).

Secondary inorganic ions and crustal dust contributed more in P1, while during P2 the temporal variation of PM_{10} was controlled almost totally by components not differentiated chemically here, most probably organic carbon. The mean unidentified fraction was 45% and 69% in P1 and P2, respectively. This fraction was at its maximum on 13 August, contributing as much as 90% of the total PM_{10}.

4.4. Source apportionment with positive matrix factorization

Application of PMF to P1 data confirmed several features which have already been found on the basis of

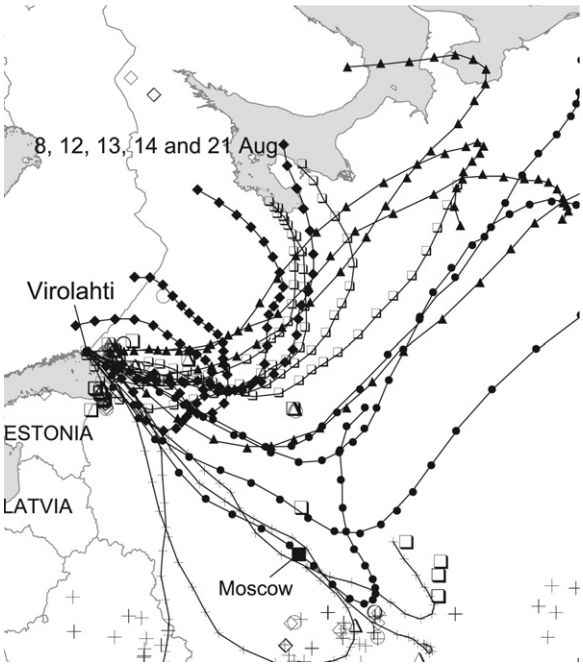

Fig. 8. Three-day backward trajectories arriving at Virolahti on 8 August (lines with squares), 12 August (triangle), 13 August (circle), 14 August (cross) and 21 August (diamond). Fire detections at each day are denoted with similar but larger open symbols.

the tracer species and trajectory analyses, but some new patterns also emerged. In P1 PMF yielded five physically meaningful PM_{10} sources: secondary inorganic ions, sea spray, soil dust, oil combustion and biomass fires. This five-factor solution explained 93–75% of the variation of each component. The factor compositions and the temporal variations of each source contribution are presented in Fig. 10.

The secondary inorganic ions formed their own factor with low loadings of other species. This LRT source has a strong peak on 2–4 May (Fig. 10). During these three days the major ions contributed as much as 20–25% to the total PM_{10}. Based on the trajectories, the source area was Eastern Europe (Fig. 7a and b).

In the next factor (sea spray) Na^+, Mg^{2+} and Cl^- appear in concentrations relatively close to fresh sea salt. Here the mass ratios Na/Mg and Na/Cl were 7.7 and 1.9, respectively, while in fresh sea salt they are about 8.5 and 0.56. This factor is therefore a good representative of slightly aged sea salt aerosol.

This factor also showed a very clear episodic pattern, with a peak on 10 May. Two of the four three-day backward trajectories calculated for this date originated near Greenland in the Arctic Ocean, circulating over the Svalbard Isles, around the Kola Peninsula and the White Sea, and arriving finally at Virolahti from the north-east (not shown). This route explains well the abundance of sea spray in the aerosol on that day. On a monthly level, 16% of total Cl^- entered in the biomass factor and 7% in the secondary ions factor. These may be indications of Cl^- depletion from sea salt aerosols as maritime air passed over burning biomass fires and other anthropogenic emissions.

In the third factor the major species contributing were Al, Fe and Mn, and the source was determined to be airborne crustal dust. The factor had a clear peak, a dust episode, on 5 May. On this day air slowly circulated along the Finnish Russian border (Fig. 7b) and arrived at Virolahti from the north-east from areas with only few fires.

The fourth factor was identified as biomass fires, due to the high contribution of K^+ (Fig. 10). The PMF analysis suggests that the biomass fire episode started on 25 April and extended, while slowly decaying, up to 4 and 5 May, which is two days longer than was concluded on the basis of exK^+. On 5 May, indeed, the tails of the trajectories (Fig. 7b) cover fire areas near the Latvian and Russian border. Thus the air mass may well have contained aged biomass-burning aerosol that did not reveal itself as exK^+ due to the simultaneous strong crustal dust episode. PMF also associates Cd, Pb, Zn and SO_2 together with biomass burning.

The fifth factor was identified as heavy fuel oil combustion with its high Ni and V contributions. 60% and 50% of NO and NO_2, respectively, also entered into this

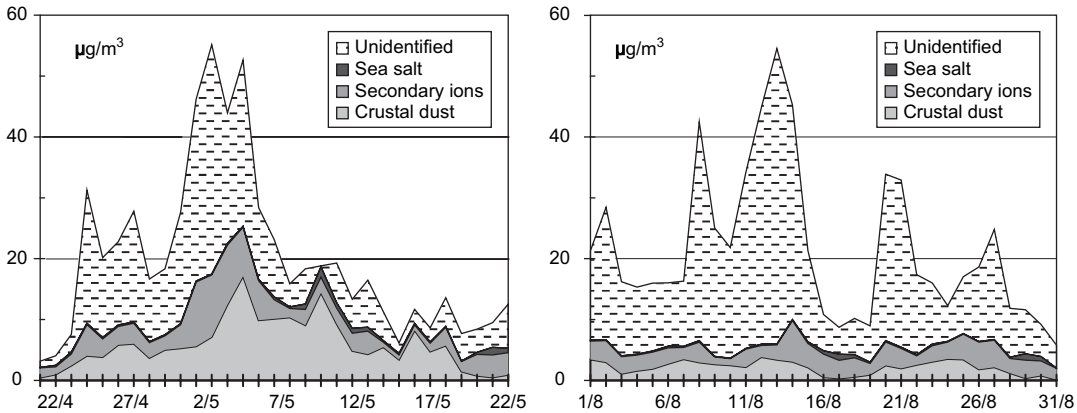

Fig. 9. Contributions of crustal dust, secondary inorganic ions and sea salt in the daily PM_{10} samples.

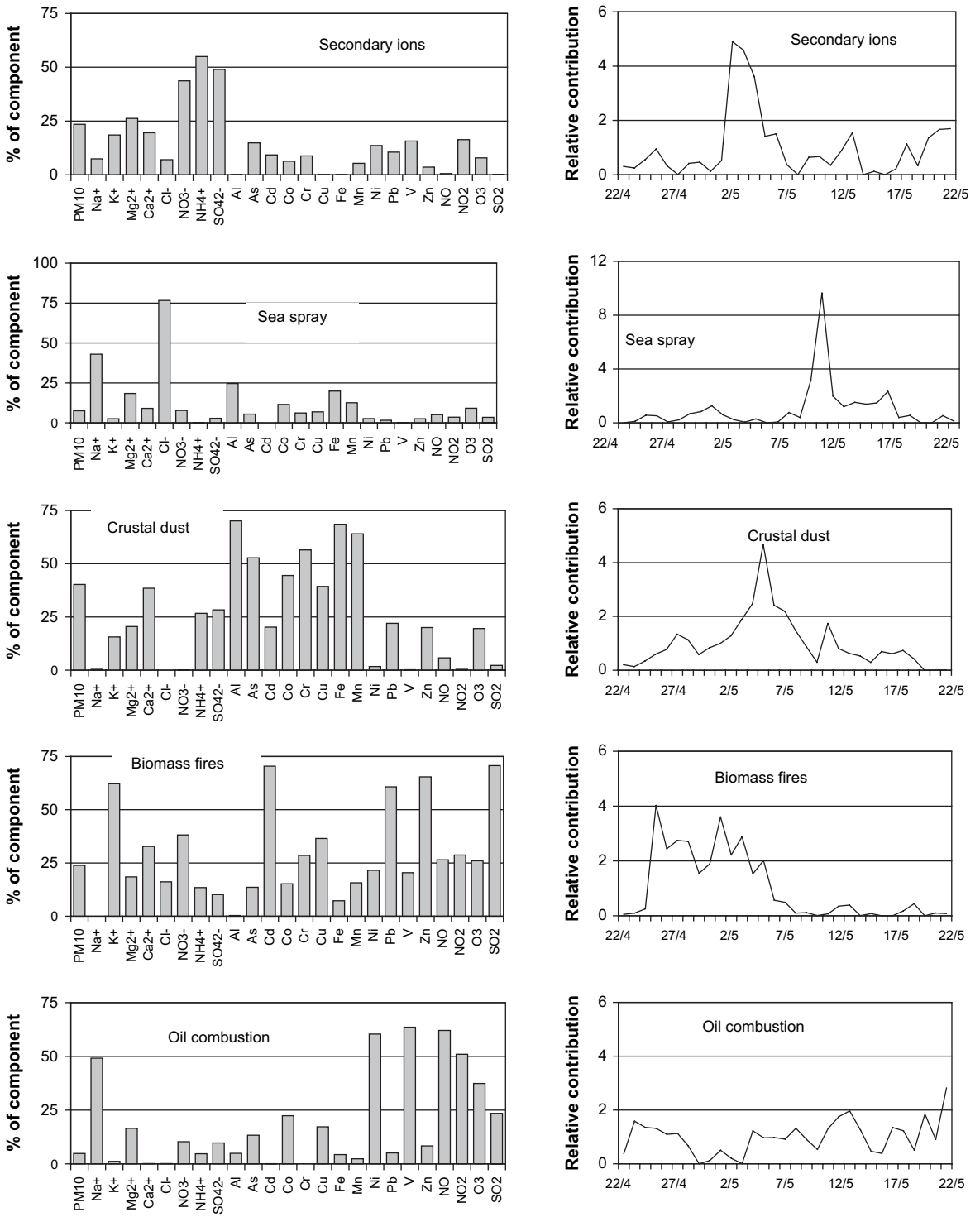

Fig. 10. The factor compositions (left column) as percentage of each species loaded into each respective factor and the relative source contribution time series (right column) during P1.

factor and at the same time very little sulphate and nitrate, which suggests reasonably close sources. This source had no specific temporal behaviour during the study period (Fig. 10).

In P2 only three physically meaningful factors were resolved: (1) combined sea spray and ship emissions, (2) combined fossil fuel combustion and industry and (3) biomass fires (Fig. 11). The PMF solution explained

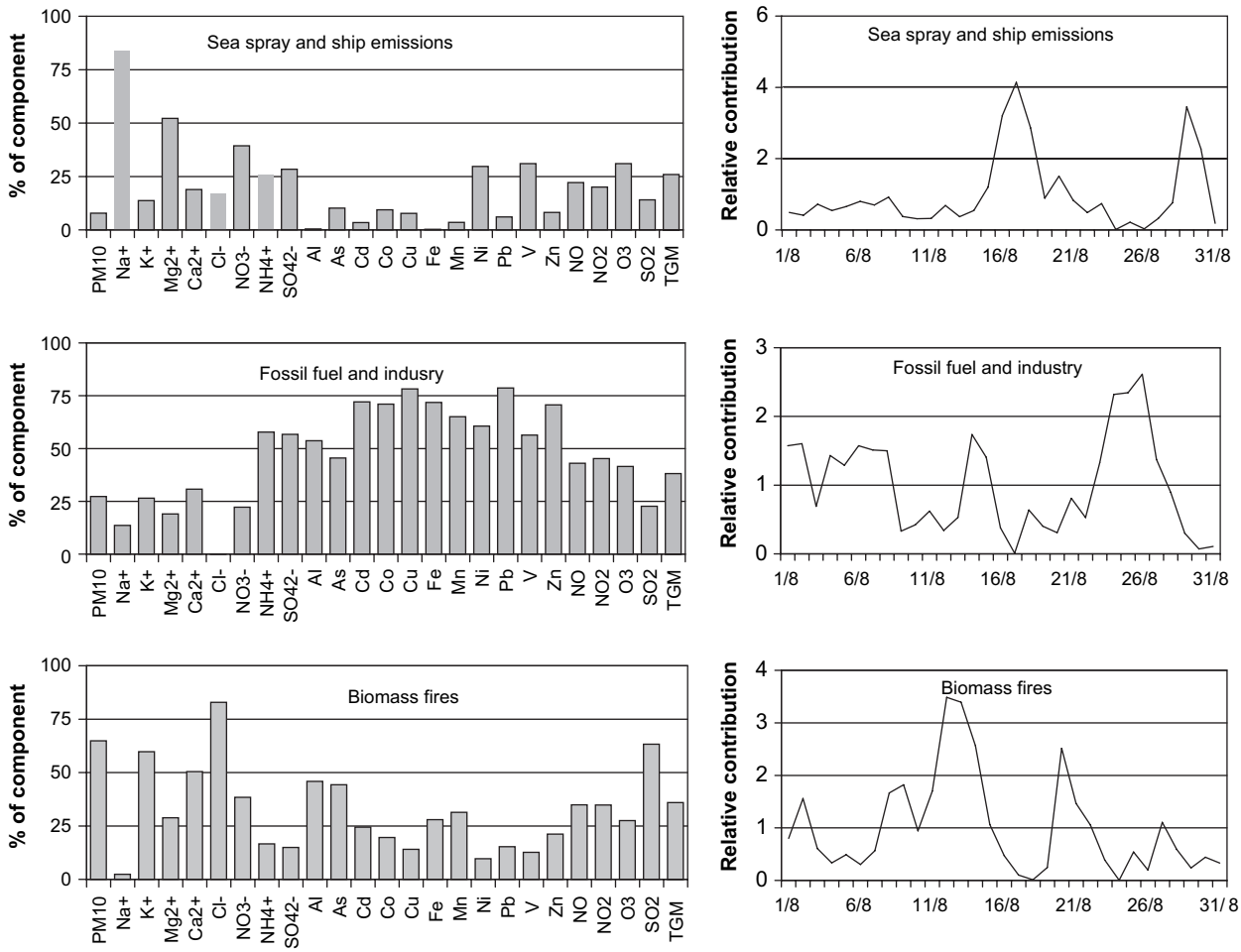

Fig. 11. The factor compositions (left column) as a percentage of each species loaded into each respective factor and the relative source contribution time series (right column) during P2.

89–76% of the variation of all components except for NO and Cl^-, which were explained to the extent of 60% and 70%, respectively. During this one-month period the biomass fire factor explained 65% of the total explained variation of PM_{10}, while fossil fuel and industry, and sea spray and ship emissions explained 27% and 8%, respectively.

The major components contributing to the first factor were Na^+ and Mg^{2+}, with a mass ratio of 6.7, thus suggesting that this material was sea spray aerosol (Fig. 11). Cl^-, on the other hand, has been seriously depleted here (Na^+/Cl^- ratio 19). The maximum days of this factor were 17 and 29 August.

Of the heavy metals, Ni and V were also slightly enriched in this factor, which suggests interference by oil combustion. Large marine diesel engines widely use low-grade residual oil. Indeed, the back trajectories of 17 and 29 August (Fig. 12), suggest that the high-density international ship route in the Gulf of Finland may play a role in the atmospheric V and Ni concentrations at Virolahti.

The second factor combined secondary ions, the majority of the trace elements and considerable fractions of major soil dust components (Al, Fe, Mn), too. No outstanding LRT, trace element or dust episodes occurred in August, and PMF also blocks all these species together. This factor was strongest on 24 and 26 August. The air-masses during these days mainly originated from northern continental Europe and circulated over Poland, the Ukraine and south-western Russia to Virolahti (not shown). These air masses may well have been a complex mixture of anthropogenic and natural emissions.

The third factor was the biomass fire factor, which we identify on the basis of its high loading of K^+. Its temporal behaviour is almost similar to that of the PM_{10} (Fig 5). Compared to P1, Cd, Pb and Zn now have clearly lower loadings, as expected (this is more exclusively caused by biomass burning), and a clearly higher loading of Cl^-. This may indicate that Cl^- was truly enriched in the primary burning emission (e.g. Hays et al., 2005; Allen and Miguel, 1995). However, Cl^- was not significantly elevated in any of the P2 episodes. Alternatively, it may be related to the atmospheric reactions between sea spray and biomass-burning aerosol when maritime air masses passed over the burning areas.

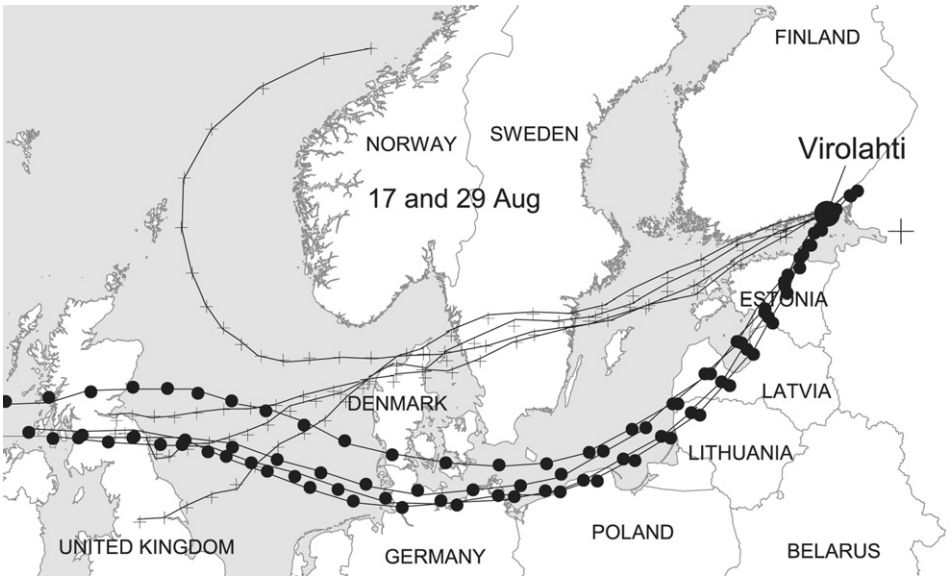

Fig. 12. Three-day backward trajectories arriving at Virolahti on 17 August (cross) and 29 August (circle).

5. Conclusions

In spring the biomass-burning aerosol detected at Virolahti originated from the south and south-east, from distances of even hundreds of kilometres, and consequently was a mixture of biomass-burning aerosol and that from other sources (both LRT and local), all of which contributed to the detected elevation of PM_{10} concentrations. The elevated concentrations of trace elements and ions were mainly explained by other sources than biomass burning. Elevated PAH concentrations occurred, however, in concurrence with the most intense biomass-burning episode.

In August, the PM_{10} at Virolahti was quite exclusively impacted by close (ca. 50–100 km) biomass fire sources. The unidentified, presumably organic component comprised, at its highest, as much as 90% of the total PM_{10}. In addition to record high PM_{10} and $PM_{2.5}$ concentrations, the concentrations of polycyclic aromatic hydrocarbons were elevated and highly variable, even reaching values that are more typical of wintertime urban environments. During the peaks of the episodes in August, the total gaseous mercury concentration in the air was more than double its background value. Release of accumulated mercury by fires from soils and foliage are a likely explanation for these mercury episodes. The trace elements in PM_{10} were not elevated from their background values during the biomass burning episodes.

Acknowledgements

NILU is acknowledged for providing the FLEXTRA trajectories, and NASA Fire Information for Resource Management System (FIRMS) for the active fire data.

References

Allen, A.G., Miguel, A.H., 1995. Biomass burning in the Amazon: characterization of the ionic component of aerosols generated from flaming and smouldering rainforest and savannah. Environmental Science and Technology 29, 486–493.

Andreae, M.O., 1983. Soot carbon and excess fine potassium: long-range transport of combustion-derived aerosols. Science 220, 1148–1151.

Andreae, M.O., Merlet, P., 2001. Emissions of trace gases and aerosols from biomass burning. Global Biogeochemical Cycles 15, 955–966.

Anttila, P., Salmi, T., 2006. Characterizing temporal and spatial patterns of urban PM_{10} using six years of Finnish monitoring data. Boreal Environmental Research 11, 463–479.

Aunela-Tapola, L., Frandsen, F., Häsänen, E., 1998. Trace metal emissions from the Estonian oil shale fired power plant. Fuel Processing Technology 57, 1–24.

Brunke, E.-G., Labuschagne, C., Slemr, F., 2001. Gaseous mercury emissions from a fire in the Cape Peninsula, South Africa, during January 2000. Geophysical Research Letters 28, 1483–1486.

Cinnirella, S., Pirrone, N., 2006. Spatial and temporal distributions of mercury emissions from forest fires in Mediterranean region and Russian Federation. Atmospheric Environment 40, 7346–7361.

Friedli, H.R., Radke, L.F., Lu, J.Y., 2001. Mercury in smoke from biomass fires. Geophysical Research Letters 28, 3223–3226.

Friedli, H.R., Radke, L.F., Lu, J.Y., Banic, C.M., Leaitch, W.R., MacPherson, J.I., 2003a. Mercury emissions from burning of biomass from temperate North American forests: laboratory and airborne measurements. Atmospheric Environment 37, 253–267.

Friedli, H.R., Radke, L.F., Prescott, R., Hobbs, P.V., Sinha, P., 2003b. Mercury emissions from the August 2001 wildfires in Washington State and an agricultural waste fire in Oregon and atmospheric mercury budget estimates. Global Biogeochemical Cycles 17, 1039. doi:10.1029/2002GB001972.

Grigal, D.F., 2003. Mercury sequestration in forests and peatlands: a review. Journal of Environmental Quality 32, 393–405.

Hays, M.D., Fine, P.M., Geron, C.D., Kleeman, M.J., Gullett, B.K., 2005. Open burning of agricultural biomass: physical and chemical properties of particle-phase emissions. Atmospheric Environment 39, 6747–6764.

Hellén, H., Hakola, H., Haaparanta, S., Pietarila, H., Kauhaniemi, M., 2008. Evaluation of importance of residential wood combustion to the local air quality in a typical Nordic residential area. Science of the Total Environment 393, 283–290.

Jalkanen, L., Häsänen, E., 1996. Simple method for the dissolution of atmospheric aerosol samples for analysis by inductively coupled plasma mass spectrometry. Journal of Analytical Atomic Spectrometry 11, 365–369.

Justice, C.O., Giglio, L., Korontzi, S., Owens, J., Morisette, J.T., Roy, D., Descloitres, J., Alleaume, S., Petitcolin, F., Kaufman, Y., 2002. The MODIS fire products. Remote Sensing of Environment 83, 244–262.

Mollicone, D., Eva, H.D., Achard, F., 2006. Human role in Russian wild fires. Nature 440, 436–437.

Niemi, J.V., Tervahattu, H., Vehkamäki, H., Kulmala, M., Koskentalo, T., Sillanpää, M., Rantamäki, M., 2004. Characterization and source identification of a fine particulate episode in Finland. Atmospheric Environment 38, 5003–5012.

Niemi, J.V., Tervahattu, H., Vehkamäki, H., Martikainen, J., Laakso, L., Kulmala, M., Aarnio, P., Koskentalo, T., Sillanpää, M., Makkonen, U., 2005. Characterization of aerosol particle episodes in Finland caused by wildfires in Eastern Europe. Atmospheric Chemistry and Physics 5, 2299–2310.

Nriagu, J.O., 1989. A global assessment of natural sources of atmospheric trace metals. Nature 338, 47–49.

Paatero, P., 1997. Least squares formulation of robust non-negative factor analysis. Chemometrics and Intelligent Laboratory Systems 37, 23–35.

Paatero, P., Tapper, U., 1994. Positive matrix factorization: a non-negative factor model with optimal utilization of error estimates of data values. Environmetrics 5, 111–126.

Saarikoski, S., Sillanpää, M., Saarnio, K., Timonen, H., Teinilä, K., Hillamo, R., 2006. Chemical composition of fine particles in major biomass burning episodes in Finland in 2006. Report Series in Aerosol Science 83, 325–329.

Saarikoski, S., Sillanpää, M., Sofiev, M., Timonen, H., Saarnio, K., Teinilä, K., Karppinen, A., Kukkonen, J., Hillamo, R., 2007. Chemical composition of aerosols during a major biomass burning episode over Northern Europe in spring 2006: experimental and modeling assessment. Atmospheric Environment 41, 3577–3589.

Salt, D.E., Smith, R.D., Raskin, I., 1998. Phytoremediation. Annual Review of Plant Physiology and Plant Molecular Biology 49, 643–668.

Samsonov, Y.N., Koutsenogii, K.P., Makarov, V.I., Ivanov, A.V., Ivanov, V.A., McRae, D.J., Conard, S.G., Baker, S.P., Ivanova, G.A., 2005. Particulate emissions from fires in central Siberian Scots pine forests. Canadian Journal of Forest Research 35, 2207–2217.

Sigler, J.M., Lee, X., Munger, W., 2003. Emission and long-range transport of gaseous mercury from a large-scale Canadian boreal forest fire. Environmental Science and Technology 37, 4343–4347.

Sillanpää, M., Saarikoski, S., Hillamo, R., Pennanen, A., Makkonen, U., Spolnik, Z., Van Grieken, R., Koskentalo, T., Salonen, R.O., 2005. Chemical composition, mass size distribution and source analysis of long-range transported wildfire smokes in Helsinki. Science of the Total Environment 350, 119–135.

Stohl, A., Berg, T., Burkhart, J.F., Fjæraa, A.M., Forster, C., Herber, A., Hov, Ø., Lunder, C., McMillan, W.W., Oltmans, S., Shiobara, M., Simpson, D., Solberg, S., Stebel, K., Ström, J., Tørseth, K., Treffeisen, R., Virkkunen, K., Yttri, K.E., 2007. Arctic smoke – record high air pollution levels in the European Arctic due to agricultural fires in Eastern Europe. Atmospheric Chemistry and Physics 7, 511–534.

Stohl, A., Wotawa, G., Seibert, P., Kromp-Kolb, H., 1995. Interpolation errors in wind fields as a function of spatial and temporal resolution and their impact on different types of kinematic trajectories. Journal of Applied Meteorology 34, 2149–2165.

Stohl, A., Seibert, P., 1998. Accuracy of trajectories as determined from the conservation of meteorological tracers. Quarterly Journal of the Royal Meteorological Society 124, 1465–1484.

Tervahattu, H., Hongisto, M., Aarnio, P., Kupiainen, K., Sillanpää, M., 2004. Composition and origins of aerosol during a high PM_{10} episode in Finland. Boreal Environment Research 9, 335–345.

Turetsky, M.R., Harden, J.W., Friedli, H.R., Flannigan, M., Payne, N., Crock, J., Radke, L., 2006. Wildfires threaten mercury stocks in northern soils. Geophysical Research Letters 33, L16403. doi:10.1029/2005GL025595.

Ward, T.J., Hamilton, R.F., Smith, G.C., 2004. The Missoula, Montana $PM_{2.5}$ speciation study – seasonal average concentrations. Atmospheric Environment 38, 6371–6379.

Wedepohl, K.H., 1995. The composition of the continental crust. Geochimica et Cosmochimica Acta 59, 1217–1232.

Wooster, M.J., Zhang, Y.H., 2004. Boreal forest fires burn less intensely in Russia than in North America. Geophysical Research Letters 31, L20505. doi:10.1029/2004GL020805.

Yamasoe, M.A., Artazo, P., Miguel, A.H., Allen, A.G., 2000. Chemical composition of aerosol particles from direct emissions of vegetation fires in the Amazon Basin: water-soluble species and trace elements. Atmospheric Environment 34, 1641–1653.

ILMATIETEEN LAITOS
METEOROLOGISKA INSTITUTET
FINNISH METEOROLOGICAL INSTITUTE

FINNISH METEOROLOGICAL INSTITUTE
Erik Palménin aukio 1
P.O. Box 503
FI-00560 HELSINKI
tel. +358 29 539 1000
WWW.FMI.FI

FINNISH METEOROLOGICAL INSTITUTE
CONTRIBUTIONS No. 163
ISSN 0782-6117
ISBN 978-952-336-101-0 (paperback)
ISBN 978-952-336-102-7 (pdf)
https://doi.org/10.35614/isbn.9789523361027

Helsinki, 2020
Edita Prima Oy